Fundamental aspects of using electric fences for groundwater remediation

Zur Erlangung des akademischen Grades eines
Doktors der Naturwissenschaften
von der Fakultät für
Bauingenieur-, Geo- und Umweltwissenschaften
der Universität Fridericiana zu Karlsruhe (TH)
genehmigte

DISSERTATION

von
Dipl.-Geol. Gabriele Gregolec
aus Krumbach (Schw.)

Karlsruhe, 14.11.2008

Hauptreferent:	Prof. Dr. Dr. K. Czurda, Karlsruhe University (TH)
Korreferent:	Dr. habil. R. Haus, Dorfner Analysenzentrum und Anlagenplanungsgesellschaft mbH, Hirschau

ABSTRACT

For the management of contaminated land the combination of different remediation techniques is more and more an object of research as clean-up practice suggests a higher potential for success, especially for complex contamination sites. Electrokinetics and permeable reactive barriers (PRBs) are frequently discussed innovative in-situ technologies. Research impulse of the present work was to investigate the potential of success of applying an electrokinetic fence upstream of the reactive barrier to enhance its long-term efficiency. Electrodes are placed into the ground to reduce the concentration of groundwater constituents that might impair the barrier function when flowing with the groundwater through the reactive material. Hence, the focus of the study laid on the investigation of fundamentals of electrokinetic retention of charged groundwater components against hydraulic flow. In particular, the influence of hydraulic flow on electrokinetically induced changes in soil/pore solution geochemistry was examined.

In all experiments, uniform middle sand was used. First, a test series of electrokinetic cell experiments was carried out. Theoretical modelling was applied to confirm experimental results. Based on these results, the experimental set-up was scaled up. Different electrode types and configurations as well as potential influence of electrokinetic processes on reactive materials (Fe^0) were studied. Finally, geochemical modelling was carried out and its applicability for predicting and analysing electrokinetically induced changes in species formation was examined.

When applying an electric gradient only, steady state conditions developed - a phenomenon that has been predicted and verified by numerical modelling. Where the electrolysis products H^+ and OH^- meet, they form water. Chemical analysis confirmed the separation of the electrolyte into two binary zones.

Laboratory experiments combining electric and hydraulic gradients proved that it is possible to hinder the bulk of charged species from moving with the groundwater flow. In particular, the electrokinetic retardation of cations seems to be very promising. It has been documented that the waterfront also develops if a hydraulic gradient is applied. Here the waterfront is transported towards the downstream electrode by the hydraulic flow. Hence, the pore solution between the electrodes is solely influenced by the geochemical conditions produced at the upstream placed electrode. However, conditions at the downstream electrode are influenced by electrochemical processes of both electrodes and are also dependent on the composition/chemistry of the flushing solution. Additionally applied acidic batch experiments proved to be a helpful tool to distinguish between retention by electrokinetic mechanisms and retention by electrokinetic induced precipitation reactions.

Bench scale experiments showed that the observed electrokinetic retention of ions can be transferred into larger scales. Installing plane electrodes generating an electric field parallel to hydraulic flow identified that for this set-up combined electrokinetic and hydraulic processes may negatively affect the stability of Fe^0. If the electric field is directed perpendicular to hydraulic flow, steady state conditions develop that are comparable to the one achieved during electrokinetic cell experiments where no hydraulic gradient was applied. The geochemical composition of the downstream effluent is affected by the position of the waterfront, precipitation reactions, hydraulic turbulences and oxygen transported electroosmotically through the anode kaolin. Using more than one electrode pair, interactions of the electrode pairs on the electric field and the geochemistry of pore and electrode solution have to be considered. Combining the results achieved by laboratory experiments and geochemical modelling, the chemical species formation with time and space can be described.

Individual Eh/pH diagrams considering changes in ion concentration and temperature during electroremediation were modelled using the software HSC Chemistry 5.1. The results demonstrated that simple Eh/pH diagrams do not reflect conditions during electrokinetic remediation sufficiently. However, the modelled complex Eh/pH diagrams are very helpful for verifying electrokinetically induced chemical species formation and optimizing chemical analysis programs, thus increasing the understanding of fundamental processes and supporting the practical application of any electrokinetic remediation technique.

The carried out laboratory experiments provide essential fundamentals of electrokinetic phenomena in sandy soil as well as interactions between electric and hydraulic induced processes. Furthermore, they offer a theoretical basis for successfully designing feasibility studies and field applications. Advantages and potential problems of applying an electric fence – in general and with respect to different electrode types/configurations – were demonstrated, discussed and solutions presented. The results show that equilibrium of the various effects can be directly controlled by the applied electric voltage and pH control. Summarizing, the retention of charged chemical species by applying an electric fence is principally a suitable and promising method. Especially the combination with other remediation techniques, e.g. as a supporting measure for enhancing the long-term-stability of PRBs, seems to be an economically viable vision.

KURZFASSUNG

Die Sanierungspraxis von Altlasten hat gezeigt, dass besonders bei komplexen Standortbedingungen die Anwendung einer Sanierungstechnologie allein oft nicht zum festgesetzten Sanierungsziel führt. Deshalb wurde in den letzten Jahren auf dem Gebiet der Altlastenbearbeitung verstärkt die Kombination unterschiedlicher Sanierungstechnologien untersucht. Die elektrokinetische Bodensanierung sowie Reaktive Wände zählen zu den innovativen in-situ Sanierungstechnologien. Die Frage, ob eine oberstromig installierte elektrische Barriere, ein so genannter „electric fence“, das Langzeitverhalten Reaktiver Wände positiv beeinflussen kann, war der Forschungsimpuls dieser Arbeit. Der Fokus dieser Studie war darauf gerichtet, grundsätzliche Erkenntnisse in Bezug auf die elektrokinetische Retardation geladener Grundwasserinhaltsstoffe gegen einen hydraulischen Gradienten zu erfassen, um eine prozessbedingte negative Beeinträchtigung der Funktion der Reaktiven Wand durch coating und clogging zu unterbinden. Insbesondere wurde dabei der Einfluss des hydraulischen Transports auf elektrokinetisch induzierte geochemische Änderungen der Porenlösung untersucht.

Vor dem Hintergrund bei gleich bleibenden Randbedingungen reproduzierbare Untersuchungsergebnisse zu erzielen wurden alle Versuche mit einem gleichförmigen Mittelsand durchgeführt. Um alle ablaufenden Prozesse qualitativ und quantitativ beurteilen zu können, wurden die Laborversuche mit kleinskaligen elektrokinetischen Laborversuchen begonnen. Numerische und analytische Modelle wurden angewandt, um die Versuchsergebnisse zu validieren. Auf der Basis dieser Ergebnisse wurden die folgenden Versuche durch Upscaling an realistische Standortgegebenheiten angepasst. Ferner wurden unterschiedliche Elektrodentypen und Elektrodenanordnungen getestet sowie der Einfluss aller elektrokinetischer Prozesse auf das reaktive Material (Fe^0) untersucht. Die gewonnen Daten flossen in eine geochemische Modellierung ein, mit dem Ziel eine Vorhersage und Analyse elektrokinetisch bedingter Speziesänderung zu untermauern.

Die in einem geschlossenen System durchgeführten elektrokinetischen Zellenversuche zeigten, dass sich bereits nach kurzer Zeit ein Gleichgewicht zwischen den elektrokinetisch transportierten Anionen und Kationen innerhalb der Porenlösung einstellt. Im Bereich, in dem sich die Elektrolyseprodukte H^+ und OH^- treffen, reagieren sie zu Wasser. Chemische Analysen haben bestätigt, dass der Elektrolyt in zwei binäre Zonen separiert wird. Die Laborversuche demonstrierten, dass der Großteil geladener Wasserinhaltsstoffe gegen einen hydraulischen Gradienten elektrokinetisch zurückgehalten werden kann. Darüber hinaus wurde gezeigt, dass sich die Wasserfront auch dann bildet, wenn ein hydraulischer Gradient auf das System wirkt. Unter diesen Bedingungen wird die Wasserfront hydraulisch zur unterstromigen Elektrode transportiert. Folglich wird die Geochemie zwischen den

Elektroden einzig von den elektrochemischen Prozessen an der oberstromigen Elektrode bestimmt. Die Bedingungen an der unterstromigen Elektrode hingegen werden von den elektrochemischen Prozessen beider Elektroden beeinflusst und sind darüber hinaus von der Zusammensetzung der Durchströmungslösung abhängig.

Die elektrokinetische Retardation von Ionen konnte auch in größerem Labormaßstab nachgewiesen werden. Verlaufen die elektrischen Feldlinien parallel zum hydraulischen Fluss, so wirken sich elektrisch und hydraulisch bedingte Prozesse negativ auf die Stabilität von elementarem Eisen (Fe^0) aus. Ist das elektrische Feld senkrecht zum hydraulischen Fluss gerichtet, entwickeln sich binäre Zonen, wie sie bei den Eingangsversuchen ohne hydraulischen Gradienten beobachtet wurden. Die Geochemie im Abstrom wird dabei maßgeblich von der Position der Wasserfront, Fällungsreaktionen, hydraulischen Turbulenzen und elektroosmotisch transportiertem Sauerstoff bestimmt. Werden mehrere Elektrodenpaare eingesetzt, muss die Wechselwirkung der Elektrodenpaare auf das elektrische Feld sowie auf die Geochemie der Poren- und Elektrodenlösung berücksichtigt werden. Geochemische Modellierungen ermöglichten Rückschlüsse über die zeitliche und räumliche Speziesbildung von Grundwasserinhaltsstoffen zu ziehen.

Für die Modellierung von Eh/pH Diagrammen wurde die Software HSC Chemistry 5.1 verwendet. Dabei fanden unter anderem elektrokinetisch induzierten Änderungen der Ionenkonzentrationen und der Temperatur Berücksichtigung. Die Ergebnisse zeigten, dass einfache Eh/pH Diagramme die Bedingungen während einer elektrokinetischen Sanierung nicht ausreichend darstellen. Die mit der Software erstellten komplexen Eh/pH Diagramme erwiesen sich dagegen als hilfreiches Werkzeug elektrokinetisch induzierte Speziesänderungen zu verifizieren und das chemische Analysenprogramm entsprechend zu optimieren. Die Modellierung trägt nicht nur zum Verständnis der grundlegenden Prozesse bei, sondern sie unterstützt auch die praktische Anwendung des elektrokinetischen Verfahrens.

Die durchgeführten Laborversuche liefern entscheidende Erkenntnisse über elektrokinetische Prozesse in sandigen Böden sowie über Wechselwirkungen zwischen elektrisch und hydraulisch bedingten Prozessen. Darüber hinaus bieten sie die theoretische Basis für die erfolgreiche Planung und Durchführung elektrokinetischer Machbarkeitsstudien und Feldanwendungen für die Grundwassersanierung. Vorteile und potentielle Probleme bei der Anwendung einer elektrischen Barriere im allgemeinen und in Bezug auf verschiedene Elektrodentypen und -konfigurationen wurden demonstriert, diskutiert sowie Lösungen präsentiert. Zusammenfassend lassen die Ergebnisse dieser Arbeit den Rückschluss zu, dass die Installation einer elektrischen Barriere ein geeignetes und Erfolg versprechendes Verfahren zur Rückhaltung geladener Grundwasserinhaltsstoffe ist. Insbesondere die Kombination mit anderen Sanierungstechnologien, beispielsweise als unterstützende Maßnahme um die Langzeitstabilität Reaktiver Wände zu verbessern, ist eine ökonomisch praktikable Vision.

ACKNOWLEDGEMENTS

This thesis was prepared at the Department of Applied Geology at the University of Karlsruhe and supervised by Prof. Dr. Dr. Kurt Czurda. First, I would like to thank him for the possibility to accomplish my PhD thesis within the framework of an international research project and for supporting me in completing this thesis with valuable suggestions and discussions.

My sincere gratitude is also to Dr. Reiner Haus from Dorfner Analysenzentrum und Anlagenplanungsgesellschaft mbH, Hirschau, for supporting this thesis and being my co-referee.

I am very grateful to Dr. Karl Ernst Roehl for his continuous interest in my studies, helpful comments and corrections. Many thanks to all the colleagues from Germany, Austria, Hungary, Poland and England of the EU-funded research project "Long-term Performance of Permeable Reactive Barriers used for the Remediation of Contaminated Groundwater" (PEREBAR) for their scientific support and cooperation.

I am deeply grateful to Dr. Hagen Steger and Dr. Roman Zorn for all the helpful discussions, technical support, corrections and close friendship.

I would like to thank Dipl.-Geol. Arndt Kurzbach for his laboratory work that contributed partly to this thesis.

My appreciation goes to all my former colleagues at the University of Karlsruhe for the good times and excellent cooperation.

Many thanks to Jennifer Stiebel for language review and for her support by taking care of my son Paul.

I would like to thank all other people that deserved acknowledgements for their help and assistance in the last few years.

Finally, I would like to express my special gratitude to my mother for her endless care and support, to Michael for his loving understanding and for giving me continuous encouragement and to my son Paul for energizing me by his blithe spirit.

CONTENTS

LIST OF FIGURES

LIST OF TABLES

1 INTRODUCTION

1.1 Background

Contaminated land and hazardous sites became generally recognised as a serious environmental problem in the seventies throughout Europe and Northern America. During the eighties most industrial nations worked on the systematisation of the decision-making processes for the evaluation and – if necessary – the treatment of contaminated land. A risk based decision-making process for remediation is now the norm in EU Member States (CLARINET/NICOLE 1998). In Germany, a federal soil protection law (Bundes-Bodenschutzgesetz) is the superior regulation instrument for the investigation and remediation of contaminated sites.

Remediation techniques of the first generation were mainly standard civil engineering techniques adjusted or transferred to the specific demands of the cleanup operation, e.g. excavation ("dig-and-dump"), engineered containment (cut-off walls and cover systems), hydraulic remediation ("pump-and-treat"), soil vapour extraction and soil washing. Especially since the nineties scientists world-wide are searching for new, more efficient and cost-effective clean-up techniques. A comprehensive overview of the state-of-the-art of implementation of remediation technologies in Europe is given in a report by CLARINET, a network funded under the Environment and Climate Programme of the European Commission (CLARINET 2002a).

Innovative remediation technologies include the following ex-situ and in-situ techniques:

- thermal ex-situ soil treatment by thermal desorption and vacuum distillation
- bioreactors
- air sparging
- thermally enhanced soil vapour extraction (SVE)
- surfactant-enhanced soil washing
- phytoextraction
- natural attenuation
- electrokinetic remediation of soils and sludges
- permeable reactive barriers

Generally, the innovative clean-up practice tends towards the application of on site technologies taking place in situ and focusing on the decontamination or control of the plume (ROEHL & GREGOLEC 2005).

Passive groundwater remediation using permeable barriers is a new and innovative technology. Permeable reactive barriers (PRB) are subsurface constructions situated across the flow path of contaminant plumes. The targeted contaminants are removed

from the groundwater flow by geochemical processes such as adsorption, chemical bonding, oxidation/reduction, and precipitation (EPA 1998, GAVASKAR et al. 1998, BLOWES et al. 2000, SIMON & MEGGYES 2000, BIRKE et al. 2003). The geochemistry of reactive barrier systems is complex, especially in cases where very reactive materials are used which might lead to drastic changes of the geochemical conditions in the groundwater (e.g. elemental iron). Laboratory and field data have shown that the behaviour of major groundwater constituents, e.g. calcium, magnesium, bicarbonate and sulphate, is very important for the long-term effectiveness of the attenuation process within the barrier material since they tend to precipitate and form secondary minerals in the barrier matrix under certain conditions (O'HANNESIN & GILLHAM 1998, MACKENZIE et al. 1999, MCMAHON et al. 1999, VOGAN et al. 1999, BLOWES et al. 2000, KLEIN & SCHAD 2000, PHILLIPS et al. 2000, YABUSAKI et al. 2001).

The research project “Long-term Performance of Permeable Reactive Barriers used for the Remediation of Contaminated Groundwater” (PEREBAR) was initiated within the 5th Framework Programme of the EU from 2000 to 2003 (ROEHL & CZURDA 2002, ROEHL ET AL. 2005). Investigating the feasibility of electrokinetic methods to positively affect the long-term efficiency of reactive barriers was one principal task of the PEREBAR project – and concurrently this task was the research impulse for the investigations presented in this thesis.

Electrokinetic methods are increasingly considered for the in situ remediation of contaminated sites – particularly for clayey soils where conventional methods like pump-and-treat fail (ALSHAWABKEH et al. 1999, CZURDA et al. 2001, HAUS et al. 1999, HAUS & CZURDA 1999, 2000, HAUS 2002, LAGEMANN & POOL 2001). Electrokinetic phenomena in cohesive soil have been used for geotechnical purposes since the beginning of the last century (CASAGRANDE 1952). In the environmental engineering field, most of the work on electrokinetics has been performed at the end of the eighties and during the nineties (LAGEMAN et al. 1989, ACAR et al. 1992, BRUELL et al. 1992, PROBSTEIN & HICKS 1993, ACAR & ALSHAWABKEH 1996, ALSHAWABKEH & ACAR 1996).

For electrokinetic soil remediation, electrodes are placed into the ground and a voltage is applied which generates a direct current (dc) electric field. The principle electric driven transport processes are electroosmosis, electromigration, and electrophoresis (PROBSTEIN 1994). Since 1996 a team of researchers of the Department of Applied Geology, Karlsruhe University, has been working in the field of electrokinetic soil remediation. They used their know-how acquired by numerous laboratory experiments for scaling up their studies to container and field tests (HAUS 2002, STEGER 2005, ZORN 2005). All of these tests were carried out with and within fine-grained soils mainly studying electroosmotic transport processes with respect to soil treatment. However, during these studies laboratory experiments with sandy soil were carried out and analysed with respect to the application of electric fences for groundwater remediation. Hence, the focus is on electromigration, which is defined as the transport of ions or ion complexes in solution, with the electric potential as the

driving force. Positively charged species are migrating towards the cathode whereas negatively charged species are moving towards the anode. The chosen basic conditions of the carried out laboratory studies allowed the exclusion of electrophoresis as predominant transport mechanism.

1.2 Objectives and scope

Permeable reactive barriers are used for the treatment of contaminated groundwater plumes and therefore usually placed in aquifers which consist of coarse-grained sediments having significant effective porosity and hydraulic permeability. The question that arises when attempting to fence off groundwater constituents from entering the PRB is: can a charged species be sufficiently retarded by an electric field to stop it migrating with the hydraulic flow. Therefore, the following aspects have to be considered:

- Electrokinetics in aquifer material:

  Though literature studies show that many laboratory and field experiments proved the applicability of electrokinetics as an in situ remediation technique for the decontamination of fine-grained soils – where electroosmosis plays an important role – only little information on electrokinetic phenomena within coarse-grained soils is available (e.g., KIM & LEE 1999).

- Combined electric and hydraulic gradients:

  No quantitative experience is reported concerning the electromigrative transport of charged species in dependency on both electric and hydraulic gradient within aquifer materials or coarse-grained soils.

The feasibility of coupling electrokinetics with treatment zones within fine-grained soils has been documented in laboratory and field experiments. The so-called “Lasagna” process described by HO et al. (1995, 1999a,b) consists of a layered configuration of electrodes and treatment zones (s. Section 2.2.4). The contaminants are transported into the treatment zones by electrokinetic mechanisms with the aim to avoid additional treatment steps, for instance to recycle the water collected in the electrode reservoirs.

Fig. 1.1 shows the main possibilities for combining electrokinetic techniques with permeable reactive barriers placed in aquifers. Considering the long-term behaviour of reactive barriers the application of an electric fence upstream of the PRB appears to be the most promising and practicable approach (s. Section 2.2.4). The general aim of this approach is to reduce the concentration of groundwater constituents that might impair the barrier function by coatings or precipitates on the surfaces of the reactive material when moving with the groundwater flow through the permeable barrier.

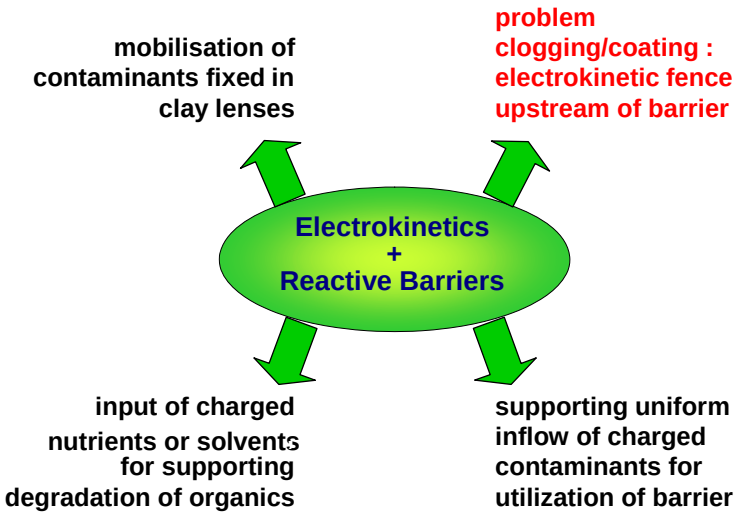

Fig. 1.1: Possibilities for the combination of electrokinetic techniques and permeable reactive barriers.

The aim of the present study was to investigate the fundamental aspects of using electric fences for groundwater remediation. First, fundamental electromigration behaviour of ions in sandy soil was investigated. Furthermore, the general influence of hydraulic gradients and the interaction between electrokinetically and hydraulically induced processes were studied. Therefore, laboratory tests were carried out focusing on electromigration, which is defined as the transport of ions or ion complexes in solution. In addition, the influence of the composition of the pore solution on electro-/geochemical conditions was considered. For sandy soils, no electric fence experiments in laboratory scale are documented in the literature – neither with plane electrodes nor with well electrodes. In this work, different electrode types as well as different configurations with respect to hydraulic flow direction are considered.

The application of a dc electric field into the ground has a substantial influence on soil pH, redox values and concentration distribution of chemical species, and usually leads to a distinct rise in temperature. To identify and visualize the influence of these dynamic changes on chemical species stability, individual Eh/pH diagrams were modelled using the software HSC Chemistry 5.1. This software allows to construct Eh/pH diagrams for selected temperatures and concentrations as well as for a selected multi-component system.

To sum up, this work included the following tasks:

- Set-up of laboratory test equipment in different scales (small-scale, bench-scale) for electrokinetic experiments with coarse-grained soil materials.
- Determination of the fundamental transport mechanisms and geochemical processes, including the influence of pore/flushing solution composition.
- Investigation of the influence of hydraulic gradients and the interaction between electrokinetically and hydraulically induced processes.
- Evaluation of different electrode types and configurations.
- Modelling of Eh/pH diagrams using the software HSC Chemistry 5.1, evaluation of the results with respect to electrokinetically induced changes on chemical species formation.
- Evaluation of the effect of electrokinetic mechanisms on the performance of PRBs.
- General recommendations for the assessment of the suitability of electrokinetic techniques in PRB systems.

1.3 Structure of the work

First, theoretical aspects that have to be considered for this study are introduced. The brief description of principles of permeable reactive barriers (PRBs) is followed by a detailed review of the principles of electrokinetic remediation. In this content, an overview of the history as well as the state-of-the-art of electrokinetic techniques is presented. Next, the most important electric variables and interacting mechanisms are introduced with focus on electrokinetic mass transport processes and effects of electrode reactions during electroremediation. As the electrokinetic phenomenon electroomosis is subject of most research undertaken in this field, its principles are presented although electroomosis can be neglected for the main practical part of this work. In addition, the Lasagna^{TM} technique, as an example for combining electrokinetics with treatment zones, and a literature survey with respect to electric fences are described. Practical aspects that have to be considered if applying electrokinetics as remediation technology close the theoretical treatise.

The theoretical models applied to verify the experimental results are explained in Chapter 3. The experimental set-ups are presented in Chapter 4. Furthermore, the methods of parameter analysis before, during, and after the individual experiments are described. In addition, the physicochemical data of the model soils, reactive materials and model solutions used in the experiments are listed.

The results obtained are described and discussed in detail in Chapter 5 to 7. The results distinguish between electrokinetic cell (small scale) and container (bench scale) laboratory experiments and Eh/pH diagrams obtained by geochemical

modelling. First, a test series of electrokinetic cell experiments was carried out. Applying only an electric gradient allowed testing the optimized test set-up. Afterwards, the influence of pore/flushing solution composition and hydraulic flow on retention of anions and cations were examined. Additionally the possibility of mobilising contaminants from clay lenses into coarser material was studied in laboratory experiments. Based on these results, the experimental set-up was scaled up. Different electrode types and configurations as well as potential influence of electrokinetic processes on zero-valent iron (Fe^0) as a reactive barrier material were studied by container experiments. Finally, geochemical modelling with HSC Chemistry 5.1 was carried out and its applicability for predicting and analysing electrokinetically induced changes in chemical species formation was examined.

2 THEORETICAL ASPECTS

2.1 Principles of Permeable Reactive Barriers

IRTC (2005) defines a permeable reactive barrier (PRB) as *"a continuous, in situ permeable treatment zone designed to intercept and remediate a contaminant plume"* (Fig. 2.1). The term "barrier" is intended to the idea of a barrier to contaminants, but not to groundwater flow. PRBs are designed to be more permeable than the surrounding aquifer materials so that contaminants are treated as groundwater readily flows through it by natural gradients and without significantly altering the hydraulic groundwater regime.

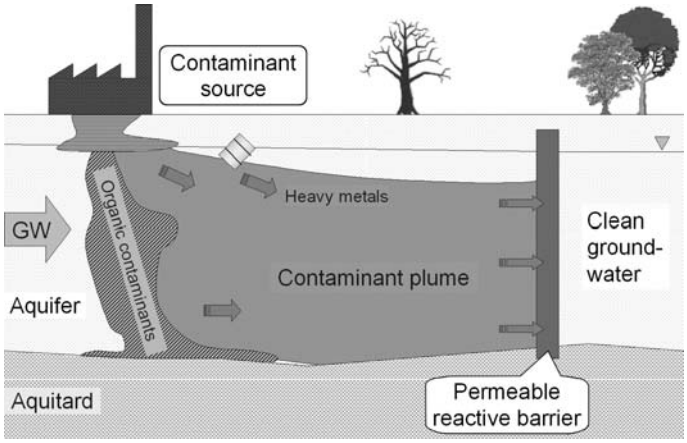

Fig. 2.1: Principle of the permeable reactive barrier PRB concept; GW groundwater flow direction (ROEHL et al. 2005).

The treatment zone may be created directly by using reactive materials such as zero-valent iron or activated carbon, or indirectly by using materials designed to stimulate secondary processes, such as by adding carbon substrate and nutrients to enhance microbial activity. In this way, contaminant treatment may occur through physical, chemical, or biological processes. Basic process categories include:

- chemical dehalogenation,
- pH control,
- reduction-oxidation,
- sorption, and
- biological enhancements.

Depending on these reaction mechanism various types of PRBs are distinguished (U.S. EPA 1996):

- Sorption barriers (e.g. zeolites, activated carbon): contaminants are removed by adsorption or complexation.
- Precipitation barriers (e.g. limestone): contaminants are changed into insoluble compounds and minerals.
- Degradation barrier (e.g. zero-valent iron): contaminants are cracked into non-toxic products (e.g. dehalogenation, reduction).

Advantages of in-situ PRBs include (O'HANNESIN & VOGAN 2005):

- low maintenance costs,
- no operating costs,
- long-term passive treatment,
- absence of waste materials requiring treatment or disposal,
- absence of invasive surface structures and equipment, and
- conservation of groundwater resources.

Several types of materials have been suggested for use in PRBs. To date, granular zero-valent iron (ZVI) has been the most widely used reactive media in full-scale permeable reactive barriers. Zero-valent iron is used mainly to treat chlorinated solvents although it is also applied to other contaminants such as chromium and arsenic (WILKIN & PULS 2003). Under highly reducing conditions and in the presence of metallic surfaces, certain dissolved chlorinated organic compounds in groundwater degrade to non-toxic products such as ethane, ethene and chloride (GILLHAM & O'HANNESIN 1994). Other reactive media, such as limestone, compost, zeolites, granular activated carbon, apatite, have also been used (ROEHL et al. 2001). Solid carbon-based PRBs promote the removal of trace metals, organics and nitrate via microbial processes (ITRC 2005). While still at the research stage, other sorbent type PRBs are being evaluated for the removal of harmful pathogens (bacteria, viruses etc.) from groundwater (RUST et al. 2005).

The PRB technology has now been applied at more than 200 sites worldwide. 83 of which are considered full scale, including 72 full-scale installations to treat chlorinated solvent compounds. In the United States, there have been more than 90 applications of iron-based PRBs, 67 of which are full scale (IRTC 2005).

In Germany, nine permeable reacitve barriers (PRBs) for passive in situ remediation of contaminated groundwater have been erected since the end of the nineties. BIRKE et al. (2003) provide a good review of the German PRB projects. Further reviews and guidance/regulatory documents are given by U.S. EPA (1996, 1998, 2002), ITRC (1999a, 1999b, 2000), GAVASKAR et al. (2000) and VIDIC (2001).

Online information platforms are for example:

http://www.prb-net.org
http://www.rtdf.org
http://www.clu-in.org
http://www.rubin-online.org
http://www.itrcweb.org

The two main PRB configurations are the continuous reactive barrier (CRB) and the funnel-and-gate (F&G) system (Fig. 2.2). A continuous reactive barrier consists only of a permeable section filled with the reactive medium, whereas a funnel-and-gate system has both permeable (gate) and impermeable (funnel) sections (ESTCP 2003).

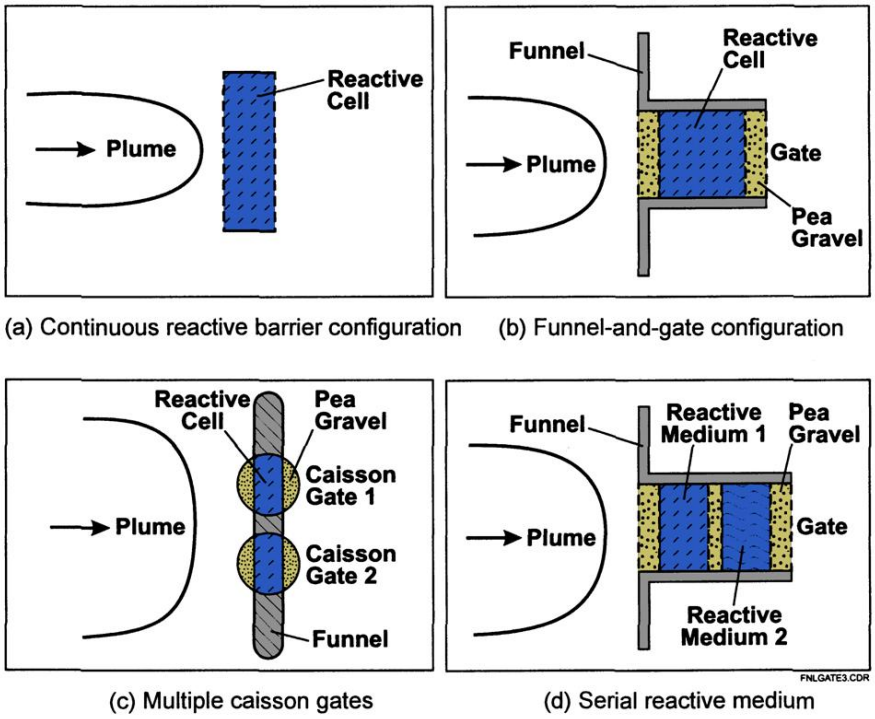

Fig. 2.2: Schematic illustration of different PRB configurations (GAVASCAR et al. 1998)

Many different construction methods are available for PRBs (MEGGYES 2005). These include simple unsupported excavation or excavation with temporary support, such as trench boxes or plane piling, for applications at shallow depths (< 6 m). Continuous trenching machines can be used to depths of 10-12 m. Biopolymer trenching is a commonly used method to depths of about 20 m, in which a biodegradable guar-based liquid is used to support the trench walls and the iron is placed through the biopolymer via a pipe.

Recently developed injection methods can be used to install granular iron PRBs to depths greater than 30 m. These methods involve suspending the granular iron in biodegradable slurry and injecting this slurry through boreholes into the subsurface (O'HANNESIN & VOGAN 2005).

Most PRBs are around or less than 10 years old, and it is not known whether they will remain effective over the lifetime of the contaminant plume, which could be on the order of decades or more. Therefore, especially within the last 5 years much research has focused on changes in PRB reaction rates over time or its long-term stability, respectively. ROEHL et al. 2005 describe methods for the evaluation and enhancement of the long-term performance of PRB systems. Processes that impair the barrier performance during PRB operation and technologies to enhance the long-term efficancy of PRB systems were studied qualitatively and quantitatively. Accelerated laboratory simulations of the long-term operation of PRBs were carried out by several authors (e.g. GAVASKAR et al. 2002, WILKIN et al. 2001).

When ZVI contacts groundwater corrosion takes place and ferrous iron and hydrogen (reducing agents) as well as hydroxyl ions are produced (Re. 1).

$$Fe^0 + 2H_2O \Leftrightarrow Fe^{2+} + H_2(g) + 2OH^- \qquad \text{Re. 1}$$

Thus, strongly reducing conditions and a high-pH milieu is often created within iron barriers. The solubility, and thus mobility, of many organic and inorganic compounds strongly depends on pH conditions. The direct effect of a pH shift on the carbonate equilibrium has been well documented with respect to the use of granular iron for PRBs. Field studies (WILKIN & PULS 2003, SASS et al. 2002, PHILLIPS et al. 2003) have shown that several inorganic constituents transfer from the solution phase onto the surface of the iron particles.
This can lead to formation of molecular or particulate films on the iron surfaces (coating). Thus, not only iron mass is consumed in these reaction, but the formation of potentially passivating films on the iron surfaces can reduce the reactivity of the remaining iron mass (ITRC 2005). The implication of this observation is that the reactivity of the PRB can potentially decline, even while considerable iron mass still remains in the PRB (GAVASKAR et al. 2002).

Coatings might block access to the reactive surfaces (Fig. 2.3). Further precipitation blocks the pore spaces between some iron particles (clogging) increasing flow velocity and decreasing the residence time.

Investigations of laboratory and field operations identified relatively similar precipitates, which primarily consisted of carbonates, hydroxides, sulphides, oxides, and silicates of calcium, iron, and, to some extent, magnesium (ROH et al. 2000).

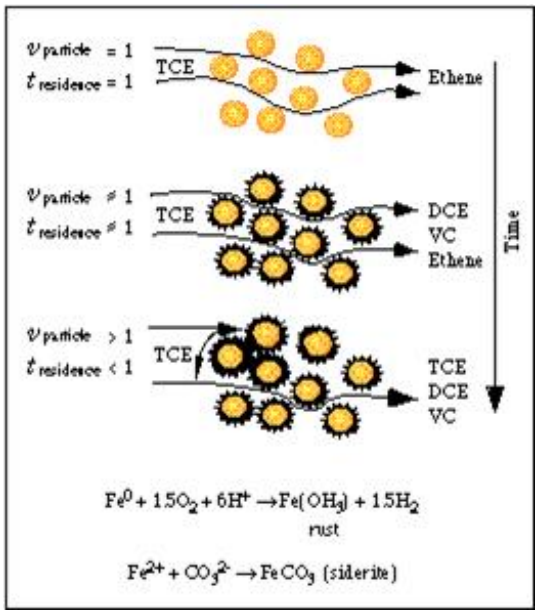

Fig. 2.3: Effects of coating of granular ZVI over time (www.powellassociates.com).

LO et al. (2004) estimated that about 1% of the original porosity in the granular-iron PRB at the Vapokon site in Denmark was being lost every year due to deposition of precipitates. A lithium tracer test carried out appears to indicate that after four years of operation, mineral precipitation and consequent changes in permeability were already causing groundwater to move through preferential pathways through the iron. At the Elizabeth City site, WILKIN & PULS (2003) estimated that the iron medium porosity in the PRB was being lost at the rate of 1 - 4% per years. At this site, the porosity losses appeared to be unevenly distributed through the PRB. Whereas approximately 7% of the original porosity was lost near the upgradient edge of the Elizabeth City PRB after five years of operation, less than 1% of the original porosity was lost near the downgradient edge. At the Denver Federal Center site, the maximum porosity loss in the PRB was estimated at 17% of the original porosity after five years of operation (ITRC 2005). Similar effects were observed by many laboratory and field tests (e.g. VOGAN et al. 1999, YABUSAKI et al. 2001, MORRISON 2003, U.S. EPA 2004).

Evidence of PRBs affecting not only the target contaminants but the entirety of groundwater chemistry comes from groundwater monitoring of the influent and effluent water. Table 2.1 illustrates the changes in common groundwater constituents during flow through the iron medium in a field test PRB installed in Pécs, Hungary. A drastic reduction of dissolved components is the rule. GAVASKAR et al. (2002) observed even up to 99% reduction of individual components and 89% of total dissolved solute (TDS) during groundwater flow through an iron PRB. These constituent losses between influent and effluent indicate that inorganic species are depositing on the iron surfaces. Decreasing sulphate concentrations for example may

indicate precipitation of sulphate-containing green rust ($[Fe_4Fe_2(OH)_{12}][SO_4x3H_2O]$) or iron sulphide caused by the reduction of sulphate to sulphide (U.S. EPA 2004).

Table 2.1: Change in water chemistry through the iron barrier at Pécs, Hungary (CSÓVÁRI et al. 2005).

	Ca^{2+}	Mg^{2+}	SO_4^{2-}	HCO_3^-	TDS	pH	Eh, mV
inflow, mg/l	167	62	397	610	1224	7.15	206
outflow mg/l	30	30	118	248	522	9.10	16
change %	**- 82**	**- 52**	**- 70**	**- 59**	**- 57**	**- -**	**- 92**

Concerning other PRB material such as activated carbon, important factors influencing their life-time are groundwater composition and formation of biomass. For example, natural groundwater constituents and contaminants compete for the adsorption sites. Furthermore, the formation of biomass and gas leads to a clogging effect of the free pore space (NIEDERBACHER & NAHOLD 2005).

As several PRBs are now more than 10 years old and show no significant deterioration of performance, it is reasonable to expect that granular iron PRBs will last 15 years or more in most environments, prior to requiring rejuvenation or replacement (O´HANNESIN & VOGAN 2005). However, the monitoring of PRBs shows that the geochemical constituents of the groundwater appear to affect the reactivity of the iron on long-term exposure to groundwater. The rate of decline in iron reactivity over times is dependent on the native level of certain dissolved solids (e.g. alkalinity, sulfate, calcium, magnesium, and silica) in the groundwater. KORTE (2001) and BENNER et al. (2001) for example identified that sites with high levels of carbonate and sulfate are potentially more susceptible to clogging than groundwater with low TDS.

The rate of decline in iron reactivity over time is also dependent on the number of pore volumes of groundwater flowing through the PRB. Therefore, sites with high groundwater flow rates are likely to encounter higher rates of decline compared to similar sites (with similar levels of TDS) with low groundwater flow rates. Over the long term, the PRB is likely to be passivated before the entire mass of ZVI is used up unless some way of regenerating or replacing the reactive media is developed and implemented (ITRC 2005).

In addition to the destructive nature of the process, PRBs offer a significant cost-advantage when compared to pump-and-treat technologies or those requiring frequent addition of reactants. While capital costs are comparable, the low maintenance costs associated with PRBs make this technology very cost-effective.

Estimating the real costs for a PRB deployment is difficult since a number of factors need to be evaluated, many of which are not well understood or documented. The cost factors that should be evaluated for a PRB installation include the following (ITRC 2005):

- site characterization costs
- design costs
- construction costs
  - purchase and installation or reactive media
  - licensing fees
  - reporting
  - monitoring costs
- O&M (operating and maintenance) costs
  - annual monitoring and reporting costs
  - media replacement rejuvenation
  - institutional controls
- unexpected and miscellaneous costs

Note that the PRB technology has limitations and should not be considered as the only possible remediation technique for a site. For example, a PRB may be used in combination with one or more other remedial approaches, such as monitored natural attenuation (MNA), bioremediation or electrokinetics. Additionally, since most PRBs operate passively, site remediation may take several years or even decades, requiring the use of long-term institutional controls for site management. Therefore, a PRB should be considered within the context of overall long-term site remediation goals.

2.2 Principles of Electrokinetics

The electrokinetic decontamination of polluted sites has become one of the most promising in situ treatment technologies particularly for fine-grained soils where conventional methods like pump-and-treat fail. Its advantages include close control over the direction of water flow and dissolved contaminants, even through heterogeneous soils, retention of contaminants within a confined zone, and low power consumption.

2.2.1 Overview

In 1808, REUSS observed the electrokinetic phenomena when a dc current was applied to a clay-water mixture. Water moved through the capillary towards the cathode under the influence of the induced electric field. When the electric potential was removed, the flow of water immediately stopped. NAPIER (1846) distinguished electroosmosis from electrolysis, and in 1861, QUINCKE found the electric potential

difference through a (charged) membrane resulted from the streaming of a fluid containing charge carrier.

HELMHOLTZ first treated electroosmotic phenomena analytically in 1879. A mathematical basis was provided. SMOLUCHOWSKI (1921) later modified it to apply it to electrophoretic velocity. Out of this treatise of the subject the well-known HELMHOLTZ-SMOLUCHOWSKI (H-S) theory was developed.

In 1939, CASAGRANDE demonstrated that when applying electroosmosis to soils with high water content the resulting increase in the effective stress in the soil will increase its shear strength to such a degree that even steep cuts remained stable. Practice indicated that small reductions in water content by electroosmosis could produce significant increases in soil strength (CASAGRANDE 1952, 1983). Therefore, electrochemical treatment of cohesive soils has been investigated and used in many geotechnical field projects, such as slope stabilisation or improvement of excavation stability, electrochemical induration/hardening, fine-grained soils stabilization, consolidation and densification (PAMUKCU 1997). In the late 1960s and early 1970s, direct current was applied successfully to recover residual oil from deep-seated geological formations (Enhanced Oil Recovery) (WAXMAN & SMITS 1967).

In the field of geo-environmental engineering, most of the work on electrokinetics was undertaken at the end of the 1980s and in the 1990s (e.g., LAGEMAN et al. 1989, ACAR et al. 1992, BRUELL et al. 1992, PROBSTEIN & HICKS 1993, PROBSTEIN 1994, ACAR & ALSHAWABKEH 1996, ALSHAHWABKEH & ACAR 1996, HAUS & ZORN 1998, HAUS et al. 1999, HAUS & CZURDA 1999).

By the term „electrokinetic“ all electrically induced mass transport processes are embraced (GERTHSEN 1989). For electrokinetic soil remediation, at least one pair of electrodes is placed in the ground and a direct current is applied. The generated electric field varies with electrode configuration and geological condition and induces the movement of contaminants and water towards the electrode reservoirs (Fig. 2.4). When an electric field is applied to a wet soil mass, different electrokinetic phenomena occur simultaneously. These electrokinetic phenomena include the flow of fluids and the movement of charged particles and ions towards the electrodes. The fundamental transport mechanisms caused by an electric field are (Fig. 2.5):

- **Electroosmosis**
  movement of liquid relative to a charged stationary surface
- **Electromigration**
  transport of charged ions or ion-complexes in solution
- **Electrophoresis**
  movement of charged particles/colloids relative to a stationary fluid

In general, the two major physical mechanisms of the electric-field-driven transport of contaminants in soils are electromigration and electroosmosis (PROBSTEIN & HICKS 1993). Both electromigration and electroosmosis will occur in fine-grained soils, whereas in coarse-grained soils electromigration accompanied by electrophoresis is the principal transport process.

In other words: Electromigration is dominant when dealing with soluble charged species such as heavy metal cations (e.g., Pb^{2+}, Cd^{2+}, Cu^{2+}, Zn^{2+}) and when the soil zeta potential is absent or small (JACOBS et al. 1994, HICKS & TONDORF 1994). In contrast, electroosmosis is the major mechanism of removal of uncharged and/or weakly dissociated contaminants (phenols, for instance) when the soil has a finite zeta potential (ACAR et al. 1992, SHAPIRO & PROBSTEIN 1993). The velocity of electromigration of ions is forty fold higher than electroosmotic flow rates and is not directly affected by variations in the zeta potential of the soil (ACAR & ALSHAWABKEH 1993).

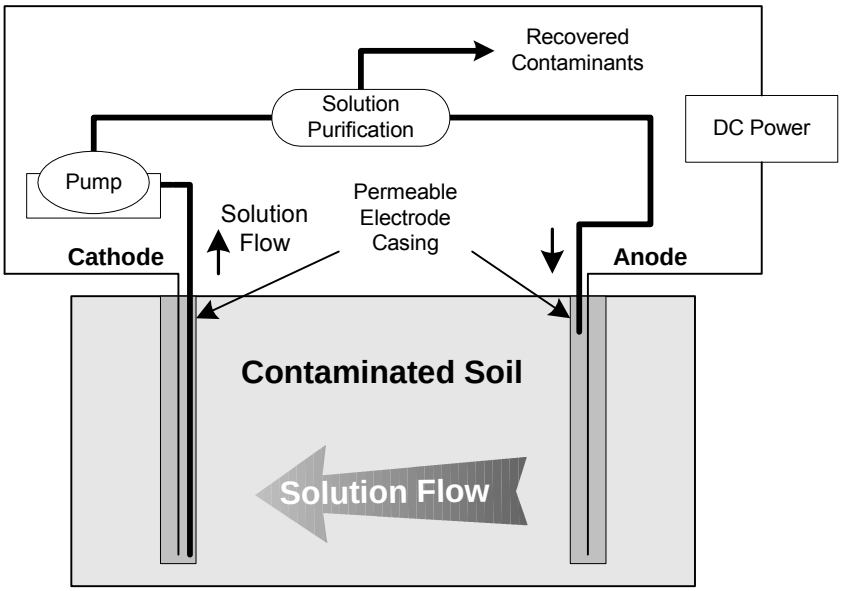

Fig. 2.4: Schematic representation of electrokinetic soil remediation (HAUS & ZORN 1998).

Most experimental data obtained to date indicate that ionic migration is the dominant mechanism (e.g., ACAR et al. 1997). However, results obtained by HSU (1997) on the removal of lead and cadmium from kaolinite indicate that electroosmotic advection can be a more effective transport mechanism than ionic migration under certain circumstances.

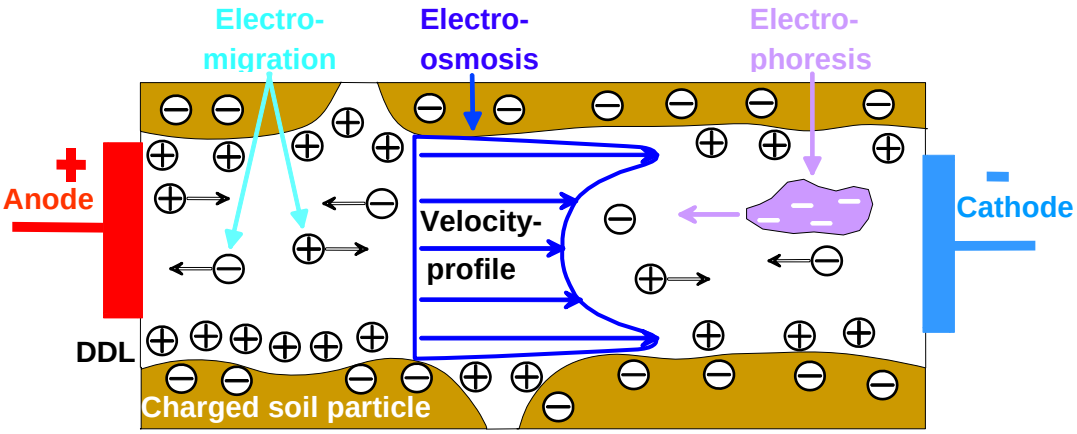

Fig. 2.5: Electrokinetic transport processes induced by an applied electric field.

In addition to mass transport processes, chemical reactions take place at the electrodes. Compounds subject to oxidation or reduction reactions are constituents of the soil matrix and/or pore water, the pore water itself, and the electrode materials. The principal electrode reaction observed is the electrolysis of water. At the cathode, water is reduced leading to the production of hydrogen gas and hydroxide ions. At the anode, water is oxidized and oxygen gas and hydrogen ions are generated.

A number of other physicochemical processes may accompany transport of the contaminants in soils. Examples are:

- diffusion of the dissolved species,
- adsorption/desorption of the species in the soil,
- chemical reactions occurring in the bulk of the pore solution (e.g., mutual neutralization of H^+ produced at the anode and OH^- produced at the cathode),
- buffering of the induced pH change by the soil-fluid-contaminant system,
- changes in species and/or charge of the species and hence transport behaviour due to changes in Eh/pH-conditions.
- precipitation of the dissolved components (when their local concentrations exceed the solubility limits and/or Eh/pH-conditions change),
- and/or dissolution of the precipitates.

The situation is particularly complex in fine-grained soils because of their large specific surface areas which provide numerous active sites for soil-contaminant interactions. Moreover, these dynamic interactions are dependent on Eh, pH, soil mineralogy, water content, temperature, presence of competing ions and concentration of the contaminants in the pore fluid.

The state of the art of electrokinetic remediation was surveyed and is described in the following to provide background information on this matter. Various authors (e.g., ACAR et al. 1993, 1995) described the main aspects of electrokinetics and its status. PAGE & PAGE (2002) and VIRKUTYTE et al. (2002) present the latest detailed reviews.

Much of the practical work on electroremediation has been undertaken in the laboratory on spiked synthetic soils (PAGE & PAGE 2002). YEUNG et al. (1997a) have presented a review of the apparatuses used. The most commonly used artificial soil is kaolinite, but experiments have been performed using other clay minerals, peat, artificial clay mixtures, and natural soils (RÖHRS et al. 2001, ZORN 2005, STEGER 2005).

A constant voltage dc power supply, generating potential gradients in the range of 20 to 200 Vm^{-1}, is often used so that a small variable current passes through the soil (PROBSTEIN & HICKS 1993). Alternatively, the current density may be maintained at a constant value, commonly in the range of 0.025 to 5 Am^{-2} (ACAR et al. 1991, HAMED et al. 1991). Experiments are run for times varying from a few hours to several months, with low currents being necessary to avoid adverse heating effects.

Electroremediation can be used for a wide range of contaminant species, e.g. charged and uncharged, organic and inorganic, radionuclides, etc. (U.S. EPA 1995, 1997, 1998). Contaminants affected by electrokinetic processes include (VIRKUTYTE et al. 2002):

- Heavy metals
- Radioactive species (Cs_{137}, Sr_{90}, Co_{60}, uranium)
- Toxic anions (nitrates and sulphates)
- Dense, non-aqueous-phase liquids (DNAPLs)
- Cyanides
- Petroleum hydrocarbons (diesel fuel, gasoline, etc.)
- Mixed organic/ionic contaminants
- Halogenated and non-halogenated pollutants

To remove heavy metals electroremediation was first applied in the 1980s (e.g., SEGALL et al. 1980). Since then the remediation of a large number of heavy metals has been proved successfully by laboratory tests (e.g., PAMUKCU & WITTLE 1992, ACAR et al. 1994, YEUNG et al. 1996, WENG & HUANG 2004). An overview is given by PAGE & PAGE (2002). The first breakthrough in the application of electroremediation at field scale was achieved in 1987 (LAGEMAN et al. 1989, LAGEMAN 1993), followed by various other field tests (e.g., HAUS 2002).

It has been proved by experiments that when heavy metals enter into basic conditions, they adsorb to soil particles or precipitate as hydroxides, oxyhydroxides, etc. In acidic conditions, those ions desorb, solubilise and migrate. To overcome adsorption/precipitation of heavy metals due to alkaline pH conditions in the vicinity of the cathode and/or to increase mobility/solubility of metals in soil, respectively, the electroremediation process often is enhanced by acidic purging solutions and/or

complexing or chelating agents (REED et al. 1995, YEUNG et al. 1996, LI & LI 2000, REDDY & CHINTHAMREDDY 2004, 2003, REDDY et al. 2004, YEUNG & HSU 2005).

In addition, organic compounds have been subject of successful electrokinetic investigations (ACAR et al. 1992, BRUELL et al. 1992, STEGER 2005, ZORN 2005). The possibility of enhancing electroosmotic mobilisation of non-polar and weak polar organic contaminants by tenside solutions and solvents is mentioned amongst others by ACAR et al. (1995) and SAICHEK & REDDY (2005).

During electroremediation, the temperature of the subsurface may increase distinctly. This heating originates from the fact that electric energy partly is transferred into so-called Joule-Heating. This heating effect has been observed during several electrokinetic field applications (e.g., HO et al. 1999a,b, LAGEMAN & POOL 2001, GODSCHALK & LAGEMAN 2005, STEGER 2005). Note that, depending on the level of the applied electric power and the type of contaminant, heating effects or kinematic processes (electromigration and electroosmosis) will dominate (PAMUKZU 2005).

Several studies, such as those by GRAY & MITCHELL (1967), EYKHOLT (1992), ACAR & ALSHAWABKEH (1993), EYKHOLT & DANIEL (1994), and ACAR et al. (1995) have described different factors and processes that affect electrokinetic remediation. Parameters influencing the electrokinetically induced mass transport are, for instance, saturation, porosity, type of contaminant, initial contaminant concentration, redox and pH conditions, electric potential, zeta-potential, soil nature, and soil mineralogy.

In recent years, progress has been made in modelling electroremediation processes. A one-dimensional coupled flow theory, taking into account all likely transport processes, was developed (YEUNG 1990, MITCHELL & YEUNG 1991, YEUNG & MITCHELL 1993) but did not include chemical reactions. The model has since been adapted to include pH changes and adsorption reactions (YEUNG & DATLA 1995). SHAPIRO & PROBSTEIN (1993) included in their model various chemical equilibria considering the effect of pH and adsorption reactions. Numerical solutions showed reasonable agreement with experimental results obtained. Non-uniform contributions to electroosmosis of, e.g., field strength, zeta potential, and/or pH, have been incorporated into various formulations (SHAPIRO & PROBSTEIN 1993, EYKHOLT & DANIEL 1994, MENON et al. 1996).

Variations in ion transport and electroosmotic flow were modelled by DZENITIS (1996, 1997a). Furthermore, DZENITIS (1997b) demonstrated steady state conditions within the electric field, which refers to the correlation between changes in pH and ion concentration (s. Section 4.1). Models have been developed for situations where relatively uniform conditions have been maintained by buffering (BAURAUD et al. 1997, 1998).

A two-dimensional model, taking into account the geometry of the electrode array, has been devised to describe the transport of phenol; acid/base reactions of the phenol and the soil were also included (JACOBS & PROBSTEIN 1996). On basis of this

complex numerical model ZORN (2005) advanced a model regarding the mechanisms of electrokinetic mass transport as well as the development of the electric field in dependence of electrode array and conductivity aspects. ALSHAWABKEH & ACAR (1996) developed a numerical model concerning complex chemical reactions but no variation in electroosmotic flow.

The literature survey shows that electrokinetic studies mainly were carried out using fine-grained soils dominated by electroosmosis. In contrast, experiments on sand rarely have been undertaken (e.g., LI et al. 1997, HANSEN et al. 1997, KIM & LEE 1999). Thus, for coarse-grained soils only little information on electrokinetic phenomena is available.

LINDGREN et al. (1991, 1994) demonstrated the electromigration of anionic food dye ions and chromate in unsaturated sands. They determined the effect of soil heterogeneities on the electrokinetic processes. Electromigration was accelerated in fine sand and slowed down in medium sand of layered experiments when compared to the corresponding individual experiments. This discrepancy was explained by estimating the current density in each layer, which was proportionally higher in the fine layer and lower in the medium layer. Furthermore, they investigated electromigration rates at various moisture contents. At lower moisture contents the electromigration rate decreased due to rapid increase in pore tortuosity. The drop of the migration rate at higher moisture content is explained by the expected decrease in the pore water current density. Thus, the optimum moisture content for electromigration is less than saturation due to competing effects of tortuosity and pore water current density.

LI et al. (1997) investigated the removal of Pb(II), Cd(II) and Cr(III) from sand. They demonstrated that heavy metals could be removed by using electromigration alone. Precipitation of heavy metals within the soil was hindered by inserting a conductive solution between the cathode and the soil being treated. Thus, the porosity and the tortuosity of the soil did not significantly change and a decrease in the apparent hydraulic conductivity, as caused by precipitation of metals in soil, had been avoided.

For the future, the combination of electrokinetics and other conventional remediation technologies seems to be very promising. HO et al. (1999), MAINI et al. (2000) and ELEKTOROWICZ & JU (2001) successfully applied a combination with bioremediation. In situ biodegradation of organics in clayey soils has been enhanced by electrokinetic supply of nutrients (SEGALL & BRUELL 1992, ELECTOROWICZ & BOEVA 1996, ACAR et al. 1997, BUDHU et al. 1997, THEVANAYAGAM & RISHINDRAN 1998). Organic contaminated soils have been treated by moving the contaminates into treatment zones containing bacteria (HO et al. 1995, DAVIS-HOOVER et al. 1999, JACKMAN et al. 1999, 2001). DEFLAUN & CONDEE (1997) have demonstrated that bacteria can be moved through aquifer material, towards a polluted area, by electrokinetic transport.

Very few studies where electrokinetics is coupled with treatment zones were carried out. All of them used fine-grained soils with electroosmosis being the main transport mechanism. The results of the Lasagna™ technique of HO et al. (1995, 1997, 1999a,b) are presented in Section 2.2.4.

CHEW & ZHANG (1997) demonstrated the feasibility of using electrokinetics coupled with a zero-valent iron (Fe^0) treatment wall to abiotically remediate nitrate-contaminated soils. They present the preliminary results of nitrate transformation using electrokinetics/iron wall processes, including the effects of different voltages, current, and iron well on transformation of NO^{3-}-N in saturated artificial clay/sand mixture. Furthermore, they determined operational conditions and parameters under which the process can achieve their optimal operational effect. The iron powder wall placed between the electrodes was near the anode to intercept nitrate ions migrating to the anode during the electrokinetic process.

The addition of a Fe^0-promoted treatment zone enables the in situ treatment of contaminants which otherwise need to be collected at the electrode and then treated by conventional means. Two localized pH conditions exist in the system, a low-pH region near the anode and a high-pH region near the cathode. Placing an iron zone near the anode increases the pH in that area over time, which is consistent with the phenomenon of pH increase in Fe^0-water systems. Movement of the acid front did not flush across the cathode. It is estimated that for a 75% NO^{3-}-N removal approximately 13.5 kWh/m^3 would be required (CHEW & ZHANG 1997).

Combining PRBs and electric fences for groundwater remediation is described further in Section 2.2.4.

2.2.2 Characteristic Electrical Variables

When an electric field is applied to a wet soil mass, an electric current is induced. In contrast to metals, the electric current in fluids does not result from moving electrons but from the motion of charged particles or ions, respectively. Ohm´s Law $U = R \cdot I$ applies for electrolytes (U = voltage [V], R = electric resistance [Ω], I = current [A]). The electric resistance R of an electrolyte measured between two electrode areas A [m^2] with a distance l [m] is described by:

$$R = \rho \cdot \frac{l}{A} \qquad [\Omega] \qquad \text{(Eq. 1)}$$

where ρ is the specific resistance [Ωm]. The reciprocal of the specific resistance is the electric conductivity σ:

$$\sigma = \frac{1}{\rho} = \frac{I \cdot l}{U \cdot A} \quad [\Omega^{-1}m^{-1} \text{or } Sm^{-1}] \qquad \text{(Eq. 2)}$$

Electrolytes are ion-conductive media, with their electric conductivity being a result of the dissociation of ions.

The electric conductivity depends on:

- amount of ions (concentration),
- specific mobility of the ions,
- temperature
- viscosity of the fluid, and
- dielectric constant/permittivity ε.

The electric conductivity of soils is composed of the electric conductivity of both the electrolyte and the soil.

The current density *j* is equal to the quotient of current and cross sectional area of the electric conductor and is proportional to the electric conductivity and the applied electric field:

$$j = \frac{I}{A} = \sigma \cdot E \qquad [Am^{-2}] \qquad \text{(Eq. 3)}$$

The electric field is displayed by equipotential lines or streamlines of the field, respectively. The type of charge carrier, e.g. plane of punctiform source, as well as the structure of the subsoil affects their distribution (parallel or dipole).

2.2.3 Interacting Mechanisms during Electrokinetics

Electrokinetic soil treatment relies on several interacting mechanisms, including various mass transport mechanisms and electrode reactions. The total movement of the matter of the contaminant solution in the dc electric field can be expressed as the sum of four components (CHILINGAR et al. 1997):

- **diffusion**: the movement of components dissolved in the flowing solution due to a concentration gradient;
- **hydraulic advection**: the hydrodynamic flow of liquids driven by the hydraulic pressure gradient;
- **electroosmosis**: the electrokinetic flow of fluids due to interaction of the diffuse double layer with the dc field;
- **electromigration**: the migration of ions inside moving fluids due to the attraction of charged particles to the electrodes; and
- **electrophoresis**: movement of charged particles/colloids relative to a stationary fluid.

It is very difficult to distinguish very clearly between the relative contributions of the different transport mechanisms. This thesis presents the results of combined hydraulic and electrokinetic gradients in sandy soil. Since the model sand used in this study is free of clay minerals, electroosmosis is negligible whereas the dominant transport mechanism for ionic species will be electromigration and hydraulic advection.

Beside these mass transport mechanisms, further soil physical and chemical processes induced by an applied electric field, e.g. electrode reactions, are presented in this chapter.

2.2.3.1 Diffussion

Diffusion is the process by which both ionic and molecular species dissolved in water move from areas of higher concentration to areas of lower concentration. Adolf Fick derived Fick's laws of diffusion in the year 1855. Fick's First Law describes the flux of a solute under steady-state conditions, i.e., when the concentration within the diffusion volume does not change with respect to time:

$$j_i^d = -D_i \cdot \frac{dc}{dx} \qquad [\text{mol m}^{-2}\,\text{s}^{-1}] \qquad \text{(Eq. 4)}$$

where

j_i^d is the diffusion flux in dimensions of [mol m^{-2} s^{-1}]

D_i is the diffusion coefficient in dimensions of [m^2 s^{-1}]

$\frac{dc}{dx}$ is the concentration gradient in dimensions of [mol dm^{-3}].

The negative sign indicates that the movement is from greater to lesser concentrations. Values for D_i are well known for electrolytes in water. For the major cations and anions in water, D_i ranges from $1 \cdot 10^{-9}$ to $2 \cdot 10^{-9}$ m^2/s. For systems where the concentrations may be changing with time, Fick´s second law may be applied:

$$\frac{\partial c}{\partial t} = D_i^* \cdot \frac{\partial^2 c}{\partial x^2} \qquad [\text{mol s}^{-1}] \qquad \text{(Eq. 5)}$$

where $\frac{\partial c}{\partial t}$ is the change in concentration with time.

Both Fick´s first and second law are expressed above for the one-dimensional case. For three-dimensional analysis, more general forms would be needed.

In porous media, diffusion cannot proceed as fast as it can in water because the ions must follow longer pathways as they travel around minerals grains. To consider this, an effective diffusion coefficient D_i^* must be used. The value of D_i^* can be determined from the relationship

$$D_i^* = wD \qquad [\text{m}^2\,\text{s}^{-1}] \qquad \text{(Eq. 6)}$$

where w is an empirical coefficient that is determined by laboratory experiments (FETTER 1994). For species that are not adsorbed onto the mineral surface it has been determined that w ranges from 0.5 to 0.01 (FREEZE & CHERRY 1979). Diffusion coefficient values can be taken from, e.g., VANCÝSEK (1993).

The process of diffusion is complicated by the fact that ions must maintain electrical neutrality as they diffuse. If we have a solution of NaCl, the Na^+ cannot diffuse faster than the Cl^-, unless there is some other negative ion in the region into which the Na^+ is diffusing.

In rock and soil with very low permeability, the water may be moving very slowly. Under these conditions, diffusion might cause a solute to travel faster than the groundwater is flowing. Under such conditions, diffusion is more important than advection (WAGNER 1992).

Comparing effective diffusion coefficient and electrical mobility of different species lead to the conclusion that diffusion is a minor contributing component to the total flux if an electrical gradient is applied (ACAR & ALSHAHWABKEH 1993). Under such conditions, corresponding to many real situations, the ionic velocity in the pore solution is particularly related to the ionic properties in the electric field as well as to spatial soil characteristics (ionic mobility, porosity, tortuosity).

2.2.3.2 Hydraulic Advection

Hydraulic advection is the process by which moving groundwater carries with it dissolved solutes. Changes in hydraulic head (*h*) are the driving force which causes water to move from one place to another. The head gradient is the change in hydraulic head per length of flow path, and appears in Darcy's law as being proportional to the discharge.

Darcy's Law describes the flow of a fluid through a porous medium (typically water through an aquifer). The law was formulated by HENRY DARCY based on the results of 1855 and 1856 experiments on the flow of water through beds of sand. It, along with the conservation of mass, comprises the groundwater flow equation, which is one the basic building relationships of hydrogeology.

Darcy´s Law is analogous to Fourier's Law in the field of heat conduction, Ohm's Law in the field of electrical networks, or Fick's Law in diffusion theory (Section 2.2.3.1). This simple relationship relates the instantaneous discharge rate through a porous medium to the local hydraulic gradient (change in hydraulic head over a distance) and the hydraulic conductivity (k_f) at that point:

$$Q = -k_f A \cdot \frac{dh}{dl} \qquad [m^3 s^{-1}] \qquad \text{(Eq. 7)}$$

It shows that the total discharge, *Q* (units of volume per time) is proportional to the hydraulic conductivity, k_f, the cross-sectional area to flow, A, and the hydraulic gradient (the hydraulic head drop between two points, divided by the distance between them). The negative sign is needed because water flows from high head to low head.

Since the fluid potential, Φ, is equal to $g \cdot h$ (g = acceleration of gravity, 9,81 ms^{-2}), DARCY´s law can also be expressed in terms of potential as

$$Q = -\frac{k_f A}{g} \cdot \frac{d\Phi}{dl} \qquad [m^3 s^{-1}] \qquad \text{(Eq. 8)}$$

As expressed here, DARCY´s law is in a one-dimensional form, as if water flows through a pipe in only one direction. Dividing both sides of Equation 8 by the area and using more general notation leads to

$$v_f = \frac{Q}{A} = -k_f \nabla h \qquad [m\,s^{-1}] \qquad \text{(Eq. 9)}$$

where v_f is the specific discharge per unit area (with units of length per time) and ∇h indicates the mathematical gradient of the hydraulic head. This value of specific discharge is often referred to as the Darcy flux. It is an apparent velocity, representing the velocity at which water would move through an aquifer if the aquifer were an open conduit.

The cross-sectional area of flow for a porous medium is actually much smaller than the dimensions of the aquifer since the water can move only through the open pore spaces. Moreover, part of the pore space is occupied by stagnant water which clings to the rock material. The effective porosity is that portion of the pore space through which saturated flow occurs.

To find the velocity at which water is actually moving, the specific discharge is divided by the effective porosity to account for the actual open space available for the flow. The result is the seepage velocity, or average linear velocity, a velocity representing the average rate at which the water moves between two points:

$$v_a = \frac{Q}{n_e A} = -\frac{k_f dh}{n_e dl} = \frac{v_f}{n_e} \qquad [m\,s^{-1}] \qquad \text{(Eq. 10)}$$

where v_a is the average linear velocity [ms^{-1}] and n_e is the effective porosity [-] (FETTER 1994). Concerning to HÖLTING (1992) typical effective porosity values for clastic sediments are:

Clay	< 5%	Gravel sand	16-28%
Fine sand	10-20%	Pea gravel	15-25%
Middle sand	12-25%	Gravel	14-24%
Coarse sand	15-30%		

Note that the average linear velocity is an average because the water molecules follow various tortuous paths through the porous medium. The value obtained above is the average linear velocity, representing the average path of water through the medium. Non-reactive solutes that are transported by advection are travelling at the same rate as the average linear velocity of the ground water.

2.2.3.3 Electroosmosis

Electroosmosis is based on the theory of diffuse double layers (DDL) around charged soil particles. Diverse models were developed to describe this theory, the so-called Stern-Gouy-Chapman model (STERN 1924) being one of the most popular for explaining electrokinetic processes.

Fine grained sediments are often dominated by clay minerals. Usually their surfaces are negatively charged as a result of isomorphous ion substitution within the crystal lattice (BRINDLEY & BROWN 1980, MERMUT 1994). An excess negative surface charge exists in all kinds of soil, for example, many clays are anionic, colloidal poly-electrolytes. The surface charge density increases in the following order: sand < silt < kaolinite < Illite < montmorillonite.

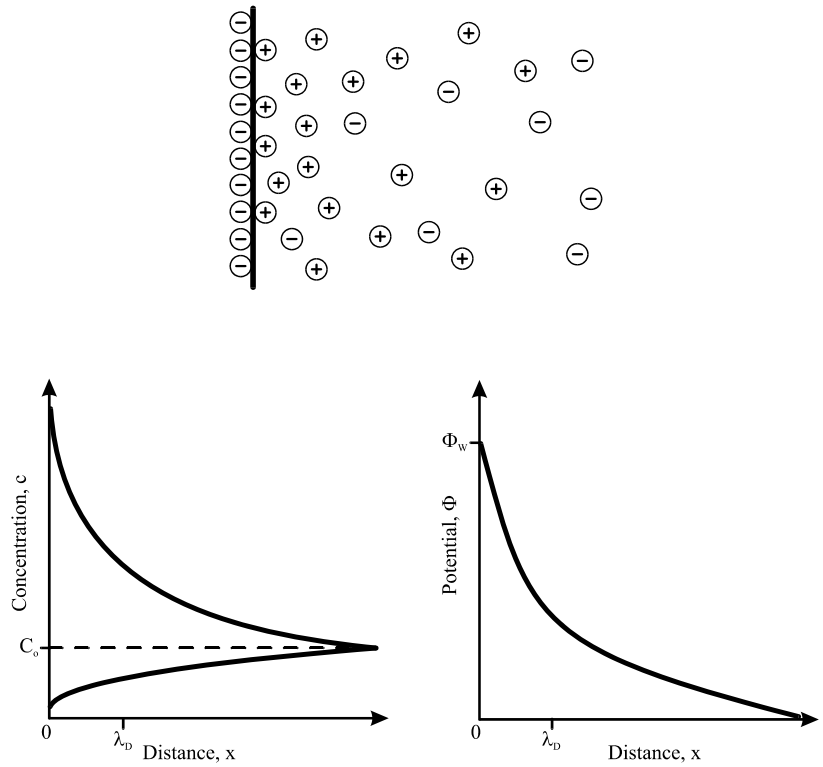

Fig. 2.6: Schematic draw of the distribution of ions and potential relative to a charged surface (after PROBSTEIN 1994).

The negatively charged surface influences the nearby distribution of ions in solution, attracting ions of opposite charge (counterions) towards the surface and repelling ions of equal charge (co-ions) away from the surface (Fig. 2.6). At the same time, the counterions tend to diffuse away from soil particle surface to equilibrate the ion concentration in solution. The simultaneity of both processes results in a random thermal motion of the ions which form an "ion cloud" around the charged soil particles, the so-called diffuse double layer (DDL). The diffuse double layer is defined

as the region in the vicinity of a charged surface with an excess of counterions over co-ions (PROBSTEIN 1994). With increasing distance from a negatively charged surface counterion concentration increases whereas co-ion concentration decreases until the concentration of the balance solution c_0 (mol/m^3) is achieved (Fig. 2.6).

The thickness of the diffuse double layer is defined as the position where the potential energy of the surface is approximately equal to the thermal energy of the counterions. The electric double layer has a typical thickness between 1 and 10 nm (PROBSTEIN & HICKS 1993).

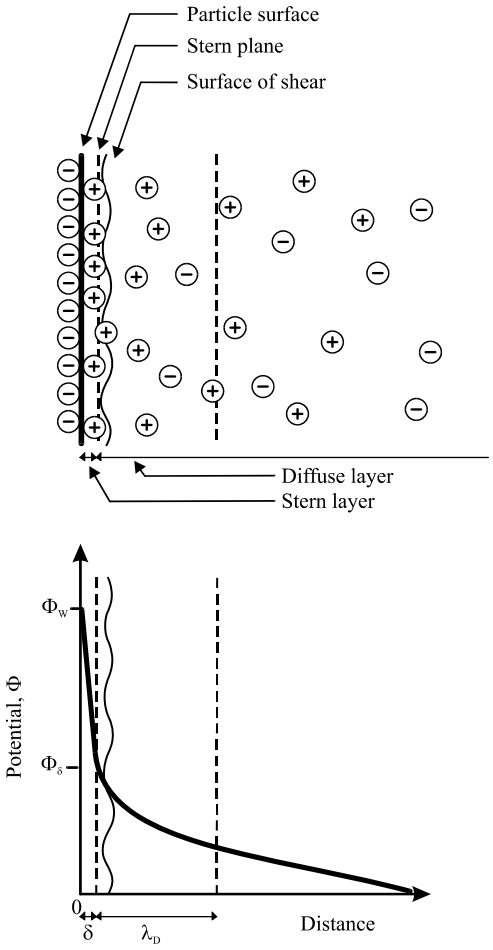

Fig. 2.7: Structure of the electrical double layer and potential distribution within the electrolyte (after PROBSTEIN 1994).

Since the ions are of finite size and the centre of an ion can only approach the charged surface to within its hydrated radius without becoming specifically adsorbed, the inner boundary of the diffuse part of the double layer is limited. This inner part next to the surface is called STERN layer, and the plane separating the STERN layer and the diffuse part of the double layer is called STERN plane (Fig. 2.7). The position of the latter is approximately defined by the hydrated radius of the ions.

By applying an electric field tangentially along the charged surface this electric field will exert a force on the charge of the diffuse layer. A movement of ions will only take place if the force of the applied electric field is exceeding the electrostatic force of attraction of the surface. These results in a slip or shear plane parallel to the surface, which is characterized as the plane at which the mobile portion of the diffuse layer can “slip” or flow past the charged surface. The potential at this plane is equal to the electrokinetic potential or zeta (ζ) potential, which is similar to the potential at the STERN plane.

The mobile shell of ions within the diffuse double layer is assumed to drag water through the capillary towards the electrodes by viscous interaction. Since the double layer is containing more cations than anions there is a net water flow towards the cathode. This process is called electroosmosis. Electroosmosis is a coupled flow as a flow of one type (hydraulic) is generated by a driving force of another type (electric) (MITCHELL 1993).

The electroosmotic velocity U of a water flow parallel to a charged surface (x-axis) is described by the HELMHOLTZ-SMOLUCHOWSKI equation, which is valid for the assumption that the thickness of the diffuse layer λ_D is very small compared to the radius of the capillary a ($\lambda^* = \lambda_D/a << 1$):

$$U = \frac{\varepsilon \cdot \zeta \cdot E_x}{\mu} \qquad [ms^{-1}] \qquad \text{(Eq. 11)}$$

ε	=	permittivity	[Fm^{-1}]
ζ	=	zeta potential	[V]
E_x	=	electric field (// x-axis) parallel to the flow direction	[Vm^{-1}]
μ	=	viscosity	[Pa s]

Thus, the electroosmotic velocity is proportional to the zeta potential, which is directly related to the specific surface of the solid, and the electric field strength. The value of the zeta potential depends on the soil properties as well as the ionic strength and pH of the saturating liquid. A typical zeta potential is about -10 to -100 mV, and in a 100 V/m electric field, water will flow towards the cathode at a velocity of around 10 cm/day (HICKS & TONDORF 1994).

Outside of the diffuse double layer, the velocity U is constant and is decreasing discontinuously from U to 0 within the double layer. Therefore U is equal to the electroosmotic velocity at the border of the diffuse double layer.

The electroosmotic flow rate Q_e is described by an equation analogous to Darcy's law:

$$Q_e = k_e \cdot i_e \cdot A \qquad [m^3s^{-1}] \qquad \text{(Eq. 12)}$$

k_e	=	coefficient of electroosmotic conductivity	$[m^2V^{-1}s^{-1}]$
i_e	=	electric field strength (= $\nabla(-\phi)$) or negative potential gradient	$[Vm^{-1}]$
ϕ	=	electric potential applied	[V]
A	=	total cross-sectional area perpendicular to the direction of fluid flow	$[m^2]$

Values of the coefficient of electroosmotic conductivity k_e of different soils lie in the narrow range of $1 \cdot 10^{-9}$ to $1 \cdot 10^{-8}$ m^3s^{-1} (ACAR & ALSHAWABKEH 1993, MITCHELL 1993, YEUNG 1994). MITCHELL (1993) reported that values of k_e range from $1.5 \cdot 10^{-9}$ $m^2V^{-1}s^{-1}$ for a clayey silt to $1.2 \cdot 10^{-8}$ $m^2V^{-1}s^{-1}$ for a sodium-bentonite slurry. For most clays k_e is around $5 \cdot 10^{-9}$ $m^2V^{-1}s^{-1}$.

The magnitude of the electroosmotic flow is a function of the applied electrical gradient, just as the rate of hydraulic flow is a function of the hydraulic gradient. However, unlike hydraulic flow, electroosmotic flow is relatively independent of pore size and porosity so that problems associated with preferential paths are reduced (PROBSTEIN & HICKS 1993). Hence, electroosmotic flow can sweep more uniformly across the media than flow induced by hydraulic gradients and permits a high degree of control of the flow direction.

Another fundamental difference between hydraulically and electroosmotically induced flows are the changes brought about by chemical reactions in the electroosmotic process. Electroosmotic conductivity is time-dependent and greatly influenced by moisture-content changes, chemical reactions, and reaction kinetics that occur at electrodes (SEGALL & BRUELL 1992).

The efficiency of electroosmosis depends on various factors. The most important parameters are dielectric constant, temperature, viscosity, electrolyte concentration, electric gradient and the zeta potential. There is also a strong dependency on the mineralogy of the soil (MITCHELL 1993). The zeta potential of the soil also varies during the process and can affect the rate and direction of electroosmotic flow (SHAPIRO & PROBSTEIN 1993, EYKHOLT & DANIEL 1994, WEST & STEWART 1995).

2.2.3.4 Electromigration

By applying an electric field across a wet soil mass, a force is exerted on the charged particles (ions and ion complexes) within the pore fluid. This force leads to a mass transfer of the charged particles, which is called electromigration. Anions (negatively

charged ions) are moved toward the anode (positive electrode) and cations (positively charged ions) are moved toward the cathode (negative electrode). Thus, metal ions, ammonium ions, and positively charged organic compounds move toward the cathode. Anions such as chloride, cyanide, fluoride, nitrate, and negatively charged organic compounds move toward the anode.

Movement of ionic species in the aqueous pore solution depends principally on electromigration together with other effects of electrolysis, including diffusion, adsorption, complexation, and precipitation reactions (PROBSTEIN 1994). The force the applied field exerts on particles within a diluted solution is proportional to the gradient of the electrostatic potential $\nabla\phi$. The electric field E is equal to the negative gradient of the electrostatic potential:

$$E = -\nabla\phi \qquad [\mathrm{Vm^{-1}}] \qquad \text{(Eq. 13)}$$

The force that affects the particle can be calculated by multiplying the charge z_i with the sign of the charge and the electric field. The force per mol is therefore $-z_i \cdot F \cdot \nabla\phi$, with the FARADAY Constant $F = 9.65 \cdot 10^4$ $\mathrm{Cmol^{-1}}$. Taking into account the mobility $u_i = -D_i/RT$ $[\mathrm{m^2/(V \cdot s)}]$, with D_i = diffusion coefficient $[\mathrm{m^2/s}]$, R = retardation factor, T = temperature and the tortuosity τ the electromigration velocity v_{ei} can be calculated:

$$v_{ei} = -u_i \cdot z_i \cdot F \cdot \tau \cdot \nabla\phi \qquad [\mathrm{ms^{-1}}] \qquad \text{(Eq. 14)}$$

The mobility is defined as the average velocity of a charged particle when a force of 1 $\mathrm{Nmol^{-1}}$ is applied and its unit therefore is $\mathrm{molN^{-1}ms^{-1}}$ or $\mathrm{molskg^{-1}}$. Therefore, the electromigration velocity is proportional to the product of the local electric field strength, the charge and the mobility of the particle (PROBSTEIN & HICKS 1993, PROBSTEIN 1994).

The molar flux j_i^m of electromigration in turn is proportional to the electromigration velocity multiplied with the concentration of the particle c_i.

$$j_i^{\,m} = (v_{ei})c_i \qquad [\mathrm{molm^{-2}s^{-1}}] \qquad \text{(Eq. 15)}$$

The ionic mobility of ions in free dilute solution, i.e., the velocities of the ions under the influence of a unit electric field, is in the range of $3 \cdot 10^{-8}$ to $1 \cdot 10^{-7}$ $\mathrm{m^2/Vs}$ (DEAN 1992). However, the effective ionic mobility of ions in soils is considerably lower than the lower bound of this range of values as the flow paths in soils are much longer and more tortuous than those in aqueous solutions. Practical ranges of effective ionic mobility of ions in fine-grained soils are given by MITCHELL (1993).

Transport of charged ions by electromigration is generally more rapid than by electroosmosis. In cases where the ionic strength is high due to the presence of inorganic contaminants, the zeta potential is small and transport occurs mainly by electromigration (HICKS & TONDORF 1994). The average mobility of ions is around ten times greater than that of the electroosmotic mobility. Therefore, the energy

necessary to move all ions over an average distance of 1 m through 1 m^2 soil section is ten times less than with electroosmosis (LAGEMAN et al. 1989).

Applying a field strength in the range of 25 to 100 V/m electroosmotic velocities of several centimetres per day can be reached. Electromigration velocities on the other hand are 5 to 40 times higher (ACAR et al. 1993) and thus can reach up to several ten centimetres a day.

The ionic mobility is related to electrical conductivity of the solution and is therefore affected by concentration, ionic charge, and temperature. The major influences on electromigration during electroremediation are (VAN CAUWENBERGHE 1997):

- field strength (as for electroosmosis),
- contaminant concentration,
- total ionic concentration,
- charge of ionic species,
- soil pore water current density,
- ionic mobility, and
- grain size.

The process efficiency is not as dependent on the fluid permeability of soil as it is on the pore water electrical conductivity and path length through the soil, both of which are a function of the soil moisture content (PAGE & PAGE 2002). Typically, electromigration is more efficient than electroosmosis as the applied force directly affects the molecules and not the free pore solution. This is the rule especially for charged contaminant species. Electromigration as dominant transport mechanism was proved successfully for many heavy metal contaminated fine-grained soils (e.g. HAMED et al. 1991, PAMUKCU & WITTLE 1992, LAGEMAN 1993, HICKS & TONDORF 1994, HAUS et al. 1999a,b, ZORN et al. 2001e, ZHOU et al. 2003, ZORN et al. 2003b). As electromigration does not depend on the pore size, it is equally applicable to coarse and fine-grained soils (PAGE & PAGE 2002).

2.2.3.5 Electrophoresis

Electrophoresis is defined as the migration of charged colloids in solid-liquid mixtures under electric potential gradient. Here the movement of colloidal particles is meant, not small ions. PROBSTEIN (1994) describes the transport mechanism of electrophoresis in detail.

If we place a direct current field across a clay-water suspension, negatively charged clay particles migrate toward the anode. Hence, for remediation purpose, electrophoresis plays a significant role for the treatment of sludges (ACAR & ALSHAWABKEH 1993).

According to PAMUKCU (1997), in a compact system of porous plug, electrophoresis is of less importance due to restrained solid phase. But in the process of soil decontamination, electrophoresis of clay colloids could still play an important role if

the migrating colloids have the chemical species of interest adsorbed on them. This was demonstrated by GROLIMUND et al. (1996) whereby strongly sorbing lead was transported by mobile colloids.

An important contribution of electrophoretic movement to contaminant transport may occur when the contaminants are in the form of *colloidal electrolytes* or *ionic micelles*. Micelle formation is promoted as the concentration of the aggregating groups increase. Ionic micelles often carry a high charge and exhibit high conductance in dilution (PAMUKCU 1997). Evidence of micellar transport was observed in a study by PAMUKCU (1994) where highly mobile anionic-surfactants facilitated the transport of non-polar organic compounds as micelles toward the anode in the opposing direction of electroosmotic flow.

In this work, none of the pore water substitutes observed tends to form colloidal electrolytes or ionic micelles nor were suspension conditions obtained. Hence, electrophoresis played no role as an electrokinetic transport process and was not included in this work either.

2.2.3.6 Electrode Reactions

When a dc electric field is applied to a wet soil mass, the system consisting of two electrodes, a power supply, and water-saturated soil between them behaves as an electrolytic cell. Current flow is from positive anode to negative cathode, opposite to electron flow. The power supply acts as an electron pump pushing electrons in at the cathode and removing them at the anode. To maintain electrical neutrality, oxidation/reduction reactions take place within the cell. Ions or molecules receiving electron at the cathode are reduced. At the anode, electrons are liberated from ions or molecules that are oxidized.

The preferential oxidation-reduction reactions that occur at electrodes are those that require the least energy. Compounds subject to oxidation or reduction are constituents of the soil matrix or pore water or the electrode materials. The principal electrode reaction observed is the electrolysis of water. At the cathode, water is reduced leading to the production of hydrogen gas and hydroxide ions:

Cathode: $2H_2O + 2e^- \Leftrightarrow 2OH^- + H_2\uparrow$ $E_0 = -0.83$ V (Re. 2)

At the anode, water is oxidized and oxygen gas and hydrogen ions are generated:

Anode: $2H_2O \Leftrightarrow 4H^+ + O_2\uparrow + 4e^-$ $E_0 = -1.23$ V (Re. 3)

Therefore, a high-pH front is produced at the cathode whereas at the anode a low-pH front is generated. Both fronts advance towards the opposite charged electrode by electromigration, diffusion and advection (including electroosmotic flow). When the two fronts meet, hydroxide and hydrogen ions react to form water, the reaction zone

being characterised by a decrease in conductivity and increase in voltage drop (EYKHOLT & DANIEL 1994, GREGOLEC et al. 2001).

The soil between the electrodes is divided into two zones, a low- and a high-pH zone, with a sharp pH jump in between. The location of the pH jump depends on several factors and usually locates closer to the cathode. One factor affecting the location of the pH jump is the relative mobility of hydrogen ions and hydroxide ions. Hydrogen ion has about twice as high ionic mobility as the hydroxide ion (VANCYSEK 1993). Electroosmotic flow typically favours transport towards the cathode. Thus, the advancement of the acid front is favoured and H^+ ions will dominate the system chemistry.

The concentration and mobility of other ions present in the solution will also affect the location of the pH jump by influencing the distribution of the electric field and forming complexes with hydroxide ions or hydrogen ions. In addition, the pH buffer capacity and cation exchange capacity of the soil and interactions of the pore solution with the solid soil material may affect the speed of advancement of the acid and base fronts and the location of the pH jump (LI et al. 1997).

The development of the pH gradient can have a significant effect on the zeta potential, which is strongly pH dependent, and hence on the magnitude of electroosmosis, as well as on solubility, ionic state and charge, and level of adsorption of the contaminants (PROBSTEIN & HICKS 1993).

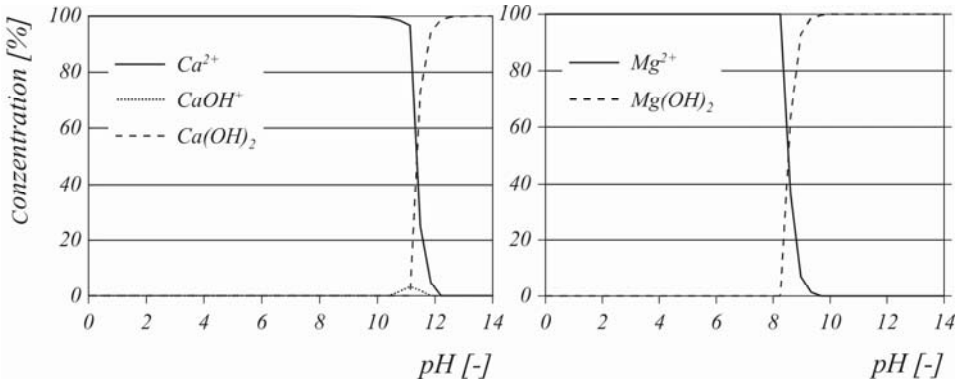

Fig. 2.8: Ca and Mg species for different pH conditions modelled by Mineql+® (after HAUS 2002).

Particular ions may be stable at different pH values. Thus, if the development of an acidic and alkaline front is not hindered by adequate methods like the addition of a neutralising solution (WILSON et al. 1995a,b, WONG et al. 1997) or the use of membranes (HANSEN et al. 1997) precipitation and solution tendency of various species can be strongly influenced by electrokinetics. Al^{3+} can dissolve at acidic conditions (WEST et al. 1997). Hydroxides can precipitate near the cathode due to alkaline conditions (Fig. 2.8). As the soil pore solution is typically dominated by

calcium, sodium or magnesium ions, corresponding hydroxides are found to precipitate preferentially.

The precipitation of hardly soluble metal hydroxides at the cathode has often been observed experimentally for many metal ions (e.g. HAMED et al. 1991):

$$Me^{2+} + 2OH^- \Leftrightarrow Me(OH)_2\downarrow \qquad \text{(Re. 4)}$$

If an iron anode is used, the principal reaction according to the NERNST Equation is iron oxidation and dissolution:

$$Fe^0 \Leftrightarrow Fe^{2+} + 2e^- \qquad E_0 = +0.44\ V \qquad \text{(Re. 5)}$$

Fe^{2+} precipitates at the cathode, preferentially as a carbonate or as a hydroxide. If chlorides are present at elevated levels, the production of chlorine gas can occur at the anode (STUMM & MORGEN 1996):

$$Cl^-(aq) \Leftrightarrow Cl_2(g) + 2e^- \qquad E_0 = -1.36\ V \qquad \text{(Re. 6)}$$

2.2.3.7 Parameter Effects on Electrokinetics

An important number of contributions have been devoted to identify driving parameters in electroremediation. The most common approach is to study the effect of a suspect parameter on the process (i.e. REDDY et al. 1997, YANG & LONG 1999, RÖHRS et al. 2002). According to CAIRO et al. (1996) electrokinetic remediation of soils generally depends on two factors:

- soil properties (e.g., soil porosity, electrical conductivity, and liquid dielectric constant)
- electrical parameters (e.g., electrode composition and spacing, voltage, and electrochemical processes)

The decontamination velocity depends on the following parameters (BARAUD et al. 1997, 1998):

- Contaminant concentration in the soil solution, which is related to the various possible solid/liquid interactions (adsorption/desorption, complexation, precipitation, dissolution, etc.) and to the speciation of the target species.
- Velocity in the pore solution when species are in the soil solution and not engaged in any reactions or interactions. The velocity depends on different driving forces (electrical potential gradient, hydraulic head differences and concentration gradient) and is not closely related to soil properties, except for the electroosmosis phenomenon.

VIRKUTYTE et al. (2002) summarize the following variables that have impact on the efficiency of removing contaminants from soils:

- chemical processes at the electrodes
- pH and pH gradients
- water content of the soil
- soil type and structure
- saturation of the soil
- type and concentration of chemicals in the soil
- applied current density / electrical field
- sample conditioning

According to PAGE & PAGE (2002) electric conductivity and field strength have a major affect on electroremediation:

The process of electrode reactions and pH changes is described in Section 2.2.3.6. Due to changes in pH and ionic strength, which arise during electroremediation, non-uniform electrical conductivity and voltage profiles quickly develop (SEGALL & BRUELL 1992, GREGOLEC et al. 2005). The most noticeable drop in conductivity and therefore rapid change in field strength appear to correspond to the sharp pH jump and to the precipitation of cations/metals as solid hydroxides (HAMED et al. 1991).

In clayey soils with electroosmosis as driving transport mechanism, the resultant steep potential gradient near the cathode initially causes a higher rate of electroosmotic flow in this region (HAMED et al. 1991, ALSHAWABKEH & ACAR 1996). As the acid front produced at the anode passes through the soil, the pH dependent zeta potential becomes less negative reducing the overall flow.

As long as the concentration of ions in solution is sufficient, electromigration results in significant removal of ions (PROBSTEIN & HICKS 1993, ACAR et al. 1994). However, as ions are removed, by means of water formation, precipitation or adsorption, conductivity falls especially in the region of the pH jump. Electromigration and therefore the rate of removal of contaminant ions become slow.

In some experiments with industrially contaminated soils, the conductivity of the soil actually increases with time, probably because ionic species dissolve as a result of pH changes (ACAR & ALSHAWABKEH 1996) or because of temperature rises (HO et al. 1997).

Many soils contain a carbonate minerals content of several percentages. Hydronium ions react with the carbonate according to Reaction 7. Hence, the acidic front only moves a few centimetres into the soil - depending on remediation time and current flow.

$$CaCO_3 + 2H_3O^+ \Leftrightarrow CO_2\uparrow + Ca^{2+} + 3H_2O \qquad \text{(Re. 7)}$$

PAGE & PAGE (2002) review the influence of the nature and arrangement of electrodes. The choice of electrode material affects the electrode process but is limited in practice by cost considerations, ease of manufacture and robustness. The size, shape, and arrangement of electrodes and the distance between them will also affect rates of decontamination. Very little research has been carried out to obtain optimum values for these parameters. ALSHAWABKEH et al. (1999) have modelled the distance between one-dimensional arrangements of electrodes and various two-dimensional arrays.

2.2.4 Lasagna™ Technique and Electric Fence

Permeable reactive barriers are used for the treatment of contaminated groundwater plumes and therefore usually placed in aquifers which consist of coarse-grained sediments having significant effective porosity and hydraulic permeability. Fig. 1.1 shows the main possibilities for combining electrokinetic techniques with permeable reactive barriers. In recent years, research increasingly has considered the application of electrokinetic permeable reactive barriers, which is electrokinetic remediation coupled with permeable reactive barrier systems (URSINI et al. 2005, CHUNG & LEE 2007, GIOANNIS et al. 2007). They principally are used for the decontamination of clayey soils. In the following principles and results of the Lasagna™ technique as well as the so-called electric fence, as examples for combining electrokinetics with treatment zones, are summarized.

Lasagna™ Technique

In 1995, a novel integrated method for in situ electrokinetic remediation of soils, called Lasagna™, was developed (HO et al. 1995) and implemented at the Paducah site, in Kentucky, USA (HO et al. 1999a,b, http://www.rtdf.org). This technology is useful for removing organic contaminants as well as heavy metal contaminants from heterogeneous, low-permeability soils (HO et al. 1997, 1999b). The Lasagna™ technique represents the successful combination of both the principles of PRBs and electrokinetics.

In brief, the Lasagna™ process contains the following concepts (VIRKUTYTE et al. 2002):

- The creation of several permeable “treatment” zones in close proximity through the whole soil matrix by adding sorbents, catalytic reagents, buffering solutions, oxidising agents, etc.
- Application of an electric current in order to transport contaminants into the “treatment” zones by electroosmosis.

The Lasagna™ process has several advantages in comparison to other techniques. First, it is possible to recycle the cathode effluent by directing it back to the anode compartment, which would favour neutralising of the pH and simplify water

management. In addition, the fluid flow may be reversed by simply switching the polarity (HO et al. 1995, 1999a). The switching of polarity promotes multiple contaminant passes through the "treatment" zones and helps to diminish the possibility of non-uniform potential and pH jumps in the soil system.

Two schematic Lasagna™ model configurations were suggested: horizontal and vertical (HO et al. 1999a). The process was called "Lasagna" due to the layering of treatment zones between the electrodes (Fig. 2.9). The technology could conceptionally treat organic and inorganic contamination as well as mixed wastes.

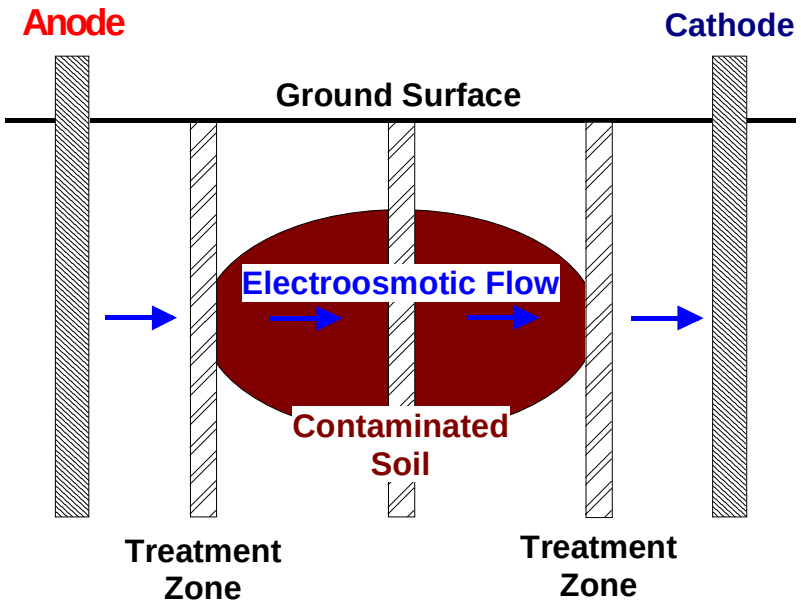

Fig. 2.9: Schematic diagram of a typical configuration of electrodes and treatment zones used by the "Lasagna" technique (HO et al. 1995).

Various configurations of the technology have been studied at various scales, including solid (graphite or steel plate) and granular carbon electrodes; adsorption and degradation treatment zones; and various soil matrixes such as homogeneous clay, sand mixed with clay, and a number of actual soils (HO et al. 1995, 1997). An overview is given in Table 2.2.

HO et al. (1995) demonstrated the successful PNP removal from clayey soils by various electrodes, treatment material mixtures, and effects of polarity reversals. In addition, they proved the effectiveness of electroosmosis in removing PNP from a heterogeneous soil matrix.

DAVIS-HOOVER et al. (1999) demonstrated the application of in situ horizontal Lasagna™ combined with methanotrophic bioremediation of TCE by a small field test (4x4 m) at Rickenbacker Air National Guard Base in Ohio. Between January 1997 and November 1998, the concentration of TCE in the biocell soil was reduced to near zero. During the same period, in the untreated natural attenuation area, little change in TCE concentration was observed.

Table 2.2: Lasagna™ experiments.

Laboratory Experiments:		
Soil	**Contaminant**	**Treatment Material**
Georgia kaolinite	p-nitrophenol (PNP)	sand and/or activated carbon
Clay surrounded by sand	p-nitrophenol (PNP)	Sand/activated carbon
Padukah soil (clay loam)	p-nitrophenol (PNP)	Activated carbon
Field Experiments:		
Soil	**Contaminant**	**Treatment Material**
Padukah soil (clay loam)	trichloroethylene (TCE)	Activated carbon
Padukah soil (clay loam)	trichloroethylene (TCE)	Zero-valent iron

HO et al. (1999a) tested the coupling of electroosmotic removal of TCE from the contaminated soil with in situ adsorption by carbon-containing treatment zones. The test lasted four months; in the last week the voltage was reversed. As the small field test was very successful, removing over 98% TCE from the contaminated soil, a full-scale field test in which TCE was degraded in place was carried out (HO et al. 1999b).

The test covered an area of 6.4 m x 9.2 m and reached a depth of 13.7 m. Zero-valent iron was chosen as reagent to degrade TCE (thickness of treatment zones was 3.8 cm), suspended in wet kaolin clay to provide a stabilized medium for keeping the iron well dispersed throughout the 14-m depth. The operation lasted for 1 year. The applied voltage varied between 120 and 200 V, and two polarity reversal periods were carried out. The treatment cost for a one-acre site (= around 4046.86 m^2) ranges from 49 € to 86 € per cubic meter depending on depth of contamination (4.2 to 13.7 m) and remediation time (from 1 to 3 years). Electrodes were 6.4 m apart, with three treatment zones inserted in between. Water was electroosmotically transported to the cathode and was recycled back to the anode. Iron filings were added to promote iron corrosion over water electrolysis as the predominant reaction at the anode. Thus, acid formation that would reduce the effectiveness of electroosmosis was minimized.

Soil temperature played a key role in this field test in several respects. First, elevated temperatures cause an increase in the rate of TCE degradation with iron filings. Second, the diffusion and dissolution rates of TCE in water would increase with temperature, which would result in accelerated TCE removal from the soil matrix by electroosmosis. Note, one of the biggest technology drawbacks is the entrapment of gases formed by electrolysis and the assurance of good electrical contact to the electrodes.

Electric Barrier/Fence

Considering the long-term behaviour of reactive barriers the application of an electric fence upstream of the PRB appears to be the most promising and practicable approach (Fig. 2.10). The general aim thereby is to reduce the concentration of groundwater constituents that might impair the barrier function when flowing with the groundwater through the reactive material. Thus, the question that arises when attempting to fence off groundwater constituents from entering the PRB is: can a charged species be sufficiently retarded by an electric field to stop it migrating with the hydraulic flow. Since in literature rarely answers to this question can be found it was the main motivating factor for this work.

YEUNG & MITCHELL (1993) developed the general formulation of coupled flows that are caused by hydraulic, electrical, and chemical gradients. The theory has predicted reasonably the migration of cations and anions in compacted clay in simultaneously imposed laboratory experiment. The idea behind is the possible use of so-called electrokinetic barriers for hazardous waste management. The applied electrical potential gradient causes the movement of ions, which in turn imposes a viscous drag on the pore water. In clayey soils, this viscous drag can generate a high enough pore water pressure capable of counteracting the ground water gradient. This will halt the movement of water within that region and prevent the migration of contaminants.

Hence, considering fine-grained soils, the idea is to create an electroosmotic counter-gradient in opposite direction to that of the groundwater gradient by the continuous or periodic application of an electric potential difference between the electrodes. Considering coarse-grained soils, the idea is to create electromigration rates of the target ions that are high enough to counteract that of the groundwater gradient by the application of an electric field.

NARASIMHAN & SRI RANJAN (2000) considered the application of an electrokinetic barrier down gradient to a contaminated zone in the subsurface in clayey soils, too. They developed a one-dimensional finite element model to predict the contaminant migration under hydraulic, electrical and chemical gradients based on theoretically formulated equations. This coupled flow model was validated using experimental data taken from literature.

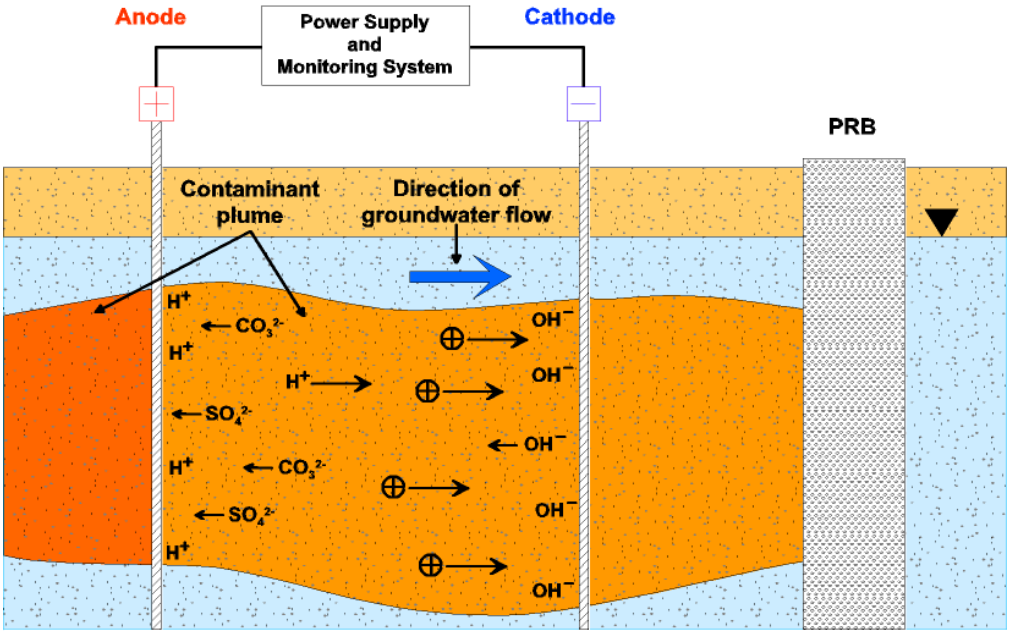

Fig. 2.10: Schematic diagram of an electric fence combined with a PRB.

The literature survey shows that electric fence studies were mainly carried out using fine-grained soils dominated by electroosmosis. In contrast, electrokinetic barrier experiments on sand have rarely been undertaken.

GODSCHALK & LAGEMAN (2003) applied an electrokinetic bio-fence within a contaminated aquifer to provide nutrients for the biological degradation of lightly volatile chlorinated hydrocarbons. An electric fence can also be installed within an aquifer as capture zone for ionic species (LAGEMAN & POOL 2001). Note that in contrast to clays, where mainly the electroosmotic counter-gradient prevails, the application of an electric fence in coarse-grained soils focuses on the electromigrative flow of charged species opposite to the hydraulic flow.
EID et al. (1999, 2000) investigated nitrate electromigration in sandy soil in constant electrical current (3 mA) laboratory soil column experiments. Electromigration was found to be an effective means for concentrating and retaining nitrate close to the anode.

2.2.5 Practical Aspects of Electrokinetics

Generally chemically inert and electroconductive media should be used to prevent dissolution of the electrode as well as generation of undesirable corrosion products in an acidic environment. Under certain conditions, the use of sacrificial electrodes, such as iron anodes, makes sense (HARAN et al. 1996, HO et al. 1999a,b, HAUS et al. 1999, HAUS & CZURDA 2000). For instance, HAUS et al. (1999) and HAUS & CZURDA (2000) used for their field application iron electrodes to reduce cancerous chromate by released iron ions.

Any conductive materials that do not corrode in a basic environment can be used as cathode. A common choice of material for both electrodes in laboratory studies is graphite, while in field applications materials such as activated titanium with an electrocatalytic coating of mixed oxides or conductive ceramics are sometimes used. Regardless of the electrode material selected, the electrode has to be installed properly to assure good electrical contact to the subsurface. Furthermore, they need to have porous casings and open access to the electrode compartments so that solutions and gases can flow through them.

Usually electrodes are installed vertically. Nevertheless, for example STEGER (2005) successfully applied horizontal electrodes during both laboratory and field tests. Limited research has been carried out to study the effect of the electrode configuration on the efficiency of electrokinetic extraction. Most laboratory and field studies on electrokinetic remediation performed to date have been used plane electrodes (one-dimensional electrode configuration). In order to enhance the electrokinetic remediation process, several authors recommend the use of a multiple electrode system or two-dimensional well electrodes, respectively (HAUS et al. 2002, U.S. EPA 1998).

These configurations of electrodes, which generate nonlinear electric fields, are more efficient for treating larger contaminated areas or contaminant plumes in great depths. Factors affecting the selection of electrode spacing include costs and processing time required. Larger electrode spacing will reduce the installation costs, but will increase the processing time required as well as operation costs. The processing time required is a function of the rate of contaminant transport and electrode spacing (ALSHAWABKEH et al. 1999b).

Total energy consumption W to treat a unit volume of contaminated soil is given by Ohm´s Law:

$$W = E \cdot i \cdot t \qquad [kWh] \qquad \text{(Eq. 16)}$$

E = electric field [Vm^{-1}]
i = current density [Am^{-2}]
t = time [s]

As the total mass of the contaminants usually represent only a percentile of the total electrolyte content of the pore fluid (HICKS et al. 1999) energy consumption increases with the ratio f of total electrolyte concentration to contaminant concentration:

$$W' \approx E \cdot i \cdot t / f \qquad \text{(Eq. 17)}$$

W´ corresponds to the energy consumption per unit contaminant. Thus, energy costs increase is inversely proportional to the ratio f (HAUS 2002).

Energy consumption depends on many factors, such as soil and contaminant properties. A high concentration of contaminants or a high ionic strength of the pore fluid will increase the electrical conductivity of the soil and thus increase the energy expenditure. Energy consumption also increases with electrode spacing and electric field strength. Small electric gradients decrease energy costs but increase remediation time and therefore personnel costs and operating costs. High coefficient of electroosmotic conductivity or a high ionic mobility of the contaminant reduces energy expenditure. The smaller the electrode spacing is, the lower energy costs will occur, but more electrodes are necessary and consequently investment and operating costs are higher. Remediation time is directly affected by ionic velocity of the electrolyte, by the electrode spacing and by the electric field strength.

The prediction of the decontamination time is of great importance to estimate energy consumption. This time is all the lower when the effective transport velocity of contaminants is high. Recapitulating, energy consumption increases with:

- ratio f of total electrolyte concentration to contaminant concentration
- ionic strength of the pore fluid
- electrical conductivity of the soil
- electrode spacing
- electric field strength
- low coefficient of electroosmotic conductivity
- low ionic mobility of the contaminant

Small and pilot scale laboratory tests document values of electric power consumption in the range of 10 to 700 kWh per cubic meter of clayey soil (ACAR & ALSHAWABKEH 1996, PROBSTEIN & HICKS 1993, HAMED et al. 1991). For sandy soils, no values of electric power consumption are available in the literature.

THORNTON & SHAPIRO (1995) and ALSHAWABKEH et al. (1999) present a cost model for estimating costs of electrokinetic remediation. According to them, remediation costs can be divided into the following direct costs:

- Fixed cost of capital: - capital investment (e.g. electrodes, electric system)
  - indirect costs (e.g. manpower, plant construction)
- Running costs (e.g. sampling, analysis, dumping, energy)

HAUS et al. (2002) give an overview of cost estimations documented by field and pilot scale tests. Remediation costs strongly vary depending on soil and contaminant properties, contamination depth and running time. Total costs of a chromate contaminated soil volume of 1880 m^3 (30 m x 30 m x 2 m) are about 125 €/t, and amounts to 75 €/t for contamination depth being 4 m (THORNTON & SHAPIRO 1995). Considering a silty clay volume of 50 m x 100 m x 5 m, a remediation time of six months and an applied voltage of 187.2 V (58,5 V/m) total costs of 48 €/m^3 can be assumed (ALSHAWABKEH et al. 1999). Extending remediation time up to 20 months

and in parallel decreasing the applied voltage down to 100 V (23 V/m) the remediation costs can be reduced to 40 €/m3. HO et al. (1999b) calculated treatment costs between 49 € and 86 € per cubic meter for a TCE-contaminated site of one acre (= around 4046.86 m^2), depending on depth of contamination (4.2 to 13.7 m) and remediation time (from 1 to 3 years). Apparently, electroremediation can compete with conventional remediation technologies and dumping.

3 THEORETICAL MODELLING

3.1 Binary Electrolyte Regions

Under certain conditions the movement of solutes in the pore solution can cease completely when applying an electric field (HICKS & TONDORF 1994, ACAR et al. 1995, ZORN et al. 2000). These situations have been identified as a result of the electrolysis products. Therefore, during electroremediation the anolyte and catholyte solutions are used to maintain contaminant removal. Without anolyte and catholyte chemical control, quasi-steady state conditions could be established. In the steady state, ions produced at each electrode meet within the soil at a reaction plane (DZENITIS 1997). By using inert electrodes, the electrolysis of water leads to the production of H^+ at the anode and OH^- at the cathode. This results in the development of a low-pH front migrating from the anode to the cathode and a high-pH front migrating from the cathode to the anode. Where these fronts meet they react to form water. In the case of electrokinetic separation of NaCl, two binary solutes develop: HCl at the anode region and NaOH at the cathode region (Fig. 3.1).

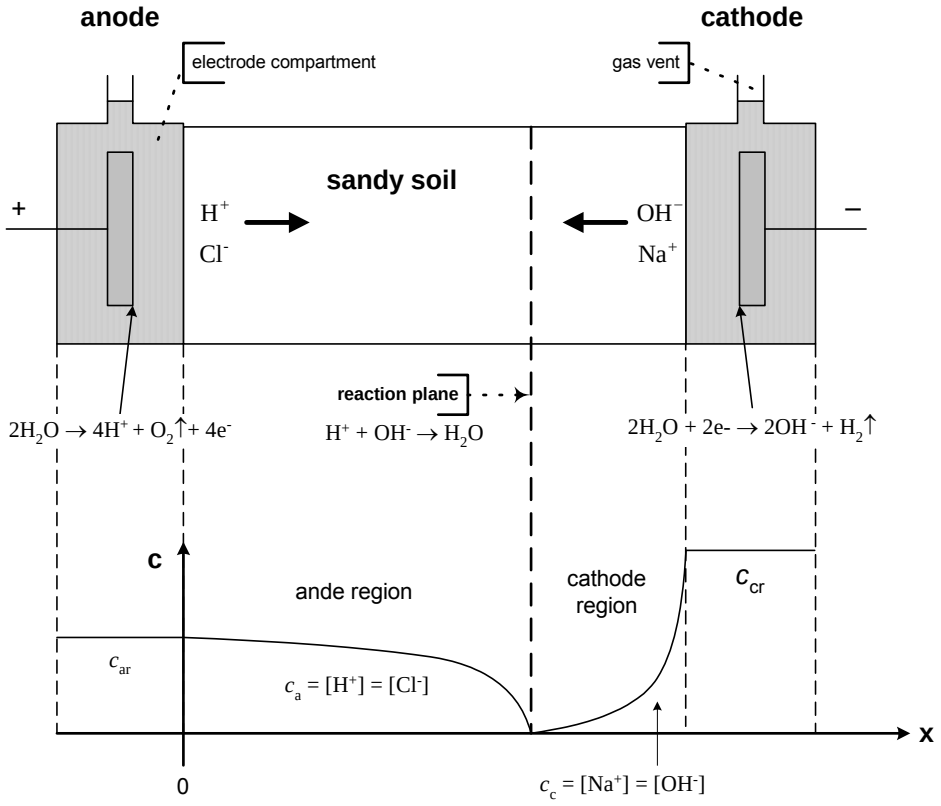

Fig. 3.1: Schematic diagram of electroremediation and binary electrolyte regions for the case when NaCl is the initial electrolyte and H^+ and OH^- are the primary electrode products (after DZENITIS 1997).

Mass conservation for the steady state distribution of a dilute species *i* in the absence of homogeneous reaction equals (DZENITIS 1997):

$$\overbrace{v_c \cdot \frac{\partial c_i}{\partial x}}^{\text{bulk convection velocity}} = - \overbrace{z_i u_i F \nabla \cdot \left(\frac{\partial c_i}{\partial x} \mathrm{E} \right)}^{\text{migration}} + \overbrace{D \frac{\partial^2 c_i}{\partial x^2}}^{\text{diffusion}} \qquad \text{(Eq. 18)}$$

where c is the molar concentration (molm^{-3}), t the time (s), v_c is the bulk convection velocity (ms^{-1}), v_c hydraulic velocity (ms^{-1}), z_i is the valence, u_i the mobility (molskg^{-1}), F the Faraday constant (96487 Cmol^{-1}), E is the electric field strength (Vm^{-1}), and D (m^{2}s^{-1}) is the molecular diffusion coefficient.

When only two charged species (H^+ and Cl^- for the anode region and OH^- and Na^+ for the cathode region) with constant diffusion coefficients are involved, the electric field could be eliminated in (Eq. 18), assuming electroneutrality. According to DZENITIS (1997) the concentration distribution for one binary region is:

$$\overbrace{v_c \frac{\partial c_*}{\partial x}}^{\text{convection}} = \overbrace{D_* \frac{\partial^2 c_*}{\partial x^2}}^{\text{diffusion}} \qquad \text{(Eq. 19)}$$

where c_* is a reduced ion concentration formed from the cation molar concentration c and the stoichiometric coefficients of dissociation ν:

$$c_* = \frac{c_{*_+}}{\nu_{*_-}} = \frac{c_{*_-}}{\nu_{*_-}} \qquad \text{(Eq. 20)}$$

D_* is the binary diffusion coefficient (PROBSTEIN 1994):

$$D_* = \frac{z_{*_+} \nu_{*_+} D_{*_-} - z_{*_-} \nu_{*_-} D_{*_+}}{z_{*_+} \nu_{*_+} - z_{*_-} \nu_{*_-}} \qquad \text{(Eq. 21)}$$

The analytic solution of (Eq. 18) is given by DZENITIS (1997). Computed steady state conditions for different convective velocities for a NaCl separation are given in Fig. 3.2.

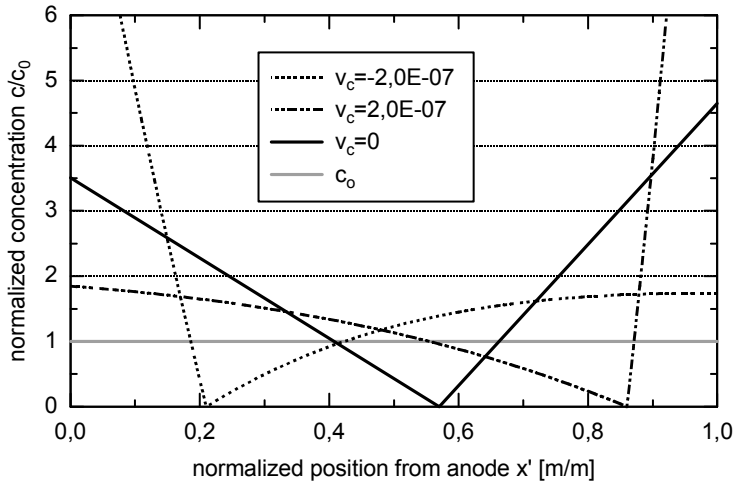

Fig. 3.2 Steady-state concentration distribution for different convective velocities (negligible convective displacement).

3.2 Eh/pH Diagrams

During electroremediation not only mass transport processes but also electrode reactions take place. The principal electrode reaction observed is the electrolysis of water. At the cathode, water is reduced leading to the production of hydrogen gas and hydroxide ions (Re. 2). At the anode, water is oxidized and oxygen gas and hydrogen ions are generated (Re. 3). Therefore, the redox conditions at the electrodes are changed. Furthermore, a high-pH front is produced at the cathode whereas at the anode a low-pH front is generated (s. Section 2.2.3.6.). Both fronts advance towards the opposite charged electrode and thus cause changes in soil pH. In addition, in low permeable soils O_2 gas generated at the anode is transported towards the cathode by electroosmosis, leading to more oxidative soil conditions.

Soil pH affects the solubility of many elements. Only a few ions as Na, K, and Cl ions are dissolved over the whole range of pH. Most metals are soluble under acidic conditions whereas increasing pH leads to precipitation of hydroxides or alkaline salts. Beside the transfer of protons, oxidation and reduction (redox) reactions determine the mobility of many inorganic compounds as well as biologically important materials such as nitrogen and sulphur. Redox reactions are defined as reactions in which electrons are transferred. The species receiving electrons is reduced, the one donating electrons is oxidized.

Eh/pH diagrams show the thermodynamic stability areas of the dominant aqueous species and stable solid phases on a plane defined by the Eh and pH axes. Usually the upper and lower stability limits of water are also shown in the diagrams. The most well-known study on comprehensive Eh/pH diagrams is from Pourbaix (1966). This work has been followed by many thermodynamic databases. The most prominent Eh/pH diagram is the one of the system Fe-C-H_2O. Important relationships for the practice are given by Reactions 8 to 10.

$$Fe(OH)_3(\text{amorphous, s}) + 3H^+ + e^- \Leftrightarrow Fe^{2+} + 3H_2O \qquad \text{Re. 8}$$

$$Fe(OH)_3(\text{amorphous, s}) + 2H^+ + HCO_3^- + e^- \Leftrightarrow FeCO_3(s) + 3H_2O \qquad \text{Re. 9}$$

$$FeCO_3(s) + H^+ \Leftrightarrow Fe^{2+} + HCO_3^- \qquad \text{Re. 10}$$

Eh/pH diagrams can be taken from different handbooks - though in most handbooks these diagrams are available only for a limited number of temperatures and concentrations (usually 25°C and 1 mol/l) and for the simple system of one element and water solution. However, the application of a dc electric field in the subsoil has a substantial influence on soil pH, redox values and concentration distribution of species and usually leads to a distinct rise in temperature. Consequently, species

changes within the electric field and at or near the electrodes occur. In addition, these changes are dynamic processes varying in time and space.

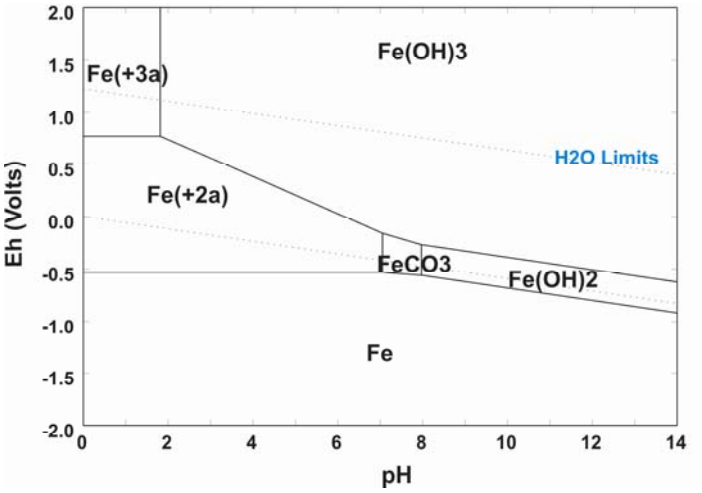

Fig. 3.3: Eh/pH diagram modelled for the system Fe-C-H_2O (CO_3^{2-} phase and sum of Fe^{2+} and Fe^{3+}), T = 25°C, Fe = 10^{-2} mol/l, C = 10^{-3} mol/l.

Although normally used, the quite simple Eh/pH-diagrams of handbooks do not meet the requests of species change caused by electrokinetics. In this work, HSC Chemistry 5.1 was used for modelling individual Eh/pH diagrams for specific cases. This software was developed at the Charles Sturt University, Australia. The software allows constructing Eh/pH diagrams for selected temperatures and concentrations as well as for a selected multi-component system. The Eh/pH module of HSC Chemistry 5.1 is based on STABCAL - Stability Calculations for Aqueous Systems - developed by HUANG (2006).

Usually the redox potential axis is based on the Standard Hydrogen Electrode (SHE) as calculated by the Nernst equation:

$$Eh = E^0 + \frac{RT}{nF} \ln K_{sp} \qquad \text{(Eq. 22)}$$

where E^0 is the standard electrode potential, R is the universal gas constant (8.314472 J $K^{-1}mol^{-1}$), T is the absolute temperature (T_K = 273.15 + $T_{°C}$.), n is the number of electrons transferred in the cell reaction or half-reaction, and K_{sp} is the solubility product (equilibrium constant $\frac{a_{red}}{a_{ox}}$, with a representing the chemical activities of the reduced and oxidized species respectively; since activity coefficients tends to unity at low concentrations, activities in the Nernst equation are frequently replaced by simple concentrations). At room temperature (25 °C), RT/F may be treated like a constant and replaced by 25.679 mV.

The redox potential of the system represents its ability to exchange electrons. The system tends to remove electrons from the species when the potential is high (Eh > 0). These conditions may exist near the anode in the electrochemical cell. In reducing conditions, when potential is low (Eh < 0), the system is able to supply electrons to the species, for example with a cathode electrode. Note that the soil itself is not a electron conductor; current solely flows by ions.

The pH of the system describes its ability to supply protons (H(+a)) to the species and is calculated by the -log function of the H^+ ion concentration:

$$pH = -Log[H^+] \qquad \text{(Eq. 23)}$$

In acid conditions (pH < 7) the concentration of the protons is high and in caustic conditions (pH > 7) the concentration of protons is low.

Generally, a large amount of different species exists simultaneously in the aqueous mixtures in fixed Eh/pH conditions. The Eh/pH diagrams simplify this situation a lot by showing only the predominant species which content is highest in each stability areas. The lines in the diagrams represent the Eh-pH-conditions where the content of the adjacent species is the same in the equilibrium state. However, these species always exist in small amounts on both sides of these lines and may have an effect on practical applications.

The lines in the diagrams can also be represented with chemical reaction equations. These reactions may be divided into three groups according to reaction types:

1. **Horizontal lines**: these lines represent reactions where electrons are involved, but which are independent of pH. Neither H(+a) ions nor OH(-a) ions participate in these reactions.

2. **Diagonal lines**: these lines have either positive or negative slope. They represent reactions that are involved with both electrons and H(+a) and OH(-a) ions.

3. **Vertical lines**: these lines represent reactions that are involved either with H(+a) or OH(-a) ions, but are independent of Eh. In other words, electrons do not participate in these reactions.

The chemical stability area of the water in the Eh/pH diagrams is depicted by dotted lines. The upper stability limit of water is based on the potential when the oxygen generation starts on the anode (Re. 3). The lower stability limit is based on hydrogen formation on the cathode (Re. 2).

The EpH module of HSC Chemistry 5.1 allows the construction of the diagrams by a quite simple way. However, the users manual (ROINE & ANTTILA 2006) point out that several aspects must be taken into account when specifying the chemical system and analyzing the calculation results, for example:

- A basic knowledge of chemistry, aqueous systems and electrochemistry is needed in order to draw the correct conclusions
- The EpH module does not take into account the non-ideal behaviour of aqueous solutions. However, in many cases these ideal diagrams give a quite good idea of the possible reactions in aqueous solutions, especially if the driving force of the reactions is high.
- It has to be considered that thermochemical calculations do not take into account the speed of the reactions (kinetics). In these cases meta-stable diagrams created by removing such species from the system may give more consistent results with the experimental laboratory results.

Thus, the HSC Chemistry user must be very careful when drawing conclusions from Eh/pH diagrams due to these limitations and assumptions.

However, these diagrams may offer extremely valuable information when combining the results with the experimental work and with a good knowledge of aqueous chemistry. There is no universal kinetic or thermochemical theory available, which could entirely substitute traditional experimental laboratory work with pure theoretical calculation models. More information on Eh/pH diagrams, calculation methods and applications can be found in different handbooks, for example from the POURBAIX Atlas (POURBAIX 1966).

The first step for the calculation of Eh/pH diagrams is that the user must specify the chemical system used. This specification of the chemical system by the user includes the following steps:

- Selection of the main element and further elements.
- Selection of the type of species which will be collected from the database (e.g. condensed = solid substances, aqueous ions = dissolved ions, gases = gaseous species).
- Selection of the species from the database.
- Selection of the temperature (combined diagrams show the effect of various temperatures).

The species selection is the most critical step of the Eh/pH calculation specifications. Principally, all species can be selected for the diagram. In some cases, however, it is useful to remove unnecessary species from the system. This will decrease calculation time and simplify diagrams. Due to kinetic reasons the formation especially of large molecules may take quite a long time in aqueous solutions. For example, the formation of large polysulfide, sulphate, etc. molecules (S_4O_6(-2a), HS_2O_6(-a), HS_7O_3(-a), ...) may take quite a while. If these are included into the

chemical system then they may easily consume all the sulphur and the formation of simple sulphides decreases due to lack of sulphur. Therefore, in some cases large molecules should be rejected from the chemical system. The data of some species may also be unreliable. Such species may be rejected from the chemical system, too.

Beside the normal Eh/pH diagrams, which show the effect of pH and potential on the stability areas of different species, the program offers the 'combine option', which enables to see the effect of other variables on the same diagram. Basically, these combined diagrams are made by superimposing up to four normal diagrams. These separate diagrams can be calculated using the main element, temperature, molality (concentration) or pressure as a variable. Combined diagrams make it easy to compare the effect of the main process variables on the chemical system behaviour. The 'combine option' only draws combined diagrams for the same chemical system. Other limitations correspond to those of the normal Eh/pH diagrams.

4 EXPERIMENTAL SET-UPS AND METHODS

4.1 Electrokinetic Cell

Small-scale laboratory experiments were carried out in an electrokinetic cell (Fig. 4.1). Its voltage feed was given by a Hewlett-Packard power supply unit (6645A; 120V/1.5A). The special feature of this construction is that there are two pairs of electrodes installed (remote sensing): active electrodes (Ø 100 mm, thickness 0,5 mm) are placed within the electrode chambers while passive electrodes (80 x 50 mm, thickness 0,5 mm) are placed at each end of the soil body (Fig. 4.2). The voltage applied at the active electrodes is regulated by the passive electrodes and is held constant during the experiment. The advantage of this system is the possibility to monitor a transition resistance which might occur between soil and filter plate and within the anode and cathode chambers. Furthermore, the electrokinetic cell consists of inert materials and allows balancing of the used water constituents.

The electrodes are made of an iridium oxide coated titanium grid (De Nora). The soil core is placed in a plexiglass cylinder of a length of 22 cm and a diameter of 10 cm. At each end, a filter plate made of borosilicate (Ø 100 mm, Robu) and additionally a special filter membrane (E-CTFE 08-1033-SK 060, Büttner GmbH) is used as suffusion protection.

The weighted soil mass was placed into the cylinder in layers of approximately 2 cm. Each layer was compacted mechanically. After waterproof sealing, five titanium potential probes were installed to detect changes of the composition of the pore solution throughout the treatment. Finally, the soil core was slowly infiltrated with the defined soil solution to assure complete saturation. For experiments where only an electric gradient was applied, the inlets and outlets were closed and only gas produced at the electrodes was allowed to escape out of the system. Thus, assuming diffusion as negligible, mass transport has taken place solely due to electromigration. For experiments combining electric and hydraulic gradients, a defined water flow was generated by pumping solution through the soil core.

During all experiments, the voltage gradient between the passive electrodes was held constant. Voltages at the electrodes and potential probes were recorded continuously by a computerised data acquisition unit. Eluates, if arisen, were sampled at least daily and were analysed (unfiltered) for pH (DIN 38404 T1, WTW pH 197, probe Mettler Toledo InLab 417-pH), redox potential (DIN 38404 T6, WTW pH 197, probe Mettler Toledo InLab 501-Redox) and electrical conductivity (WTW LF 197, probe Tetra-Con).

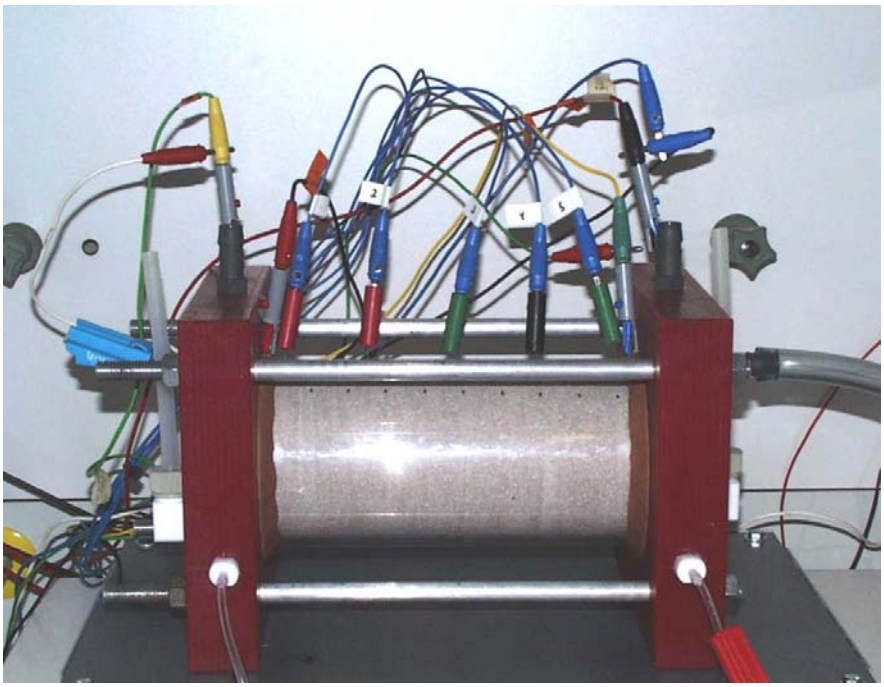

Fig. 4.1: Electrokinetic cell. Note the 5 probes distributed along the soil core. The red PE compartments contain the active electrodes and the electrode chambers.

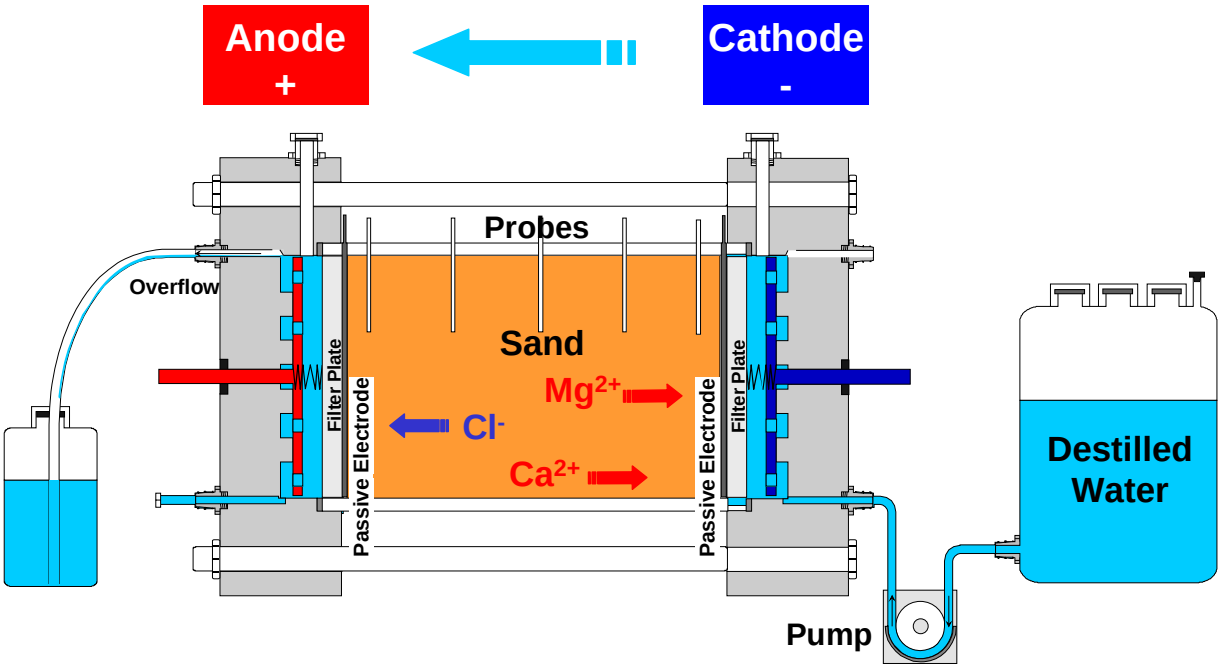

Fig. 4.2: Schematic graphic of an electrokinetic cell (modified after STEGER et al. 2001).

After the experiments, the electrode eluate was drained and weighed. Furthermore, pH, redox potenial and electrical conductivity of the eluate was measured. The soil cores were dissected into ten slices. Each slice was weighed and homogenised before its moisture content (DIN 18 121 T1) and soil pH (DIN 19 684 T1, WTW pH

197, probe Neukum pH 120) was determined following standard procedures. To analyse the ionic concentrations of the salts used in the model solutions, batch experiments with deionised water (40 ml/4 g) were carried out on the wet soil slices as well as on the original soil (DIN 38 414 T4). For experiments with Ca/Mg enriched tap water, an acidic batch (0.1% HNO_3) was applied additionally.

The ion concentrations of the aqueous eluate of the batch experiments as well as the filtrated (40 μm) eluate collected during and at the end of the experiment were analysed for hydrochemical parameters. Anions were measured using spectral photometry (WTW, MPM 3000). Chloride concentrations were determined photometrical using the Spectroquant Chloride Test (Merck), sulfate concentrations turbimetric by the precipitation rate of $BaSO_4$ at a wavelength of 445 nm. Cations were analysed using atomic adsorption spectrometry (PERKIN-ELMER 3030B).

Previously, the electrokinetic cell set-up at the AGK has been used solely for the treatment of clayey - low permeable - soils. First runs with sandy - highly permeable - soils showed that several changes were necessary to prevent unintentional hydraulic flow and to get additional process information. The modifications included:

- use of coarser filter plates and special filter membranes
- enlargement of overflows and gas outlets
- construction of an adjustable base frame which allows the exact horizontal placement of the electrokinetic cell
- addition of 5 potential probes across the soil core which allow the monitoring of changes in pore fluid conductivity/composition with time and place

Table 4.1 gives an overview of the different experimental series carried out in the small-scale electrokinetic cells. Note that in these experiments, sand is used and the ions are artificially spiked into the sand, for which the removal is probably not as difficult as for real contaminated soils. Natural soils usually contain fine particles such as clay particles, which have a high surface area, causing a larger retention time for dissolved species. The chemical and physical characterisation of the materials (soils, reactive material) and solutions used in the experiments are described in the following sections.

4.2 Container

To scale up the experiments a special bench-scale apparatus, the so-called “container”, was designed and constructed (Fig. 4.3). The dimensions of the “container” are 30 cm width, 60 cm length and 30 cm height. This experimental set-up allows to vary electrode configurations as well as to implement reactive materials.

To prevent gas embedding and to minimise layer formation the soil was build in and mixed under water. The applied hydraulic gradient was 0.001, and the average

velocity about 15 cm/day. The voltage applied varied between 20 and 40 V and was held constant by a set of passive and active electrodes. Effluent and - if possible - electrode solution was sampled at least once a day. Beside chemical analysis of ion concentrations, the parameters determined were pH, redox potential and electric conductivity. Principally, all chemical and physical methods applied before, during and after the container experiments were the same as for the electrokinetic cell experiments. At the end of the experiment, the soil body was cut into slices perpendicular and parallel to the electrical field. The analytical programme of various chemical and physical parameters and ion concentrations in the soil samples was equal to the electrokinetic cell experiments.

Two experiments with plane electrodes and one with well electrodes were carried out. For the plane electrode experiments, the linear electric field direction was parallel to the hydraulic flow direction. For the experiment with well electrodes, the nonlinear electric field was directed perpendicular to the hydraulic flow by two sets of well electrodes. An overview of the test conditions is given in Table 6.1.

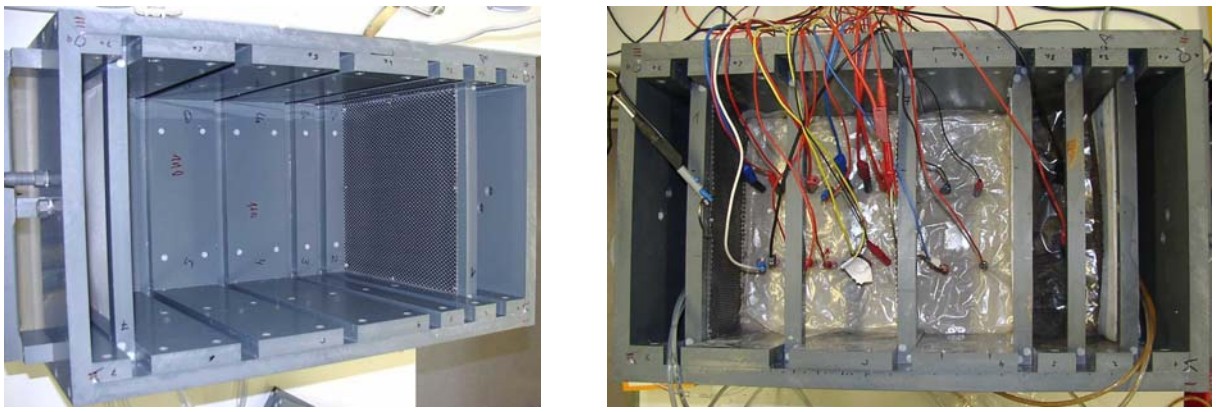

Fig. 4.3: Container test apparatus with a length of 60 cm, width of 30 cm and height of 30 cm. Left: without soil; right: during a plane electrode experiment.

Like for the electrokinetic cell experiments the experimental series started with a simple soil solution system. The aim of the NaCl experiment was to test the function of the facility in principle. The sand body was saturated with a 0.01 molar NaCl solution and flushed with deionized water from the anode towards the cathode. The retention of Cl^- was reflected by its discharge rate at the anode and soil concentration after the experiment, respectively. For soil analysing, the soil body was dissected into a total of 30 portions.

Table 4.1: Overview of the electrokinetic experiment series.

Set-up	Exp. series	Material	Hydraulic gradient	Model contaminant	Matrix solution	Flushing solution
Electrokinetic cell	1	sandy soil	-	NaCl	dist. water	-
	2	sandy soil	-	$CaSO_4$	dist. water	-
	3	sandy soil / loess loam	-	Na_2CO_3	dist. water	-
	4	sandy soil	anode → cathode	NaCl	dist. water	NaCl
	5	sandy soil	anode → cathode	$CaSO_4$	dist. water	
	6	sandy soil	anode → cathode	tap water		dist. water
	7	sandy soil	cathode → anode	NaCl	dist. water	
	8	sandy soil	cathode → anode	$Ca/MgCl_2$	tap water	dist. water
	9	sandy soil	cathode → anode	$Ca/MgCl_2$	tap water	$Ca/MgCl_2$ enriched tap water
Container	1	sandy soil	anode → cathode	NaCl	dist. water	
	2	sandy soil / Fe^0	cathode → anode	$Ca/MgCl_2$	tap water	dist. water
	3	sandy soil	perpendicular to electric gradient	$Ca/MgCl_2$	tap water	$Ca/MgCl_2$ enriched tap water

In the next plane electrode experiment the case of an electric fence, which is the most promising and practicable approach of combining electrokinetic and reactive barriers, was simulated. The soil was saturated with 0.002 molar $CaMgCl_2$ enriched tap water and flushed with deionized water. The pair of plane electrodes was placed upstream of the reactive material (Fig. 4.3). The retardation of cations was investigated with the cathode being placed upstream of the anode. As elemental iron barriers are common, the reactive material implanted was cast iron grit (Table 4.6), which also was used by other PEREBAR project partners.

The plane electrodes were made of an iridium oxide coated titanium grid (De Nora). Two rows of potential probes registered the voltage development across the soil body over time. The soil was separated from the reactive material and the electrode chambers, respectively, by using a permeable filter membrane (E-CTFE 08-1033-SK 060, Büttner GmbH) which is stable even under extreme pH conditions. Pistol pumps continuously circulated the anode and cathode chamber solutions. All in all 57 soil samples were taken after the experiment; 27 between the electrodes, 12 between anode and iron and 18 within the elemental iron.

In order to enhance the electrokinetic remediation process, several authors recommend the use of a multiple electrode system or two-dimensional well electrodes, respectively (HAUS et al. 2002, U.S. EPA 1998). For the container test two pairs of well electrodes (Anode1 A1 - Cathode C1 and Anode2 A2 - Cathode2 C2) generate an electric field which is perpendicular to the hydraulic flow direction (Fig. 4.4). The distance between A1-C1 was 12 cm, for A2-C2 10 cm and for A1-A2 and C1-C2 11 cm each. The soil was saturated and flushed with 0.002 molar CaMgCl2 enriched tap water. After the saturation process, the anode chambers were pumped dry and spiked with 0.02 molar LiCl enriched tap water.

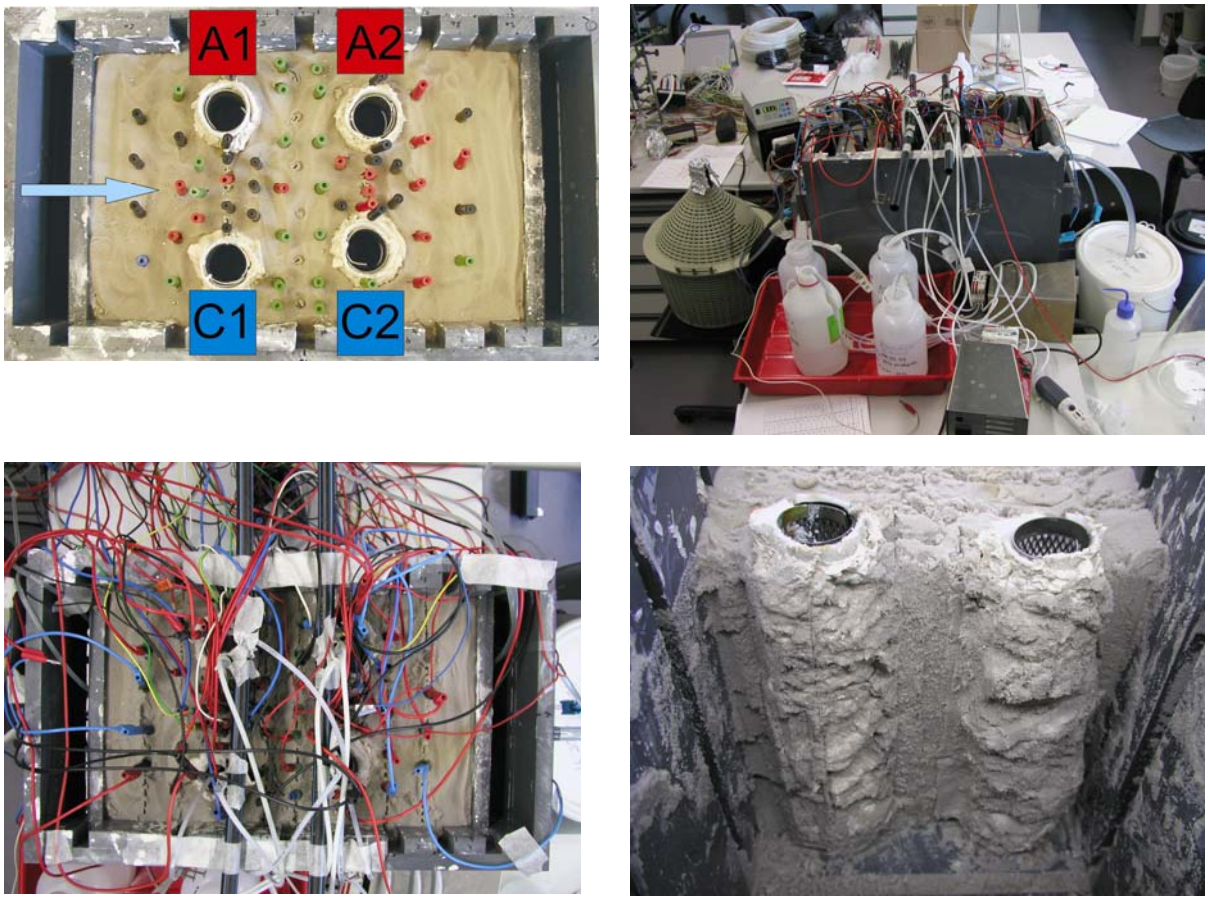

Fig. 4.4: Container test apparatus for the well electrode experiment. Top left: before the experiment; top right and down left: during the experiment; down right: during disassembly.

The well electrodes were 4.5 cm in diameter and 23 cm in height and were made of iridium oxide coated titanium grid (De Nora). The titanium grid was coated by fleece and kaolin (2 cm). The fleece was used as suffusion protection; kaolin was used to seal the electrode compartments and to provide better electrical connection between the electrode and the soil. Within the kaolin coat, electroosmotically induced water and mass transport takes place. Thus, at the anode there is an electroosmotic water flux through the kaolin into the sand whereas at the cathode water flows through the kaolin into the cathode compartment. To prevent drying-up of the anode the supply of

(LiCl) solution was ensured throughout the experiment. At the cathode, the eluate was collected. The water level within each electrode compartment was held constant by fixing a tube at the wanted water level and connecting it with a pump.

To register the development of the nonlinear electric dipole field a net of 66 voltage probes was installed across the soil body - 60 of them being read automatically, six of them being measured manually two times a day.

After a successful preliminary test, the well electrode experiment was run over 13 days. To test the electrodes and monitor the dipole field generated by a single pair of well electrodes or by the superposition of two dipole fields first the power supply was turned on before the hydraulic gradient was applied. For this, each set of electrodes was powered separately and then both electrode pairs were powered simultaneously. From day 1 to 8 the applied voltage was 20 V, from day 8 to 14 the applied voltage was 40 V.
During the experiment sampling of the four electrode solutions and the in- and outflow was done at least once a day. After the experiment the soil was divided into a three-dimensional grid of 41 soil samples. The analytical programme was equal to the electrokinetic cell experiments described above.

4.3 Model Soil and Reactive Material

To avoid additional and difficult controllable geochemical reactions such as adsorption/desorption processes and to create known basic conditions, for all experiments quartz sand was used as a model soil (Table 4.2, Table 4.3). The sand is produced and distributed by Gebrüder Dorfner GmbH & Co.Kaolin- und Kristallquarzsand-Werke KG and has the designation DORSILIT® 9 S. The sand originates from Hirschau, which is 12 km to the northeast of Amberg, Germany. The deposit is placed within the Oberfränkisch-Oberpfälzische fault-block area, which was the sedimentary basin of the Naab-mountains in the south (during Permian and Trias). The deposition of the model soil took place during the Early Trias (sm2). The up to 60m thick arkose was formed from the weathering of granitic rocks. The kaolinite transformation took place after sedimentation (WALTER 1995). Due to tertiary fault-block tectonics and/or erosion, the arkose of the Early Trias partially is found at the surface. During wet processing the clay and sand fraction are separated. According to the supplier, the crystal quartz sand is washed several times and is characterised by its high SiO2 – content. Furthermore, the sand is free from humic substances and other impurities. Thus, the uniform sand has a low retention capacity. The average grain size is 0.38 mm. Its hydraulic conductivity (determined by calculation after HAZEN and BEYER) is approximately $8 \cdot 10^{-4}$ m/s and its porosity 38%, both typical values for sandy aquifers.

The natural loess loam used for the experiment examining electrokinetic mass transport from low permeable soil to high permeable soil is characterised in Tables 3 and 4. The relocated loess loam was used as its positive properties with respect to electroosmotic water transport already has been documented by field and laboratory applications (HAUS 2002, STEGER ET AL. 2003, STEGER 2005). The loess loam originates from the contaminated land "Hammerwerk Pfinztal", which is located 15 km east of Karlsruhe, Germany. The thickness of the loess loam deposit is between 2 and 10m. It is a weathering product of loess, an aeolian sediment transported by west winds during the cold stages of the Pleistocene. The fine-grained loess is decalcified and silicates are transferred into clay minerals by alteration processes.

As reactive material zero-valent iron (ZVI) was chosen as it was also used by other PEREBAR project partners (Table 4.6, Table 4.7).

Table 4.2: Chemical composition of DORSILIT® 9 S quartz sand (data given by supplier).

Oxides	**Percentage [%]**	**Oxides**	**Percentage [%]**
SiO_2	89.40	K_2O	4.97
Al_2O_3	4.68	Na_2O	0.29
Fe_2O_3	0.05	CaO	0.03
TiO_2	0.20	MgO	0.02

Table 4.3: Soil-physical parameters of DORSILIT® 9 S quartz sand (data given by supplier).

Parameter	**Unit**	
Particle size distribution::		
> 1.0 mm	%	1
0.63 - 1.0 mm	%	2
0.5 - 0.63 mm	%	6
0.4 - 0.5 mm	%	16
0.315 - 0.4 mm	%	23
0.2 - 0.315 mm	%	29
0.1 - 0.2 mm	%	19
< 0.1 mm	%	4
Loss of ignition at 550°C	%	0.28
Porosity	%	38
Initial soil pH	-	5.5
Grain density	g/cm^3	2.65
Hydraulic conductivity (BEYER/HAZEN)	m/s	$7.7 / 8.4 \cdot 10^{-4}$

Table 4.4: Mineralogical composition of loess loam (STEGER et al. 2003).

Minerals	**Percentage [%]**
Quartz	40.0
Illite	15.0
Calcite	12.0
Chlorite	10.0
Dolomite	5.5
Smectite	5.0
Feldspars	5.0
Kaolinite	5.0
Organics	2.5

Table 4.5: Soil-physical parameters of loess loam (STEGER 2005).

Parameter	**Unit**	
Grain size distribution:		
< 0.002 mm	%	13
0.002 - 0.06 mm	%	75
0.06 - 2 mm	%	12
Electroosmotic conductivity	m^2/Vs	$3 - 9 \cdot 10^{-10}$
Hydraulic conductivity	m/s	$2.94 \cdot 10^{-8}$
Loss of ignition at 400 °C	%	2.4
Loss of ignition at 550°C	%	3.6
Plastic limit	%	21.1
Liquid limit	%	26.5
Plasticity index	%	6.4
Porosity	%	44
Cation exchange capacity	mmol(eq)/100g	13.05
Proctor density	g/cm^3	1.69
Grain density	g/cm^3	2.71

Table 4.6: Chemical composition of GOTTHART MAIER cast iron grit FG 0200/1000/GG (data given by supplier).

Element	**Percentage [%]**	**Element**	**Percentage [%]**
C	2.8 - 3.6	Ni	0.05 - 0.3
Si	1.8 - 2.1	Al	0.01 - 0.1
P	0.04 - 0.4	Fe	92% typically
Cr	0.05 - 0.4		

Table 4.7: Physical parameters of GOTTHART MAIER cast iron grit FG 0200/1000/GG (data as given by supplier).

Parameter	**Unit**	
Granulometry	mm	0.20 - 1.0
Density	g/cm^3	6.7 - 7.2
Apparent Density	g/cm^3	2.7 - 2.9

4.4 Model Solutions

To verify the function of the experimental set-up and examine fundamental electromigration behaviour in coarse-grained soils, it was decided that simple solutions should be used as model solutions in the laboratory experiments. A 0.01 M NaCl (MERCK, 1.06404) solution was chosen because of its stability and low attenuation in soil. A 0.01 m $CaSO_4$ (MERCK, 1.02161) solution was used as sulphate-rich solution because dissolved sulphate is a common groundwater constituent and can cause unfavourable precipitates in reactive iron barriers. Gradually the solutions chosen became more complex to simulate more realistic conditions. Tap water (Table 4.8) and tap water enriched with 0.002 M $CaCl_2$ (Merck, 2382) and 0.002 M $MgCl_2$ (Merck, 1.05833) were used as representative for multi-component systems and to determine possible interactions between various ions. Regarding the main ion components, the composition of the latter was in accordance with the groundwater composition of a test site of the PEREPAR project in Pécs (Hungary). For experiments examining the electroosmotic transport of ions through low permeable soil into high permeable soil (Table 8) an 0.02 M Na_2CO_3 (Merck, 1.06398) solution was used. For the container experiment with well electrodes the anodes were spiked with 0.02 M LiCl (Merck, 5679.0250) enriched tap water.

Table 4.8: Selected parameters of the tap water of Karlsruhe (SCHNELL 2001).

Parameter	**Unit**	**Average over 19 analyses**
pH	-	7.28
Electric conductivity	µS/cm	626
Oxygen content	mg/l	5.80
Sulphate	mg/l	76
Chloride	mg/l	25
Bicarbonate	mg/l	316
Calcium	mg/l	116
Sodium	mg/l	13.9
Magnesium	mg/l	13.0

5 RESULTS - ELECTROKINETIC CELL EXPERIMENTS

To investigate the fundamental electromigration behaviour of ions under the combined influence of electric and hydraulic gradients in coarse-grained soil a series of electrokinetic cell experiments was carried out.

Initial experiments showed that the conventional experimental apparatus that has been used at the Department of Applied Geology of Karlsruhe University (AGK) - the so-called electrokinetic cell - had to be adapted for runs with coarse-grained soil materials (s. Section 4.1). To test this modified electrokinetic cell preliminary experiments were carried out in a closed system without applying hydraulic gradients (s. Section 5.1). Furthermore, to verify the function of the experimental set-up and examine fundamental electromigration behaviour in coarse grained soils, simple solutions were used as model solutions in the laboratory experiments. A theoretical model (as described in Section 3.1) was applied to predict the formation of steady state conditions. This numerical model couples different mass transport mechanisms, like electromigration, hydraulic flow and diffusion, with the electric field distribution (conservation of charge) and chemical reactions (ZORN 2005). The chemical reactions considered are the electrolysis of water at the electrodes and the dissociation and formation of water.

To simulate groundwater flow, further experiments were carried out where a defined hydraulic flow was generated by pumping solution through the soil core (s. Section 5.2). Objective of these experiments was to investigate the electrokinetic retention potential of ionic species against hydraulic flow. Furthermore, the focus was to observe the influence of a hydraulic flow on the Eh/pH conditions within the soil and at the electrodes, respectively.

Note that in the following charts the voltages are normalized to the applied passive voltage during the experiment, distance to the electrodes (anode and cathode) is normalized to the total distance between the electrodes, and concentrations of ions are normalized to their initial concentration. Furthermore, at the normalized distances to the anode of 0.0 and 1.0, the normalized potentials are measured at the passive electrodes and concentrations are determined for the electrode chambers solutions.

Initial experiments where only an electric gradient was applied on different pore solution systems will be presented first (s. Section 5.1). Experiments where electric and hydraulic gradients are combined (s. Section 5.2) are subdivided into electrokinetic retention of anions and cations, respectively.

5.1 Electric Gradient Only

Initial experiments were carried out in a closed system without applying an hydraulic gradient. Thus, assuming diffusion to be negligible, changes in ion concentration within the model soil (sand) are solely due to electromigration.

First experimental runs with sandy - highly permeable - soils in conventional electrokinetic cells showed that several changes were necessary to prevent unintentional hydraulic flow and to get additional process information. The modifications included:

- use of coarser filter plates and special filter membranes (160-250 µm)
- enlargement of overflows and gas outlets
- construction of an adjustable base frame which allows the exact horizontal placement of the electrokinetic cell
- addition of 5 potential probes across the soil core which allow the monitoring of changes in pore fluid conductivity/composition with time and place

Thus, prior objective was to test the function of the modified experimental set-up. In addition, theoretical models were used to predict the formation of steady-state conditions and were compared with the experimental results.

The soil used has been characterised in Chapter 4.3. The model contaminants were NaCl, $CaSO_4$ and Na_2CO_3, respectively. An overview of the test conditions for the experiments with electric gradient only is given in Table 5.1.

According to their charge, Na^+, Ca^{2+} and H^+ are migrating towards the cathode while Cl^-, SO_4^{2-}, CO_3^{2-} and OH^- are migrating towards the anode. Theoretical analysis and numerical simulations presented by DZENITIS (1997) postulated that in such a simple system steady state conditions are reached where the current density is low and contaminant transport by migration is very slow (s. Section 2.3). The electrolysis products H^+ and OH^- meet within the soil at a reaction plane where they form water. This region is characterised by low electric conductivity and high electric field strength. As a consequence the electrolyte of the system is separated by this reaction plane into two binary zones: the anode zone on one side, dominated by $HCl/H_2SO_4/H_2CO_3$, and the cathode zone on the other side, dominated by $NaOH/Ca(OH)_2$.

In nature, this phenomenon has to be considered in aquifers where the groundwater velocity is very slow or where the soil system chemistry is very simple and pore solution chemistry is the dominant parameter, e.g. in sandy aquifers.

In addition, to consider the well-known problem of decontamination of clay lenses within aquifers, the electroosmotic mobilisation of species from low into high

permeable soil has been demonstrated by an experiment with the model solution Na_2CO_3.

Table 5.1: Test conditions for experiments with electric gradient only.

Parameter	**Unit**	**NaCl sand**	**$CaSO_4$ sand**	**Na_2CO_3 sand/loam**
Voltage	V	20	20	20
Current	mA	3-23	3-32	12-103
Electric Field	V/m	89	89	160
Length of soil core	cm	22,5	22,5	12
Pore Volume	cm^3	545	576	-
Duration	h	10 / 90	97	68
Build in Density	g/cm^3	1.60	1.51	-
Model Solution	mol/l	0.01	0.01	0.02
Initial Soil Conc. Cation	mg/kg	43	88	-
Initial Soil Conc. Anion	mg/kg	74	248	-
Final Soil Conc. Cation	mg/kg	34	35	-
Final Soil Conc. Anion	mg/kg	43	205	-
Balance Cation	%	99	56	97
Balance Anion	%	64	98	-

5.1.1 Model Contaminant NaCl

Applying an electric gradient only, two tests with NaCl as model contaminant were carried out just differing in duration (KURZBACH 2001). The first test (experiment duration 10 h) was stopped before, the second (experiment duration 90 h) after reaching steady-state conditions. The development of potential gradients, current and concentration profiles of both experiments exactly match within the first 10 h, indicating good experimental reproducibility. Hence, mainly the results and conclusions of the 90 h test are presented in the following.

The current trace shows an increase within the first 10 h (Fig. 5.1). After reaching a maximum value of approximately 24 mA it drops steeply before reaching a constant value of approximately 3 mA. The initial rise in current represents an increased electric conductivity within the soil, which results from additional ions produced by the electrolysis of water. H+ and OH- ions produced at the electrodes move faster into the soil as other ions out of the soil towards the electrodes. The subsequent steep decrease in current arises from the formation of water within the soil core, which leads to a zone of low electric conductivity.

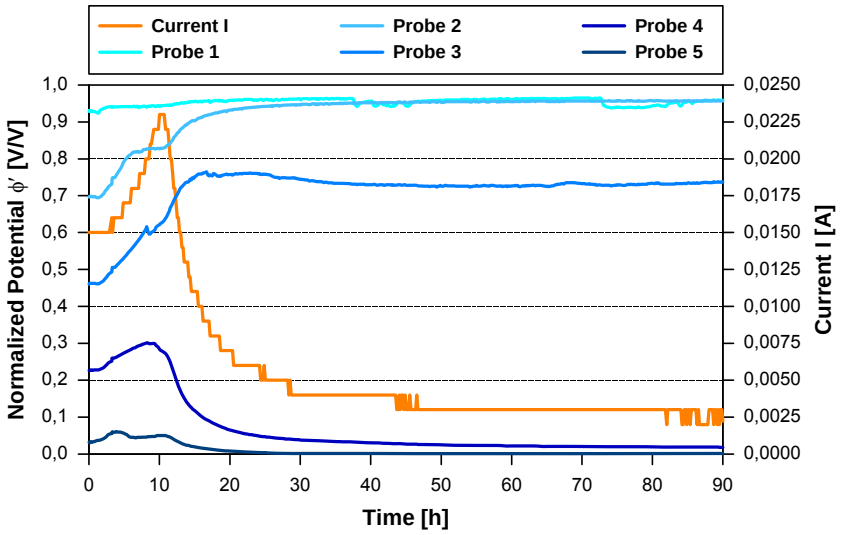

Fig. 5.1: Temporal developing of current and voltage across the soil - NaCl experiment with electric gradient applied only.

The formation of water also is reflected by the development of the potential gradient within the soil core, documented by the traces of the five potential probes. Probe 1 is located next to the anode, probe 5 next to the cathode. Voltages of probes 1 to 3 increase whereas voltages of probes 4 and 5 decrease before they reach constant values after circa 50 hours. The maximum in voltage difference between probes 3 and 4 accompanies with the maximum of potential gradient or zone of water formation, respectively. Based on the traces of the current and the voltages it can be concluded that within approximately 50 hours steady state conditions were reached. Note, the trace of probe 2 indicates inadequate connection probe/soil.

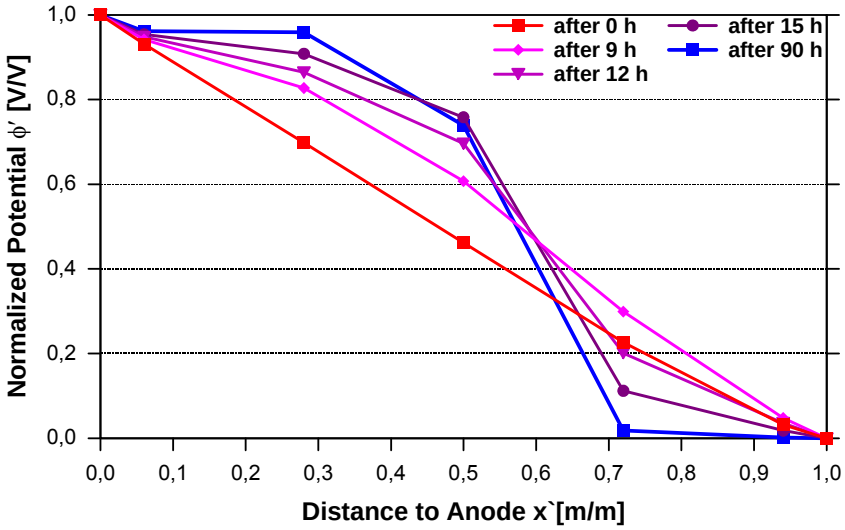

Fig. 5.2: Developing of potential gradient across the soil with time and place – NaCl experiment with electric gradient applied only.

The development of steady state conditions with time and space is also documented by the developing of the voltage gradients between the probes (Fig. 5.2). In the beginning, the voltage gradient is linear. In the end, there is a steep gradient within a small zone while across the rest of the soil core gradients are negligible. The linear voltage gradient in the beginning indicates that ion concentration or in other words conductivity are constant across the soil. The electromigration of ions leads to local changes of ion concentration, which in turn results in local changes of the electric field. As the electromigration velocity of a species is proportional to the electric field, velocity is high where steep voltage gradients exist and vice versa. Thus, ions entering the region with high electric field strength will migrate out readily whereas migration ceases in the nearby region with low voltage gradients - steady state conditions are reached.

According to DZENITIS (1997), this region with steep electric gradient coincides with the reaction plane where the electrolysis products H^+ and OH^- meet and form water. The reaction plane separates the electrolyte of the system into two binary zones: the anode zone on one side, dominated by HCl, and the cathode zone on the other side, dominated by NaOH. To prove this theoretical prediction, Na^+ and Cl^- concentrations as well as soil pH across the soil were determined after the experiments.

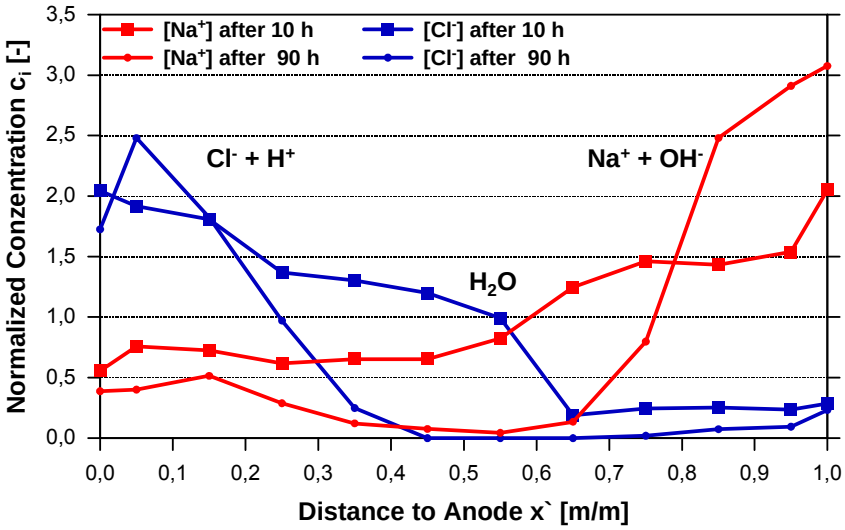

Fig. 5.3: Distribution of Na^+ and Cl^- in soil before (after 10 h) and after steady state conditions are reached (after 90 h) - NaCl experiment with electric gradient applied only.

Fig. 5.3 shows the development of the Na^+ and Cl^- distribution for different periods of the experiment. After 10 h the electromigration of Na^+ and Cl^- already is evidenced by an increase of the Na^+ and Cl^- concentrations at the cathode side and anode side, respectively. At the end of the 90 h test steady-state conditions are reached. Now, the distribution of the Na^+ and Cl^- concentrations clearly shows that there is a zone depleted in ions whereas towards the electrodes the ion concentrations increase very steeply. Within the cathode chamber, the Na^+ concentration rises up to triple of the

initial value. In contrast, the Cl^- concentration within the anode chamber is reduced compared to the concentration in the soil close to the anode region. This is a sign for the oxidation of chloride to chlorine gas at the electrode - an effect that is not considered in DZINITIS' model. Furthermore, the trace of the Na^+ and Cl^- concentrations indicates that the waterfront formed at a distance of about 0.6 from the anode. This placement coincides with the fact that the electromigration velocity of H^+ ions generally is about two times higher than the one of OH^- ions.

In addition, to test the experimental set-up, DZENITIS' (1997) analytical model was used to predict the Na^+ and Cl^- concentration distribution at the end of the experiment (Fig. 5.4). Indeed the experimental results are clearly in accordance with the theoretical predicted development of the two binary zones. Furthermore, the experimental results show that water does not form only at a distinct reaction plane but rather forms within a wider zone.

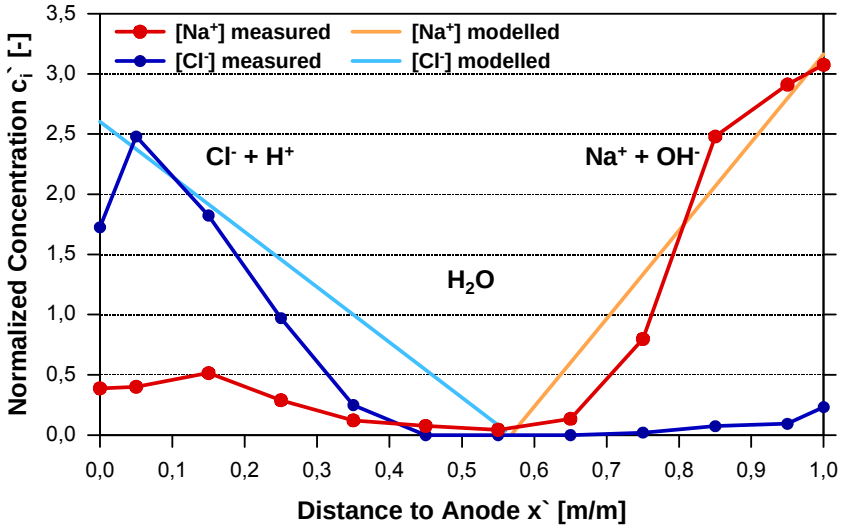

Fig. 5.4: Experimental and modelled distribution of Na^+ and Cl^- in soil under steady state conditions (after 90h) - NaCl experiment with electric gradient applied only.

The position of the reaction zone is also displayed by the distribution of the soil pH across the soil core at the end of the experiment (Fig. 5.5). The soil pH ranges from 4 to 9. At the anode zone, acidic conditions develop (HCl) whereas at the cathode zone an alkaline pH forms (NaOH). Note, soil pH values were determined following standard procedures after DIN 19 684 T1. They are not equal to the pH of the pore solution, which cannot be identified because of the experimental set-up. However, changes in soil pH do reflect the tendency of changes in pore solution pH.

During electrokinetic experiments using clayey soils, usually the electroosmotic water transport leads to changes of the soils´ water content (STEGER 2005). The soil water content at the end of the present experiment is at a constant level across the soil body and equals the initial water content. In addition, during the dissection of the soil core no increased wetness at the cathode side of the soil core was noticed. Thus,

considering the nature of the soil system used, the occurrence of an electroosmotic water transport can be neglected.

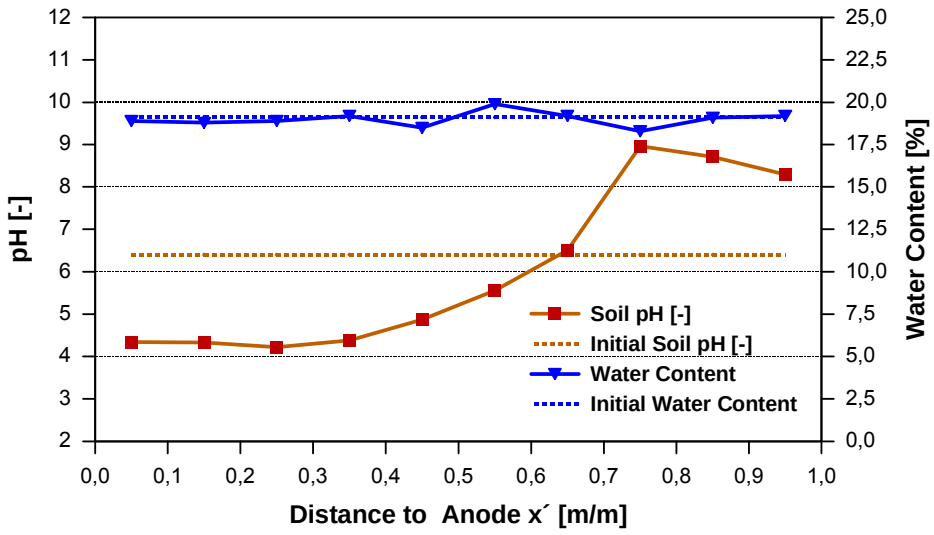

Fig. 5.5: Soil pH and water content before and after the NaCl experiment with electric gradient applied only.

5.1.2 Model Contaminant $CaSO_4$

The electrokinetic cell experiments with a soil/solution system consisting of a uniform middle sand and NaCl showed very satisfactory results. To verify these findings the experiment was repeated under similar conditions but now using $CaSO_4$ as model contaminant. The 0.01 molar $CaSO_4$ solution was used representatively for a sulphate-rich solution as dissolved sulphate is a common groundwater constituent and can cause unfavourable precipitates in reactive iron barriers (s. Section 2.1).

Regarding the development of current, potential gradients, change in ion concentration, pH, and water content the results absolutely coincided with the NaCl experiment. Hence, the correct reproducibility of the experiment for different type of solutions is given. In the following, the results are explained quite briefly, for details in explanation see Section 5.1.1.

Like for the NaCl experiment the current trace reflects the processes of:

- electrolysis of water at the electrodes,
- subsequent formation of water where the two pH fronts meet within the soil
- development of steady state conditions with two binary zones.

These phases are documented by the initial increase of current, followed by its steep drop before reaching a constant value of approximately 3.5 mA (Fig. 5.6). The position of the waterfront at a distance of circa 0.55 is marked by the maximum in voltage difference or potential gradient between probe 3 and 4 (probe 1 is next to the anode, probe 5 is next to the cathode). Note, the unsteady trace of probe 3 indicates misconnection of probe/soil.

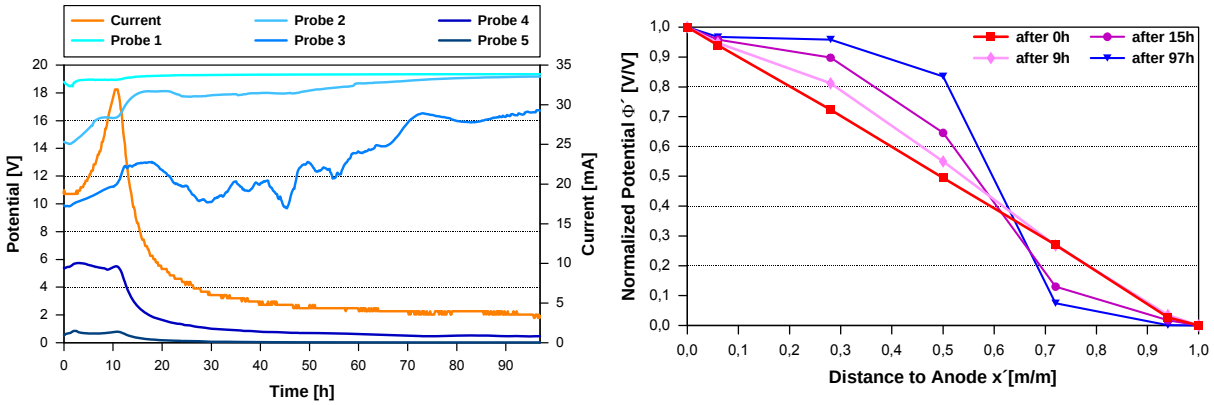

Fig. 5.6: Temporal developing of current and potential at the different probes (left) and potential gradient across the soil body with time and place (right) – $CaSO_4$ experiment with electric gradient applied only.

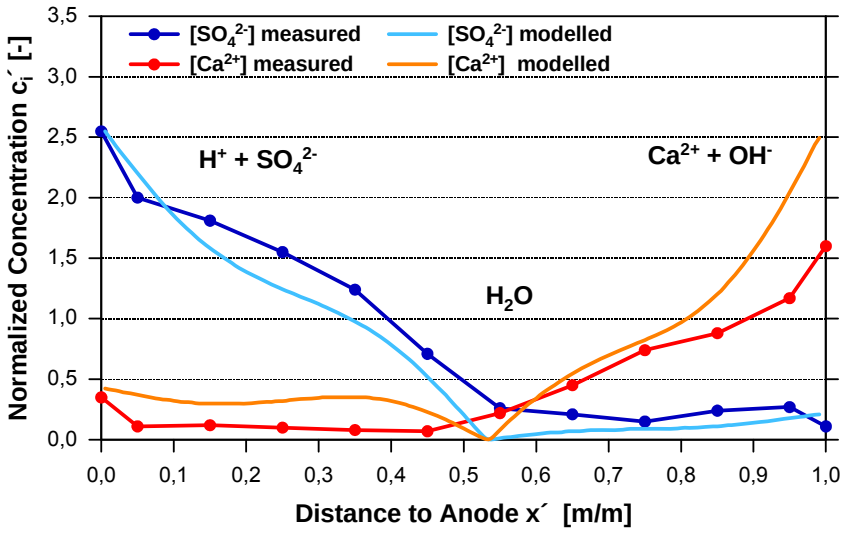

Fig. 5.7: Experimental and modelled distribution of Ca^{2+} and SO_4^{2-} in soil under steady state conditions - $CaSO_4$ experiment with electric gradient applied only.

Analogous to the previously described NaCl case, Ca^{2+} and SO_4^{2-} were transported towards the oppositely charged electrodes by electromigration. As a consequence two binary zones enriched in ions separated by a zone depleted in ions formed and steady-state conditions were achieved. Within the zone depleted in ions water is formed. This zone is characterised by a steep voltage gradient which in turn is an indication factor for the separation of ions.

This phenomenon is not only validated by the described experimental results but also by different theoretical simulations. For NaCl the analytical model of DZINITIS (1997) was used (Section 5.1.1). For $CaSO_4$, the numerical model described by Zorn (2005) was applied. Again, the experimental and modelled results of the ion distribution at the end of the experiment coincide very well (Fig. 5.7). According to the ion mass balance 98% of SO_4^{2-}, but only 56% of Ca^{2+} is found at the end of the experiment. The lack in Ca^{2+} can be explained by precipitation of $Ca(OH)_2$ within the cathode chamber (for details see chapter 7).

The development of two binary zones, dominated by H_2SO_4 and $Ca(OH)_2$ respectively and separated by the water zone, is also reflected by the soil pH after the experiment (Fig. 5.8). Note that all parameters considered - ion distribution (experimental + modelled), soil pH or potential gradient - display the same position for the waterfront at around 0.55 distance from the anode. No significant water changes are determined at the end of the experiment. As the initial soil water content was higher than in the NaCl experiment, the effects of electrolysis and evaporation are more visibly.

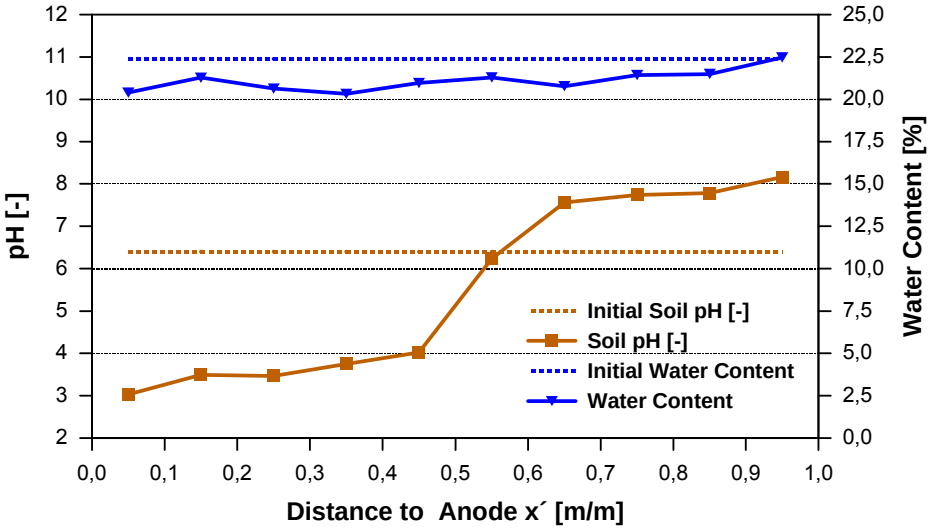

Fig. 5.8: Soil pH and water content before and after the $CaSO_4$ experiment with electric gradient applied only.

5.1.3 Model Contaminant Na_2CO_3

Clay lenses are a common problem with regard to the decontamination of aquifers. They often contain a substantial amount of contaminants. However, due to the intrinsic properties of clays, like low hydraulic permeability, large specific surfaces and negative surface charge, the contaminants are released slowly and cannot be treated efficiently by conventional technologies. On the other hand, the electrokinetic processes of electroosmosis and electromigration allow the transport of contaminants within a defined zone - especially in fine-grained soils. Thus, the electrokinetic

transport processes can be applied to treat clay lenses. For instance, contaminants can be mobilised from clay lenses into the aquifer where they can flow with the groundwater into the reactive barrier.

To investigate the electroosmotic transport of water and the mobilisation of species through low permeable soil into sand a small-scale experiment was carried out. Of special interest was to observe variations in potentials across the soil during the experiment. The electrokinetic cell was filled half with loess loam half with sand (Fig. 5.9) and was saturated with deionized water. After saturation was achieved, a voltage of 20 V was applied with the anode being at the side of the loam and the cathode at the side of the sand. During the experiment the anode chamber was rinsed with 0.02 molar sodium carbonate solution stored in a reservoir at the anode side. Hence, the migration of an acidic front into the soil and potential negative effects on the efficiency of electroosmosis was hindered.

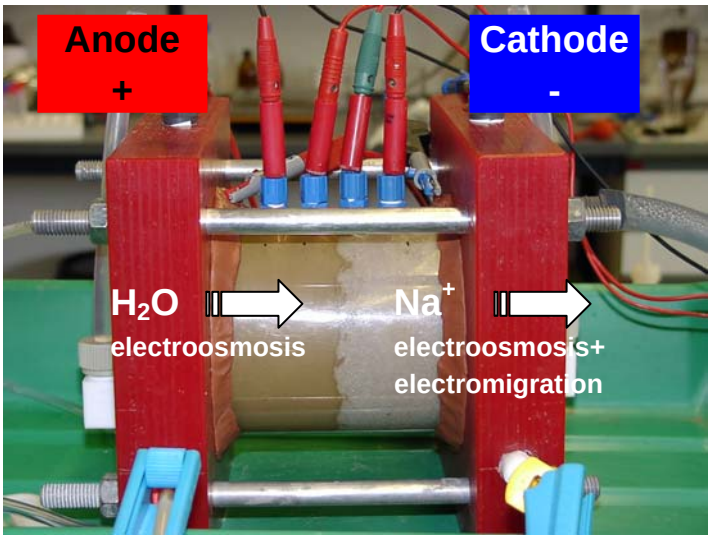

Fig. 5.9: Experimental set-up for the Na_2CO_3 experiment.

Beside the discharge rate of Na^+ and effluent at the cathode, the change in Na^+ concentration in the anode reservoir over time was monitored (Fig. 5.10). After the experiment, more than 95% of Na^+ was released from the anode compartment. The total discharge of sodium at the cathode displays the breakthrough of sodium at the cathode within a few hours. Its linear increase after 26 hours indicates constant discharge rates. The lower discharge rate of sodium at the beginning probably is caused by the excess supply of sodium that leads to sorption/desorption mechanisms within the clayey loam. In addition, the electroosmotic driven increase in water content within the loam (STEGER 2005) results in an delayed effluent and mass transport (see also Fig. 5.14).

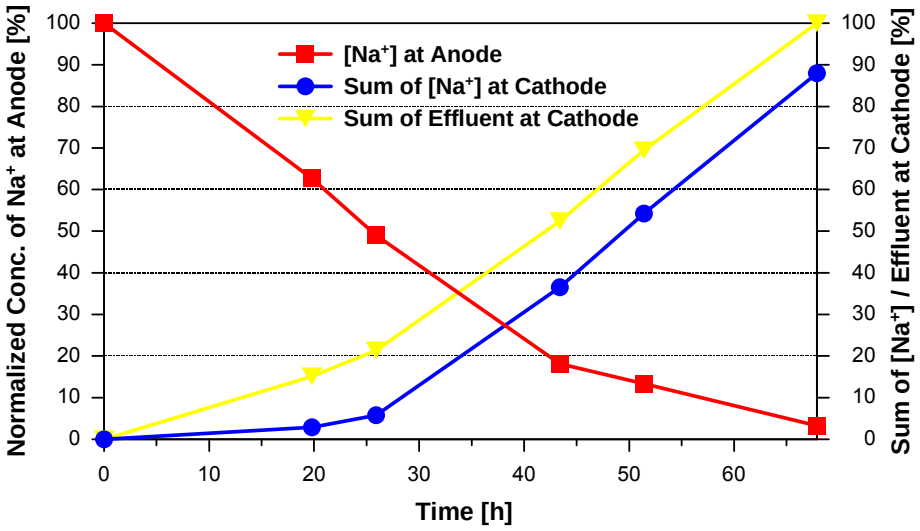

Fig. 5.10: Normalized Na^+ concentration at anode, summarized total discharge of Na^+ concentration as well as total effluent volume at cathode over time.

The almost linear increase of the total amount of effluent at the cathode over time not only prove that indeed an electroosmotic water transport from the loam into the sand takes place but also indicates that the electroosmotic flow rate/k_e of average $7 \cdot 10^{-10}$ $m^2V^{-1}s^{-1}$ is quite constant (Fig. 5.11). Thus, the positively charged sodium is transported towards the cathode not only by electromigration but also by electroosmosis/convective flow. With regard to the remediation success, this means that not only charged but also uncharged contaminants will be transported by electric induced processes.

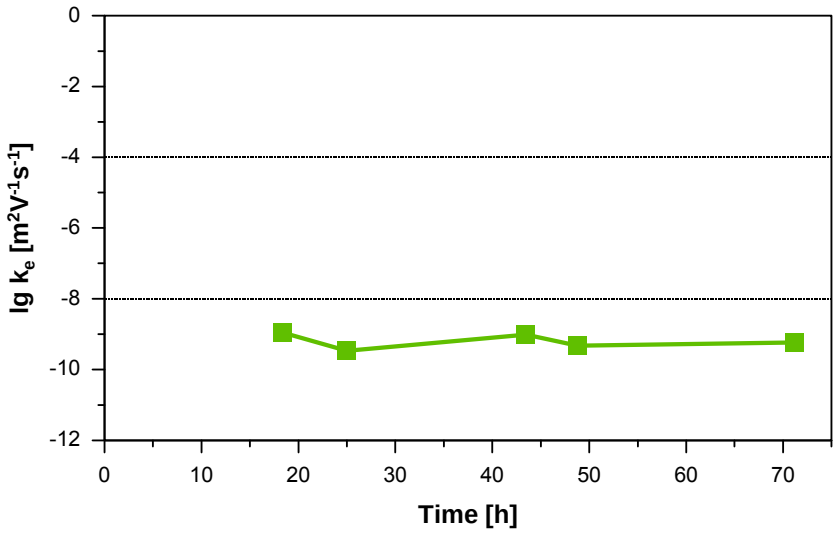

Fig. 5.11: Developing of k_e-values at the cathode.

As for the sodium breakthrough at the cathode, the water discharge rate increases after 26 hours. By applying an electric field sodium and hydrogen ions move into the loam. After sorption/desorption mechanisms are in equilibrium the electrolyte concentration in the soil increases. In addition, initial electroosmotically induced saturation effects (Fig. 5.14) result in a delayed effluent before nearly constant flow rates supported by the continues inflow of Na^+ ions are reached. These effects are also reflected by the developing potential gradients within the loam, which are low in the beginning, increasing within the first 26 hours and keep quite constant from then on (Fig. 5.12).

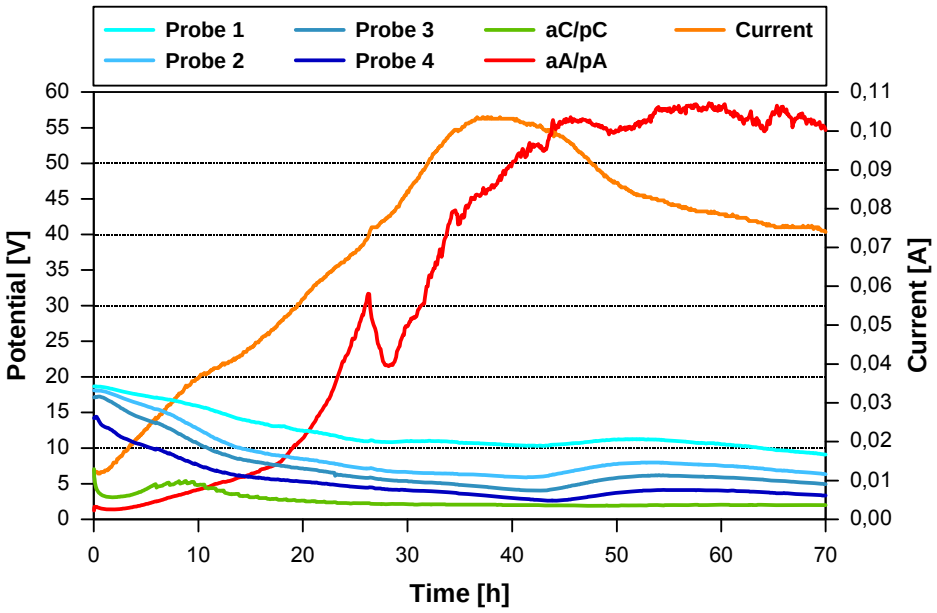

Fig. 5.12: Development of current and potentials at the different probes and between active and passive electrodes – $CaSO_4$ experiment with electric gradient applied only.

The increase in current within the first 40 hours is caused by the increase in water content in the loess loam (Fig. 5.12). STEGER (2005) noticed an increase of up to 25% in laboratory experiments with the same loess loam. This saturation effect is accompanied/superimposed by the electrolysis of water and the electromigration of Na^+ into the soil core. Both result in an enrichment of ions in the soil and increase in electrical conductivity and current, respectively. The subsequent decrease in current is because the soil system depletes in Na^+ as no further Na^+ is supplied at the anode.

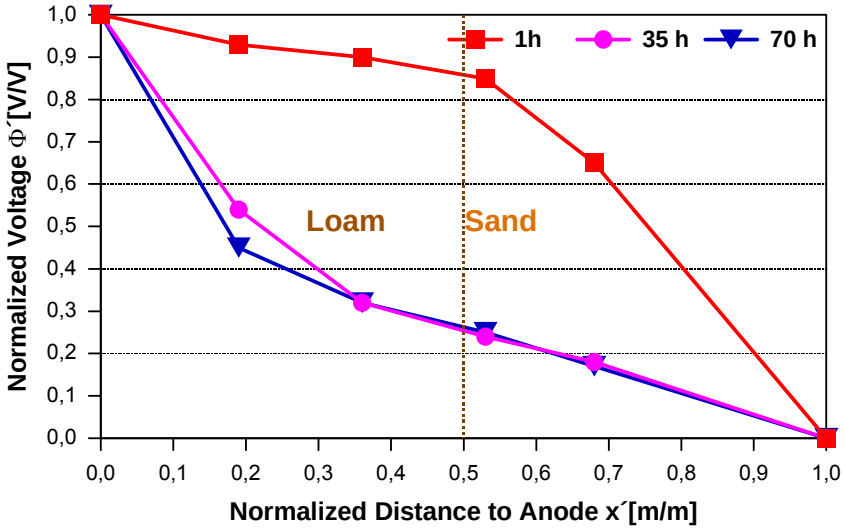

Fig. 5.13: Potential gradient across the soil body over time and place – Na_2CO_3 experiment with electric gradient applied only.

Of high interest is the variation in potential gradient across the soil body during the experiment (Fig. 5.12, Fig. 5.13). Different soil media show different electrical characteristics: Lower potential gradients in fine grained soils with high ion concentrations and electric conductivity. Higher potential gradients in coarse grained soil with lower ion concentrations and electric conductivity. Thus, to avoid unnecessary high energy input and remediation time/costs in real case it should be ensured that the electrode array is conform to the position of the clay lenses.

Subsequently, the maximum in potential gradient moves towards the anode with time. The potential at probe 1 decreases and potential between active and passive anode (UaApA) increases. In principle, H^+ ions generated at the anode will be transported towards the cathode by electromigration and electroosmosis. Consequently, soil pH of the loess loam may decrease and hence the surface charge of the clay minerals changes. Here, the anode is rinsed by a sodium solution. Hydronium ions are mainly buffered by the presence of carbonate ions and hence no acidic front develops within the soil. According to their charge, carbonate ions keep being at the anode whereas Na^+ ions do move into the soil. Hence soil solution chemistry is dominated by Na^+ and OH^- ions. The final soil pH is alkaline and varies between 8.3 and 8.7 (Fig. 5.14). The waterfront (characterised by a depletion in ions and high potential gradient) forms directly at the anode side. The formation of water (insulation effect) could be one explanation for the steep increase in voltage drop between active and passive anode (UaApA). Additionally the H^+ production at the anode could lead to dissolution effects within the loam which causes an impairment of the interconnection electrode/soil.

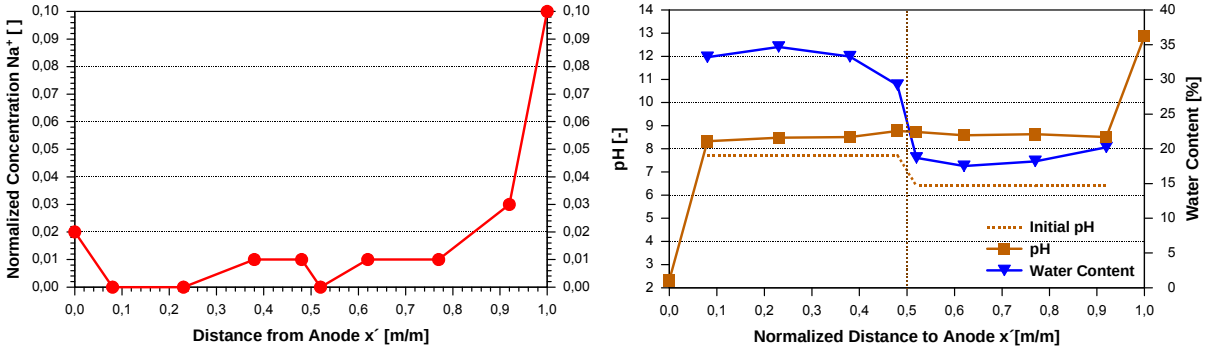

Fig. 5.14: Distribution of Na^+ across the soil (left); Soil pH and water content before and after the NaCl experiment with electric gradient applied only (right).

In summary, the results prove that the theoretically predicted transport of water and species through low permeable soil into high permeable soil indeed takes place. Therefore, electrokinetics principally can be utilised for the decontamination of clay lenses within an aquifer to provide enhanced treatment rates. Nevertheless, different soil types show different electrical characteristics. Hence, the placing of the electrode array is very important to avoid high energy consumption.

5.2 Combined Electric and Hydraulic Gradient

To investigate the fundamentals of electrokinetic retention of ions against hydraulic flow electrokinetic cell experiments combining electric and hydraulic gradients were carried out. Of special interest was the influence of the hydraulic flow direction on the development of the electric field and on the geo-/electrochemical milieu. For all experiments, the hydraulic gradient generated by pumping solution through the soil core was approximately 0.001 and average linear velocity was between 15 and 20 cm/d, respectively. These realistic boundary conditions allow to adjust the various electric gradients and to control their efficiency. During almost all experiments (except the NaCl experiment), voltage was held constant at 20 V, which equals a field strength of 89 V/m. The model solutions were NaCl and $CaSO_4$ in deionized water, tap water and $Ca/MgCl_2$ enriched tap water. Thus, the composition of pore solution gradually became more complex and realistic.

To examine the electrokinetic retention of anions the hydraulic gradient was applied from the anode towards the cathode with model solutions being NaCl, $CaSO_4$ and tap water. The effect of electrokinetic retention of cations was investigated by applying the hydraulic gradient from the cathode towards the anode using NaCl and $Ca/MgCl_2$ solutions.

Making mass balancing easier and understanding the basics of electrokinetic retention, the soil core was first saturated with model solution but then - during the

experiment - flushed with deionized water. To simulate more realistic conditions where a constant supply of ions is given, the experiment with $Ca/MgCl_2$ was also carried out by flushing the soil core with the same solution.

High sulphate concentrations are often typical for contaminated groundwater. Thus, the electrokinetic retention of sulphate was the objective of the experiment, using $CaSO_4$ as model solution and flushing the soil core from the anode towards the cathode.

Table 5.2: Test conditions for experiments with combined electric and hydraulic gradient.

Parameter	**Unit**	**NaCl**	**NaCl**	**$CaSO_4$**	**tap water**	**$Ca/MgCl_2$ tap water**	**$Ca/MgCl_2$ tap water**
Retention of		***Anion***	***Cation***	***Anion***	***Anion***	***Cation***	***Cation***
Voltage	V	20 /10	20	20	20	20	20
Current	mA	-	5-14	16-38	3-7	3-18	7-17
Electric Gradient	V/m	89	89	89	89	89	89
Hydraulic Gradient		0.001	0.001	0.001	0.001	0.001	0.001
Length of Soil Core	cm	22.5	22.5	22.5	22.5	22.5	22.5
Pore Volume	cm^3	713.28	738.35	686	587	643	643
Duration	d	6.3	14.9	5.8	4.8	9	15
Build in Density	g/cm^3	1.58	1.61	1.61	1.76	1.59	1.61
Model Solution	mol/l	0.01	0.01	0.01	0.01	0.002	0.002
Flushing solution		NaCl	Dist. water	Dist. water	Dist. water	Dist. water	Ca/MgCl2 tap water
Initial Soil Conc. Cation	mg/kg	75 Na	58	73 Ca	15 Na	39 Ca, 13 Mg	42 Ca, 15 Mg
Initial Soil Conc. Anion	mg/kg	98 Cl	69 Cl	221 SO4	6 Cl	66 Cl	66 Cl
Final Soil Conc. Cation	mg/kg	27 Na	42	0.3 Ca	0.2Na	27 Ca, 3 Mg	53 Ca, 22 Mg
Final Soil Conc. Anion	mg/kg	18.7 Cl	0 Cl	170 SO4	4 Cl	0 Cl	32 Cl
Balance Cation	%	-	94 Na	91 Ca	78 Na	88 Ca, 38 Mg	23 Ca, 20 Mg
Balance Anion	%	-	115 Cl	100 CO4	99 Cl	110 Cl	72 Cl
Contaminant Retention	%		54	54	49	70 Ca, 20 Mg	88 Ca, 91 Mg
Passed through pore Volume		4.9	7.6	3.9	5	4.8	12

5.2.1 Electrokinetic Retention of Anions

The electrokinetic retention of anions was investigated by applying the hydraulic gradient from the anode towards the cathode. The model solutions used were NaCl and $CaSO_4$ dissolved in deionized water and tap water.

5.2.1.1 Model solution NaCl

First, experiments combining electric and hydraulic gradient were carried out with the non-reactive NaCl as model solution (KURZBACH 2001). The soil core was saturated as well as flushed with the NaCl solution.

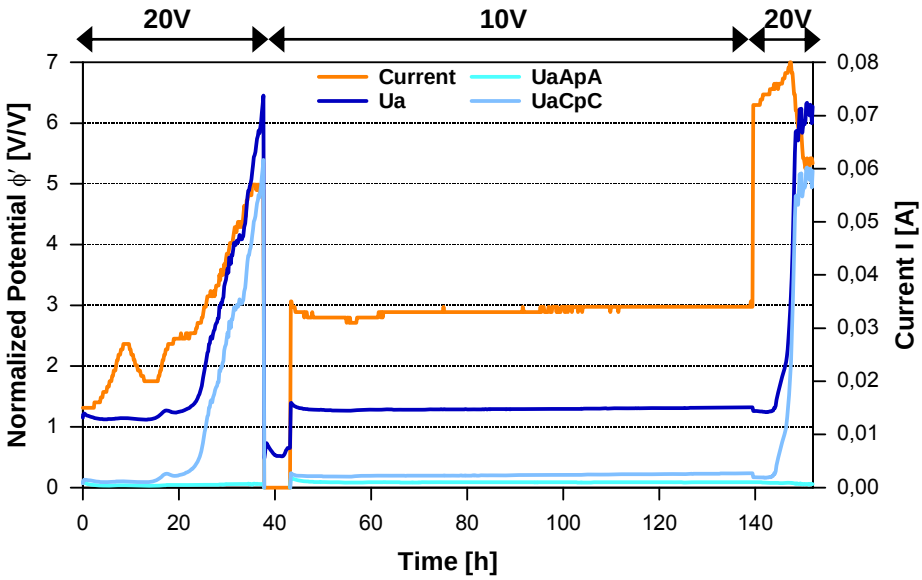

Fig. 5.15: Trace of current, active potential (Ua) and potentials within the anode chamber (UaApA) and cathode chamber (UaCpC), respectively (NaCl).

Fig. 5.15 shows the trace of current and potentials with time. Note that different voltages were applied for particular periods, which were 20 V up to 30 h and at the end and 10 V between 45 and 145 h. Within the first hours, the current trace is concordant to the experiments without hydraulic flow. The current rises due to the increase of soil conductivity by the electrolysis products followed by a decrease. Obviously, the electromigration velocity of the hydroxide ion exceeds hydraulic velocity and the hydroxide ions move against hydraulic flow into the soil. Where hydroxide and hydronium ions meet, low-conductive water is formed separating the soil into two binary zones (s. Sections 4.1, 5.1.1). Hydronium ions are transported by electromigration and hydraulic flow whereas hydroxide ions are transported by electromigration only, against the hydraulic flow. Hence, the water reaction zone shifts towards the cathode and is located between probe 4 and 5 at a distance of 0.85 from the anode (Fig. 5.16).

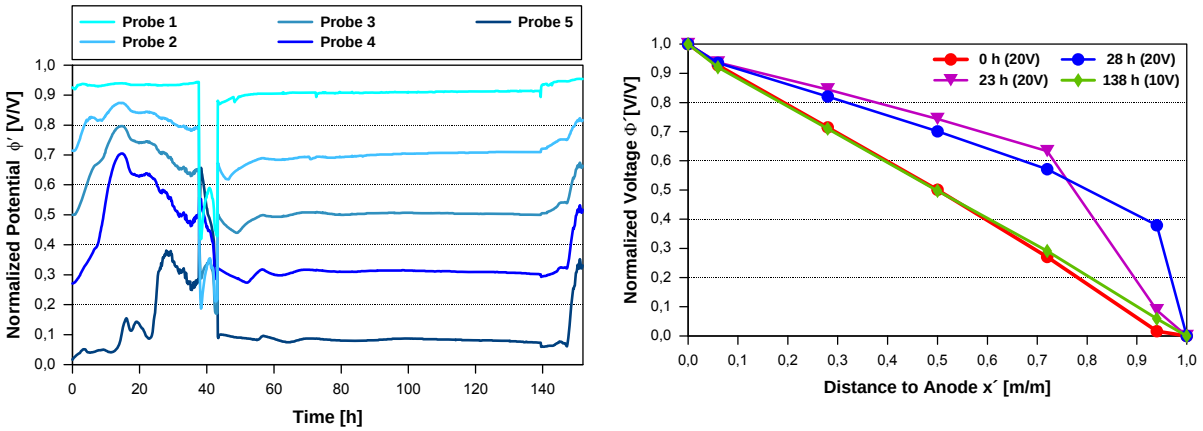

Fig. 5.16: Temporal development of potential at the different probes (left) and of voltage gradient across the soil body with time and place (right).

Contrary to the previous experiments without hydraulic gradient, current starts to rise again after 16 h. The reason is that the waterfront is more and more shifted towards the cathode chamber by the hydraulic flow and at the same time the actual “reaction zone” decreases. A fact that is also documented by the development of the electric gradients across the soil (Fig. 5.16, right). Hence, the whole soil body is dominated by the acidic anode zone (HCl).

Once the waterfront reaches the cathode chamber its resistance increases strongly. The computerised experimental control system is set to keep the potential gradient (measured at the passive electrodes) throughout the soil at a constant value by increasing the active voltage. One possible explanation is that the active electrode within the cathode chamber is passivated by Na^+ ions forming a so-called HELMHOLTZ layer around it. This layer to some extent counterbalances the negative charge of the electrode. The additional resistance leads to further increase in voltage. Finally, the system switched off automatically due to technical limitations of the power supply.

Reducing the applied voltage to 10 V, current as well as measured potentials, including the potentials in electrode chambers, remain constant. The electric field is not strong enough to generate cationic electromigration against hydraulic flow into the soil. Increasing the voltage again towards the end of the experiment (145 h) led to renewed current and potential rise. Considering the potentials measured at the probes, the voltage gradient remains linear across the whole soil core at lower applied voltage whereas higher voltage causes local changes (Fig. 5.16).

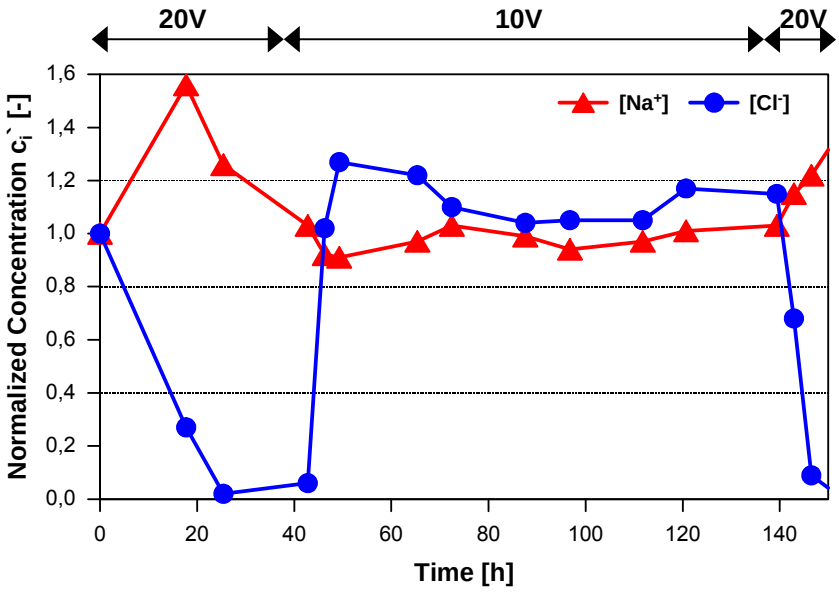

Fig. 5.17: Development of Na^+ and Cl^- concentrations of the cathode effluent during the experiment (concentrations normalised to initial concentrations of the compounds).

The local changes in voltage gradient are caused by local changes in ion distribution, which are reflected by the development of the concentrations of Na^+ and Cl^- in the cathode effluent (Fig. 5.17). For high electric field strength, the electromigration velocity of Cl^- is high enough to counteract hydraulic gradients. Cl^- concentration in the cathode effluent decreases whereas Na^+ concentration increases by the combined effect of electromigration and hydraulic transport. Obviously, the separation of ions also takes place when a hydraulic gradient is applied. Once the waterfront, which is depleted in Na^+, arrives at the cathode (20h), Na^+ concentrations decline in the effluent. At the same time, the outflow of Cl^- ceases signifying complete retardation within the anode-dominated zone.

At lower applied voltages (42-140h), when the average linear velocity exceeds electromigration Na^+ and Cl^- concentrations of the effluent is equal to the one of the influent. Thus, the input of ions is equal to the output and hydraulic flow is the dominating transport mechanism. Increasing the applied voltage at the end of the experiment (140h) leads to increased Na^+ and decreased Cl^- concentrations in the electrode effluent.

Fig. 5.18 shows Na^+ and Cl^- concentrations across the soil body after the experiment. Na^+ concentration is half of the initial value. In contrast, Cl^- concentration is around triple of the primary quantity, a sign for the successful electrokinetic retention against hydraulic flow. The results again were confirmed by numerical modelling after ZORN (2005). Principally, two binary zones formed. As the waterfront is moved towards the cathode, HCl dominates the complete soil system, whereas NaOH dominates the cathode chamber. Hence, soil pH is acidic (Fig. 5.20); effluent pH is alkaline (Fig. 5.19).

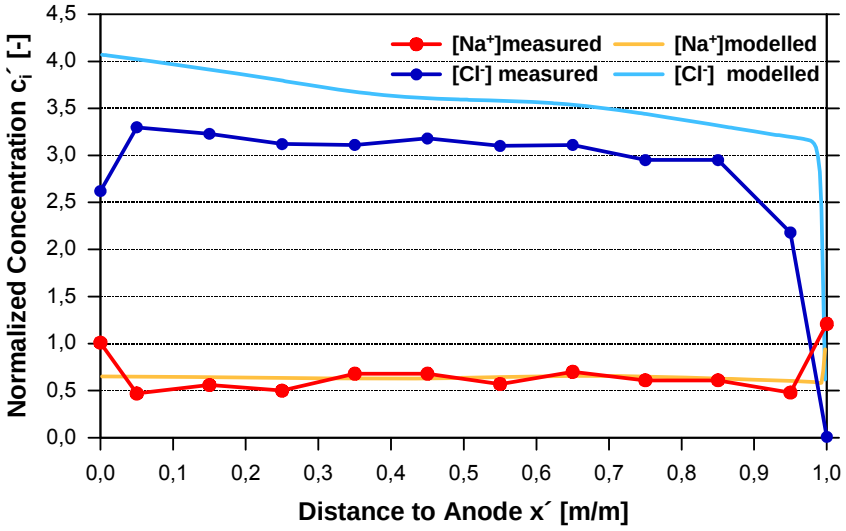

Fig. 5.18: Experimental and modelled distribution of Na^+ and Cl^- in soil after the experiment.

The development of pH, redox and electric conductivity of the cathode effluent (Fig. 5.19) reflect the processes described above. As soon as the electric gradient dominates there is a fall in redox potential and rise in pH. The interaction between electrolysis and waterfront leads to neutralized conditions. Principally, conductivity development is more complex. Here, the rise in conductivity is due to the rise in active voltage at the cathode which leads to a higher OH^- production. Further experiments (not shown here) gave similar results concerning the development of soil pH and water content and confirmed the reproducibility of the findings.

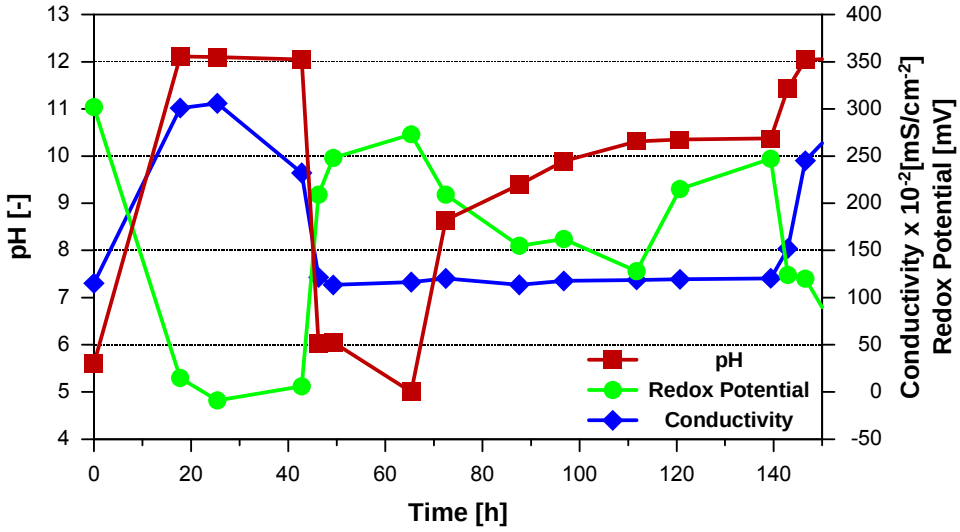

Fig. 5.19: Development of pH, redox and electric conductivity of the cathode effluent during the experiment.

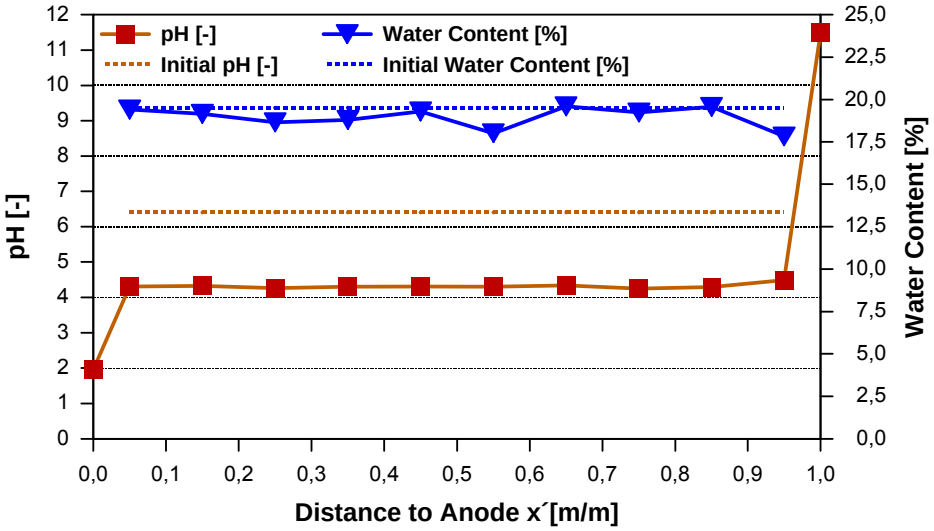

Fig. 5.20: Soil pH and water content before and after the NaCl experiment with electric and hydraulic gradient directed from anode towards cathode.

To verify experimental results, the development of the voltage gradients across the soil body was modelled for different experimental times (Fig. 5.21, right). The modelling is based on numerical algorithms described by ZORN (2005). The modelled results show exactly the same trend of voltage gradient as the measured one do and hence prove the reliability of the experimental set-up. In addition, numerical modelling after ZORN (2005) validated the experimental results achieved for the distribution of Na^+ and Cl^- across the soil, too (Fig. 5.18). Note that the transformation of Cl^- to chlorine gas is not considered in the model.

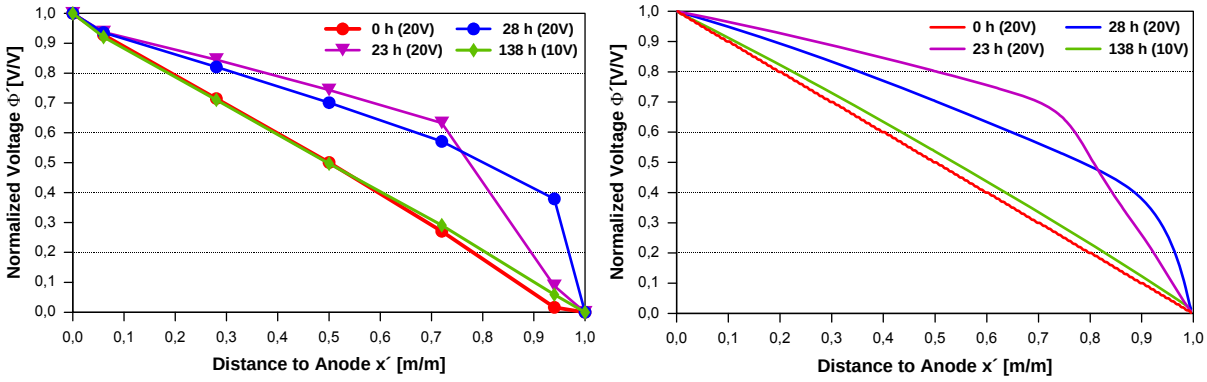

Fig. 5.21: Developing of voltage gradient across the soil body with time and space (NaCl). Experimental results (left), modelled results (right).

The results of the NaCl experiment prove that it is possible to hinder charged species from moving with the groundwater flow by applying an electric field. Electromigration dominates at higher voltages and hydraulic flow overcomes electromigration when lower voltages are applied. Again, hydronium and hydroxide ions react to water

separating two binary zones. As the waterfront is moved towards the cathode by hydraulic flow, the whole soil body is anode-dominated (acidic).

5.2.1.2 Model solution $CaSO_4$; Flushing Solution Deionized Water

Since the results achieved with NaCl were quite promising, further experiments were carried out using $CaSO_4$ as model solution. To avoid the passivation of the active cathode and making mass balancing easier the soil core was saturated with $CaSO_4$ solution but then flushed with deionized water. The pore volume was passed through 4 times.

The developing of potentials across the soil body for different times show the same features as for NaCl systems. Again, a waterfront (characterized by steep voltage gradient) forms between probe 4 and 5 and is transported with the hydraulic flow towards the cathode (Fig. 5.22). The unstable trace of the passive probes reflect that the connection probe/soil is not well achieved.

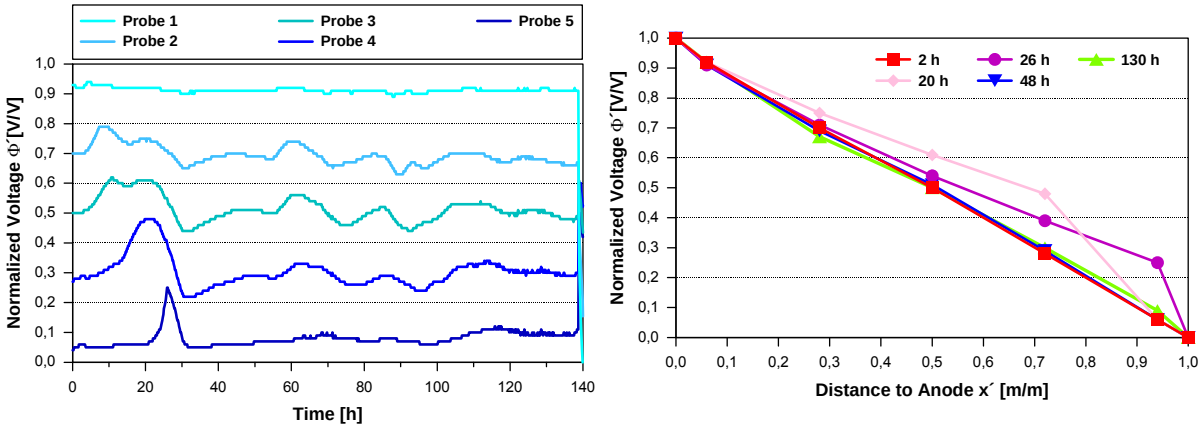

Fig. 5.22: Temporal developing of voltage (left) and of voltage gradient across the soil body with time and place (right).

After the waterfront was flushed into the cathode chamber, linear voltage gradients across the soil body develop indicating even distribution of SO_4^{2-} across the soil. The development of ion separation is also reflected by the total discharge of Ca^{2+} and SO_4^{2-} at the cathode (Fig. 5.23. left). Ca^{2+} is transported by electromigration and hydraulic flow, both directed towards the cathode. In contrast, electromigration of SO_4^{2-} is directed opposite to the hydraulic flow. Thus, the removing rate of SO_4^{2-} is much lower. The discharge of both ions increases linear in the beginning but almost ceases after the waterfront was moved out of the soil body by the hydraulic flow. Consequently, from that time on the electromigration of sulphate and the hydraulic flow are in balance proving that the retardation of sulphate against a hydraulic flow is possible. Fig. 5.23 (left) also demonstrates that the major amount of sulphate is remaining within the soil whereas calcium is discharged completely. 7% of the SO_4^{2-}

carried out derives from the initial cathode solution outside of the electric field. Hence, the retention rate is around 70% (Fig. 5.23, right).

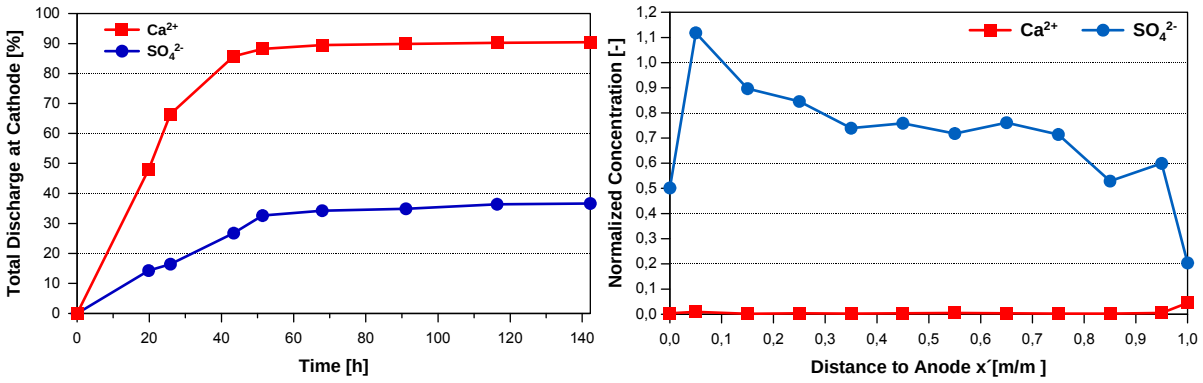

Fig. 5.23: Total discharge of Ca^{2+} and SO_4^{2-} at the cathode effluent (left). Distribution of Ca^{2+} and SO_4^{2-} across the soil body after the experiment, with concentrations normalised to initial concentrations of the compounds (right).

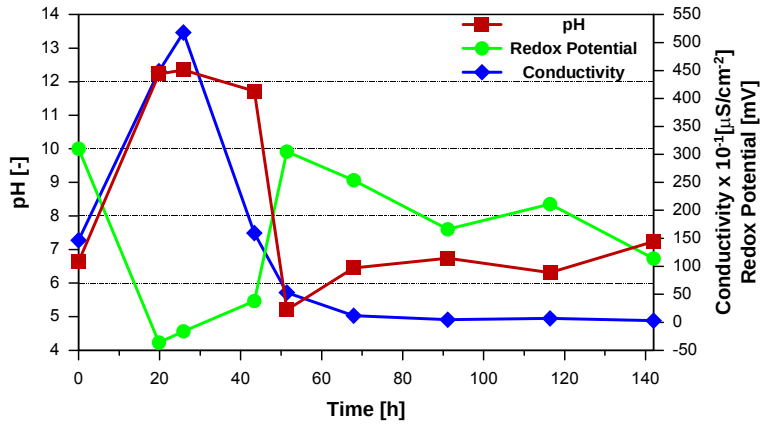

Fig. 5.24: Development over time of pH, redox potential and conductivity of the cathode effluent.

The trace of conductivity of the cathode effluent (Fig. 5.24) reflects the change of the ion concentrations in the effluent with time. First conductivity increases steeply due to the formation of electrolysis products and the accelerated discharge of Ca^{2+}, followed by an abrupt decrease indicating rapid depletion in ions. The latter is a result of the waterfront entering the cathode chamber, the complete discharge of Ca^{2+} and finally the flushing with deionized water. The waterfront also influences pH and redox potential at the cathode. After the waterfront passed, pH drops down from alkaline to roughly neutral values and the reductive redox potential changes towards more oxygen conditions. Both parameters remain constant from then on, indicating that steady state conditions developed. According to the pH development in the cathode effluent, the whole soil became acidic. Note that in the beginning precipitation of

$Ca(OH)_2$ may have taken place in the cathode chamber. However, the drop in pH leads to re-dissolution, and no further precipitation reactions occur.

5.2.1.3 Model Solution Tap Water, Flushing Solution Deionized Water

To investigate changes of geochemical parameters and ion migration behaviour for multi-component systems, tap water was chosen as a representative model solution and the described experiment repeated under same conditions. The soil body was saturated with tap water and flushed with deionized water. The pore volume was passed through 4 times.

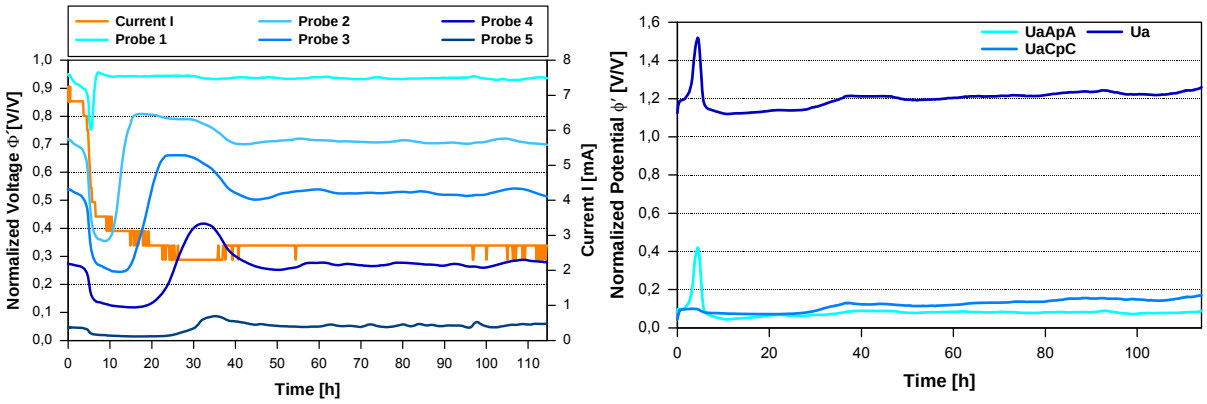

Fig. 5.25: Development over time of current and voltage (left) and trace of the active potential (Ua) and potential within the anode chamber (UaApA) and cathode chamber (UaCpC), respectively.

In the beginning, the current decreases steeply before reaching a constant value of about 2.7 mA (Fig. 5.25, left). This trace results from the electromigrative depletion in ions, the formation of the waterfront and the flushing with deionized water. For tap water (600 μScm^{-2}) the dilution effect of deionized water is much more distinct than it was for the relatively high concentrated $CaSO_4$ experiment (1600 μScm^{-2}). After five hours, the initial solution at the anode compartment is totally displaced by deionized water. This point of the experiment is characterized by an increase in fall of potential between the active anode in the anode chamber and the passive anode at the soil (Fig. 5.25, right). The movement of the front of deionized water through the soil body is reflected by increased voltage gradients moving from the anode towards the cathode. This front of deionized water is superimposed by the waterfront, which forms at the point where OH^- ions meet H^+ ions.

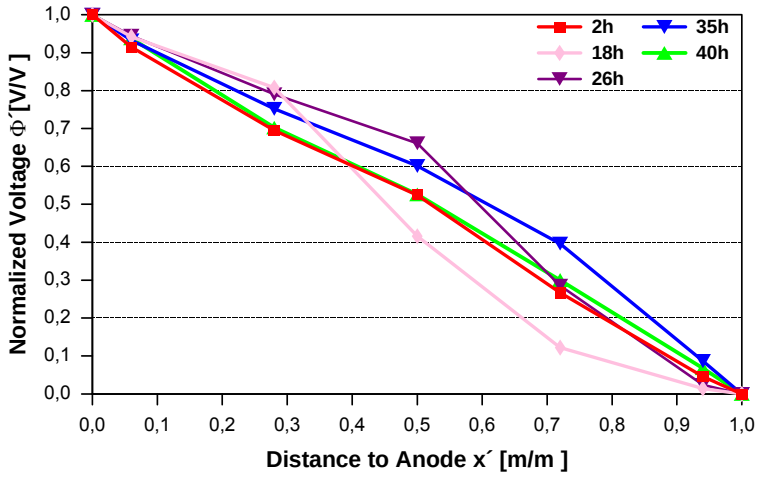

Fig. 5.26: Development of voltage gradient across the soil body with time and place.

Like for the more simple NaCl or $CaSO_4$ systems the waterfront forms between probes four and five and is moved towards the cathode by hydraulic flow (Fig. 5.25 left, Fig. 5.26). The following linear voltage gradients across the soil body indicate even ion distribution. From then on, the main anions of the tap water (bicarbonate, sulphate, nitrate, chloride) and the electrolysis product H^+ dominate the soil solution.

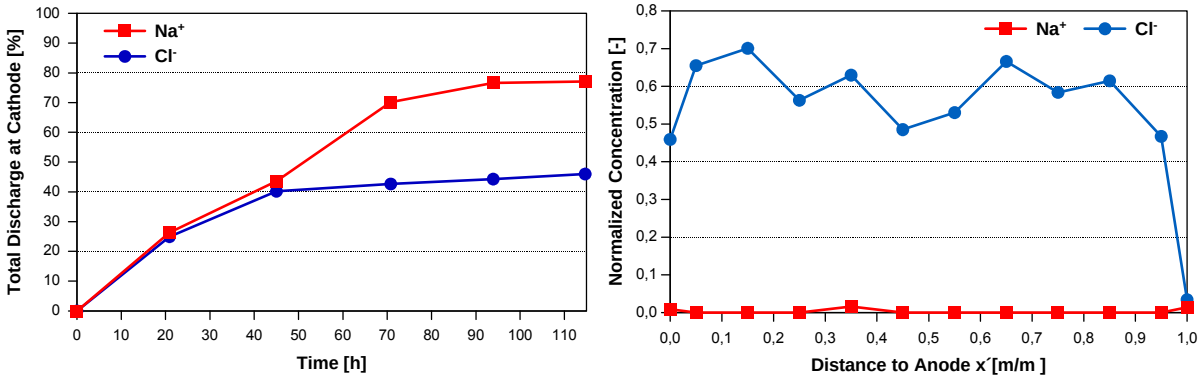

Fig. 5.27: Total discharge of Na^+ and Cl^- at the cathode (left). Distribution of Na^+ and Cl^- as representative ions across the soil body (right).

Representatively for cations, Ca^{2+} and Na^+ were analysed; for the anions, SO_4^{2-} and Cl^- were measured. The development of ion separation is shown by the total discharge at the cathode (Fig. 5.27 left, Fig. 5.28 left). Only 45% of Cl^- and 32% of SO_4^{2-} was flushed out by the hydraulic flow. Obviously, the electrokinetic retention of anions is effective also in systems that are more complex. The distribution of SO_4^{2-} and Cl^- ions across the soil body after the experiment show different retention rates. Although effluent rates of Cl^- was 13% higher, in average 60% of Cl^- but only 15% of SO_4^{2-} is found in the soil after the experiment (Fig. 5.27 right; Fig. 5.28 right). The diffusion coefficients of Cl^- and SO_4^{2-} are approximately equal. According to Eq. 14 the electromigration velocity of SO_4^{2-} ions is two times higher and hence they move

faster towards the anode. Furthermore, it is likely that SO_4^{2-} is involved in precipitation reactions (s. Chapter 7).

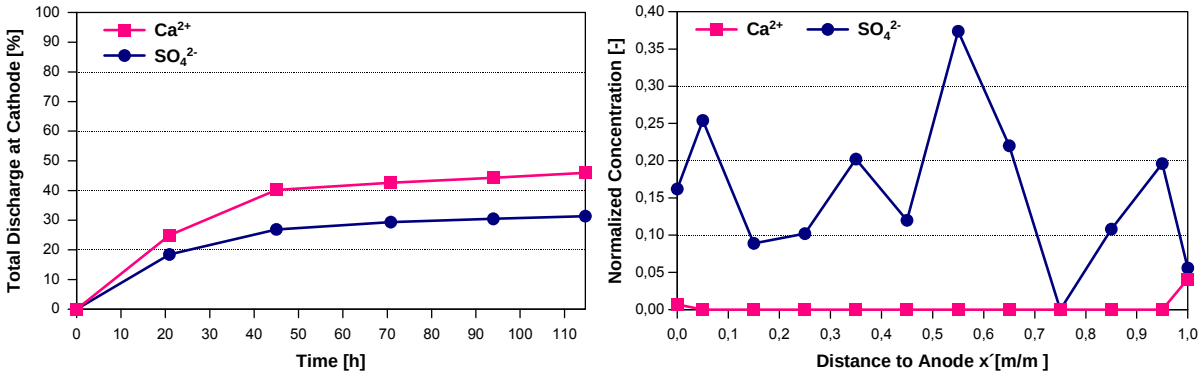

Fig. 5.28: Total discharge of Ca^{2+} and SO_4^{2-} at the cathode (left). Distribution of Ca^{2+} and SO_4^{2-}across the soil after the experiment (rigt).

The presence of competitive ions or more mineralised solution, respectively, also has a great influence on the developing of pH, redox potential and electric conductivity of the cathode effluent during the experiment. Furthermore, according to the law of electric neutrality, precipitation reactions are affected by the composition of the solution. In comparison to the $CaSO_4$ experiment, the discharge of SO_4^{2-} is somewhat lower (8%) but that of Ca^{2+} is much lower (45%). The great lack of Ca^{2+} is can be attributed to precipitation reactions. According to the results of modelling (s. Chapter 7), $CaSO_4$ may precipitate at the anode and within the soil. Furthermore, precipitation of $CaCO_3$ in the soil is likely and alkaline pH at the cathode (Fig. 5.29 right) leads to precipitation of $Ca(OH)_2$.

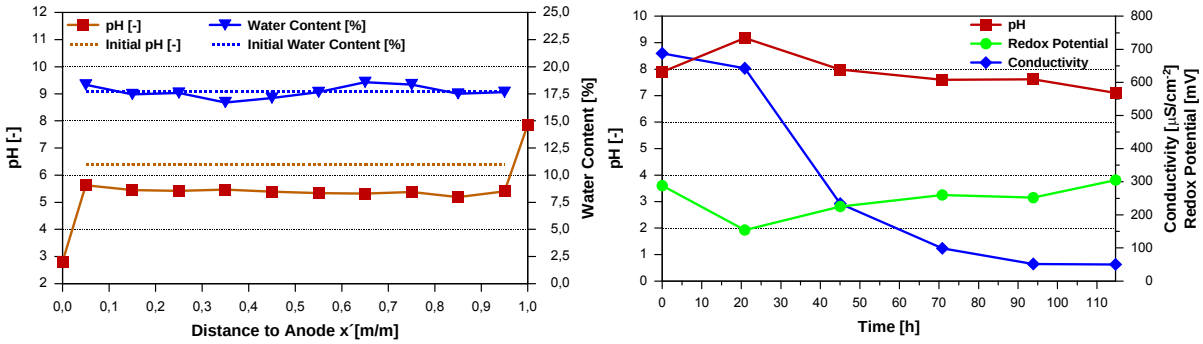

Fig. 5.29: Soil pH and water content after the experiment (left). Development of pH, redox potential and electric conductivity during the experiment (right).

5.2.2 Electrokinetic Retention of Cations

The electrokinetic retention of cations was investigated by applying a hydraulic gradient directed from the cathode towards the anode. The model solutions used were NaCl dissolved in deionized water and $Ca/MgCl_2$ dissolved in tap water. With the latter solution, two types of experiments were carried out: one with flushing the soil core with deionized water, the other flushing the soil core with the solution itself to simulate conditions that are more realistic.

5.2.2.1 Model Solution NaCl, Flushing Solution Deionized Water

The soil core was saturated with 0.002 molar NaCl solution and flushed with deionized water. The waterfront causes a steep potential gradient and a decrease of the current, respectively. Contrary to the experiments before (s. Section 5.1), voltage gradients are not linear across the soil core (after the waterfront is flushed out), but a steep voltage gradient between probe 5 and the anode develops (Fig. 5.30). The electromigration velocity of H^+ is 1.8 times higher than the one of OH^-. In this experiment, the electromigration velocity of H^+ is obviously high enough to overcome the hydraulic flow and move into the soil body. The waterfront is not flushed out completely but remains a few millimetres within the soil. On the one hand there is a loss in voltage within a very small zone. On the other hand high ion migration velocities characterize the zone of steep voltage. Hence, the flushing out of cations with the hydraulic flow is impeded.

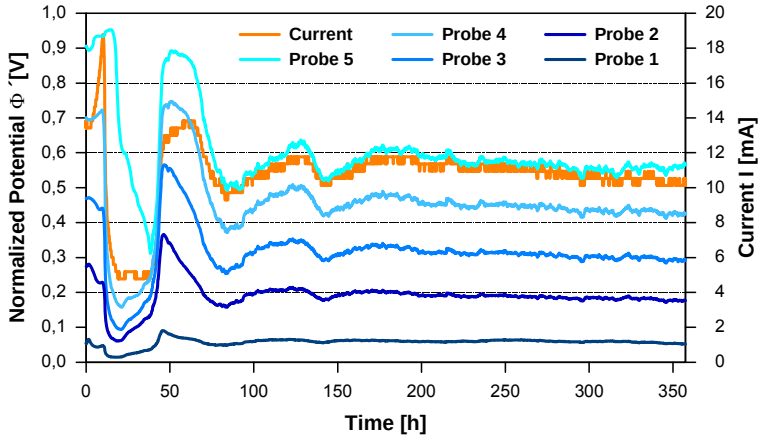

Fig. 5.30: Developing of current and voltage across the soil (NaCl).

The total discharge of ions of the NaCl experiment shows exactly the same features as the previously described experiments targeted at the electrokinetic retardation of anions (Fig. 5.31 left). Cl^- was transported towards the anode by both electromigration and hydraulic flow indicated by the high discharge rate. Electromigration of Na^+ was directed opposite to the hydraulic flow. Thus the discharge rate as well as the total amount of Na^+ transported to the anode (37%)

were much lower compared to Cl^- (100%). Again, the discharge rate of both ions ceases after a while. Thus, separation of ions takes place and electromigration of Na^+ is in balance with hydraulic flow. Consequently, no Cl^- but approximately 75% of Na^+ remained in the soil core (Fig. 5.31 right). The very good overall recovery of 95% of Na^+ proved the plausibility of the experiment.

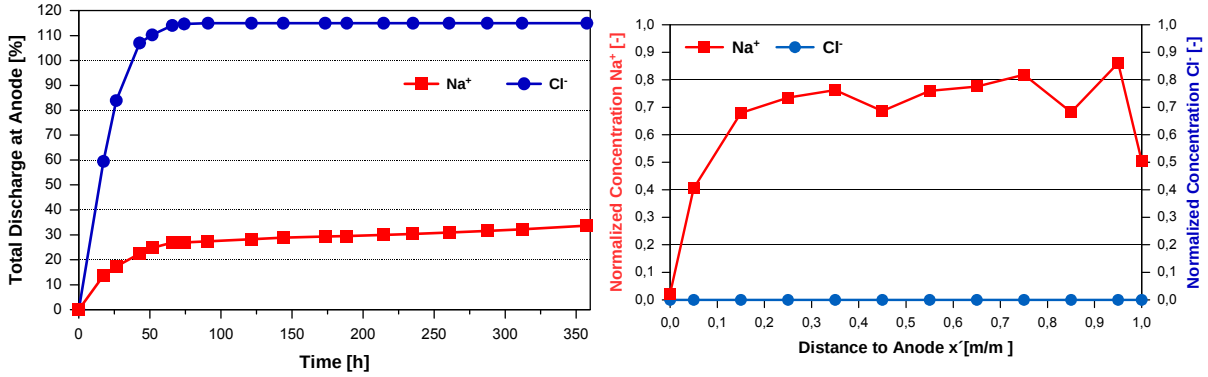

Fig. 5.31: Total discharge of Na^+ and Cl^- at the anode (left). Distribution of Na^+ and Cl^- across the soil after the experiment (right).

The development of pH, redox potential and conductivity of the anode effluent with time show that after around 25 hours the breakthrough of the anode front is achieved (Fig. 5.32 left). The oxidising conditions of the effluent turn into more reducing conditions and the pH becomes neutral. Electric conductivity becomes very low, indicating that electrolysis products H^+ and OH^- react to neutral water, Na^+ is flushed out completely and Cl^- is retarded within the soil by electrokinetic forces. The cathode zone domination within the soil is also reflected by the alkaline soil pH values after the experiment (Fig. 5.32 right).

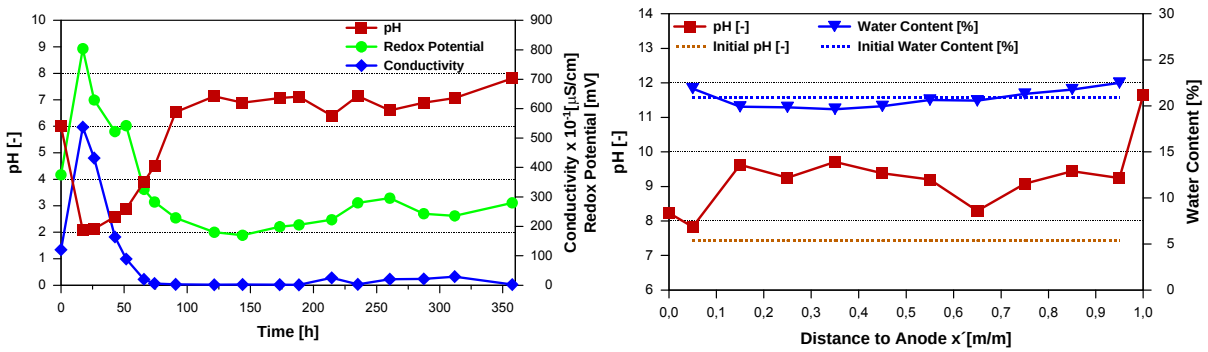

Fig. 5.32: Developing of pH, redox potential and conductivity of the anode effluent (left). Soil pH and water content before and after the NaCl experiment (right).

5.2.2.2 Model Solution $Ca/MgCl_2$ enriched tap water, Flushing solution deionized water ($Ca/MgCl_2$_Z1)

To determine the electrokinetic retention of cations in the presence of competing ions, tap water enriched with $Ca/MgCl_2$ was used as model solution. Fig. 5.33 illustrates the development of the electric field during the experiment. In the beginning, the voltage gradient is linear across the soil. Within a few hours, the voltage gradient starts to increase between probe 5 and the cathode and moves on towards the anode. After 25 hours a steep voltage gradient between probe 2 and the anode has developed, where about 85% of the applied voltage falls. After 80 hours about 35% of the voltage falls near the anode and keeps quite constant until the end of the experiment. Across the rest of the soil, the voltage gradient is linear.

In the beginning, ion distribution across the soil is homogenous leading to constant voltage gradients. The rise in voltage gradient close to the cathode within the first couple of hours marks the position of a zone depleted in ions. There are two possible explanations:

- OH^- produced at the cathode causes precipitation when entering the soil. The depletion in ions causes an increase in voltage gradient near the cathode. OH^- ions move to the anode by electromigration and hydraulic flow. The trace of this "precipitation front" is documented by the trace of steeper voltage gradient from the cathode towards the anode within the first 15 hours.
- The flushing solution is deionized water. Once the low mineralised solution enters the soil it causes an increase in voltage gradient. The trace of steeper voltage gradient from the cathode towards the anode marks the trace of deionized water.

Which effect - "precipitation front" or "deionized waterfront" - is dominating is not determinable. The same phenomenon has been observed during an experiment, where flushing direction was from the anode towards the cathode (5.2.1.3) and during experiment $Ca/MgCl_2$-Z2 (s. Section 5.2.2.3) where not deionized water but the initial solution was also the flushing solution.
Between probe one and two OH^- ions meet H^+ ions and form water. This waterfront is characterised by depletion in ions, which causes a steep voltage gradient that superimposes the one caused by the "deionized waterfront" and/or the "precipitation front". After circa 70 hours all of the initial $Ca/MgCl_2$ solution is displaced by deionized water and the soil core is cathode dominated.

As H^+ ions overcome hydraulic flow and move into the soil, the waterfront is not flushed out completely but forms close to the anode characterised by a voltage fall of circa 35%. The quite unstable trace of potentials (Fig. 5.33) may be due to disturbed pumping rate.

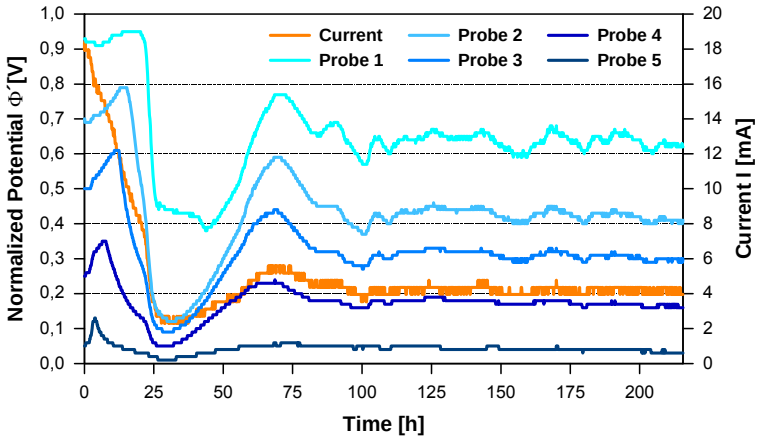

Fig. 5.33: Development of current and voltage across the soil during the Ca/$MgCl_2$_Z1 experiment.

The total discharge of Ca^{2+} and Mg^{2+} at the anode (Fig. 5.34 left) shows the same features as the more simple sodium solution in the experiment before. After 70 hours, steady-state conditions are reached and flushing out of cations ceases.

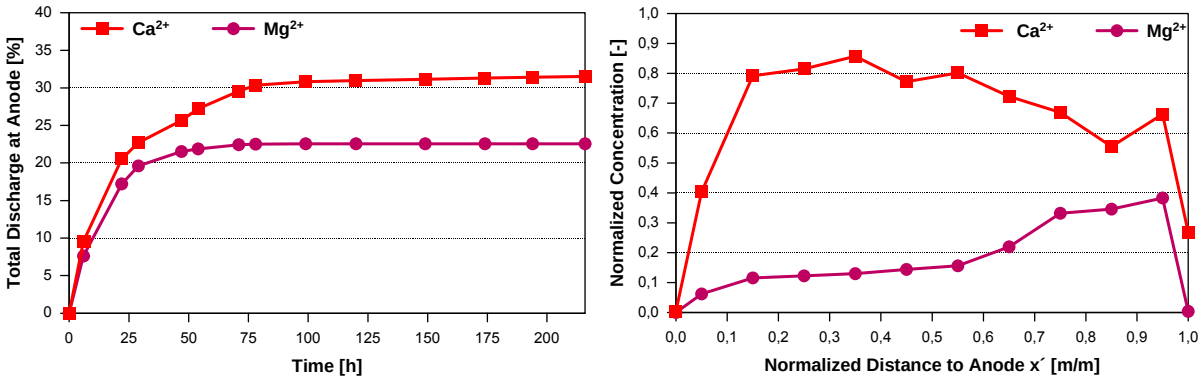

Fig. 5.34: Total discharge of Ca^{2+} and Mg^{2+} at the anode (left). Distribution of Ca^{2+} and Mg^{2+} across the soil after the Ca/$MgCl_2$_Z1 experiment (rigt).

The total discharge rate of Ca^{2+} is higher than that for Mg^{2+}. But the distribution of Ca^{2+} and Mg^{2+} across the soil after the experiment showed that the major amount of Ca^{2+} remained within the soil whereas only around 20% of Mg^{2+} could be recovered (Fig. 5.34 right). Furthermore, a quite great lack in the mass balances of these two cations was observed (12% for Ca^{2+} and 60% for Mg^{2+}).

This phenomenon can be explained by electrochemical reactions that occur at the electrodes. The electrolysis of water at the cathode led to the formation of hydroxide which is flushed with the hydraulic flow through the soil core towards the anode. Thus, an alkaline soil pH develops during the experiment (Fig. 5.35, right) resulting in the precipitation of Ca^{2+} and Mg^{2+} compounds. The lower precipitation tendency of Ca^{2+} is reflected by its higher discharge rate as well as its lower lack in balance.

Considering the pH at the cathode and in the soil, as well as the modelling results described in Chapter 7, Mg^{2+} will precipitate as hydroxide in both the cathode and the soil. Precipitation of $Ca(OH)_2$ will occur predominantly at the cathode whereas in the soil carbonates will precipitate. For further explanations, see Chapters 6 and 7. In addition, precipitation within the soil leads to a slower rise in pH and a decrease in redox conditions at the anode effluent, respectively (Fig. 5.35 left).

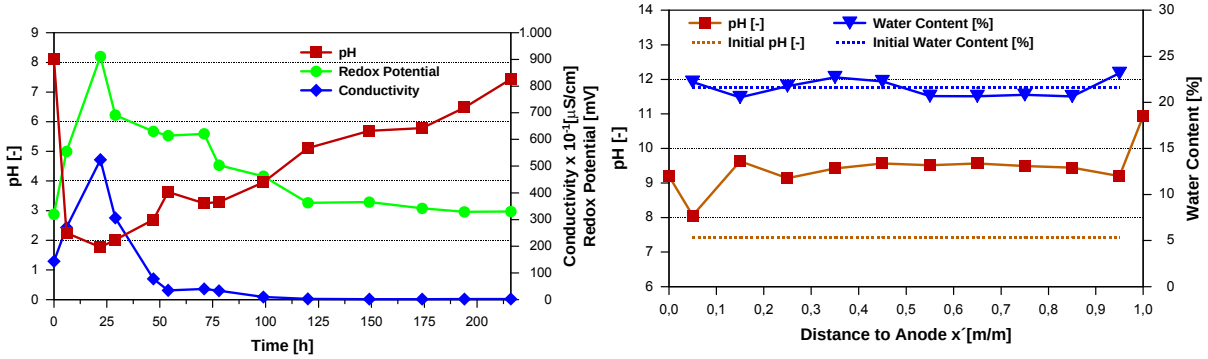

Fig. 5.35: Development of pH, redox potential and conductivity at the anode (left). Soil pH and water content before and after the $Ca/MgCl_2$_Z1 experiment (right).

5.2.2.3 Model Solution $Ca/MgCl_2$ enriched tap water, Flushing solution $Ca/MgCl_2$ enriched tap water ($Ca/MgCl_2$_Z2)

The experiment with $Ca/MgCl_2$ enriched tap water and deionized water as flushing solution showed positive results concerning the retardation of cations. Furthermore, it points out that distinct precipitation takes place as alkaline pH develops across the soil. Precipitation within the soil leads to porosity losses and should be avoided with respect to hydraulic flow variations. To verify the observations described above a second experiment with $Ca/MgCl_2$ enriched tap water was carried out. This time, constant ion supply should be simulated. Furthermore, the portion of precipitation at the cathode and within the soil were investigated. Hence, the flushing solution used was not deionized water but the soil solution itself.

Contrary to the experiments without constant ion supply, the current now increases as soon as the waterfront is moved out towards the anode (Fig. 5.36). Here the current attains constant values of about 16 to 18 mA. In the experiment with deionized water as flushing solution the current kept constant at only 4 mA. As soon as the “precipitation front” and the waterfront passed through the soil, a constant voltage gradient develops, indicating constant ion distribution. From that point on, electromigration and hydraulic flow are in equilibrium. Between probe 5 and the anode a higher voltage gradient develops implying the position where water is formed. Note that in this experiment the voltage gradient induced by precipitation is much more distinct as more ions for precipitation are available.

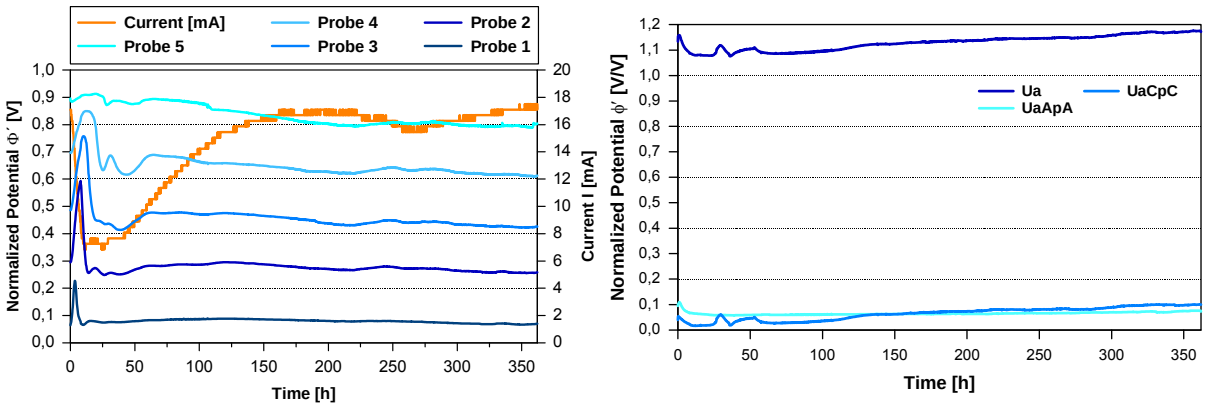

Fig. 5.36: Development over time of current and voltage (left) and trace active potential (Ua) and potential fall within the anode chamber (UaApA) and cathode chamber (UaCpC), respectively (Ca/$MgCl_2$_Z2).

The linear increase of the chloride discharge at the anode indicates that the volumetric flow rate during the experiment was constant over time (Fig. 5.37). Although constant ion supply is given, the total discharge of the cations stops like in the experiments with deionized water after three to four days. Only 8% of the total mass (including flushing volume) of Mg^{2+} and 10% of Ca^{2+} was discharged at the anode. Hence, electrokinetic retention seems to be higher than for the experiment with deionized water as flushing solution.

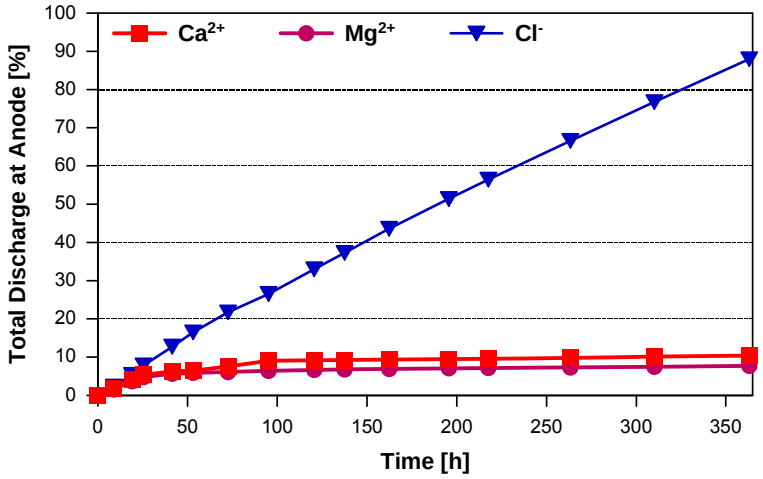

Fig. 5.37: Total discharge of Ca^{2+}, Mg^{2+} and Cl^- at the anode (Ca/$MgCl_2$_Z2).

Total recovery of Ca^{2+} and Mg^{2+} was with 19% and 12% very low. As alkaline soil pH developed during the experiment (Fig. 5.39 right), precipitation seems to be likely. The conventional eluate solution for batch experiments is deionized water. To recover potentially Ca^{2+} and Mg^{2+} precipitates an acidic eluate was used. This acidic batch experiment leads to a total recovery of 23% Ca^{2+} and 20% Mg^{2+}. Inspection of the cathode after the experiment showed that substantial precipitation took place

directly at the cathode grid (Fig. 5.40). Hence, not electromigration against hydraulic flow but precipitation because of electrochemical reactions at the electrodes is the main retardation factor.

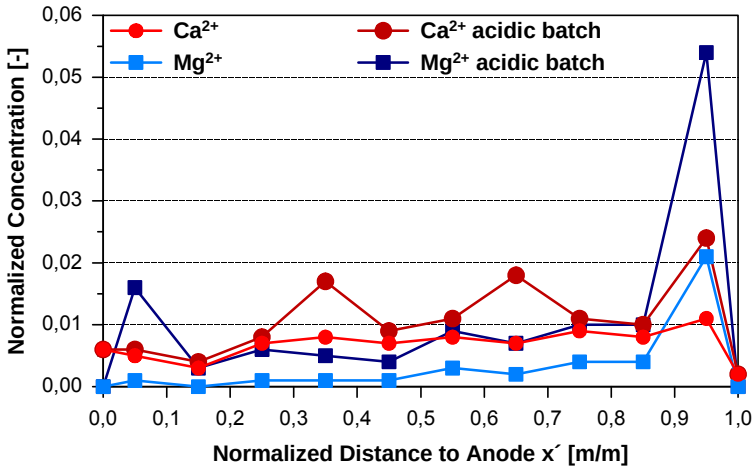

Fig. 5.38: Distribution of Ca^{2+} and Mg^{2+} across the soil body after electrokinetic experiment coupled with hydraulic gradient from cathode to anode and simulating constant ion supply (Ca/MgCl2_Z2).

The constant ion supply leads to a constant buffering of the alkaline, reducing conditions produced at the cathode. Therefore, the effluent at the anode is not neutralized like in the experiments before but is dominated by the electrolysis products of the anode. The pH, redox potential and electric conductivity develop accordingly to the break through of the flushing solution, which is also documented by the current trace (Fig. 5. 36, left).

Considering the combination of electrokinetics and reactive barriers, the results achieved implicate that a substantial amount of cations could be hindered from entering the barrier. Thus, clogging and coating within the barrier can be reduced significantly. For the constellation that the cathode is placed upstream of the anode, precipitation mainly takes place at the cathode. Hence, porosity losses and consequently changes in hydraulic parameters of the soil will be small. Nevertheless, the buffer capacity of natural soil is much higher, and soil pH will not become that alkaline as in the small-scale laboratory experiments, and as a result precipitation tendency will be even lower.

The experiments show that OH^- ions are mainly consumed by precipitation reactions. At the anode acidic and oxidative conditions develop. This high acidic and oxidative water will be transported with hydraulic flow. Hence, the changed Eh/pH conditions generated by electrokinetic processes have to be considered and their effect on the reactive barrier has to be investigated.

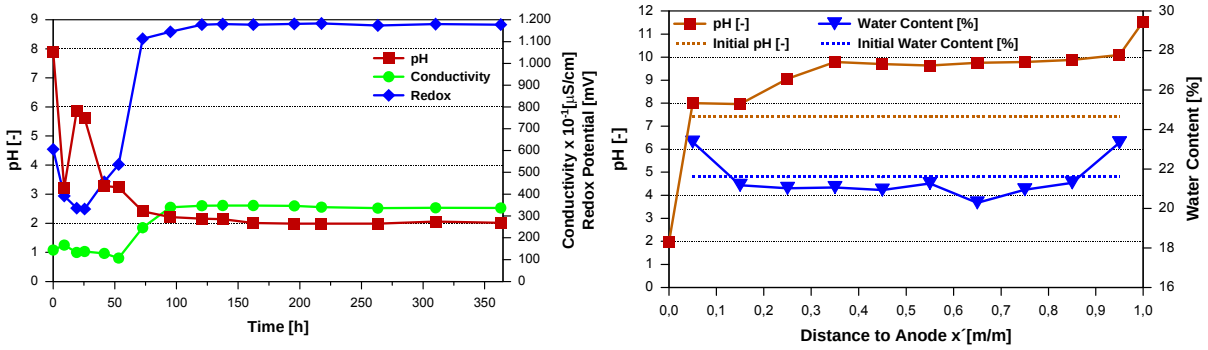

Fig. 5.39: Development of pH, redox potential and conductivity of the anode effluent (left). Soil pH and water content before and after the Ca/$MgCl_2$_Z2 experiment (right).

Fig. 5.40: Cathode after the electrokinetic experiment coupled with hydraulic gradient from anode to cathode and simulating constant ion supply (Ca/$MgCl_2$_Z2).

6 RESULTS - CONTAINER EXPERIMENTS

Small-scale experiments showed very promising results regarding the electrokinetic retention against a hydraulic gradient of both anions and cations (Section 5.2). On basis of these experiments, the test-apparatus was scaled up. The dimension of the experimental set-up was 60 cm x 30 cm x 30 cm (the so-called "container", s. Fig. 3.3 in Section 3.2). The soil/materials used have been characterised in Section 4.3. The model contaminants were NaCl, and $CaMgCl_2$ enriched tap water, respectively (s. Section 4.4). Li^+ was used as tracer. An overview of the test conditions for the container experiments is given in Table 6.1.

As discussed in Chapter 1 the implementation of an electrokinetic fence seems to be the most promising and reasonable combination with reactive barriers. The constructed container set-up allows simulating different electrode and electric/hydraulic field configurations (Fig. 4.3). Both, plane or well electrodes can be installed. An electric field parallel as well as perpendicular to the hydraulic flow direction can be generated. Furthermore, the implementation of reactive material is possible. Thus, various construction methods for an electrokinetic fence can be tested.

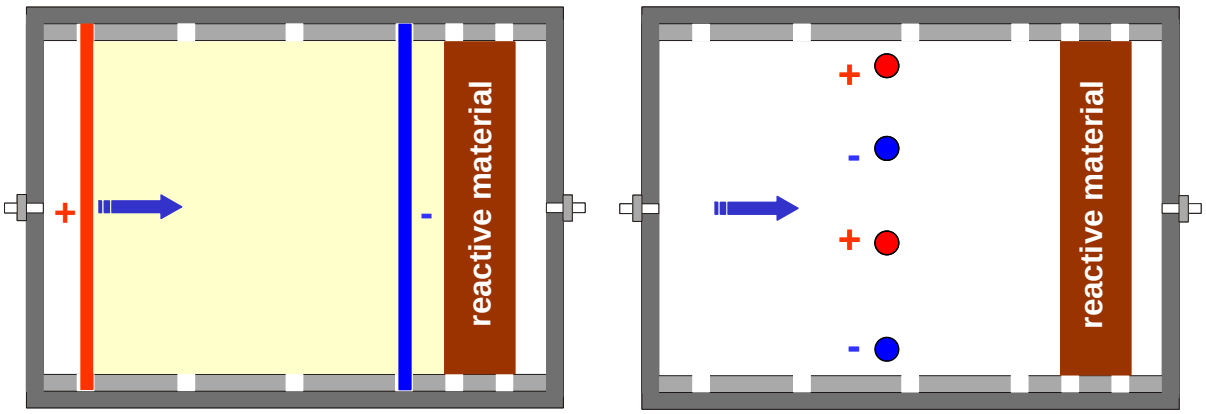

Fig. 6.1: Examples for container tests. Left: plane electrodes, electric and hydraulic gradient parallel. Right: well electrodes, electric and hydraulic gradient perpendicular.

In this work, the results of three different container experiments are presented. To test the correct function of the container and plane electrodes, the experiment series starts with a simple and relatively easy to handle experiment. Comparable to the electrokinetic cell experiments, NaCl was used as model solution and the retardation of Cl^- was investigated.

For simulating an electrokinetic fence, two different methods concerning type of electrodes and direction of electric/hydraulic field were tested. For both experiments $CaMgCl_2$ enriched tap water was used as model solution. The first test/method investigated the retardation of cations for the case of plane electrodes being installed upstream of reactive material (Fe^0). Thus, electrical and hydraulic gradients were directed parallel. This construction is for example applicable if certain groundwater constituents, such as calcium, have to be hindered from moving into the barrier to prevent unfavourable precipitation reactions. Uncharged organic molecules would flow unhindered through the electrokinetic fence into the reactive barrier.

The use of well electrodes is even more variable in respect of application possibilities. Nevertheless, literature review shows no laboratory-scale experiments with well electrodes in sandy soil in laboratory scale. In the present study, two pairs of well electrodes were installed in a way that their generated electric field is directed perpendicular to the hydraulic flow (Fig. 6.11). One of the main advantages of this electrode array is that both anions and cations are retarded simultaneously. Thus, the amount of total dissolved solids in the groundwater and therefore the total precipitation rates within the reactive wall is reduced. Furthermore, this electrode array geometry can be used to introduce and transport ionic nutrients across the plume to support microbial degradation of organic contaminants. In addition, ions can be distributed more equally across the aquifer to even consumption and precipitation rates.

The basic requirement for the successful application of electrokinetics is the efficiency of the electrodes. Within fine-grained soils where electroosmosis takes place the breakthrough of oxygen at the cathode and the rise in redox potential, respectively, is a common indicator for their efficiency. For coarse-grained soils where only electromigration takes place no indication method for its efficiency is mentioned in the literature. In this work, the application of Li^+ as an easy-to-handle tracer was tested for the first time. Li^+ was fed at the anodes. According to its electric charge, it moves towards the cathode by electromigration. Thus, the aim is to proof that this method is suited to check the efficiency of the electrodes on the one side and the put in of substances into the soil on the other hand.

Li^+ was chosen as tracer because of:

- its high chemical stability, particularly with regard to pH (pK LiOH = 13.4)
- its similar transport behaviour in soil solution to the primary cations Na^+ and K^+
- its physiological innocuousness
- its low sorption capacity due to its low tendency of ion exchange
- it is easy to analyse
- it is not oxidized at the anode, like many organic and inorganic tracers (e.g. bromide, iodide, uranin)

Kaolin was used to seal the electrode compartments and to provide better electrical connection between electrodes and soil. On the one hand, kaolin shows almost higher k_e-values than, e.g., bentonite. On the other hand, its sorption capacity and hence cationic exchange capacity is much lower. Thus, ions are adsorbed less to its surface.

Summarizing, the principle aims of the well electrode experiment are:

- Detection of temporal variations in electric field distribution as well as changes in pH, ion distribution and formation of species.
- Investigation of the retardation behaviour of ionic species within an electric field perpendicular to hydraulic flow direction.
- Development of an easy handling tracer method to prove the efficiency of electrodes in coarse-grained soils.

Table 6.1: Test conditions for the container experiments.

Parameter	**Unit**	**NaCl test + plane electrodes**	**$CaMgCl_2$ test + plane electrodes**	**$CaMgCl_2$ test + well electrodes**
Voltage	V	45	20	20 / 40
Current	mA	65-255	38-170	8-28
Electric Field	V/m	94	100	
Electric Field A1/K1	V/m			166/333
Electric Field A2/K2	V/m			204/408
Distance between electrodes	cm	48	20	12 (A1/K1) / 9.8 (A2/K2)
Duration	d	8.7	12.2	14
Model Solution	mol/l	0.01 NaCl	0.02 $CaMgCl_2$ enriched tap water	0.02 $CaMgCl_2$ enriched tap water
Flushing Solution	mol/l	deionized water	deionized water	$CaMgCl_2$ enriched tap water
Hydraulic Gradient	-	0.001	0.001	0.001

6.1 Model Solution NaCl, Flushing Solution Deionized Water

To evaluate the applicability of the container set-up, NaCl was used as model solution as its geochemical reactivity is low and results can be compared with those achieved in the small-scale electrokinetic cell. By applying a hydraulic gradient from the anode towards the cathode the electrokinetic retardation of Cl^- was investigated. The electric and hydraulic conditions during the container experiments were kept similar to the one of the electrokinetic cell experiments. The distance between the electrodes was 48 cm, the constantly applied voltage was 45 V. The applied field

strength was 94 V/m; the applied hydraulic gradient was 0.001. Plane electrodes were implemented directly at the ends of the soil with a filter membrane used as suffusion protection. Two rows of probes were placed across the experiment array.

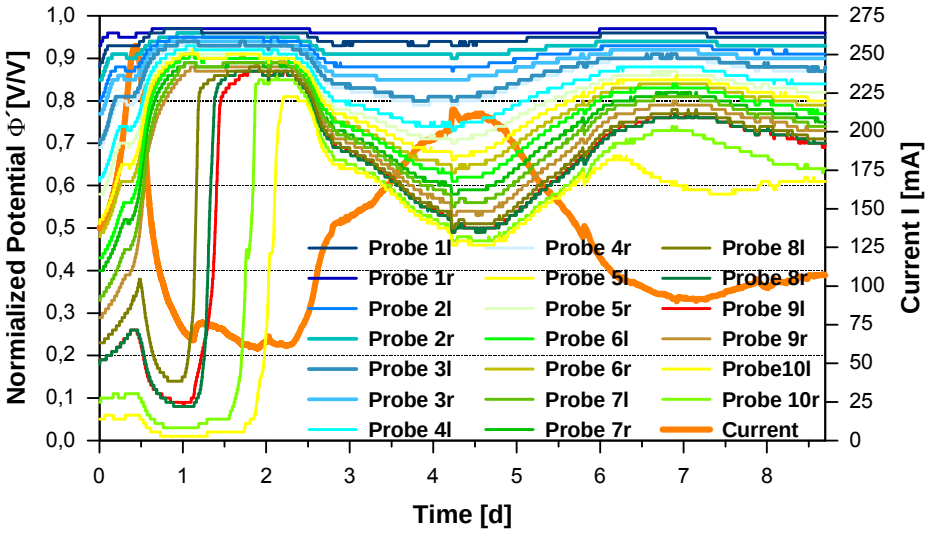

Fig. 6.2: Temporal developing of current and voltage at the different probes (NaCl). “l” marks the left, “r” the right probe row relating to flow direction, numbers increasing with flow direction (1 is close to the anode, 10 close to the cathode).

In the beginning, the voltage gradient is linear across the soil body (Fig. 6.2). After 0.5 days, the waterfront develops between Probe 8 and 9 at a distance of 6.5 cm from the cathode, indicated by a steep voltage gradient. The position of the waterfront is moved towards the cathode by hydraulic flow. The steep voltage decline between probe 10 and the cathode indicates that the waterfront is not flushed out of the soil body completely but develops close to the border between soil and cathode membrane. Obviously, the electromigration velocity of hydroxyl ions is high enough to counteract the hydraulic flow, and hence OH^- moves a few millimetres to centimetres into the soil. The variations in the voltage gradient between probes 9/10 and the cathode mark variations in the absolute position and the expansion of the waterfront which is characterised as a zone depleted in ions (Fig. 6.3). Hence, the trend of the current is inverse to the expansion (and development) of the waterfront. The increase in current in the beginning is due to the production of H^+ and OH^- ions leading to a high electric conductivity (Fig. 5.32). Flushing with deionized water and formation of the waterfront result in higher electric resistance and hence a decrease in current. Once the waterfront is positioned very close to the cathode, the current increases again. While no chloride is flushed out after one day by-and-by all the Na^+ is transported towards the cathode by electromigration and hydraulic flow. Both the discharge of Na^+ as well as the flushing with deionized water leads to a decreasing current. In the end the pore solution is solely dominated by HCl (Fig. 6.3) and current only depends on the expansion of the waterfront. Note the small differences between

left and right probes, which are related to slight differences in their absolute position within the soil body.
Like in the small-scale experiments, steady-state conditions of total discharge of Cl^- at the cathode were achieved soon (Fig. 6.3), indicating the balance of electromigration and hydraulic transport of Cl^-. Note that in the beginning almost 10% of the initial Cl^- content of the whole system was within the cathode chamber. Thus, the registered Cl^- discharge principally can be attributed to the Cl^- placed within the cathode chamber.

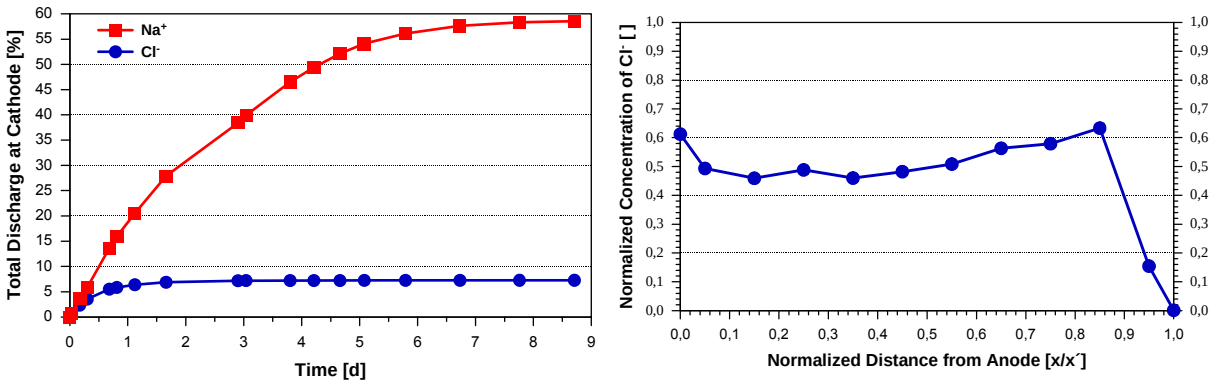

Fig. 6.3: Total discharge of Na^+ and Cl^- at the cathode during (left) and distribution of Cl^- across the soil body after (right) the NaCl container experiment.

This fact is also documented by the distribution of Cl^- across the soil after the experiment (Fig. 6.3 right). About 50% of Cl^- remained in the soil body proving the successful electrokinetic retention of Cl^-. 10% of it is discharged at the cathode; the lack in the balance (37%) can be explained by oxidation of chloride to chlorine gas at the anode (s. Section 2.2.3.6). Furthermore, there is a zone depleted in Cl^- close to the cathode, which coincides with the position of the waterfront and a steep voltage gradient, respectively (Fig. 6.2).

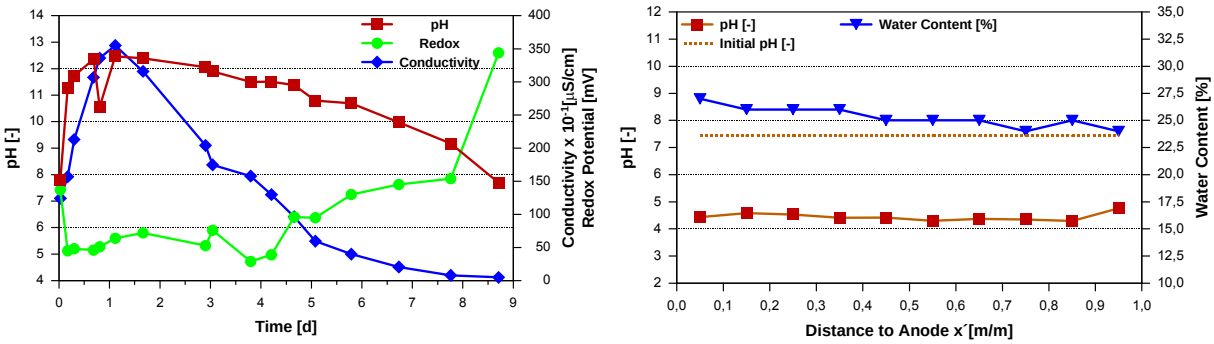

Fig. 6.4: Temporal development of pH, redox potential and conductivity of the anode effluent during the NaCl container experiment.

The development of electric conductivity and pH of the cathode effluent reflects the development of ion concentrations over the experiment time (Fig. 5.32). First, conductivity increases steeply due to the formation of electrolysis products and the accelerated discharge of Na^+, followed by an abrupt decrease indicating rapid depletion in ions. The latter is a result of the waterfront entering the cathode chamber and flushing with deionized water. At the cathode, reductive conditions develop due to electrochemical electrode reactions. The steep increase in redox at the end of the experiment is probably caused by dissolved oxygen that was transported by hydraulic flow from the anode towards the cathode.

The results of the NaCl bench-scale container experiment coincides with the small-scale electrokinetic cell experiments. Hence, it is possible to transfer the principle mechanisms to larger dimensions.

6.2 Model Solution $Ca/MgCl_2$ enriched Tap Water, Flushing Solution Deionized Water

The results of the previous experiments show that electrochemical reactions and hydraulic flow have a great influence on the variations in Eh/pH conditions. Retention processes within permeable reactive barriers are strongly dependent on Eh/pH conditions (Section 2.1). For simulating an electrokinetic fence, electrodes were placed upstream of reactive material. Fe^0 was chosen because it is one of the most established materials used in permeable reactive barriers. Aim of the experiment was to investigate the influence of electrokinetic processes on the reactive material as well as on chemical species formation and distribution. The two-dimensional developing of the electric field was measured by two rows of passive probes to get information of ion distribution and pH conditions during the experiment.

The experiment was carried out with 0.002 molar $Ca/MgCl_2$ enriched tap water. To make balancing easier the flushing solution used was deionized water. A pre-test was undertaken to optimise the test conditions for this experimental set-up. The hydraulic flow direction was adjusted from the cathode towards the anode to examine electrokinetic retardation of cations. In addition, elemental iron (properties s. Section 3.3) was implemented as a reactive material. Plane electrodes were implemented directly into the soil with a filter membrane used as suffusion protection. To simulate realistic conditions the electrodes were placed upstream of the reactive material forming an electrokinetic fence (Fig. 6.5). Hence, electric and hydraulic gradient were directed parallel. The distance between the electrodes was 20 cm, between anode and iron 10 cm, and the iron layer was 10 cm thick. Note that the electric field only acts between the electrodes and thus only affects ions that are present between the electrodes. Therefore, ions outside of the electric field are transported by hydraulic

flow and diffusion soluly. Two rows of probes (passive electrodes) are placed across the experiment array (Fig. 6.5).

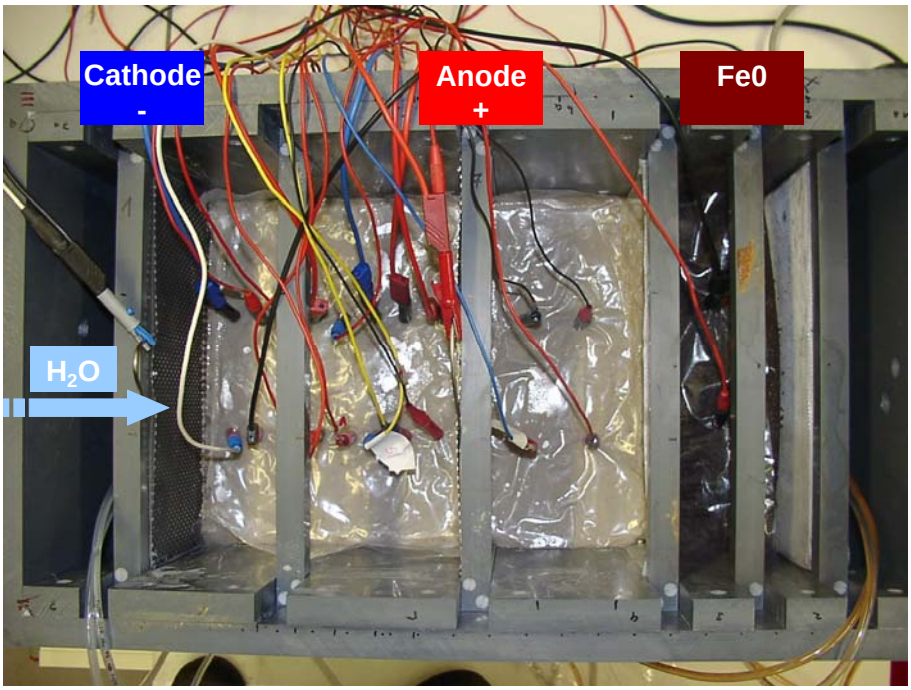

Fig. 6.5: Container experiment with electrokinetic fence upstream of reactive material.

Fig. 6.6 illustrates the development of voltage gradients during the experiment. In addition, the distribution of the electric field for different times is visualised in Fig. 6.7. Note the lines displayed in Fig. 6.7 are equipotential lines, connecting points with equal potential values. The migration direction of the ions is perpendicular to these lines.

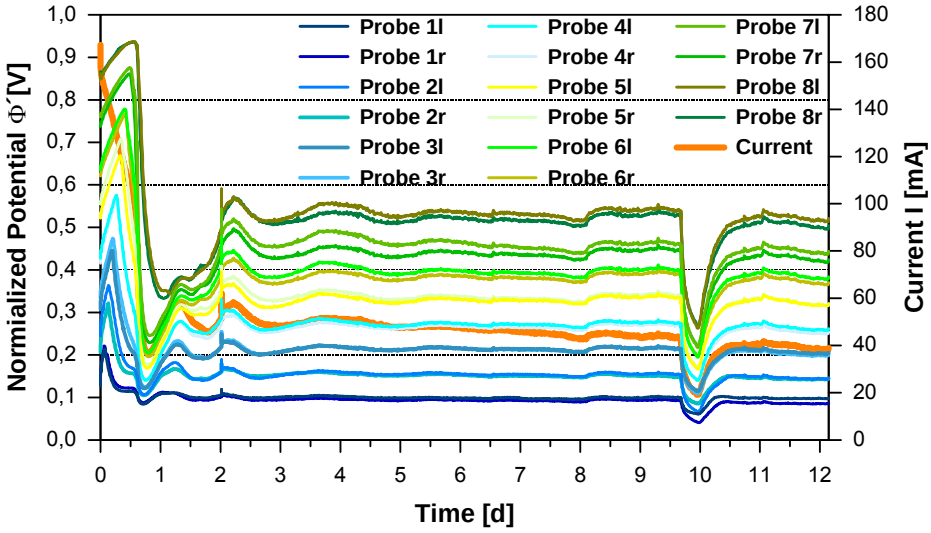

Fig. 6.6: Temporal development of current and voltage at the different probes ($CaMgCl_2$). Two rows of electrodes, “l” marks the left, “r” the right probe row relating to flow direction, probe 1 is next to the cathode, probe 8 is next to the anode.

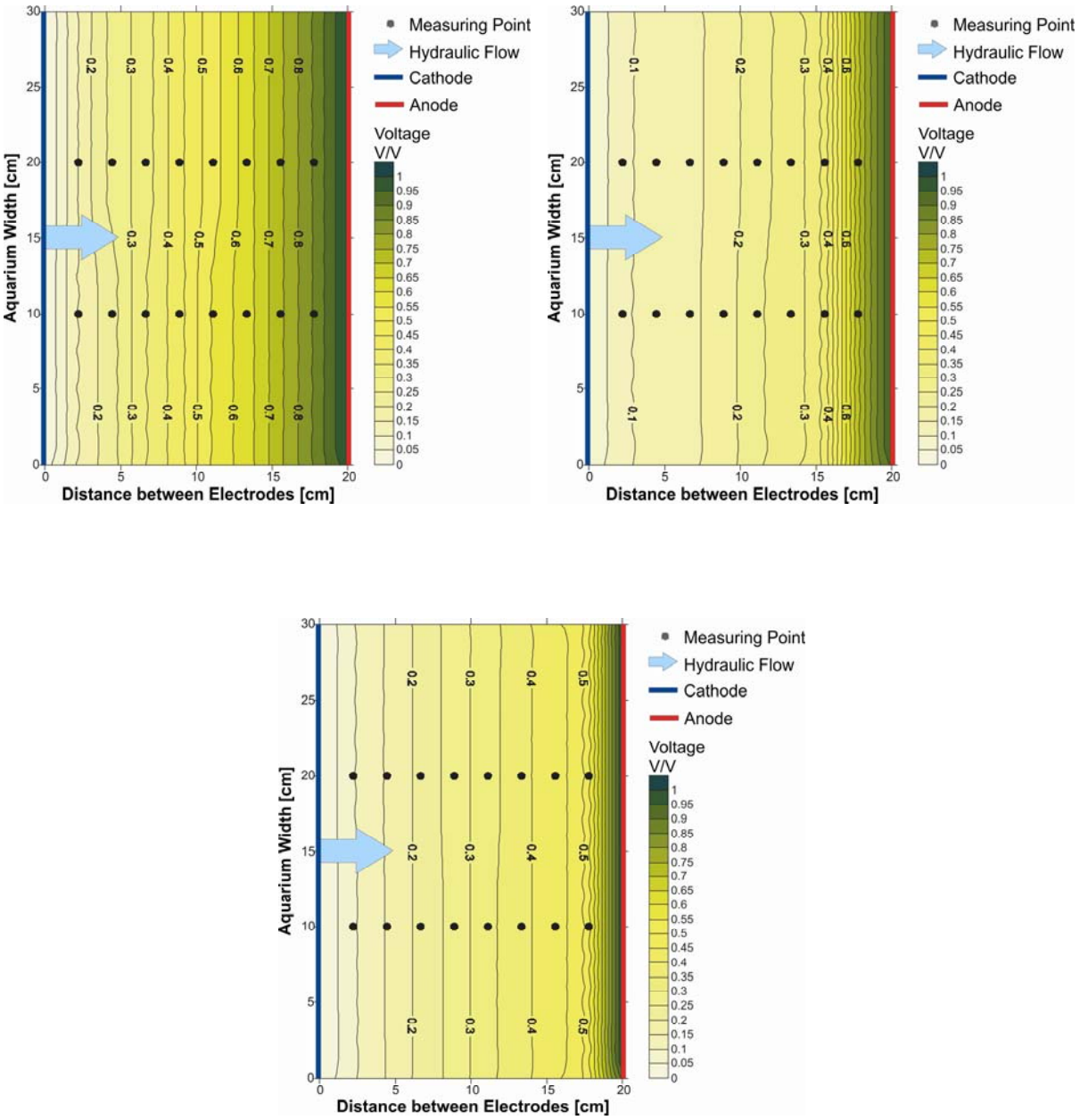

Fig. 6.7: Distribution of the electric field for different times; top left t = 0 days, top right t = 0.65 days, bottom t = 6 days.

In the beginning, the voltage gradient is linear across the soil body. Like during the electrokinetic cell experiments (Fig. 5.36), a steep voltage gradient develops, where about 60% of the applied voltage falls. After 2 days, 45 % of the voltage falls near the anode and keeps constant until the end of the experiment. Across the rest of the soil, the voltage gradient is linear. Note the increase in voltage fall at day ten is due to technical problems, which caused failure of the hydraulic gradient and lead to a wider zone of water formation. In the beginning, ion distribution across the soil is

homogenous leading to constant voltage gradients. OH^- production at the cathode causes precipitation within the cathode and in the soil. In addition, the flushing solution used is deionized water characterised by low mineralization. Hence, both processes result in depletion in ions, which causes an increase in voltage gradient near the cathode. OH^- ions move to the anode by electromigration and hydraulic flow, deionized water by hydraulic flow.

The trace of this “low ion concentration front” is documented by the trace of a steeper voltage gradient from the cathode towards the anode within the first 15 hours. Which effect – “precipitation front” or “deionized waterfront” – is dominating is not determinable. The same phenomenon has been observed during electrokinetic cell experiments (Section 5.2.2). Between probe 7 and 8, at a distance of 4.4 cm from the anode, OH^- ions meet H^+ ions and form water, and a steep voltage gradient develops. After two days all of the initial $CaMgCl_2$ solution between the electrodes is displaced by deionized water. Hence, electric conductivity differences between pore solution and waterfront decrease. From then on voltages are constant across the soil body, indicating an even ion distribution controlled by the equilibrium between electromigration, precipitation and hydraulic flow. The depletion in ions by precipitation, the development of the waterfront and the flushing with deionized water leads to a distinctive decrease in current.

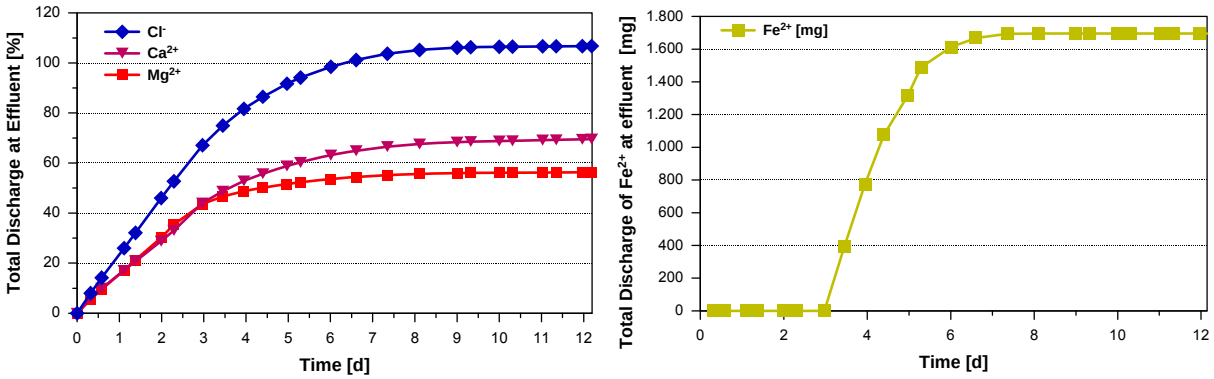

Fig. 6.8: Total discharge of Ca^{2+}, Mg^{2+} and Cl^- (left; %) and Fe^{2+} (right; mg) at the effluent.

The trace of total discharge of the main ions (related to the total volume at the beginning of the experiment, including influx and efflux reservoirs) show the same features as in the experiments before, indicating the separation of ions and the balance between electromigration and hydraulic flow (Fig. 6.8). Within the first three days, discharge rates are linear and particular high because ions placed outside of the sphere of action of the electrical field are released; the flushed volume is equal to the pore volume outside of the electric field. These ions are transported by hydraulic flow and diffusion. The slope of Cl^- discharge is steeper due to the fact that between the electrodes Cl^- transport is accelerated by electromigration and hence, more Cl^- is

flushed out per unit of time. In addition, Ca^{2+} and Mg^{2+} may be retarded within the Fe^0.

From day three onwards, the discharge of cations decreases indicating successful retention of ions´ portion located between the electrodes. After eight days, the volume of the $CaMgCl_2$ solution is displaced by deionized water completely. Discharge of Ca^{2+} and Mg^{2+} and Cl^- cease, indicating a balance between electromigration/precipitation and hydraulic flow. At the end of the experiment, no Cl^- but about 30% of Ca^{2+} and over 40% of Mg^{2+} is retarded. In relation to the portion placed within the electrodes almost total retention took place (Fig. 6.9). The lower Mg^{2+} discharge is mainly related to its higher precipitation tendency at lower pH. Note that to a minor extent Ca^{2+} may react with CO_3^{2-} of the tap water to form carbonates (Chapter 7).

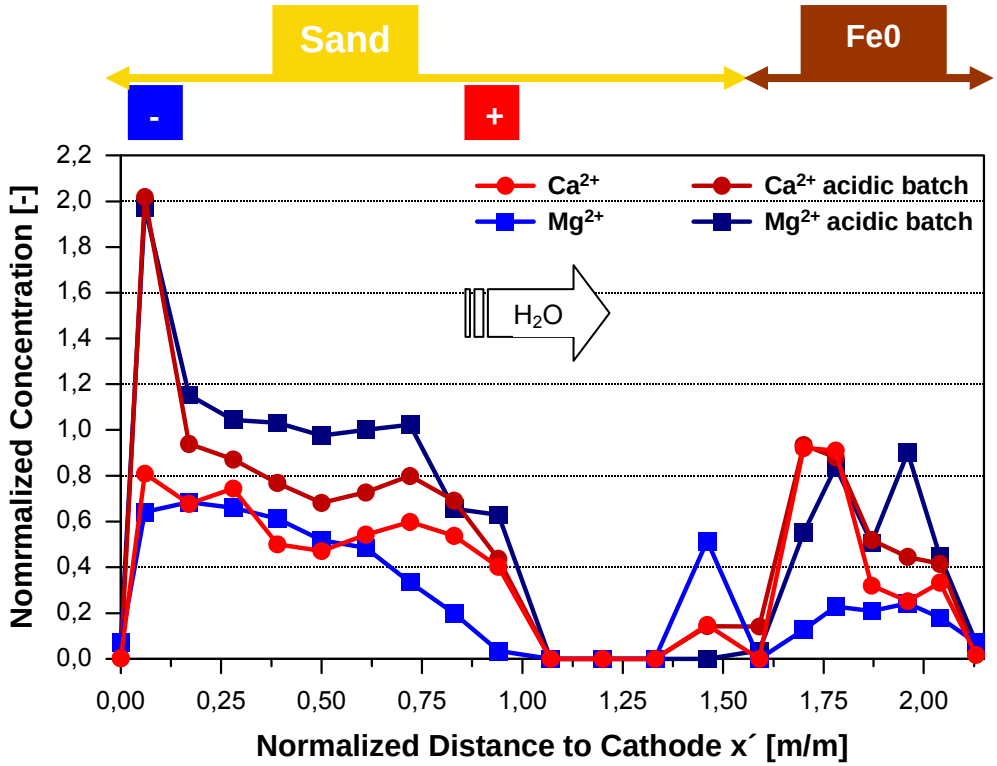

Fig. 6.9: Distribution of Ca^{2+} and Mg^{2+} across the soil body after container experiment coupled with hydraulic gradient from cathode to anode (concentrations normalised to initial concentrations of the compounds)

After the experiment, the soil was eluated with both deionized water and acidic eluate to recover potential precipitates. Note that the soil core can be separated into three different zones with regard to application of an electric field and differences in material. These three zones are “sand within the electric field”, “sand outside the electric field”, and “reactive material outside of the electric field”. The distribution of

the cations across the soil after the experiment reflects the different retention tendencies of these three zones (Fig. 6.9).

Within the electric field, the cation concentration in the pore solution increases towards the cathode and is low in the zone of water formation. All in all the final cation content is almost equal to the initial one. The acidic batch shows that the precipitation rate clearly is highest in the cathode's vicinity and is higher for Mg^{2+} than for Ca^{2+}. Distinct precipitation of Mg^{2+} also takes place within the elemental iron, but only for a minor extent of Ca^{2+}. In contrast, in the sand zone between anode and iron (outside of the electric field) virtually no cations are retarded.

The distribution characteristics of the cations after the experiment can be explained by the distribution of soil pH (Fig. 6.10). Between the electrodes, pH is approximately 9.5, within the elemental iron close to 9, whereas in the sand in-between soil pH is around 6. Thus, the precipitation tendency within the different zones is a result of the pH development within the soil. The soil pH itself is a result of electrochemical reactions at the electrodes, hydraulic flow and geochemical conditions within the Fe^0 zone. At the cathode, hydroxide ions are produced which are flushed towards the anode by both electromigration and hydraulic flow. Hence, the zone between the electrodes is cathode-dominated (alkaline), with the cations Ca^{2+} and Mg^{2+} and the electrolysis product OH^- being the main ions in soil solution. Close to the cathode OH^- concentration is highest leading to high precipitation rates. The higher Mg^{2+} concentration appears simultaneously with its higher precipitation tendency (for more detailed explanations see Chapter 4 and explanations in Section 6.3).

At the anode, hydronium ions are generated reacting with hydroxide ions to water. Soil pH between the anode and the iron is more acidic than the initial pH. Obviously H^+ ions dominate, as precipitation reactions consume OH^- ions. In addition, within the elemental iron, alkaline pH is generated due to redox reactions that take place within this zone, as described in the literature (s. Section 2.1). Note that Fig. 6.9 also illustrates that for Mg^{2+} precipitation at the cathode seems to be the dominating retention process, whereas for Ca^{2+} the proportion of electrokinetic retention within the soil body is much higher.

Fig. 6.10 shows the development of pH, redox and electric conductivity of the effluent during the experiment. Note that in all previous experiments the effluent was measured directly at the anode or cathode. Hence, the measured values reflect the conditions that exist at the electrodes at that time. In this case, for a particle at the anode it takes about 2.5 days until it is registered at the effluent. Furthermore, it passes the Fe^0 zone on its way. Hence, the measured values are time-delayed and reflect conditions that are altered by the Fe^0 zone.

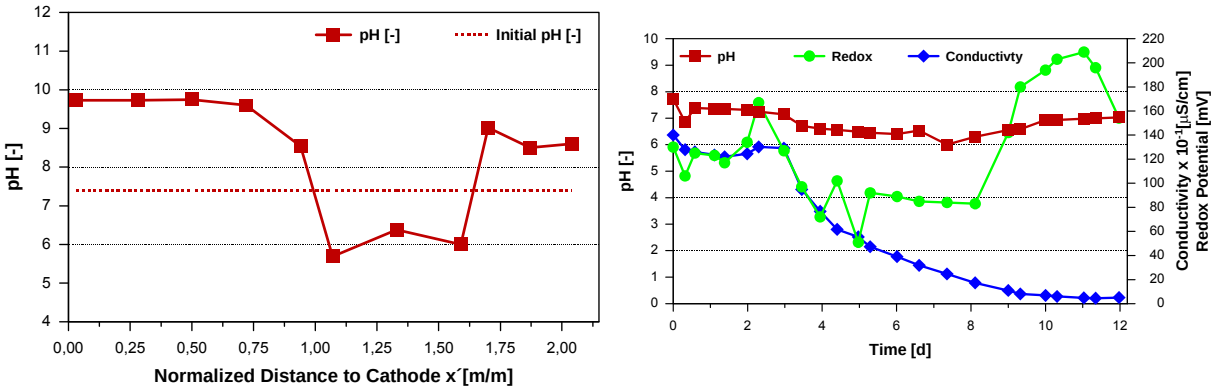

Fig. 6.10: Soil pH (left) and development of pH, redox and electric conductivity of the effluent (right) during the $CaMgCl_2$ container experiment.

Electric conductivity of the eluate is constant at first, then strongly decreases after three days and reaches constant low values at the end of the experiment (Fig. 6.10). Between day three and eight, substantial amounts of Fe^{2+} are discharged (Fig. 6.8). The period of Fe^{2+} discharge coincides with more reductive redox conditions and slightly more acidic pH values (Fig. 6.10). Once no Fe^{2+} is released anymore redox values jump towards more oxidative conditions. After three days, the portion of $CaMgCl_2$ enriched tap water located outside of the electric field is already flushed out. From then on, the flushing (and effluent) solution is depleted in ions by electromigration and precipitation within the electrodes and Fe^0 zone, respectively. Furthermore, when passing the anode, OH^- reacts with H^+ to form water, which is uncharged. Finally, deionized water with low conductivity was used as flushing solution. All these factors are leading to a depletion in ions and hence decrease in conductivity.

Considering the results of the electrokinetic cell experiment described in Section 5.2.2.2, pore solution, which passed the anode and enters the Fe^0 zone, will be acidic and oxidative in the beginning before being more and more neutralised by OH^- and H_2, which are transported from the cathode towards the anode (Fig. 5.35). Generally, Fe species are strongly dependent on pH and Eh conditions (STUMM & MORGAN 1996). Considering the Eh/pH diagram of the system Fe-C-H_2O (Fig. 3.3) oxidative acidic water may lead to the dissolution of Fe^0 (Re. 1) and - if present - of $FeCO_3$ and amorph $Fe(OH)_3$. Dissolution of Fe^0 is accompanied with the release of Fe^{2+} and the development of alkaline pH and reducing conditions, respectively.

Obviously, the electrokinetics processes lead to Eh/pH conditions that favour the consumption of Fe^0. Furthermore, the oxidative and acidic anode effluent is “neutralized” by the alkaline and reductive conditions generated within the Fe^0 zone. Once the pore volume of the initial $CaMgCl_2$ solution is flushed out totally (after eight days), only deionized water characterised by very low ion concentration is supplied. Equilibrium between precipitation and electromigration in the zone between the electrodes is reached, i.e. less OH^- is consumed by precipitation. Thus, solution that

passed the anode and enters the Fe^0 zone, is quasi-neutral in pH and less oxidative. Dissolution of Fe^0 is not favoured anymore. As soil pH within the Fe^0 zone is about nine at the end of the experiment, corrosion of Fe^0 still takes place but is not very distinct.

The results show clearly how electrokinetically induced changes in Eh/pH conditions affect the stability of the Fe^0 reactive material. In nature, not deionized water but constant ion supply by groundwater flow is provided. According to the results achieved by an electrokinetic cell experiment (Section 5.2.2.3), conditions for constant ion supply would be comparable to the one registered between days three and eight. Hence, the anode effluent remains acidic and oxidative. Dissolution of Fe^0 takes place; OH^- ions are released. However, as they are neutralized by H^+ ions of the anode effluent decrease in precipitation rates is favoured. It can be assumed, that Fe^0 consumption by additional dissolution is more problematic than Fe^0 passivation by precipitation. Thus, in practice the consumption of Fe^0 by electrokinetics definitely should be avoided by applying an adequate pH control.

6.3 Model Solution and Flushing Solution $CaMgCl_2$ enriched Tap Water; Tracer LiCl

In order to enhance the electrokinetic remediation process, several authors recommend the use of a multiple electrode system or two-dimensional well electrodes (HAUS ET AL. 2002, U.S. EPA 1998). Using well electrodes is more economical, especially for treating larger contaminated areas. Their production costs are less, the installation is easier. They are applicable for contaminant plumes in great depths and can be installed horizontal for the remediation beneath buildings.

For the container test described in the following, two pairs of well electrodes (Anode1 A1 – Cathode1 C1 and Anode2 A2 - Cathode2 C2) were installed to simulate an electrokinetic fence (Fig. 6.11). In contrast to the $CaMgCl_2$ plane electrode experiment, the electric field is directed not parallel but perpendicular to the hydraulic flow direction. Thus, both anions and cations are retarded simultaneously. The soil was saturated and flushed with 0.002 molar $CaMgCl_2$ enriched tap water. After the saturation process, the anode chambers were pumped dry and refilled with 0.02 molar LiCl enriched tap water. A 10-days long pre-test was carried out to prove the principle functionality of the electrodes and to optimise test conditions. Voltage data was registered by a small-meshed grid of 65 passive probes. Using computerized linear interpolation it was possible to visualize the developing of the electric field, especially interactions and differences between the electric fields generated by the two electrode pairs (in 2 dimensions). Hence, conclusions concerning ion distribution and pH developing during the experiment were possible.

Generally, the test results were expected to provide an informative basis for the following aspects:

- Retardation efficiency of ionic species within an electric field perpendicular to hydraulic flow direction.
- Development of an easy-to handle method for proving the efficiency of electrodes in coarse-grained soils.
- Injection of nutrients into the soil.

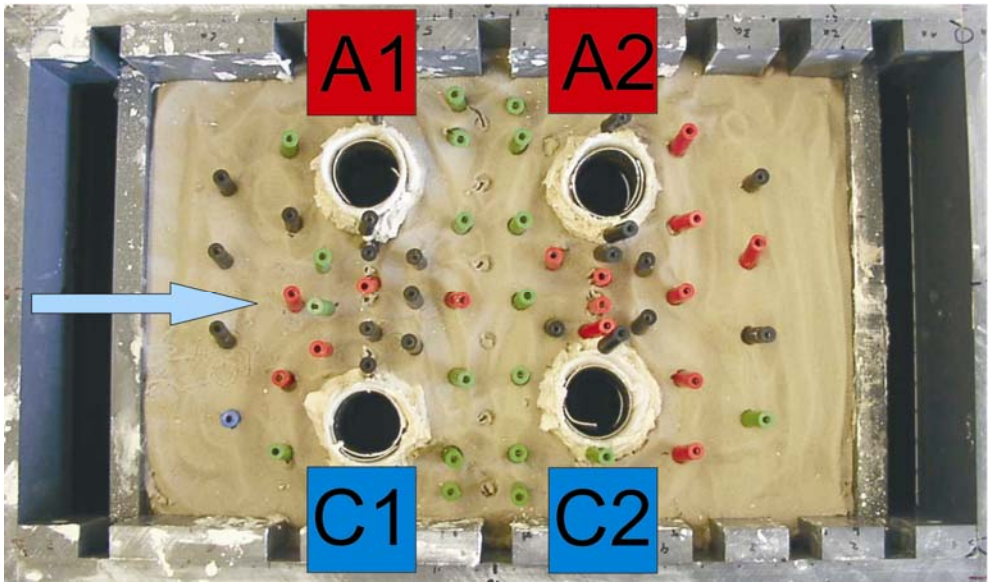

Fig. 6.11: Container test simulating an electrokinetic fence. The used array of well electrodes generate a non-linear electric field (dipole field) that is perpendicular to the hydraulic flow direction.

Computer simulations and laboratory tests of LAGEMAN & POOL (2001) showed promising results for an electrokinetic fence placed perpendicular to the groundwater flow in field scale. Nevertheless, the remediation success is only described in a quantitative way without concerning the relevant process parameters. In laboratory scale, no experiments with well electrodes in sandy soil are documented in literature. In this work, the focus is on detecting temporal variations in electric field distribution as well as changes in pH, ion distribution and formation of species. To complete the interpretation of these experimental results, a hydraulic model should be established. However, the hydraulic turbulences and pressure variations as well as hydraulic flow changes caused by the electrode array are very difficult and complex to describe by a model and go beyond the scope of this work.

For this container experiment, two pairs of well electrodes were installed. To registrate how the electric fields generated by each electrode pair influence each other, first each single pair of electrodes was connected to the dc supply separately, before switching on both simultaneously (Fig. 6.12). Note that the lines displayed in the figure are equipotential lines, connecting points with equal potential values. The

migration direction of the ions is perpendicular to these lines. The graph clearly displays that well electrodes generate an electric dipole field. Switching on both pairs of electrodes, the single electric fields superimpose each other leading to areas between the cathodes and anodes where no or only a very small electric gradient exist. Hence, within these areas electromigration rates are low and hydraulic convection may dominate. Another characteristic of the dipole field compared to the electric field generated by plane electrodes is that the electric field not only acts within the zone directly between the electrodes but in a wider area around the electrodes. Thus, groundwater ingredients within a wider area are effected by the dipole electric field. As the electric gradient is steepest in the zone directly between the electrodes (Fig. 6.12), electromigration velocities are highest in this zone (Eq. 14).

In the beginning, the steepest voltage gradient mainly occurs within the kaolin around the anodes and, to a minor extent, at the cathodes. Between the electrodes, the voltage gradient is linear. Principally, different soil media show different electrical characteristics: Lower potential gradients develop in fine-grained soils with high ion concentrations and electric conductivity; higher potential gradients in coarse-grained soil with low ion concentrations and electric conductivity. In the present experiment, the potential gradients show the opposite trends. Obviously, the connection between anode and kaolin was not sufficient and significantly influenced the voltage gradient. For practical application, it is indispensable that a good electrode/soil connection is provided to avoid unnecessary energy consumption and decreased contaminant transport, respectively.

Fig. 6.13 to Fig. 6.16 show the development of the electric field with time. Note at the beginning voltage was 20 V, whereas from day seven onwards 40 V was applied.

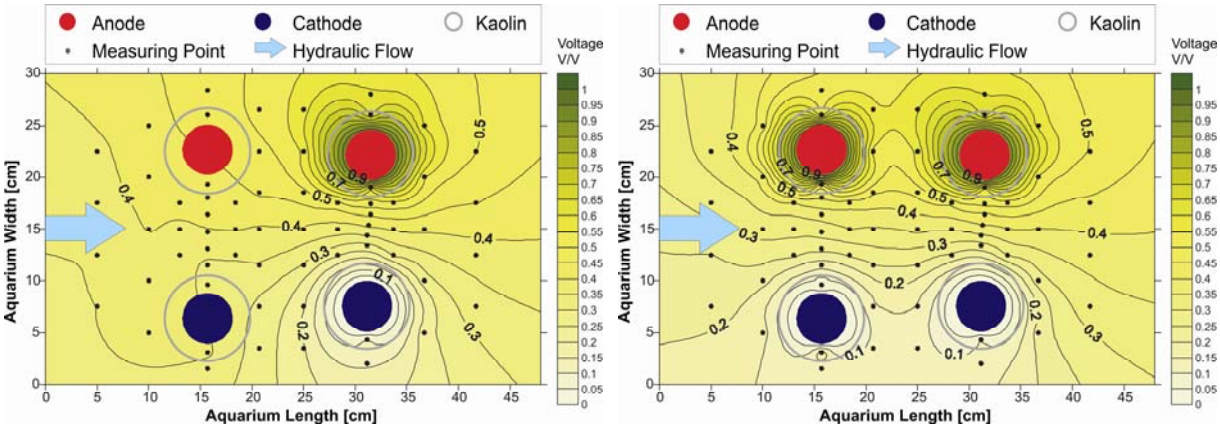

Fig. 6.12: Distribution of the electric field generated by a single pair of electrodes (left) and by both electrode pairs (right) at experiment time = 0.

Within one day, a steeper voltage gradient develops within the sand adjacent to the cathode kaolin (Fig. 6.13, Fig. 6.14). This can be explained by the depletion in ions caused by electromigration towards the cathodes and precipitation reactions as well as the development of a waterfront. All these factors result in an increase of electric resistance and hence higher voltage gradient. Principally, conditions similar to those observed during the electrokinetic cell experiments where no hydraulic gradient was applied (5.1) develop.

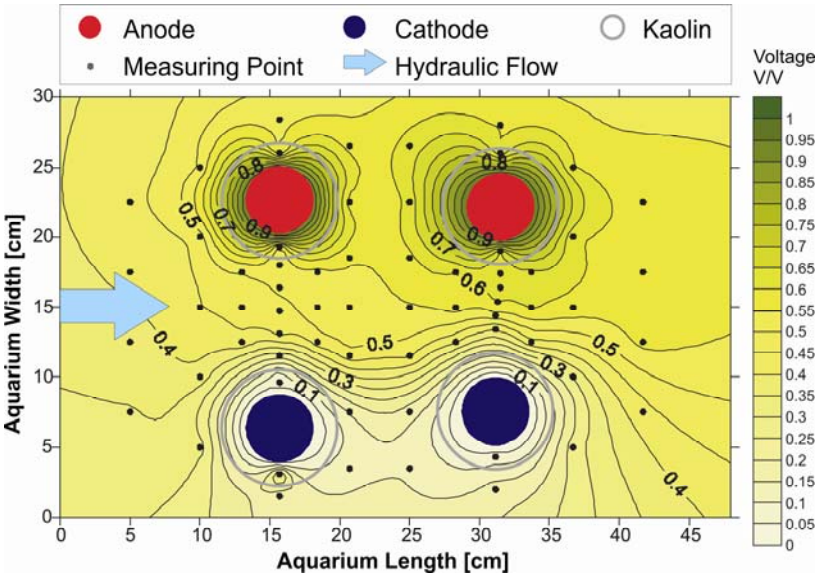

Fig. 6.13: Distribution of the electric field at day 1.

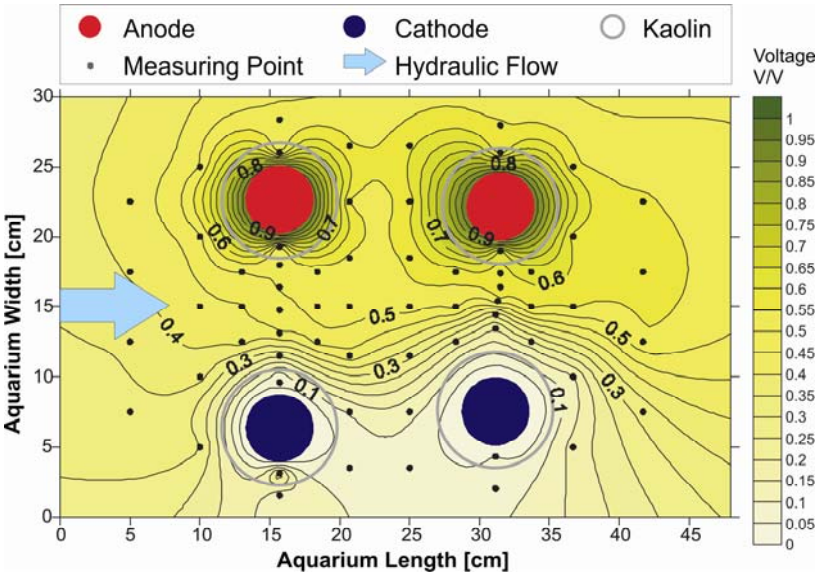

Fig. 6.14: Distribution of the electric field at day 4.

Increasing the applied voltage at day seven from 20 V up to 40 V, the drop in voltage at A1 decreases from 50% to 30% and at A2 from 40% to 25% (Fig. 6.15). Obviously, increasing voltage leads to smaller transition resistance between electrodes and soil.

From day 12 onwards, the position of the highest voltage drop between the second electrode pair is moved more towards C2. Thus, the voltage fall within the kaolin backfill at C2 increases (Fig. 6.16), which is also reflected by an increase in k_e value (Fig. 6.23). Considering the soil pH values (Fig. 6.17) it is obvious that the waterfront/acidic front migrated into the kaolin, as indicated by neutral to slightly acidic pH values (Fig. 6.17).

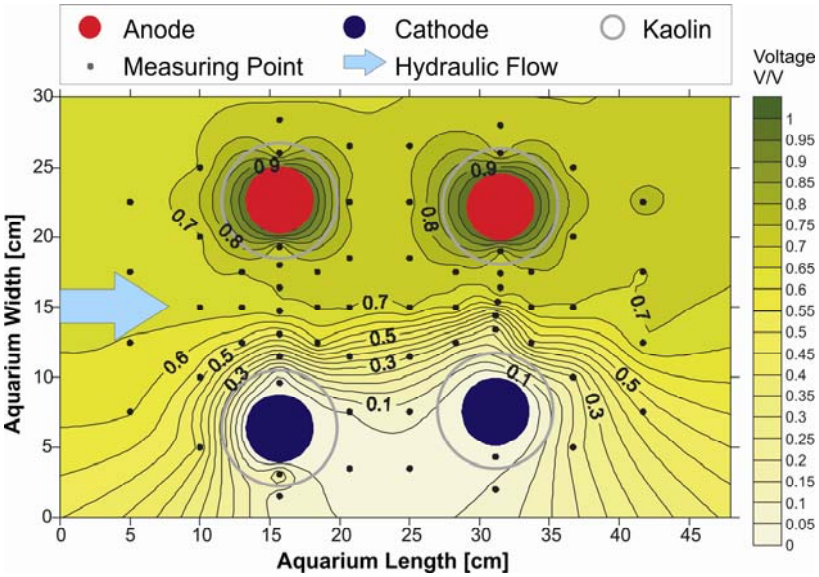

Fig. 6.15: Distribution of the electric field at day 9.

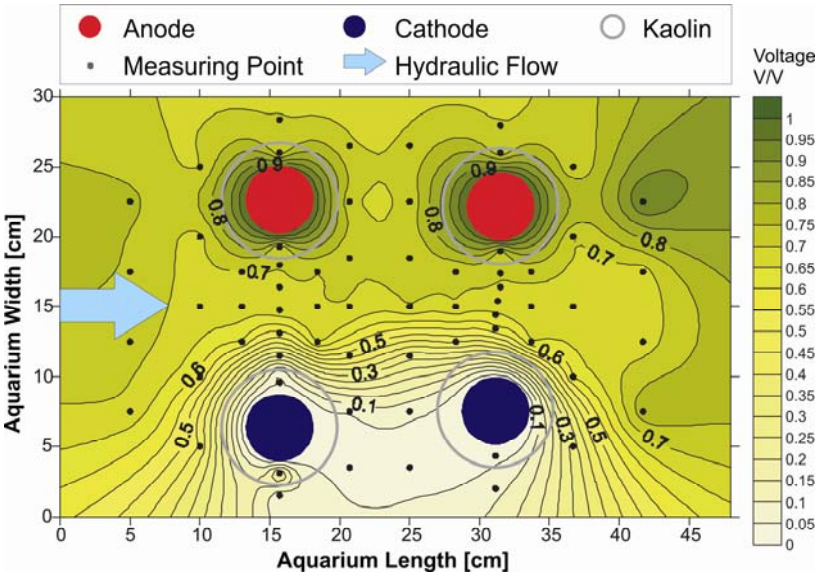

Fig. 6.16: Distribution of the electric field at day 13.5.

For all previous experiments, the position of the steepest voltage gradient coincided with the position of the waterfront and the zone depleted in ions, respectively. Here, the depletion in ions by precipitation and the accompanying increase in the voltage gradient superpose the voltage drop caused by the waterfront. According to the distribution of soil pH and electric gradient at the end of the experiment, the position of the waterfront is at the very edge of the drop in voltage (towards the anode side). Usually the position of the waterfront is closer to the cathode as the electromigration velocity of H^+ is around 1.8 times higher than that of OH^-. Fig. 6.17 shows that within the influx zone its position is shifted towards the anode whereas within the efflux zone it is shifted towards the cathode leading to a wider zone of acidic pH. The more acidic conditions at the efflux zone are also reflected by the acidic pH of the effluent (Fig. 6.26). This may be explained by turbulences caused by hydraulic flow and different consumption of OH^- by precipitation reactions due to different ion concentrations.

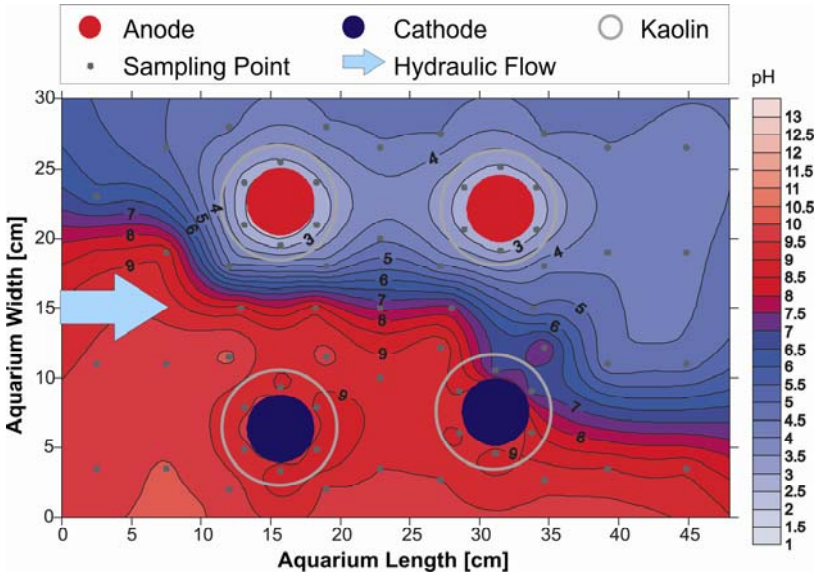

Fig. 6.17: Distribution of soil pH after the experiment.

Many soils contain a carbonate content of several percent. Hydronium ions react with the carbonate according to Reaction 7. Hence, the acidic front only moves a few centimetres into the soil – depending on remediation time and current flow. In practical applications this effect would lead to a quite broad precipitation zone. Depending on the site characteristics, the formation of an acidic and alkaline front can be avoided by addition of either a buffer or a neutralisation solution (DZENITIS 1997a, WILSON et al. 1995a,b, WILSON 1996, WONG et al. 1997), by the use of membranes (Hansen et al. 1997) or by combining the anode and cathode solution (GOLDMANN 2000).

Fig. 6.18 to Fig. 6.20 show the concentration distribution of the main ions in the soil solution. The dominating cation is Ca^{2+}, the dominating anion Cl^-. Note that the

software used (Surfer 8) interpolates linearly between two sampling points. This is correct within one soil medium (in the present case sand or kaolin). Nevertheless, between a sampling point located within the kaolin and an adjacent one located within the sand not a linear but an abrupt change in concentration would occur at the border of the two materials. In the case of Ca^{2+} this means that between the kaolin and sand at C1 a concentration drop of 600 mg/kg is more likely than the interpolated difference of 300 mg/kg. The same assumption applies for the other electrodes as well as ions. Li^{+} for example was detected solely within the kaolin but not within the sand. Furthermore, the sampling points represent concentration values of pooled/mixed samples with the sampling points being the midpoint of the sample.

The voltage gradient upstream of the electrode pair one is quite low compared to the zone directly between the electrodes. However, concentration distribution after the experiment shows that within this zone a concentration gradient already develops. Thus, electromigration velocity of the ions was high enough to counteract the applied hydraulic gradient and to move the ions to the respective oppositely charged electrodes (Fig. 6.18, Fig. 6.19, Fig. 6.20).

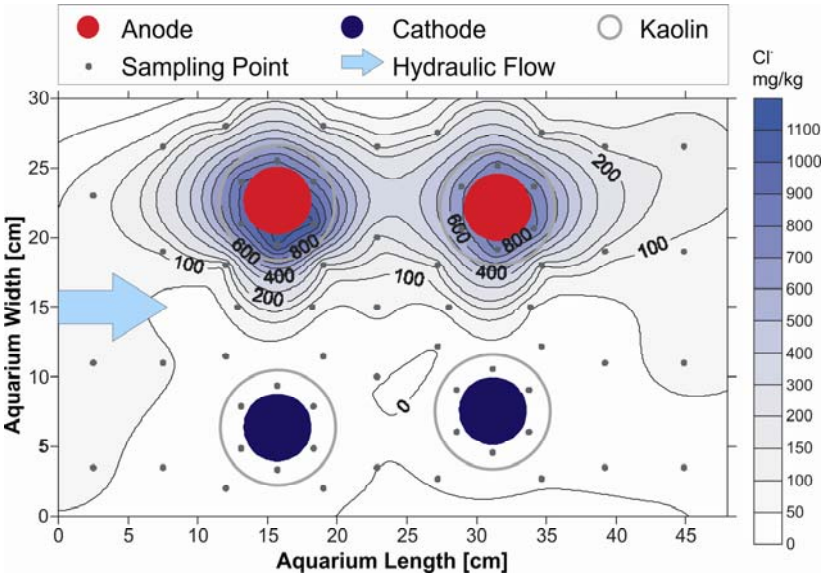

Fig. 6.18: Distribution of Cl^{-} after the experiment.

Cl^{-} is often used as anionic tracer for hydrogeological purposes. In contrast to Mg^{2+} and Ca^{2+}, Cl^{-} has no precipitation tendency over the whole range of pH (s. Chapter 7). Thus, the migration of Cl^{-} depends mainly on electromigration and hydraulic flow, and to a minor extent on diffusion. Within the influx region, Cl^{-} is distributed quite evenly across the complete lateral dimension of the soil body (Fig. 6.18). From 7.5 cm up to 42.5 cm of the container length, Cl^{-} mainly appears in the anode zone, but also to some extent in the cathode zone. From 42.5 cm to the edge of the container, the distribution of high Cl^{-} concentration (> 50 mg/kg) is broader again.

At the influx, Cl^- is added and concentrations are the same over the whole cross section. After 7.5 cm, the influence of the electric field already becomes noticeable and the Cl^- concentration increases towards the anodes. Considering the concentration distributions of Ca^{2+} and Mg^{2+} – which increase towards the cathodes – it is obvious that there is a zone depleted in ions between the electrodes. This phenomenon coincides with observations made by the electrokinetic cell experiments and predicted by theoretical models (s. Sections 4.1, 5.1). At the outflow region, the electric field is weaker and electric gradients are lower, and Cl^- disperses by diffusion and hydraulic flow. Obviously, the applied electric field is high enough to cause substantial Cl^- migration towards the anode side and into the anode, but is not high enough to cause a complete separation of ions and retardation of Cl^-, respectively. In contrast to Cl- Ca^{2+} and Mg^{2+} are additionally retarded by precipitation leading to a greater decrease in concentration while passing the first electrode pair. A complete balance is not possible as electrokinetic processes are dynamic and local (precipitation, dissolution).

Ca^{2+} and Mg^{2+} show similar concentration distribution characteristics (Fig. 6.19, Fig. 6.20), which are consistent with pH distribution. They reflect that during the experiment an anode-dominated zone and a cathode-dominated zone develop. The anode zone is characterised by low pH, the dominating ions are the main anions of the solution and H^+. The alkaline pH of the cathode zone goes along with high cation concentrations. Generally, alkaline pH values favour precipitation reactions. Batch experiments with deionized water show quite homogenous distributions of the analysed anions and cations across the soil body with low concentrations. However, the results achieved with acidic batch confirm that substantial precipitation takes place at the cathode dominated side.

Precipitation reactions are not solely dependent on pH but also on the presence of other elements, concentration ratios and temperature. With the help of chemical modelling (s. Chapter 7) the precipitation behaviour of Ca^{2+} and Mg^{2+} can be explained. Mg precipitation is quite independent on the presence of other elements and precipitates as hydroxide. Precipitation of $MgOH_2$ depends on pH and to a minor extent on concentration and temperature. Chemical modelling shows that $MgOH_2$ will precipitate from around pH 9.5 onwards (Fig. 7.1). As these pH values are achieved within the soil, precipitation indeed takes place. No Mg^{2+} is detected at the cathodes (Fig. 6.24). Hence, all residual Mg^{2+} that might migrate to the cathode chamber is consumed by precipitation.

The precipitation area of Ca^{2+} has quite the same extension as the one of Mg^{2+}. Taking the simple chemical system of Ca-O-H and Mg-O-H into account (Fig. 7.1), $Mg(OH)_2$ starts to precipitate already at pH values of about 9.5 whereas $Ca(OH)_2$ starts to precipitate only at pH values higher than 12. Thus, the phenomenon that Ca^{2+} precipitates at the same pH as Mg^{2+} remains unexplained by this simple chemical system. Further chemical modelling showed that for the given initial concentrations and in the presence of inorganic carbon species, Ca already starts to

precipitate as carbonate minerals at pH 6 (Fig 7.4). For oxidative conditions and increasing temperature and in the presence of sulphur even the precipitation of $CaSO_4$ between pH 2 and 6 is likely (Fig 7.4, Fig. 7.5).

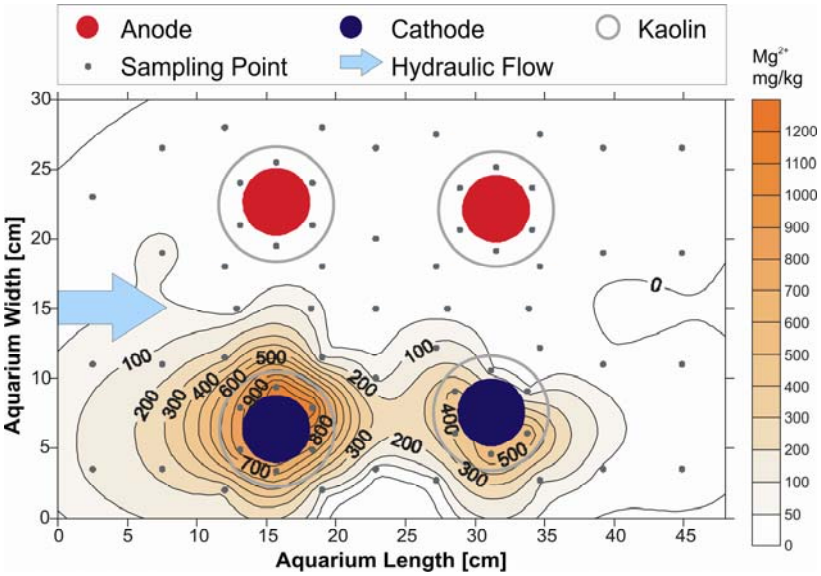

Fig. 6.19: Distribution of Mg^{2+} after the experiment (acidic batch).

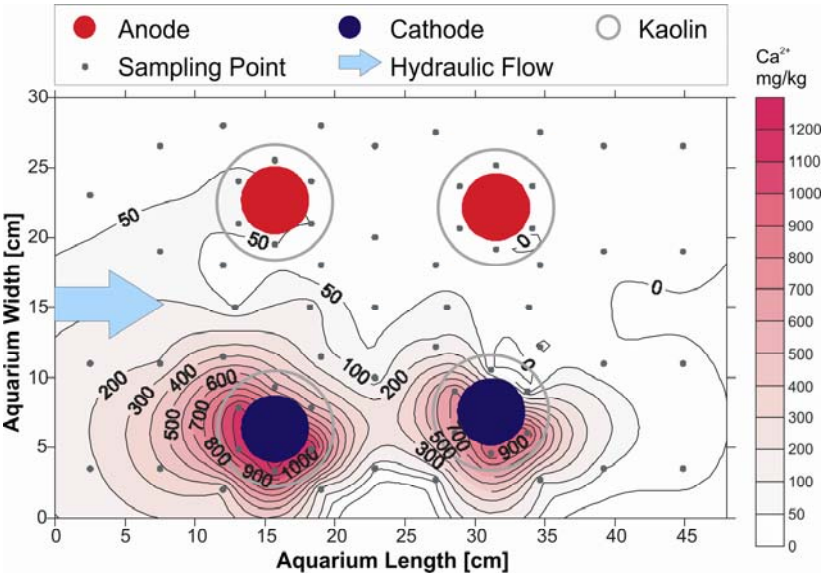

Fig. 6.20: Distribution of Ca^{2+} after the experiment (acidic batch).

Note that the analyses of soil concentrations only reflect the situation after the experiment. However, the application of an electric field causes various dynamic processes which are taking place in parallel and generally cannot be quantified separately. Thus, temporal variations in concentration, precipitation and solution reactions cannot be measured.

Combining the results of the concentration analysis at the end of the experiment and of the chemical modelling the following conclusions are most likely:

- At least in the beginning and later on within the influence area of the first electrode pair, the concentration of Ca^{2+} within the anode-dominated area should be high enough to lead to the precipitation of $CaSO_4$ under acidic conditions; towards the cathode, the concentration of HCO_3^- was sufficient to lead to the precipitation of $CaCO_3$. Near the cathode and within the cathode the precipitation of $CaOH_2$ is dominating.
- Entering the influence zone of the second pair of electrodes, the concentration of ions in the soil solution is much less than before as a substantial amount of ions is removed by electromigration towards the electrodes and by precipitation. Whether during the experiment the Ca^{2+} concentration was still high enough to lead to the precipitation of $CaSO_4$ in the sphere of influence of A2, and which portion of Ca^{2+} precipitates as carbonate and which portion as hydroxide around C2, cannot be answered easily.

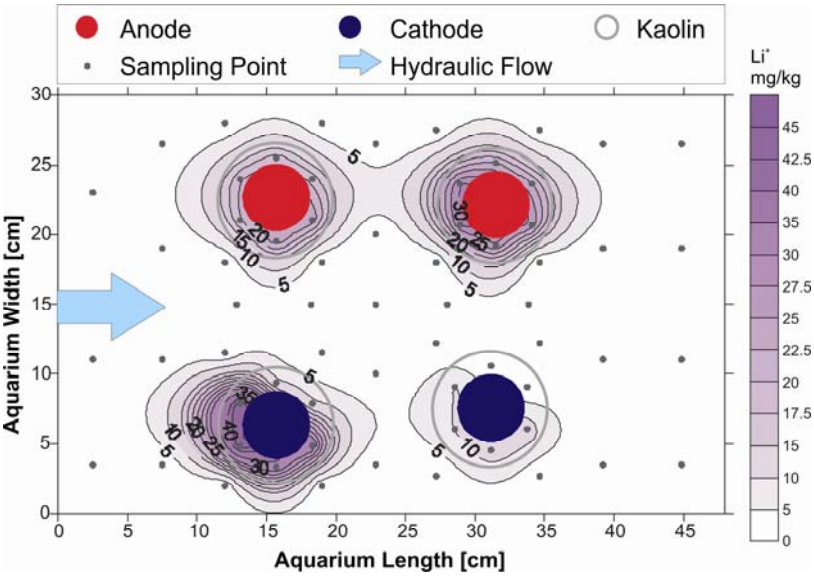

Fig. 6.21: Distribution of Li^+ after the experiment (acidic batch).

In fined grained soils, oxygen produced at the anode and transported towards the cathode by electroosmosis is an indicator for the functionality of the electrodes during an experiment. For coarse-grained soils, no comparable method is known. In the present work, the application of Li^+ as easy-to-handle tracer method was tested. The anodes were filled with 0.02 molar LiCl enriched tap water. According to its electric charge, Li^+ moves towards the cathode by electromigration. After one day, Li^+ is detected at both cathodes already (Fig. 6.25). After the experiment, a total of 85% of the Li^+ migrated out of the anodes. 15% of Li^+ were detected at the cathodes, no Li^+ was measured within the sand due to dilution effects (Fig. 6.21) and 30% were discharged with the cathode eluate. Compared with the analysed main ions, the total Li concentration/mass is very small. Nevertheless, substantial amounts of Li were detected at the cathodes, proving its very small tendency to precipitate. In contrast,

Mg^{2+} with a mass input of more than 15 times of that of Li was not registered at the cathode.

The experiment results show that the induction of Li^+ at the anode indeed is a suitable tracer method to test the functionality of the electrodes during an experiment. Beside its chemo-physical characteristics the easy analysis method and the small amount of substance/concentrations needed are of great advantage. Principally, charged nutrients favouring decomposition of organic contaminants can also be distributed across coarse-grained soils by this method.

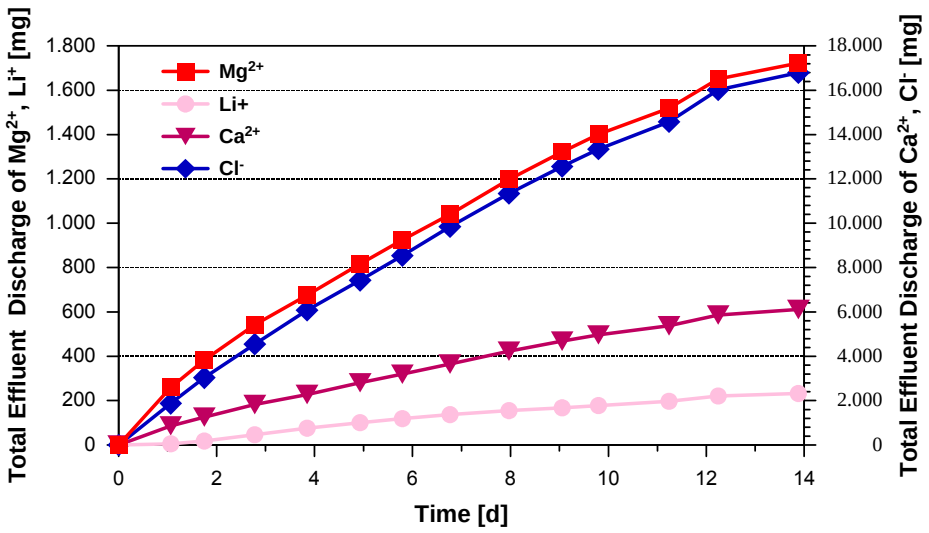

Fig. 6.22: Temporal development of the discharge of Ca^{2+}, Mg^{2+}, Li^+ and Cl^- in the effluent.

The development of electroosmotic inflow and outflow rates (Q_{eo}) at the electrodes is shown in Fig. 6.23. In the beginning, Q_{eo} at both anodes and cathodes decrease before reaching almost constant values. The efficiency of electroosmosis depends on various factors, e.g. mineralogy of the soil, pH, extent of the diffuse double layer, electrolyte concentration, electric gradient and the zeta potential. Note that the influence of a single parameter cannot be quantified. Principally the decrease in electrolyte concentration by electrokinetic transport processes and precipitation reactions leads to a decrease in k_e. Once an electrolyte balance is achieved, Q_{eo} values are almost constant. The acidic pH at the anode favours protonation of the edges of clay minerals. Thus, the surface charge becomes more positive which affects the electroosmotic flow negatively. The steep voltage gradient at the anode supports electroosmotic flow, but obviously is not high enough to outbalance the other parameters. Precipitation at the cathodes leads to coating of the clay minerals and decreasing k_e values respectively.

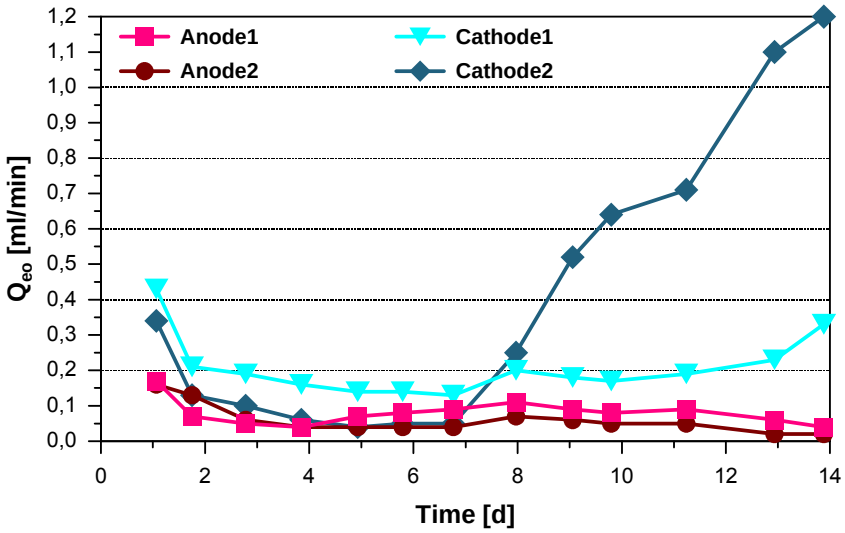

Fig. 6.23: Temporal development of electroosmotic inflow/outflow rates Q_{eo} at the electrodes.

The development of ion masses within the electrodes is displayed in Fig. 6.24 and Fig. 6.25. Principally, the ion mass within the anodes decreases constantly with time. Cations migrate towards the cathode; Cl^- is oxidised to chlorine gas (Re. 6). The increase at day seven is due to the refill of anolyte solution. Although ion masses at the anode ceases, its electric conductivity increases (Fig. 6.26). Obviously, H^+ produced by electrochemical reaction at the anode dominates electric conductivity. Note that the decrease in conductivity from day seven to eight is due to the dilution effect by the refill.

At the cathode, Cl^- migrates out of the cathode towards the anode, displayed by a decreasing Cl^- mass. Hence, the electromigration velocity of Cl^- exceeds the electroosmotic velocity within the kaolin, which is directed towards the cathode. Within one day, no Mg^{2+} is detected at the cathode. Mg^{2+} precipitates as $Mg(OH)_2$ at a pH of about 9.5 already (Fig. 7.3). Furthermore, Mg^{2+} concentration is quite low compared to the one of Ca^{2+} (by factor 10). Thus, all Mg^{2+} is consumed by precipitation within the soil and the cathode, respectively. At cathode one C1 appears a steep increase in Ca^{2+} within the first three days. From day three to seven Ca^{2+} discharge is very low. Increasing the applied voltage up to 40 V, results in an initial increase in Ca mass transport before it almost ceases from day 11.5 onwards.

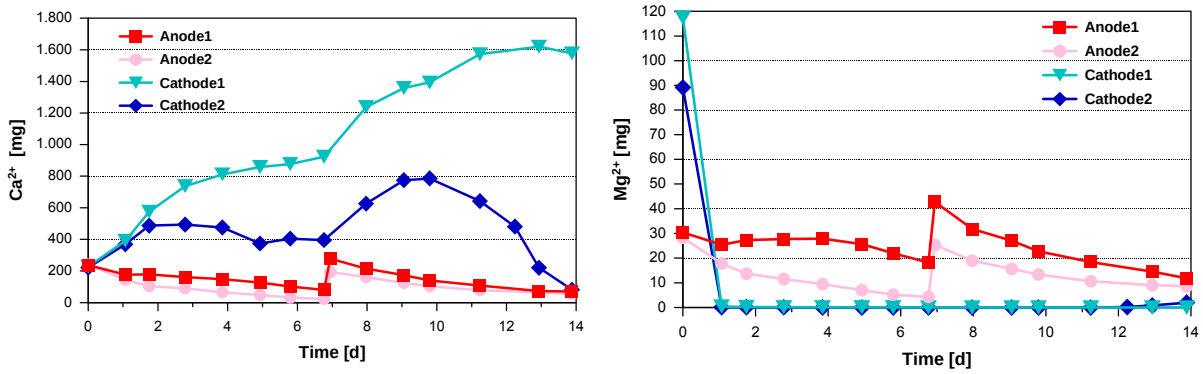

Fig. 6.24: Development of Ca^{2+} (left) and Mg^{2+} (right) at the electrodes.

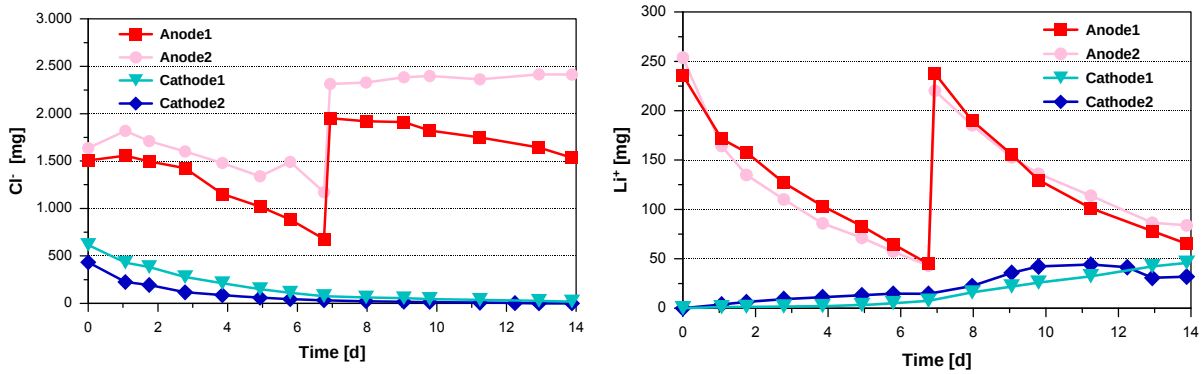

Fig. 6.25: Development of Li^{+} (right) and Cl^{-} (left) at the electrodes.

Generally, an increasing ion mass reflects that electrokinetic mass transport rates exceed precipitation rates and vice versa. A constant ion mass indicates that electrokinetic mass transport and precipitation are in equilibrium. The development of the Ca^{2+} mass at cathode two C2 shows completely different characteristics. After two days the Ca^{2+} mass keeps being constant, signifying that electrokinetic mass transport rate and precipitation rate are in equilibrium. Increasing voltage causes a rise in mass transport which results in an increase of Ca^{2+} mass at C2. After further three days there is a steep decrease in Ca^{2+} mass and no Ca^{2+} is measured at the end of the experiment. In the sphere of influence of the first electrode pair, Ca^{2+} is transported towards the cathode by electromigration (and within the kaolin additionally by electroosmosis). Furthermore, precipitation takes place within the sand. Both electrokinetic transport processes and precipitation leads to decreased concentrations within the soil solution. Hence, entering the sphere of influence of the second electrode pair Ca^{2+} concentrations are reduced and accordingly less Ca^{2+} is transported to the second cathode. Consequently, equilibrium at C2 is achieved much faster than at C1.

Increasing the applied voltage at day seven leads to an increase in retardation at C1: more Ca^{2+} is transported by electromigration, more OH^- is produced leading to higher pH and precipitation rates. The reduced Ca^{2+} mass after passing electrode pair one is reflected by the soil concentrations of Ca^{2+} after the experiment, which are a factor 3-10 lower around C2 than around C1 (Fig. 6.20). Lower Ca^{2+} and higher OH^- concentrations at C2 lead to total consume of Ca^{2+} by precipitation.

Further explanations for the high increase in Q_{eo} and decrease in Ca^{2+} mass at C2 are:

- Although the installation of the electrodes was carried out as precise as possible, distances between the two electrode vary; distance between A1 and C1 is 20% greater than between A2 and C2. Consequently, the electric field between the second electrode pair is higher than between the first one.
- Neither the amount of kaolin nor the thickness of the kaolin backfill ring is exactly the same for each electrode (due to installation conditions)
- Transition resistance between fleece/kaolin and kaolin/sand occurs resulting in differences in voltage gradients.
- It cannot be guaranteed that the structure within the kaolin is the same at all electrodes.
- Eventually some dispersion of the clay minerals at C2 occurred, which leads to higher hydraulic conductivity.
- Electroosmosis within the kaolin has to act against hydraulic pressure within the sand. The second electrode pair is located in the hydraulic lee side of electrode pair one. Hence, for the second cathode it is easier to pull water out of the sand.
- Gas production.

The pH values of the eluate decrease with time (Fig. 6.26, top left), as pro rata more OH^- than H^+ is consumed by precipitation reactions. Increasing voltage results in a short-time increase of pH. More OH^- ions are produced as OH^- precipitate. After 4 days, OH^- production and precipitation reactions seem to be in equilibrium and pH values of the eluate are constant at 4.7.

At the anodes, electric conductivity continuously increases and is dominated by H^+ production (Fig. 6.26, top right) and electromigrative transport of anions towards the anode. The refill of anode eluate at day seven causes a small decrease in electric conductivity due to dilution effect. At A1 electric conductivity is smaller. Reason could be that at the distance between A1/C1 is higher than between A2/C2. Hence, the electric field applied is smaller which results in less anion concentration as the electromigration velocity is straight proportional to the electric field. Another explanation could be that the electric connection electrode/soil at A1 is worse. At the cathodes, electric conductivity is smaller than at the anodes due to precipitation of hydroxides. At C1 the mass transport rate of Ca^{2+} towards the cathode exceeds precipitation rate leading to a continuous increase in electric conductivity. At C2

constant values are achieved quickly signifying that mass transport rate and precipitation is in equilibrium. From day nine onwards, electric conductivity decreases due to dilution effects caused by high k_e values or because of unintentional hydraulic flow resulting from the dispersion of kaolin. The trend of redox potentials (Fig. 6.26, bottom) show the conditions at the anodes and cathodes, which arise due to electrochemical reactions in dependence on ion concentration and electric parameters.

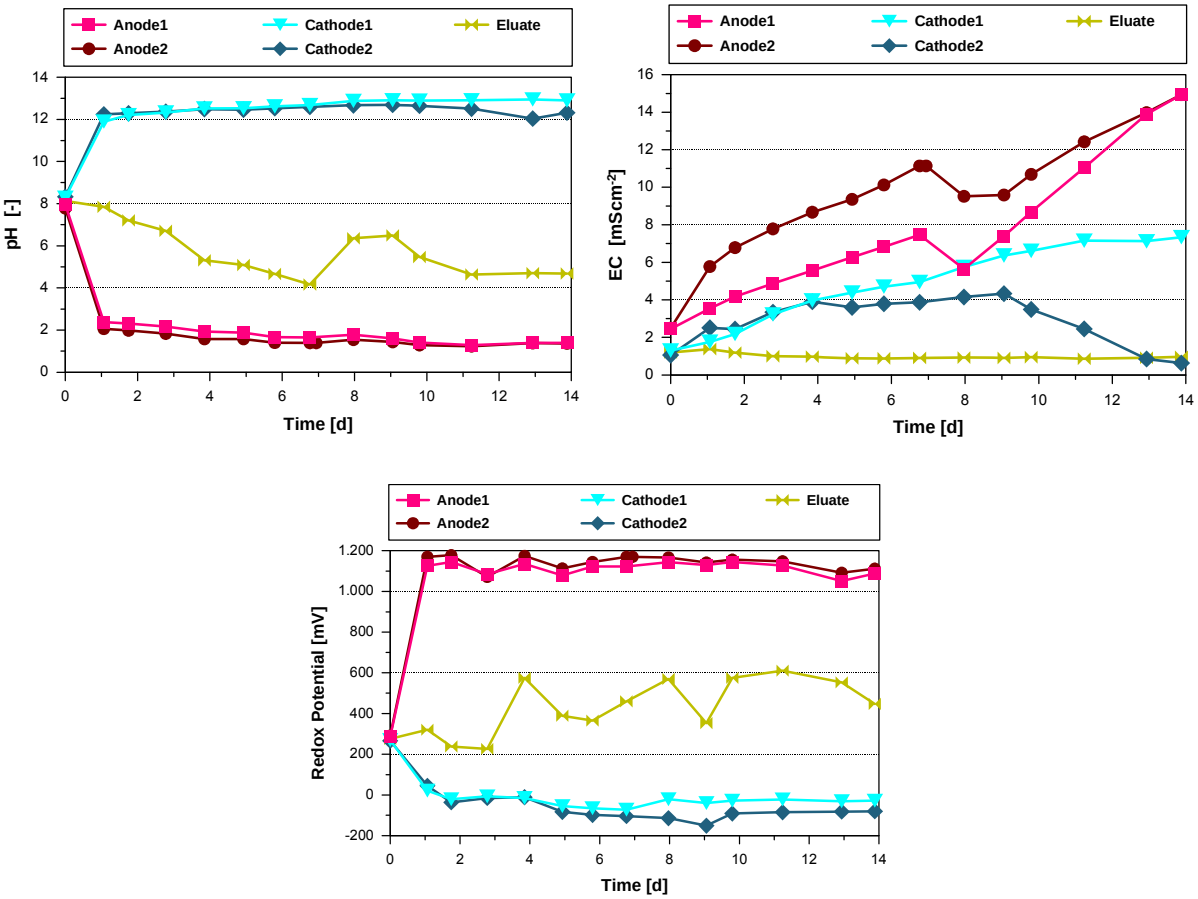

Fig. 6.26: Development of pH (top left), electric conductivity (EC, top right) and redox potential (bottom) of the electrodes and eluate.

7 RESULTS – EH/PH DIAGRAMS

Oxidation and reduction (redox) reactions play an important role in the geochemical processes that occur in soil and groundwater. Redox reactions are defined as reactions in which atoms change their oxidation state, notably by transferring electrons from one atom, ion, or molecule to another. Redox potential is an intensity parameter of the overall redox reaction potential in the system (similar in concept to pH), but does not describe the capacity of the system for specific oxidation or reduction reactions. In the literature, redox potential is generally reported as Eh, which is the potential generated between a platinum electrode and a standard hydrogen electrode (SHE) when placed into groundwater, where hydrogen is considered the reference electrode (VANCE 2002). The sign of the potential is positive if the reaction is oxidizing and negative if it is reducing (FETTER 1994).

Redox reactions determine the mobility of many inorganic compounds in groundwater. In addition, the soil pH affects the solubility of many elements in aqueous solution. The pH of the system describes its ability to supply protons (H(+a)) to the species. Natural waters contain many ionic species. If the pH and Eh of an aqueous solution are known, stable chemical species can be determined by calculation. The stability relationship is best represented in an Eh/pH diagram. The Eh/pH diagram can be used to show the fields of stability for both the dominant solids and the dissolved ionic species on a plane defined by the Eh and pH axes. Generally, it depends upon the concentrations of all ionic species present. For simplification, the molarity of the investigated species or main species of the solution can be used. Water itself is stable only in a certain part of the Eh/pH field. Usually the upper and lower stability limits of water are shown in the diagrams with dotted lines. During electroremediation, these extreme conditions exist at the electrodes.

The application of a dc electric field into the ground has a substantial influence on soil pH, redox state and concentration distribution of the chemical species present, and usually leads to a distinct rise in temperature. Consequently, species changes within the electric field and at the electrodes occur. In addition, these changes are dynamic processes varying in time and space. In literature, qualitative results of electrokinetic experiments are often explained by referring to Eh/pH diagrams taken from hand- or textbooks. Usually these diagrams are available only for a limited number of temperatures and concentrations (usually 25°C and 1 mol/l) and for the simple system of one element and water solution. Hence, these Eh/pH diagrams do not reflect the real conditions during electrokinetics.

To identify and visualize the influence of electrokinetically induced changes in pH, redox potential, concentration and temperature on species stability, individual Eh/pH diagrams were modelled using the software HSC Chemistry 5.1 (s. Section 4.2). This

software allows constructing Eh/pH diagrams for selected temperatures and concentrations as well as for a selected multi-component system.
For the modelling, data obtained from the container experiments with $CaMgCl_2$-enriched tap water were used (s. Section 6.3). For the modelling the main cations (Ca^{2+} and Mg^{2+}) and anions (HCO_3^- and $SO4_2^-$) were considered. The elements selected were inorganic carbon (C), calcium (Ca), magnesium (Mg), and sulphur (S). Although Cl^- is also a main anion of the solution, it was not included for modelling as Cl^- ions are dissolved over the whole range of pH. Note that at the anode Cl^- can be oxidised to gaseous Cl_2 (Re. 6). Table 7.1 gives an overview of the series of Eh/pH diagrams constructed. Parameters changed were the selection and concentration of the elements as well as temperature.

Table 7.1: Overview of variations in elements, temperature and concentration during modelling Eh/pH diagrams.

Test-ID	Chemical System	Concentration	Temperature [°C]	pH
A	Ca-O-H, Mg-O-H, C-O-H, S-O-H	c_0	25, 45, 60	1-14
B	Ca-O-H, Mg-O-H, C-O-H, S-O-H	c_0, x5, x20, $x10^{-1}$	25	1-14
C	C-Ca-Mg-S in H2O	c_0	25, 45, 60	1-14
D	C-Ca-Mg-S in H2O	$c_{0Cation}$x10 $c_{0Anion}x10^{-1}$, $x10^{-2}$, $x10^{-8}$	25	6-14
E	C-Ca-Mg-S in H2O	c_{0Anion}x10 $c_{0Cation}x10^{-1}$, $x10^{-2}$, $x10^{-8}$	25	0-6

with c_0 = original concentration of flushing solution in mol/l (C=0.026, Cl=0,015, Ca=0.005, Mg=0.002, S=0.002), $c_{0Anions}$ = original concentration of anions, $c_{0Cations}$ = original concentration of cations

The simple systems of test series A and B were chosen to investigate the influence of temperature and concentration on species stability fields, in principle. This case may be relevant within the electrode solution, where at the anode H^+ is the dominating cation and at the cathode OH^- is the dominating anion. In a next step, a more complex chemical system consisting of C, Ca, Mg and S in H_2O and its behaviour for different temperatures was examined (Test-ID C).

During electrokinetics, anions migrate towards the anode and cations towards the cathode. In addition, precipitation, especially close to the cathode, leads to concentration changes in the aqueous solution, too. To consider these changes in ion distribution, which are greatest close to the electrodes, the anode and cathode

dominated areas were considered separately for the modelling. Simulating the anode zone, concentration of the anions c_{0Anion} was increased and concentration of the cations $c_{0Cation}$ was decreased (Test-ID E). On the other hand, higher cation and lower anion concentration were used to reflect conditions at the cathode zone (Test-ID D). Note that only concentrations at the beginning and at the end of the experiment are known. Thus, concentration values during the experiment can only be estimated. The type of species, which were chosen to collect from the database, were solid substances, dissolved ions and gaseous species.

After the elements and the type of species were chosen, the most critical and time-consuming step of selecting the species from the database followed. Generally, the selection based on knowledge of chemistry and aqueous systems as well as literature studies (KRAUSKOPF 1979, MATTHESS 1990, SCHEFFER & SCHACHTSCHABEL 1992, FETTER 1994, STUMM & MORGAN 1996). The following modifications were carried out when specifying the chemical system and analyzing the calculation results:

- organic species were rejected (not relevant for the selected case)
- large molecules were rejected (due to kinetic reasons)
- unreliable species were removed

After the chemical system is specified, the software displays the calculated Eh/pH diagrams. For each Eh/pH diagram another “main” element is used, i.e. all species, which are shown in the diagram, will contain this element.

The Eh/pH diagrams of test series A and B in dependency on concentration (left) and temperature (right) are displayed in Fig. 7.1 and Fig. 7.2. The modelled results allow the following conclusions:

- Species of C, Ca and Mg are only dependent on pH; species of S are also dependent on redox values.
- Principally, variations in concentrations have a greater influence on the position of borders of stability fields than variations in temperature have.
- Higher concentrations shift the border to the left, e.g. towards lower pH; hence, the cations have a greater tendency to precipitate as hydroxide if concentrations are high. As an electric field leads cations to migrate towards the cathode this increase in concentration favours its precipitation tendency.
- $Mg(OH)_2$ precipitates at much lower pH than $Ca(OH)_2$.

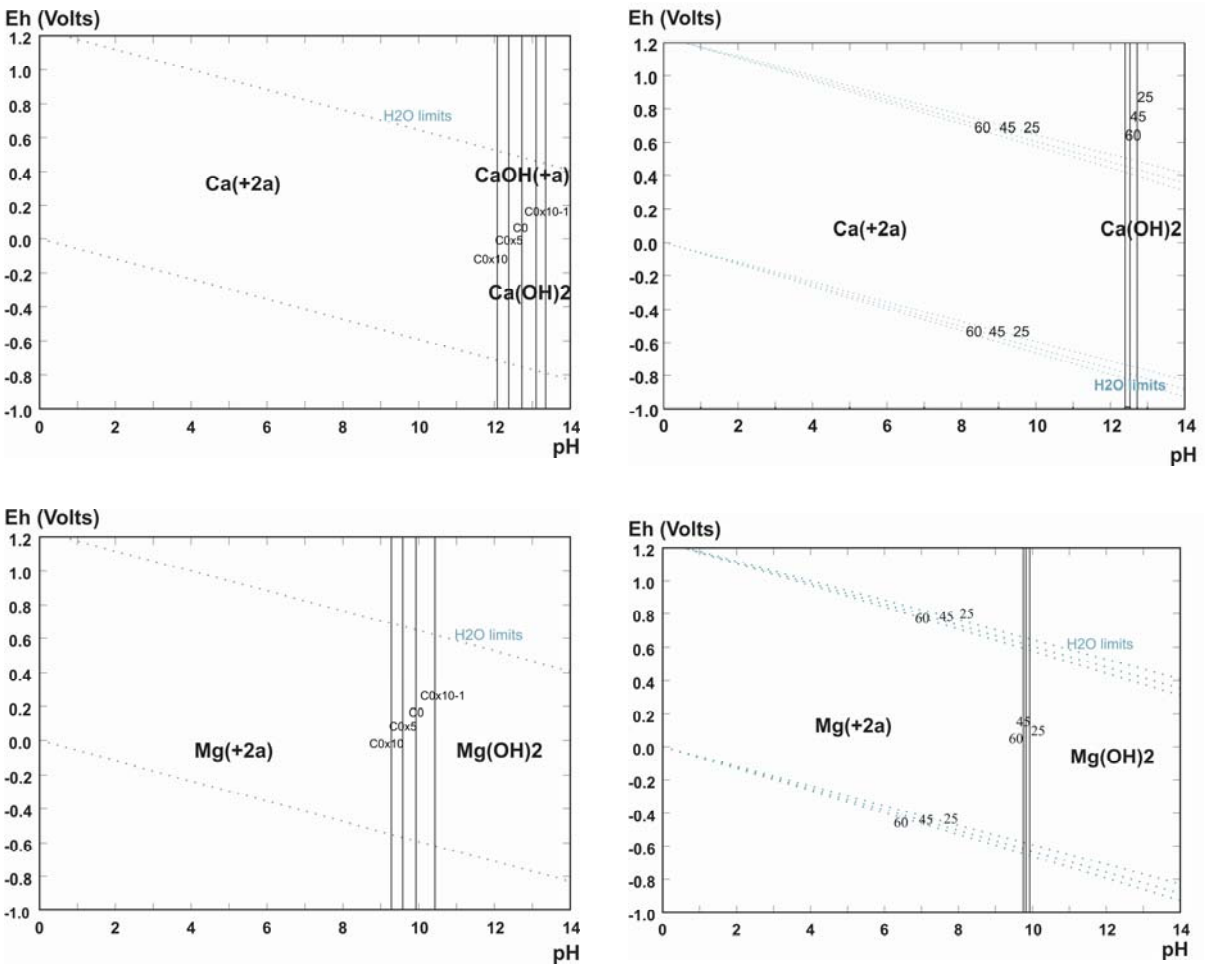

Fig. 7.1: Eh/pH diagrams for Ca-O-H (top) and Mg-O-H (down) in dependency on concentration (left) and temperature (right) and constant concentration c_0 (Test-ID A, B).

Note that dissolved sulphur in solutions at the earth's surface has only two principal oxidation states, +6 and -2; that the only important sulphur-containing ion in oxidizing solutions is SO_4^{2-}; that reducing solutions contain chiefly H_2S at acidic pH, and HS^- at alkaline pH; and that S^{2-} is never a major constituent of any geologically important solution. However, although its concentration is very minute in the fields of HS^- and H_2S, it is capable nevertheless of precipitating many heavy-metal ions as insoluble sulfides (STUMM & MORGAN 1996).

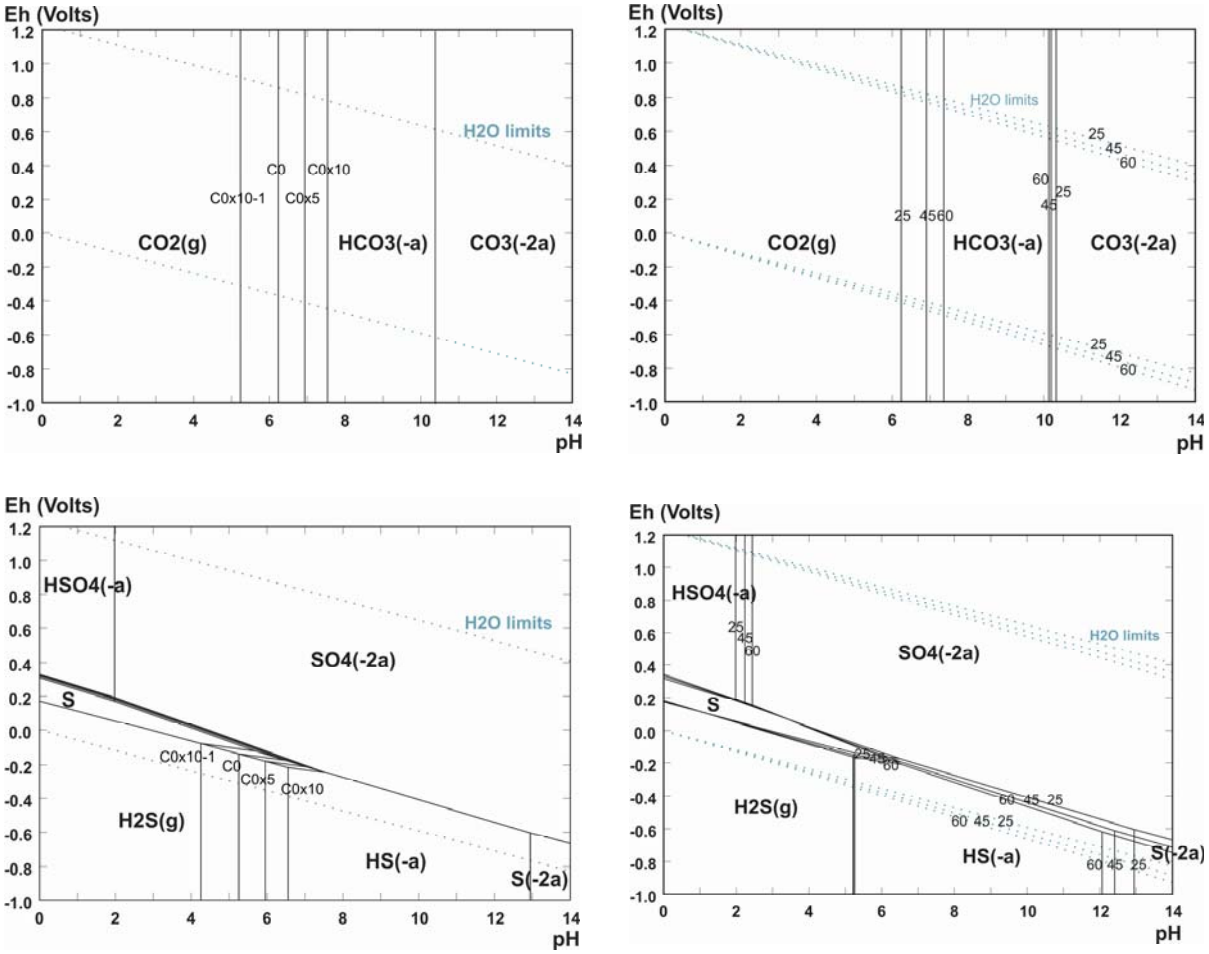

Fig. 7.2: Eh/pH diagrams for C-O-H (top) and S-O-H (down) in dependency on concentration (left) and temperature (right) and constant concentration c_0 (Test-ID A,B).

A next step investigated the influence of the presence of several elements and different temperatures on species formation (Test-ID C). Fig. 7.3 and Fig. 7.4 show the Eh/pH diagram of the species of the system C-Ca-Mg-S in H_2O for different temperatures and constant concentrations c_0. In the system Ca-O-H, Ca precipitates as hydroxide at a pH of about 12.5. If C is present, Ca does not precipitate as hydroxide but as carbonate (Fig. 7.4 left). In contrast, the presence of C does not influence Mg species (Fig. 7.3). While in the simple chemical system of test series A and B Mg tends to precipitate at much lower pH than Ca, in the multi-component system the precipitation of Ca occurs at a pH of about six already.

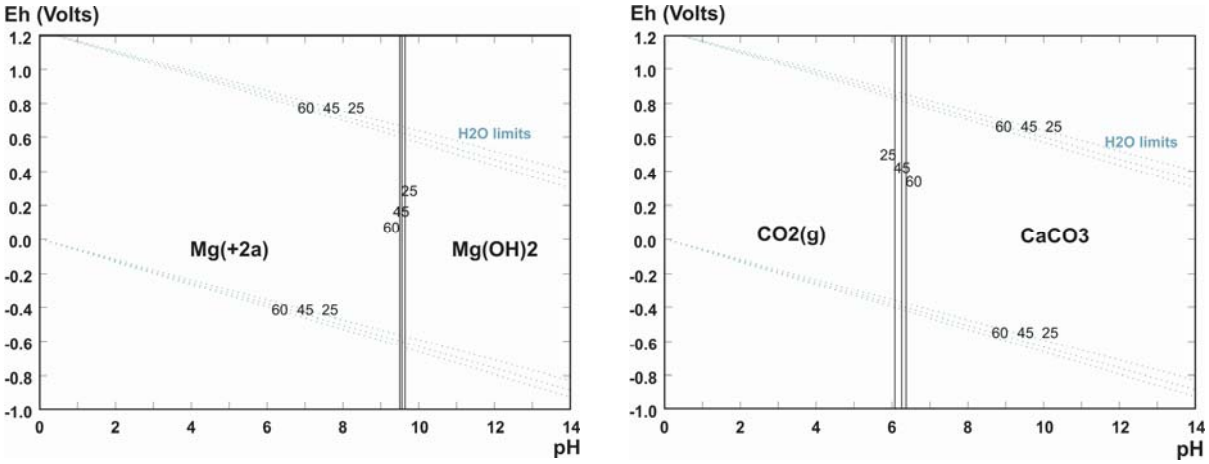

Fig. 7.3: Combined Eh/pH diagrams of Mg-C-Ca-S (left) and C-Ca-Mg-S (right) in H_2O for constant concentration c_0 and different temperatures (Test-ID C).

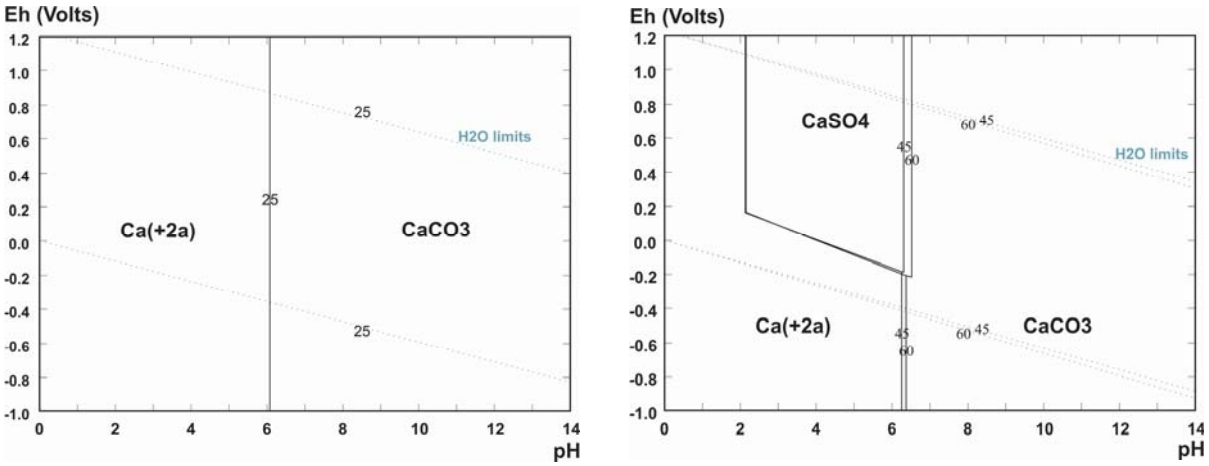

Fig. 7.4: Combined Eh/pH diagrams of Ca-C-Mg-S in H_2O for constant concentration c_0 and different temperatures (Test-ID C).

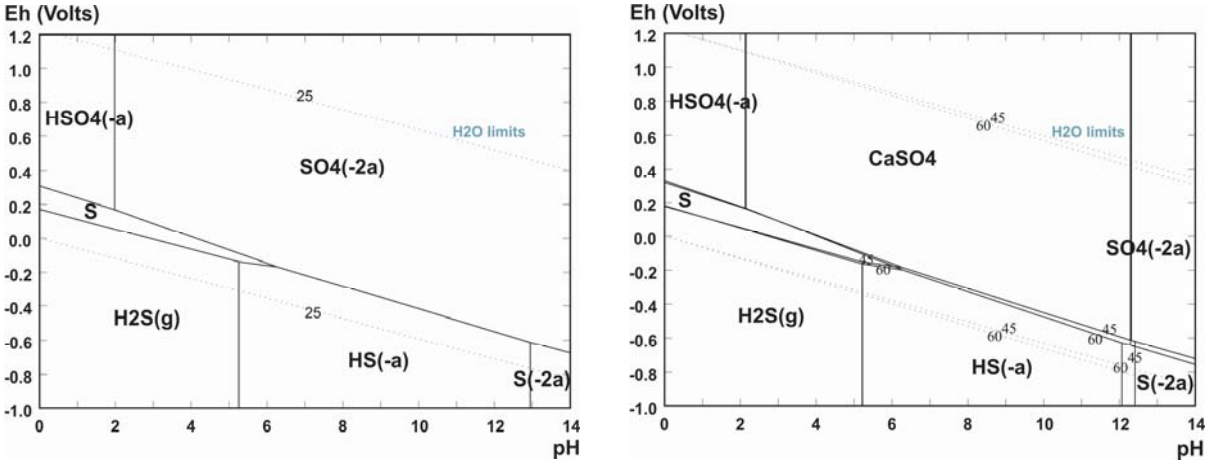

Fig. 7.5: Combined Eh/pH diagrams of S-C-Ca-Mg in H_2O for constant concentration c_0 and different temperatures (Test-ID C).

Beside the elements present in the system, temperature has a great influence on species formation. At 25 °C stable Ca species are Ca^{2+} and $CaCO_3$, respectively. However, increasing temperature leads to the formation of further species. Now, at lower pH (2-6) and oxidative redox conditions $CaSO_4$ is stable whereas at higher pH $CaCO_3$ precipitates (Fig. 7.4). Considering the possible sulphur species at 25°C, SO_4^{2-} dominates over almost the whole range of natural and electrokinetically influenced Eh/pH conditions (Fig. 7.5). At temperatures higher than 36°C, $CaSO_4$ forms. Checking only the Eh/pH diagram with S as main element, $CaSO_4$ would be the stable species from pH 2 to pH 12.

For this diagram (as for any Eh/pH diagram), it should be noted once more that the boundaries are calculated for equilibrium conditions. The single Eh/pH diagrams only show those species, which contain the selected main element. However, checking all the diagrams with different main elements in parallel is giving a good idea of the equilibrium. This example shows impressively that considering only one element cannot reflect natural conditions properly and may lead to misinterpretation. Furthermore, it reflects that for electroremediation the influence of temperature on species formation often is underestimated but definitely has to be considered.

As Mg does not undergo substantial species changes, the calculated Eh/pH diagrams for the Mg-C-Ca-S-H_2O system are not displayed for further examinations.

Applying an electric field yields to distinct changes in ion distribution and concentration relations, respectively. Cations migrate towards the cathode and anions towards the anode. Hence, within the cathode-zone concentrations of Ca and Mg increase whereas concentrations of C and S decrease (Test-ID D). Within the anode region, the concentration ratio is vice versa (Test-ID E). The influence of changes in concentration ratio on species formation was investigated in a next step. Modelling cathode conditions, ten times higher Ca and Mg concentrations were used. Concentrations of C and S were decreased gradually. This scenario is relevant for temporal changes during electroremediation or for the case described by the container experiment, where ion concentrations between the first pair of electrodes are higher than between the second pair of electrodes. Note, only concentrations and pH at the beginning and at the end of the experiment are known. Thus, concentration values during the experiment can only be estimated.

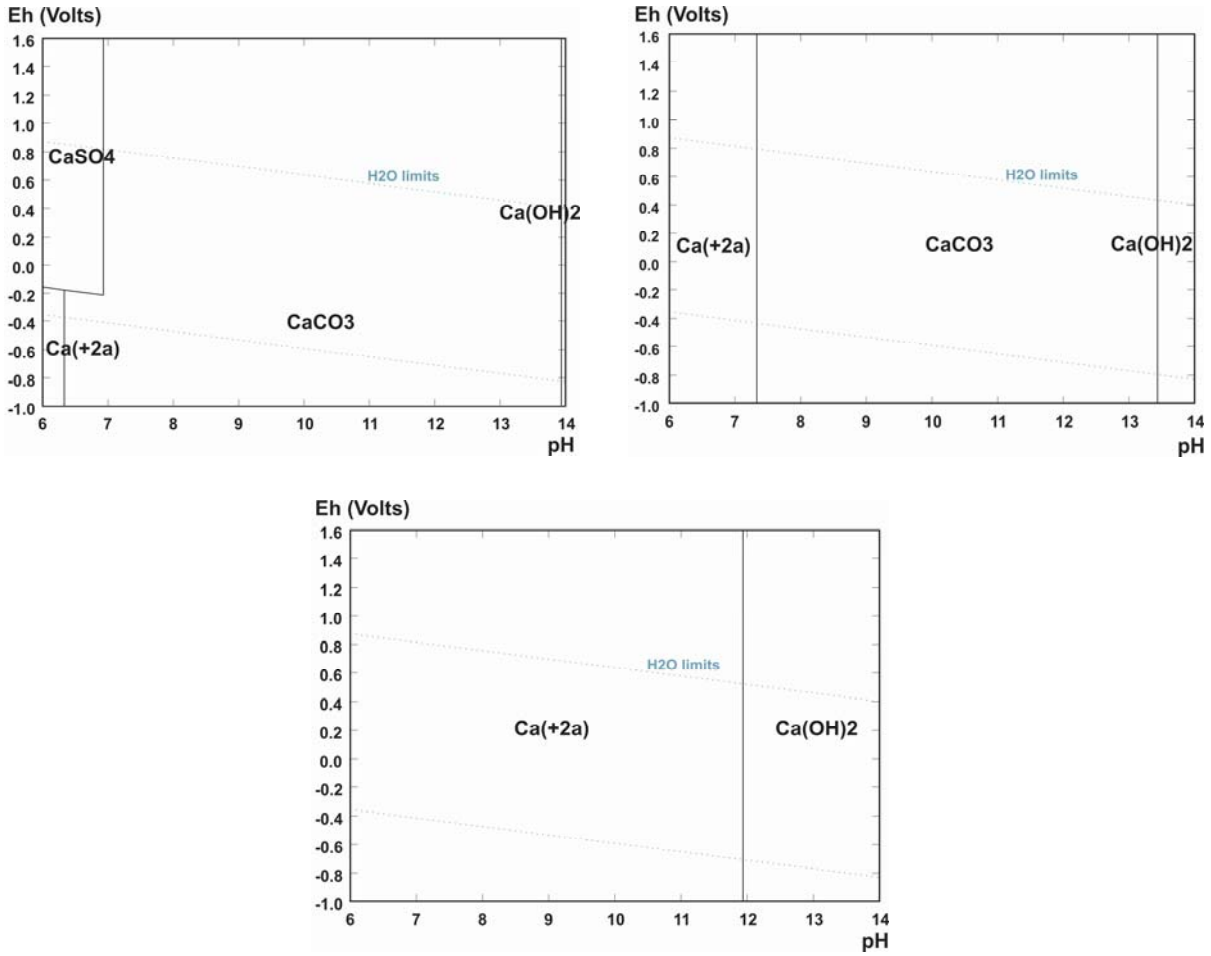

Fig. 7.6: Eh/pH diagrams of Ca-C-Mg-S-H2O system at 25 °C for different concentrations of C and S simulating cathode zone conditions; $c_{0Anion}x10^{-1}$: top left, $x10^{-2}$: top right, $x10^{-8}$: bottom (Test-ID D).

Fig. 7.6 (top left) shows that if C and S concentrations are still high enough, Ca mainly precipitates as carbonate. However, at lower pH calcium sulphate can form and at very alkaline pH $Ca(OH)_2$ starts to precipitate. Further decrease in C and S concentration leads to a shift of the stability border $Ca^{2+}/CaCO_3$ to the right whereas the border $CaCO_3/Ca(OH)_2$ shifts to the left until finally only $Ca(OH)_2$ precipitates (Fig. 7.6, top right and bottom). Fig. 7.7 and Fig. 7.8 confirm these observations. In principle, simulations for the anode regions with high C and S and low Ca and Mg lead to the same conclusions. Thus, these calculated Eh/pH diagrams are not presented.

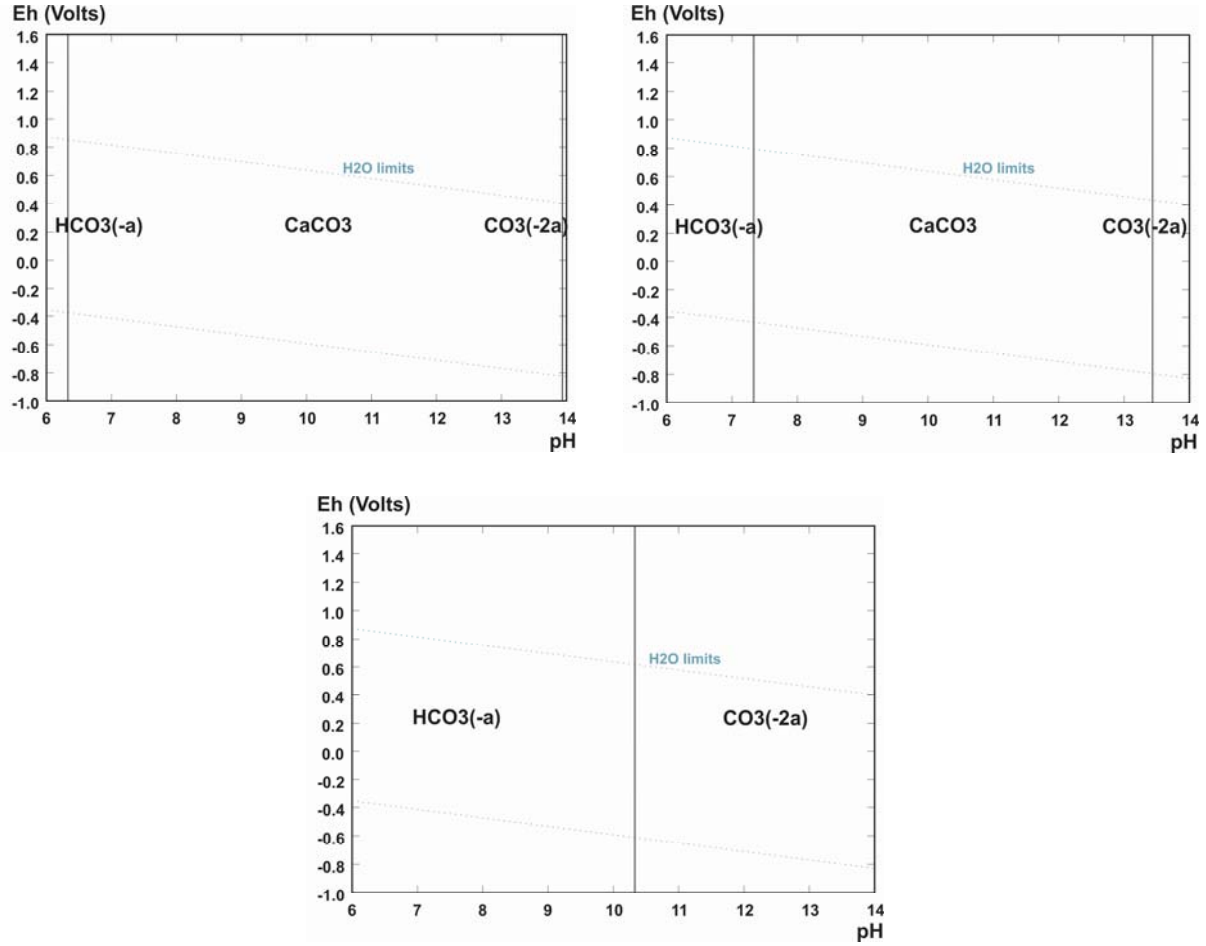

Fig. 7.7: Eh/pH diagrams of C-Ca-Mg-S-H2O system at 25°C for different concentrations of C and S simulating cathode zone conditions; $c_{0Anion}x10^{-1}$: top left, $x10^{-2}$: top right, $x10^{-8}$: bottom (Test-ID D).

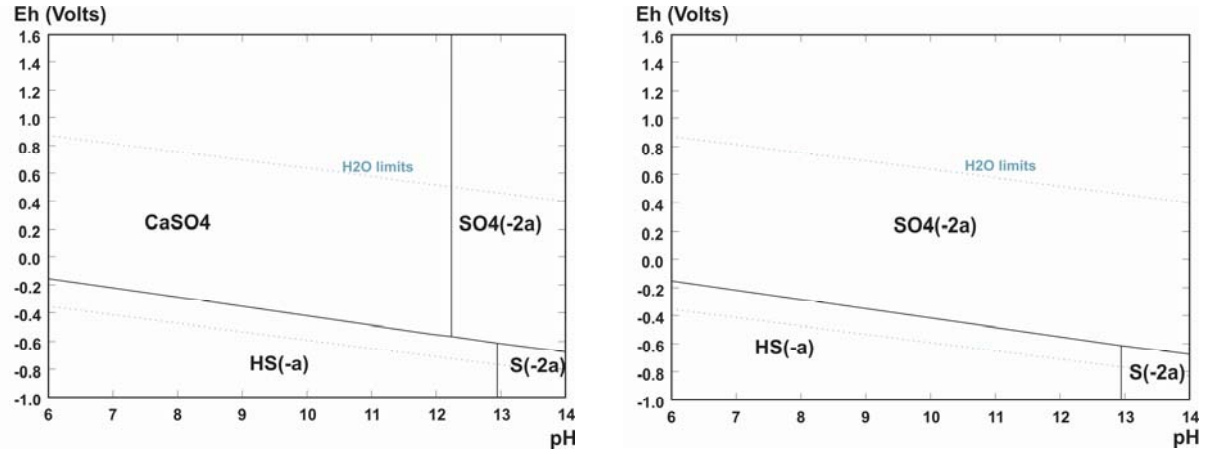

Fig. 7.8: Eh/pH diagrams of S-C-Ca-Mg-H2O system at 25°C for different concentrations of C and S simulating cathode zone conditions; $c_{0Anion}x10^{-1}$: left, $x10^{-2}$: right (Test-ID D).

On basis of the modelled Eh/pH diagrams, it is possible to describe the dynamics of the dominant species formation with time and space. In the beginning, Ca may precipitate as sulphate and/or carbonate (depending on pH) in the soil whereas at the electrode it forms hydroxides. As C and S concentrations decrease (due to electromigration towards the anode) precipitation of $CaCO_3$ within the soil and $Ca(OH)_2$ at the electrode is likely. Finally, only $CaOH_2$ may precipitate at the cathode.

For the application of electrokinetic remediation, the effect of changes in pH, ion distribution and temperature on species formation is of special interest. The results above show that simple Eh/pH diagrams considering only one element, do not display precipitation tendency sufficiently. The modelled Eh/pH diagrams also demonstrate that even in a quite simple chemical system rising temperature and shifting of ion concentrations caused by electrokinetics result in sustainable species changes. Obviously, Eh/pH diagrams offer a valuable help for predicting and interpreting species formation during electroremediation.

However, several aspects have to be considered when dealing with Eh/pH diagrams. Principally they simplify aqueous species mixtures a lot by showing only the predominant species with the highest content in each stability area. Nevertheless, adjacent species always exist in small amounts on both sides of these lines and may have an effect on practical applications. Furthermore, Eh/pH diagrams are calculated on the assumption that the chemical system has achieved equilibrium state. In contrast, environmental and electrokinetic processes are complex and typically are in thermodynamic dis-equilibrium (caused by e.g. flowing groundwater conditions, biological activity, electrokinetic mass transport and electrochemical reactions of exposed active mineral surfaces). Furthermore, especially for the processes of dissolution and precipitation in porous media the reaction kinetic plays an important role. There is an endless number of electrokinetic induced concentration and temperature combinations varying with time. Thus, one must be aware that the information gained from an Eh/pH diagram only reflects one certain moment at a certain place. On the other hand, neither exact concentrations nor redox and pH values during the application of electrokinetics are known. Consequently, only estimated values can be used; a fact that has to be considered when deriving the occurrence of a certain compound by simple classification in an Eh/pH diagram. Note that Eh/pH diagrams principally work well in a qualitative fashion, but due to conditions previously discussed are usually unsuccessful when applied to quantitative applications. In addition, for interpreting all species have to be considered. Finally, the calculated Eh/pH diagrams have to be controlled critically to exclude software, calculation or operation errors (see also www.hsc.csu.edu.au, www.outokumpu.com/hsc).

Beside these restrictions, the presented modelling series leads to the conclusion that Eh/pH diagram is a supportive tool to visualize the complexity of chemical species formation during electrokinetics. One main advantage is that possible species formation can be identified before the application and chemical analysis methods can

be adjusted, respectively. Especially, if dealing with contaminants, which species may have different algebraic signs in different pH milieus, Eh/pH diagrams are helpful to avoid unnecessary failure of the remedial action. Furthermore, the modelling of individual Eh/pH-diagrams is recommended to apply if toxic compounds are present. Dangers can be avoided as Eh/pH diagrams visualize which parameters during electrokinetic remediation have to be monitored and/or controlled to guarantee safety. Moreover, the Eh/pH-diagrams modelled in this thesis deliver the basis for almost all environmental realities as the included elements/compounds are commonly dominant or present in nature. The basis for the modelling was constructed in such way that the results not only can be applied to the experiments presented in this study but also can be transferred to field applications as they reflect natural and realistic conditions. In other words, to get individual Eh/pH-diagrams for a certain hazardous waste site the data basis of this modelling only has to be complemented by the relevant elements. Thus, the performed modelling provide a basic and quite easy handling tool for enhancing success rate and safety conditions during electrokinetic remediation.

8 DISCUSSION AND CONCLUSIONS

8.1 Summary of the Results

The combination of different techniques for soil and groundwater remediation is more and more object of research as clean-up practice suggests higher potential for success, especially for complex site conditions and contamination situations. Both passive groundwater remediation using permeable reactive barriers (PRB) and active soil remediation using electrokinetics are new and innovative technologies. The task of using electrokinetic methods to positively affect the long-term efficiency of reactive barriers was the research impulse for the investigations presented in this thesis. The application of an electric fence upstream of the PRB appears to be the most promising and practicable approach. The fundamentals of electrokinetic phenomena within fine-grained soils have already been tested and understood. The feasibility of coupling electrokinetics with treatment zones within fine-grained soils has been documented, too (s. Section 2.2.4). In contrast, only little information on electrokinetic phenomena within coarse-grained soils is available (e.g., KIM & LEE 1999, KATZORECK 2007). Furthermore, no quantitative experience is reported concerning the electromigrative transport of charged species in dependency on both electric and hydraulic gradients within aquifer materials or coarse-grained soils. Thus, the fundamental electromigration behaviour of ions in principle and under the combined influence of electric and hydraulic gradients in coarse-grained sediment was the main object of the present investigations. In addition, results were discussed with respect to the combination of an electric fence with PRBs.

First, a test series of electrokinetic cell experiments was carried out. For all experiments, a uniform middle sand was used as model soil. Model solutions became gradually more complex, the influence of pore/flushing solution composition and hydraulic flow on retention of anions and cations were examined. On basis of these results, the experimental set-up was scaled up. Different electrode types and configurations as well as potential influence of electrokinetic processes on reactive material Fe^0 were studied. Additionally, the possibility of mobilising contaminants from clay lenses into coarser material was studied in laboratory experiments. Finally, geochemical modelling using the software HSC Chemistry 5.1 was carried out and its applicability for predicting and analysing electrokinetically induced changes in chemical species formation was examined.

The conventional experimental apparatus used for clayey soils (as described by, e.g., STEGER 2005, ZORN 2005) has been adapted for tests with coarse-grained soil materials. To enable the documentation of electrochemical and geochemical

variations in the soil during the experiments, five additional passive probes were installed across the soil sample to measure the electric potential. To test this modified electrokinetic cell and to document fundamental electromigration behaviour in sandy soil, preliminary experiments were carried out in a closed system without applying hydraulic gradients. Model contaminants were NaCl, $CaSO_4$, and Na_2CO_3, respectively. The applied electric field was 89 V/m during the NaCl and $CaSO_4$ experiment and 160 V/m during the experiment with Na_2CO_3. The chosen field strengths and simple chemical systems can nevertheless simulate realistic applications. The electric field and the ionic strength are chosen to be representative for subsequent experiments as well as field applications.

The results demonstrate that indeed steady state conditions were reached as postulated by theoretical analysis and analytical simulations presented by DZENITIS (1997). It has been proved that by applying an electric field the present ions are transported towards the opposite charged electrodes by electromigration. Where the electrolysis products H^+ and OH^- meet, they form uncharged water. The characteristics of this reaction plane have been identified by the traces of the five potential probes (maximum in voltage gradient) as well as by the distribution of ion soil concentration (depletion in ions) and soil pH (pH jump) after the experiment. Thus, low electric conductivity, high electric field strength and hence high electromigration velocities occur within this water formation front. As a consequence the electrolyte of the system is separated into two binary zones: at the anode zone acidic conditions develop ($HCl/H_2SO_4/H_2CO_3$) whereas at the cathode zone alkaline pH conditions form ($NaOH/Ca(OH)_2$).

To confirm the experimental results, DZENITIS' (1997) analytical model and the numerical model described by ZORN (2005) were applied. Indeed the experimental results clearly are in accordance with the theoretical predicted development of the two binary zones. Note, in nature the described phenomenon has to be considered if groundwater is poor in constituents and/or groundwater velocity is very slow.

Clay lenses pose a frequent problem with regard to the decontamination of aquifers. Due to their intrinsic properties, contaminants cannot be treated efficiently by conventional technologies. However, electrokinetic processes of electroosmosis and electromigration allow the transport of contaminants in fine-grained soils. To investigate if an electroosmotic transport of water and simultaneously a mobilisation of species through low permeable soil into sand take place, the electrokinetic cell was filled half with loess loam and half with sand. To avoid the negative effect of acidic pH on electroosmosis, the pH of the anode was controlled by initial buffering with a 0.02 molar sodium carbonate solution. The soil core was saturated with deionized water and an electric field of 160 V/m was applied with the anode being at the side of the loam and the cathode at the side of the sand. Of special interest was the observation of variations in potentials across the soil during the experiment. The different soil media show different electrical characteristics: lower potential gradients develop in the loess loam whereas higher potential gradients occur in the sand.

Subsequently the maximum in potential gradient move towards the anode. The waterfront forms directly at the anode side, the final soil pH is alkaline. The results demonstrate that the theoretically predicted transport of water and species through low permeable soil into high permeable soil takes place indeed. The development of high voltage gradients due to material or ion distribution changes has to be considered.

To investigate the fundamentals of electrokinetic retention of ions against hydraulic flow, electrokinetic cell experiments were carried out where a defined hydraulic flow was generated by pumping solution through the soil core. Of special interest was the influence of the hydraulic flow direction on the development of the electric field and on the geo-/electrochemical milieu. The model solutions were NaCl and $CaSO_4$ in deionized water, tap water and Ca/$MgCl_2$-enriched tap water. Thus, the composition of the solution gradually became more complex and realistic. Both, the electrokinetic retention of anions and cations were examined. The electric gradient applied was 89 V/m; the hydraulic gradient was 0.001 with the average velocity being approximately 15 cm/day.

It has been documented that the electromigrative transport of OH^-/H^+ ions exceeds the hydraulic flow transport. A steep voltage gradient forms but after a while a linear voltage gradient occurs again indicating that low conductive/uncharged water forms but is now flushed out towards the downstream electrode by the hydraulic flow. Hence, according to DZENITIS´ theory of binary zones, from then on the soil milieu and pore solution composition is solely dominated by the electrochemical processes at the electrode placed upstream. In addition, these processes also influence the Eh/pH conditions at the downstream electrode, e.g. redox potentials at the downstream electrode prove that H_2/O_2 is transported by hydraulic flow. Once the waterfront is flushed out, the effluent is constant according to composition and pH, redox and conductivity. Thus, again steady state conditions develop, electrokinetic and hydraulic transport processes being in equilibrium. Modelling based on numerical algorithms confirm the experimental results. Up to 70% of the initial content of both anions and cations are retarded against the hydraulic flow.

Results achieved for anionic retention show that the presence of competitive ions or a multi-component solution, respectively, have a great influence on the development of the soil pH as well as on the redox potential, pH, electric conductivity and ion composition of the cathode effluent. Furthermore, it has been demonstrated that precipitation reactions are affected by the composition of the solution. Geochemical modelling suggests that calcium does not only precipitate as hydroxide directly at the cathode but also as sulphate and/or carbonate within the soil.

In particular, the electrokinetic retardation of cations seems to be very promising. OH^- ions produced at the cathode are transported into the soil by electromigration and hydraulic flow and may cause precipitation (Ca, Mg). The installation of the passive probes across the soil allows documenting the progression of this “precipitation

front", which is characterized by steeper voltage gradient due to depletion in ions. For constant ion supply, the proportion of discharged cations is even lower as for flushing with deionized water. Precipitation at the cathode as basic cause was proved by additionally applying acidic batch experiments. Contrary to the experiment with deionized water, here precipitation takes place mainly directly at the cathode or in the cathode chamber and not within the soil. Finally, it has been identified that constant ion supply leads to constant buffering of the alkaline reducing conditions produced at the cathode. Therefore, the effluent at the anode is not neutralized like in the experiments before but is dominated by the electrolysis products of the anode. Acidic pH and oxidising redox potential develop. Hence, the changed Eh-pH-conditions generated by electrokinetics and hydraulic flow have to be considered and its effect on the reactive barrier plays an important role.

On basis of the electrokinetic cell experiment results, a test apparatus in bench/container scale was designed and constructed. To evaluate the applicability of the container set-up, the test row started with NaCl as model solution (comparable to the electrokinetic cell experiment). The successful retardation of Cl^- (50%) was demonstrated. For simulating an electrokinetic fence, two different methods concerning type of electrodes and direction of electric/hydraulic field or electrokinetic fence configuration were tested. For both experiments, Ca/$MgCl_2$ enriched tap water was used as model solution.

The first experiment investigated the retardation of cations for the case of plane electrodes being installed upstream of reactive material (Fe^0). The influence of electrokinetic processes on the reactive material as well as on species formation and distribution and developing of the electric field were examined. Between the electrodes, the bulk of cations are retarded. Acidic batch experiments illustrate that for Mg^{2+} precipitation at the cathode seems to be the dominating retention process, whereas for Ca^{2+} the proportion of electrokinetic retention in the soil core is much higher. Within the elemental iron, distinct precipitation of Mg^{2+} but only minor precipitation of Ca^{2+} takes place. The distribution characteristics of the cations after the experiment can be explained mainly by the development of soil pH. The soil pH itself is not only a result of electrochemical reactions at the electrodes and geochemical conditions within the Fe^0 zone but is also influenced by hydraulic conditions. The experiment also shows that the steep voltage gradient that forms near the cathode supports electrokinetic retention of anions as accelerated electromigration occurs in this zone The measured dissolution of Fe^0 can be explained on basis of the Eh/pH diagram for Fe: the acidic/oxidative anode effluent causes a shift towards the stability field of Fe^{2+}.

Two pairs of well electrodes were installed in a way that they generate an electric field that is directed perpendicular to the hydraulic flow. The focus laid on detecting temporal variations in electric field distribution and interactions between adjacent electrodes as well as changes in pH, ion distribution and formation of species. Furthermore, the application of Li^+ as easy handling tracer method to prove the

efficiency of electrodes in coarse-grained soils was elaborated and documented by the experiment.

Voltage data was registered by a small-meshed grid of passive probes. Using computerized linear interpolation it was possible to visualize the development of the electric field in two dimensions. Hence, conclusions concerning ion distribution and pH developing during the experiment were possible. It has been identified that, in spite of the hydraulic flow and a constant ion supply, principally steady-state conditions develop that are similar to those achieved during the electrokinetic cell experiments where no hydraulic gradient was applied. Between the electrodes, the waterfront divides the soil into two binary zones, which differ in pH and ion composition. Furthermore, it has been recognized that hydraulic turbulences and/or precipitation can cause spatial shifting of the uncharged waterfront. Hence, composition and pH of the pore solution change. In addition, dissolved oxygen is transported from the anode into the soil by electroosmosis providing rather oxidative conditions within the sand.

Combining the results of concentration analysis within the soil at the end of the experiment with those of the chemical modelling allows to describe chemical species formation with time and space. The results lead to the conclusion that differences in hydraulic pressure ratio may contribute to differences in electroosmotic flow and ion discharge at the electrodes. Besides, it was shown that electrokinetic and precipitation reactions cause differences in pore solution composition between the electrode pairs.

The application of a dc electric field into the ground has a substantial influence on soil pH, redox values and ion concentration distribution of chemical species and usually leads to a distinct rise in temperature. Eh/pH diagrams of handbooks are often used but do not properly reflect these dynamic conditions during electrokinetics. To analyse and visualize the actual influence of electrokinetic induced changes on chemical species stability individual Eh/pH diagrams were modelled using the software HSC Chemistry 5.1. Elements selected for the modelling were C, Ca, Mg, S. Parameters changed were the selection and concentration of the elements as well as temperature.

Considering only one single element (Element-O-H-system), the modelling showed that variations in concentrations principally have a greater influence on the position of borders of the stability fields than variations in temperature have. Increased concentration leads to precipitation at lower pH. In addition, precipitation tendency/dependency in general and in comparison to other elements was determined. Species of C, Ca and Mg are only dependent on pH whereas species of S are dependent on redox values, too. $Mg(OH)_2$ precipitates at much lower pH than $Ca(OH)_2$.

Considering all elements, it has been proved that not only the elements present but also temperature strongly influences species formation. For example, Ca precipitates in presence of C as carbonate and at high temperature additionally calcium sulphate forms. The modelling demonstrated that checking all the diagrams with different main elements in parallel is giving a good idea of the equilibrium. Furthermore, it reflects that for electroremediation the influence of temperature on species formation often is underestimated though definitely has to be considered.

The influence of concentration ratio changes on species formation exemplarily was presented for pH 6 to 14 (cathode zone). On basis of the modelled Eh/pH diagrams, it is possible to describe the dynamics of species formation with time and space. In the beginning, Ca may precipitate as sulphate, carbonate in the soil and hydroxide at the electrode – depending on pH. As C and S concentrations decrease (due to electromigration towards the anode) precipitation of $CaCO_3$ within the soil and $Ca(OH)_2$ at the electrode is likely. Finally, only $Ca(OH)_2$ may precipitate at the cathode. Considering the results described above Eh/pH diagrams seems to offer a valuable help for predicting and a useful/important controlling measure for interpreting dynamic chemical species formation during electroremediation.

8.2 Discussion and Outlook

Since the 1990s, electrokinetic methods are increasingly being considered for the in situ remediation of contaminated sites, particularly for clayey soils where conventional methods like pump-and-treat fail (ALSHAWABKEH et al. 1999, CZURDA et al. 2001, HAUS et al. 1999, HAUS & CZURDA 1999, 2000, HAUS 2002, LAGEMANN & POOL 2001). Theoretic fundamentals of electrokinetic processes in fine-grained soils are well established. Numerous laboratory and field tests confirmed its successful and economical application in clayey soils (LAGEMAN et al. 1989, HAUS & CZURDA 1999, 2000, STEGER 2005, ZORN 2005). The results of this thesis provide profound knowledge of electrokinetic phenomena with respect to groundwater remediation. Fundamental aspects of electric fences have been determined and interactions between electric and hydraulic induced processes identified. In the following, the results are discussed – also with respect to the combination with permeable reactive barriers – and comprehensive solutions for future investigations are suggested.

The electrokinetic retention of charged species against hydraulic flow was proved. In principle, the electric field can be applied parallel or perpendicular to the groundwater flow direction. Regarding the former method particularly the retention of cations, where the cathode is placed upstream to the anode is promising. For both electrode arrays, changes in Eh/pH conditions of the groundwater were observed. To investigate their effect on the stability of reactive material, long-time electrokinetic cell experiments should be carried out. To accelerate testing, the pore and flushing solutions used have to be higher concentrated than at the actual field site to

accelerate alteration processes and to allow predictions concerning long-term behaviour. Furthermore, it has been identified that precipitation reactions rather than electromigration can be the major retardation factor. In future investigations, the practical control of the system should be focused on. Depending on the site characteristics, the formation of an acidic and alkaline front can be avoided by either addition of a buffer or neutralisation solution (DZENITIS 1997a, WILSON et al. 1995a,b, WILSON 1996, WONG et al. 1997), by the use of membranes (HANSEN et al. 1997) or by combining the anode and cathode solutions (GOLDMANN 2000).

To make results comparable and to investigate principles of electromigrative retention, for all experiments the same hydraulic gradient was used. In practice, groundwater velocity will vary during the years. Hence, in a next step different groundwater velocity scenario should be considered by applying different hydraulic gradients. KATZORECK (2007) used the electrokinetic cell set-up that was designed and constructed during the present study to investigate enhanced bioremediation in aquifers. He determined electromigration velocities and mass transport of various charged species/nutrients in sandy soil. On basis of the research presented here, it is recommended to further KATZORECK's investigations by additionally applying a hydraulic gradient.

In order to enhance electrokinetic remediation processes, several authors recommend the use of a multiple electrode system or two-dimensional well electrodes, respectively (HAUS et al. 2002, U.S. EPA 1998). Using well electrodes is more economical, especially for treating larger contaminated areas. Their production costs are less, the installation is easier and they can be used for contaminant plumes in great depths or can be installed horizontal. Principally, the electrode array is strongly dependent on the remediation location and goal, respectively. Here, two pairs of well electrodes were installed in the way that their generated electric field is directed perpendicular to the hydraulic flow. One of the main advantages of this electrode array is that both anions and cations are retarded simultaneously. Thus, the amount of total dissolved solids in the groundwater and therefore the total precipitation rates within the reactive wall will be reduced. In literature, the electrode array is also recommended to introduce and transport charged nutrients across the plume to support microbial degradation of organic contaminants (LAGEMAN & POOL 2001). The carried out experiments showed that the electrode array causes separation of ions and concentration gradients across the soil. Contrary to this, the electric field parallel to the hydraulic gradient provides a uniform distribution of ions between the electrodes. On basis of these results, the array displayed in Fig. 8.1 is suitable to be applied for the injection of ions/nutrients into aquifers or contaminant plumes as this array provides the most homogenous and maximal dispersion of charged species. Note that the green arrows show the case of examples for selected electromigration paths of charged species without taking into account a diversion of the species due to the hydraulic flow. The coupled electric and hydraulic gradients then cause the ideal species distribution across the aquifer.

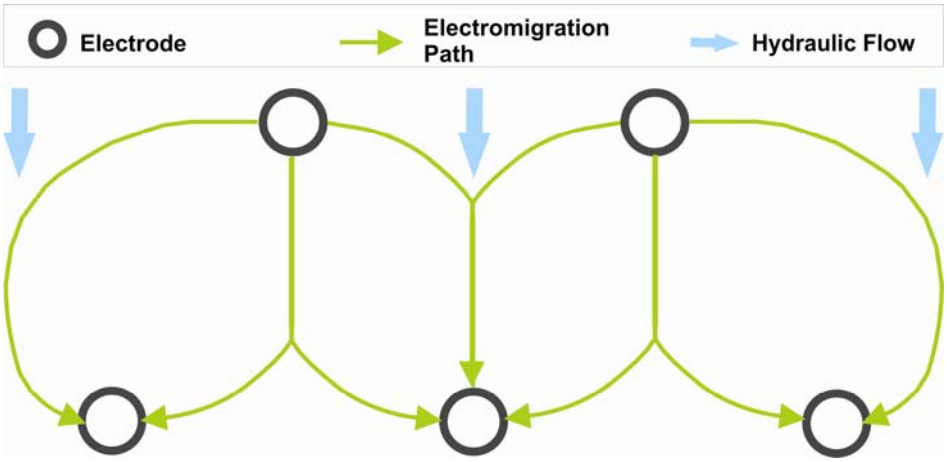

Fig. 8.1: Electrode array recommended for the injection of charged nutrients into groundwater.

Usually contaminant and/or groundwater constituent concentrations strongly vary across the whole dimension of reactive barriers. Thus, the spatial distribution of consumption and precipitation rates varies within the reactive barrier. To save costs, an electrokinetic fence could be installed to distribute charged species more evenly across the aquifer or to decrease concentrations in the plume centre, respectively. Again, the separation of ions has to be carefully considered when planning the positioning of the electrode array. Depending on groundwater composition, substantial precipitation may take place within the soil and may cause clogging of the pore spaces. To avoid changes in hydraulic conductivity, pH controlling at the electrodes is recommended. If the main aim is not to retain certain ions but to disperse them more homogenously over the barrier profile, the applied voltage and hence energy expenditure will be lower. The reduction of contaminant peak concentrations results in a reduction of reactive barrier consumption over time, hence increasing lifetime of the reactive barrier. At the same time, the design of the reactive barrier can be based on a smaller thickness, saving construction costs.

The successful application of an electrokinetic species transport is considerably dependent on the detailed knowledge of the chemical-physical characteristics of the pore solution and its constituents. Furthermore, the site conditions and soil characteristics can limit the treatment process. Experiments with very simple soil solution and deionized water as matrix solution did demonstrate that principle mechanisms and tendencies can be investigated, indeed. However, the results demonstrate that neither geo-/electrochemical processes nor species formation caused by electrokinetic and hydraulic gradient are described sufficiently by simple solutions. Hence, with respect to real case applications, the chemical system of the experiments has to be adapted to nature. To verify the findings it is suggested to conduct the experiments with actual leachate sampled at the contaminated sites.

The presented geochemical modelling showed that an Eh/pH diagram is a supportive tool to identify chemical species formation under the extreme conditions during electroremediation. On basis of the modelling, the chemical analysis program can be optimized. Especially, when dealing with ionic contaminants which easily change their electric charge from positive to negative and vice versa in different Eh and pH milieus and/or are toxic, Eh/pH diagrams are helpful to avoid dangers and unnecessary failures in the remediation success. In addition, the basis for the modelling was constructed in such way that the results not only can not only be applied to the experiments presented in this study but also can easily be transferred to field applications as they reflect natural and realistic conditions. Furthermore, these diagrams may offer extremely valuable information when combining the results with experimental work and with a good knowledge of aqueous chemistry. Thus, it is recommended to support Eh/pH diagrams by additional mineralogical analyses of the soil and/or electrode chambers. Summarizing, the performed modelling provides a basic and quite easy-to-handle tool for enhancing the success rate and safety conditions during electrokinetic remediation.

It is also recommended to integrate electrokinetic transport models into any electrokinetic remedial activity to optimise application strategy and to evaluate remediation time. ZORN (2005) introduced an improved numerical model for electrokinetic transport processes. Based on this, a model should be developed that includes all concurrent mass transport mechanisms as well as chemical specification of a multi-component system and temperature development. To explore the ideal electrode configuration and construction, the (hydro)geological situation and the variability in groundwater composition has to be known. In addition, it has to be considered that not only the targeted groundwater components but all charged species/contaminants will be transported. Experimental results suggest that hydraulic turbulences may cause changes in the position of the water formation front, which also affect the geochemical parameters of the groundwater downstream. Hence, laboratory tests should be supplemented by hydraulic modelling, which consider changes in hydraulic conditions caused by the implementation of electrodes. Summarizing, a multidimensional model should be developed that allows combining processes induced by both electric fences and groundwater flow.

Costs for the application of both electrokinetics and permeable reactive barriers depend on a multiplicity of parameters and hence differ strongly from site to site. Permeable reactive barriers are usually planned and constructed for large scale and long-time applications. In contrast, electrokinetics is rather applied for spatially well defined sites and short remediation times. Presently entire cost models for electrokinetics are given by THORNTON & SHAPIRO (1995) and ALSHAWABKEH et al. (1999); for PRBs by BURMAIER et al. (2007). Particularly for PRBs, comparison of costs with other techniques are insufficient as reliable long-time data are not yet available. Principally, capital costs for PRBs are high and are documented to be up to several million Euros. Cost statements for electrokinetics mainly refer to clayey soils.

For instance, THORNTON & SHAPIRO (1995) cite total costs of around 200,000 Euros for electrokinetic remediation of a soil volume of 30 m x 30 m x 2 m contaminated with chromate. Being only a supporting measure, costs for electrokinetics in combination with a PRB will be less than the values given in the literature. First, these costs usually refer to remediation projects completely based on the electrokinetic technique. Furthermore, most data rely on test studies and hence costs are higher than they would be under commercial conditions. Because of lower tortuosity effects and lower soil conductivities in coarse-grained soils, the needed electrical input is much lower in comparison to a pure application in a clayey soil. Thus, the required electric field strength or energy costs, respectively, will be less. Finally, several costs like for preliminary geological and hydrogeological investigations, labor and monitoring, incur for the construction of permeable reactive barriers anyway. In summary, the application of an electrokinetic fence seems to be viable from an economic point of view, too.

Clean-up practice suggests that the combination of different remediation techniques is promising, especially for complex sites and contamination situations. STEGER (2005) designed an electrokinetic test plant that enables the combination with pneumatic, hydraulic and/or microbiological techniques. Principally, there is a multitude of application possibilities for both dc and ac electric fences. This thesis shows that the installation of an electric fence is a promising method to combine with permeable reactive barriers in aquifers. The challenge of the environmental scientist will be to continue combining technologies in a way that they support each other's benefits while compensating their potential drawbacks.

9 REFERENCES

Acar, Y. B., Rabbi, F. & Ozsu, E.E. (1997): Electrokinetic Injection of Ammonium and Sulfate Ions into Sand and Kaolinite Beds.- J. of Geotechnical and Geoenv. Eng., 123 (3): 239-249.

Acar, Y.B. & Alshawabkeh, A.N. (1993): Principles of Electrokinetic Remediation.- Environ. Sci. Technol., 27 (13): 2638-2647.

Acar, Y.B. & Alshawabkeh, A.N. (1996): Electrokinetic Remediation. I: Pilot-Scale Tests with Lead-Spiked Kaolinite.- J. Geotech. Eng., 122: 173-185.

Acar, Y.B., Gale, R.J., Alshawabkeh, A.N., Marks, R.E., Puppala, S., Bricka, M. & Parker, R. (1995): Electrokinetic Remediation: Basics and Technology Status.- J. Hazard. Mater., 40 (3): 117-137.

Acar, Y.B., Hamed, J., Alshawabkeh, A.N. & Gale, R.J. (1994): Removal of Cadmium (II) from Saturated Kaolinite by the Application of Electrical Current.- Géotechnique, 44 (2): 239-254.

Acar, Y.B., Li, H. & Gale, R.J. (1992): Phenol Removal from Kaolinite by Electrokinetics.- J. Geotech. Eng. Div, ASCE, A118 (11): 1837-1852.

Alshawabkeh, A.N. & Acar, Y.B. (1996): Electrokinetic Remediation. II: Theoretical Model.- J. Geotech. Eng., 122 (3): 186-196.

Alshawabkeh, A.N., Yeung, A.T. & Bricka, M.R. (1999a): Optimization of 2-D electrode configuration for electrokinetic extraction.- J. Soil Contaminat, 8: 617-635.

Alshawabkeh, A.N., Yeung, A.T. & Bricka, M.R. (1999b): Practical Aspects of In-Situ Electrokinetic Extraction.- J. Environ. Eng., 125 (1): 27-35.

Baraud, F., Fourcade, M.C., Tellier, S. & Astruc, M. (1998): Modelling of decontamination rate in an electrokinetic soil processing.- Int. J. Environ. Anal. Chem., 68: 105-121.

Baraud, F., Tellier, S. & Astruc, M. (1997): Ion velocity in soil during electrokinetic remediation.- J. Hazard. Mat., 56: 315-332.

Benner, S.G., Blowes, D.W. & Molson (2001): Modleing preferntial flow in reacitve barriers: Implications for performance and design.- Ground Water 39 (3): 371-379.

Birke, V., Burmeier, H. & Rosenau, D. (2003): Design, Construction and Operation of Tailored Permeable Reactive Barriers.- In: Prokop, G., Bittens, M., Cofalka, P., Roehl, K.E., Schamann, M. & Younger, P. (eds.): Summary Report of the 1st IMAGE-TRAIN Advanced Study Course "Innovative Groundwater Management Technologies". Tübinger Geowissenschaftliche Arbeiten (TGA), C68: 64-94; Tübingen.

Birke, V. & Roehl, K.E. (2002): An introduction to permeable reactive barriers (PRB).- Available on www.rubin-online.de.

Blowes, D.W., Ptacek, C.J., Benner, S.G., McRae, C.W.T., Bennett, T.A. & Puls, R.W. (2000): Treatment of inorganic contaminants using permeable reactive barriers.- Cont. Hydrol., 45: 123-137.

Brindley, G.W. & Brown, G. (1980): Crystal Structures of Clay Minerals and their X-ray Indentification.- Min. Soc. Monogr., 5: 495 p.; Mineralogical Society, London.

Bruell, C.J., Segall, B.A. & Walsh, M.T. (1992): Electroosmotic Removal of Gasoline Hydrocarbons and TCE from Clay.- J. Environ. Eng, 118 (1): 68-83.

Budhu, M., Rutherford, M., Sills, G. & Rasmussen, W. (1997): Transport of nitrates through clay using electrokinetics.- J. Env. Eng. 123 (12): 1251-1253.

Casagrande, L. (1939): Die elektrochemische Bodenverfestigung.- Bautechnik, 16: 228-230.

Casagrande, L. (1952): Electroosmotic stabilization of soils.- Boston Soc. Civ. Eng., 49 (1).

Casagrande, L. (1983): Stabilization of soils by means of Electro-Osmosis. State-of-the-art.- Boston Soc. Civ. Eng., 69 (2): 255-302.

Chew, C.F. & Zhang, T.C. (1997): Nitrate removal using electrokinetic/iron wall processes.- In: Erickson, L.E., Rankin, M.M., Grant, S.C. & McDonald, J.P.: Proceedings of the 12th Annual Conference on Hazardous Waste Research; http://www.engg.ksu.edu/HSRC/97Proceed/Remediation1/nitrate.html.

Chilingar, G.V., Loo, W.W., Khilyuk, L.F. & Katz, S.A. (1997): Electrobioremediation of soils contaminated with hydrocarbons and metal: Progress report.- Energy Sources 19: 129-146.

Chung, H.I. & Lee, Y.S. (2007): Electrokinetic permeable reactive barrier for the removal of heavy metal and organic substance in contaminated soil and groundwater.- EREM 2006, 6th Symposium on Electrokinetic Remediation: Vigo, Spain.

CLARINET (2002a): Remediation of Contaminated Land, Technology Implementation in Europe. Available from www.clarinet.at

CLARINET / NICOLE (1998): CLARINET/NICOLE Joint Statement: Better Decision Making Now. October 1998. Available from www.nicole.org

Csóvári, M., Csicsák, J., Földing, G. & Simoncsics, G. (2005): Experimental iron barrier in Pécs, Hungary.- In: Roehl, K.E., Meggyes, T., Simon, F.-G. & Stewart, D.I. (eds): Long-term Performance of Permeable Reactive Barriers.- Trace Metals and Other Contaminants in the Environment, 7: 261-281; Amsterdam (Elsevier).

Czurda, K., Haus, R., Kappeler, C. & Zorn, R. (eds., 2001): EREM 2001 - 3rd Symposium and Status Report on Electrokinetic Remediation.- Schr. Angew. Geol. Karlsruhe, 63; Karlsruhe.

Darcy, H. (1856): Les fontaines publiques de la ville de Dijon.- Paris (Dalmont).

Davis-Hoover, W.J., Roulier, M.H., Kemper, M., Vesper, S.J., Al-Abed, S., Bryndzia, L.T., Murdoch, L.C., Cluxton, P. & Slack, W.W. (1999): Horizontal Lasagna to bioremediation TCE.- 2nd Symposium, Tech. Univ. of Denmark, 159-164.

DeFlaun, M.F. & Condee, C.W. (1997): Electrokinetic transport of bacteria.- J. Hazard. Mat., 55: 263-277.

Denisov, G., Hicks, R.E. & Probstein, R.F. (1996): On the Kinetics of Charged Contaminant Removal from Soils Using Electric Fields.- Journal of Colloid and Interface Science, 178: 309-323.

Dzenitis, J. M. (1996): Soil Chemistry Effects and Flow Prediction in Remediation of Soils by Electric Fields. PhD Dissertation, Massachusetts Institute of Technology, 123 S.; Cambridge.

Dzenitis, J.M. (1997a): Soil Chemistry Effects and Flow Prediction in Electroremediation of Soil.- Environ. Sci. Technol., A31 (4): 1191-1197.

Dzenitis, J.M. (1997b): Steady State and Limiting Current in Electroremediation of Soil.- The Electrochemical Society, Inc., A144 (4): 1317-1322.

Eid, N., Larson, D., Slack, D. & Kiousis, P. (1999): Nitrate electromigration in sandy soil in the presence of hydraulic flow.- J. of Irrigation and Drainage Eng., 125 (1): 7-11.

Eid, N., Slack, D. & Larson, D. (2000): Nitrate electromigration in sandy soil: closed system response.- J. of Irrigation and Drainage Eng., 126 (6): 389-397.

Elektorowicz, M. & Boeva, V. (1996): Electrokinetic supply of nutrients in soil bioremediation.- Environ. Technol., 17: 1339-1349.

Elektorowicz, M. & Ju, L. (2001): Removal of PAH using electrokinetic transport of biosurfactants in clayey soils.- In: Czurda, K., Haus, R., Kappeler, C. & Zorn, R. (eds.), EREM 2001, 3rd Symposium and Status Report on Electrokinetic Remediation. Schr. Angew. Geol. Karlsruhe, 63: 15/1-15/12; Karlsruhe.

EPA (1998): Permeable reactive barrier technologies for contaminant remediation.- U.S. EPA Remedial Technology Fact Plane, EPA 600/R-98/125, 102 p.

ESTCP (Environmental Security Technology Certification Program) (2003): Evaluating the Longevity and hydraulic performance of permeable reactive barreirs at department of defense sites.- ESTCP Cost and performance report CU-9907: 54p; Available on www.estcp.org.

Eykholt, G.R. & Daniel, D.E. (1994): Impact of System Chemistry on Electroosmosis in Contaminated Soil.- J. Geotchn. Engineering, 120 (5), 797-815.

Eykholt, G.R. (1998): Analytical solution for networks of irreversible first-order reaction.- J. of the Intern. Ass. on Water Quality, 33 (3): 814-826.

Fetter, C.W. (1994): Applied Hydrogeology.- 3rd ed.: 691p.; New Jersey (Prentice-Hall).

Fick, A. (1855): On liquid diffusion.- Phil. Mag., 294(X): 30-39.

Freeze, R.A. & Cherry, J.A. (1979): Groundwater.- Englewood Cliffs, N.J. (Prentice-Hall).

Gavaskar, A.R., Gupta, N., Sass, B.M., Janosy, R.J. & O'Sullivan, D. (1998): Permeable Barriers for Groundwater Remediation.- 176 p.; Columbus, Ohio (Batelle Press).

Gavaskar, A., Gupta, N., Sass, B., Janosy, R. & Hicks, J. (2000): Design guidance for application of permeable reactive barriers for groundwater remediation.- 167 p.; Columbus, Ohio (Battelle).

Gavaskar, A., Sass, B., Gupta, E., Drescher, E., Yoon, W., Sminchak, J., Hicks, J. & Condit, W. (2002): Evaluating the longevity and hydraulic performance of permeable barriers at department of defence sites.- 70 p.; Columbus, Ohio (Battelle).

Gerthsen, C., Kneser, H.O. & Vogel, H. (1989): Physik.- 16. Aufl.: 920 S.; Heidelberg (Springer).

Gillham, R.W. & O'Hannesin, S.F. (1994): Enhanced degradation of halogenated aliphatics by zero-valent iron.- Ground Water, 32 (6): 958-987.

Gioannis, G., Muntoni, A., Ruggeri, R., Zijlstra, H. & Floris, M. (2007): Chromate adsorbtion in a transformed red mud permeable reactive barrier using electrokinesis.- EREM 2006, 6th Symposium on Electrokinetic Remediation: Vigo, Spain.

Godschalk, M.S. & Lageman, R. (2005): Electrokinetic Biofence, remediation of VOCs with solar energy and bacteria.- Engineering Geology, 77 (3-4): 225-231; Amsterdam (Elsevier).

Gray D.H. & Mitchell J.K. (1967): Fundamental Aspects of Electro-Osmosis in Soil.- J. Soil Mech. Found., SM 6: 209-236.

Gray, D.H. & Schlocker, J.G. (1969): Electrochemical alteration of clay soils.- Clays Clay Miner., 17: 309-322.

Gregolec, G., Roehl, K.E. & Czurda, K. (2005): Electrokinetic techniques.- In: Roehl, K.E., Meggyes, T., Simon, F.-G. & Stewart, D.I.: Long-term Performance of permeable reactive barriers: 183-209; Amsterdam (Elsevier).

Gregolec, G., Zorn, R., Kurzbach, A., Roehl, K.E. & Czurda, K. (2001): Coupling of hydraulic and electric gradients in sandy soils.- In: Czurda, K., Haus, R., Kappeler, C. & Zorn, R. (eds.): Proc. EREM 2001, 3. Symposium on Electrokinetic Remediation, April 18-20, 2001, Karlsruhe. Schr. Angew. Geol. Karlsruhe, 63: 41/1-41/15; Karlsruhe.

Grolimund, D., Borkovec, M., Barttmetler, K. & Sticher, H. (1996), Colloid-Facilitated Transport of Strongly Sorbing Contaminants in Natural Porous Media: A Laboratory Column Study.- Environ. Sci. Technol., 30 (10): 3118-3123.

Hamed, J., Acar, Y.B. & Gale, R.J. (1991): Pb (II) Removal from Kaolinite Using Electrokinetics.- J. Geotech. Eng., 117 (2): 241-271.

Hansen, H.K., Ottosen, L.M., Kliem, B.K. & Villumsen, A. (1997): Electrodialytic remediation of soils polluted with Cu, Cr, Hg, Pb and Zn.- J. Chem. Tech. Biotechnol., 70: 67-73.

Haran, B.S., Popov, B.N., Zheng, G. & Whit, R.E. (1997): Mathematical modeling of hexavalent chromium decontamination from low surface charged soil.- J. Hazard. Mat., 55 (1-3): 93-107.

Haus, R. & Czurda, K. (1999): Electrokinetic Remediation of Clays.- In: Kodama, H., Mermut, A.R. & Torrance, J.K. (eds.): Clays for our future: 191-200; Ottawa, Canada.

Haus, R. & Czurda, K. (2000): Field Scale Study on In situ Electroremediation.- In: Proc. 7th Intern. KFK/TNO Conference on Contaminated Soil, ConSoil 2000: 1053-1059; London (Telford).

Haus, R., Zorn, R. & Aldenkortt (1999a). Comparison of Lab- and Field Scale Tests in Electroremediation.- Proc. 2nd Symposium Heavy Metals in the Environment and Electromigration Applied to Soil Remediation, July 7th-9th, DTU, Lyngby, Denmark, 165-170.

HAUS, R., ZORN, R. & ALDENKORTT, (1999b): Electroremediation: In situ Treatment of Chromate Contaminated Soil.- In: Yong, R.N. & Thomas, H.R. (eds.): Geoenvironmental Engineering - Ground contamination - Pollutant Management and Remediation: 384-391; London (Telford).

Haus, R. (2002): Elektrokinetische Bodensanierung.- Schr. Angew. Geol. Karlsruhe, 65: 214 p.; Karlsruhe.

Haus, R., Zorn, R., Czurda, K. & Terfehr, S. (2002): Elektrokinetische in-situ-Sanierung, Stand der Technik, Planung, Implementierung.- Schriftenreihe altlastenforum Baden-Württemberg e.V., 7: 25 p.

Helmholtz, H.L.F. (1879): Studien über elektrische Grenzschichten.- Wiedemanns Annalen der Physik, 7: 337-382; Leipzig.

Helmholtz, H.L.F. (1879): Studies of Electric Boundary Layers.- Wied. Ann., Vol. 7, pp. 337-382.

Hicks, R.E. & Tondorf, S. (1994): Electrorestoration of Metal Contaminated Soils.- Environ. Sci. Technol., 28 (12): 2203-2210.

Hicks, R.E., Probstein, R.F. & Young, W.T. (1999): In-Situ Field Test of Electroremediation of a Chromate-contaminated Site in Hudson County, New Jersey.- R2D2 Program, Northeast Hazardous Substance Research Centre; Final Report: 80 S.

Ho, S.V., Athmer, C.J., Sheridan, P.W. & Shapiro, A.P. (1997): Scale-up aspects of the Lasagna TM process for in situ soil decontamination.- J. Haz. Mat., 55: 39-60.

Ho, S.V., Athmer, C., Sheridan, P.W., Hughes, B.M., Orth, R., McKenzie, D., Brodsky, P.H., Shapiro, A., Thornton, R., Salvo, J., Schultz, D., Landis, R., Grifffith, R. & Shoemaker, S. (1999a): The Lasagna Technology for In Situ Soil Remediation. 1. Small field test.- Environ. Sci. Technol., 33 (7): 1086-1091.

Ho, S.V., Athmer, C., Sheridan, P.W., Hughes, B.M., Orth, R., McKenzie, D., Brodsky, P.H., Shapiro, A., Sivavec, T.M., Salvo, J., Schultz, D., Landis, R., Grifffith, R. & Shoemaker, S. (1999b): The Lasagna Technology for In Situ soil remediation. 2. Large field test.- Environ. Sci. Technol., 33 (7): 1092-1099.

Ho, S.V., Sheridan, P.W., Athmer, C.J., Heitkamp, M.A., Brackin, J.M., Weber, D. & Brodsky, P.H. (1995): Integrated In Situ Soil Remediation Technology: The Lasagna Process.- Environ. Sci. Technol., A29: 2528-2534.

Hölting, B. (1992): Hydrogeologie: Einführung in die allgemeine und angewandte Hydrogeologie.- 4. Aufl.: 415 S.; Stuttgart (Enke).

Huang, H.H. (2006): STABCAL - Stability Calculations for Aqueous Systems.- Software produced by Prof. H. Huang, Montana Tech (USA).

ITRC (Interstate Technology & Regulatory Council) (1999a): Regulatory guidance for permeable barrier walls designed to remediate chlorinated solvents.- PBW-1: 52 p.; Washington, D.C. Available on the internet at www.itrcweb.org.

ITRC (Interstate Technology & Regulatory Council) (1999b): Regulatory guidance for permeable reactive barriers designed to remediate inorganic and radionuclide contamination.- PRB-3: 52 p.; Washington, D.C. Available on the internet at www.itrcweb.org.

ITRC (Interstate Technology & Regulatory Council) (2000): Design guidance for application of permeable reactive barriers for groundwater remediation.- PRB-2: 167 p.; Washington, D.C. Available on the internet at www.itrcweb.org.

ITRC (Interstate Technology & Regulatory Council) (2005): Permeable reactive barriers : Lessons Learned/New Directions.- PRB-4: 202 p.; Washington, D.C. Available on the internet at www.itrcweb.org.

Jackman, S.A., Maini, G., Sharman, A.K. & Knowles, Ch.J. (1999): The effects of direct electric current on the viability and metabolism of acidophilic bacteria.- Enzyme and Mcrobial Techn., 24: 316-324.

Jackman, S.A., Maini, G., Sharman, A.K., Sunderland, G. & Knowles, Ch.J. (2001): Electrokinetic movement and biodegradation of 2,4-dichlorophenoxyacetic acid in silt soil.- Biotechn. and Bioeng., 74 (1): 40-48.

Jacobs, R.A. & Probstein, R.F. (1996): Two-Dimensional Modelling of Electroremediation.- AIChE Journal, 42 (6): 1685-1696.

Jacobs, R.A., Sengun, M.Z., Hicks, R.E. & Probstein, R.F. (1994): Model and experiment on soil remediation by electric fields.- J. Environ. Sci. Health, A29 (9): 1933-1955.

Katzoreck, D. (2007): Untersuchungen zum elektrokinetischen Transport von Nährstoffen und Elektronenakzeptoren im sandigen Boden zur Simulation des mikrobiellen Schadstoffabbaus.- 102 p.; Karlsruhe (unpublished diploma thesis).

Kim, J. & Lee, K. (1999): Effects of electric field directions on surfactant enhanced electrokinetic remediation of diesel-contaminated sand column.- J. Environ. Sci. Health, A34 (4): 863-877.

Klein, R. & Schad, H. (2000): Results from a full scale funnel-and-gate system at the Beka site in Tübingen (Germany) using zero-valent iron.- In: Proc. 7th Intern. KFK/TNO Conference on Contaminated Soil, ConSoil 2000: 917-923; London (Telford).

Korte, N. (2001): Zero-valent iron permeable barriers. A review of performance.- Oak Ridge National Laboratory Envir. Sci. Div. Pub. N05056.

Krauskopf, K.B. (1979): Introduction to Geochemistry.- New York (McGraw-Hill Book Comp.)

Kurzbach, A. (2001): Untersuchungen zur Migration von Ionen in sandigen Bpden unter Einfluss eines hydraulischen und elektrischen Gradienten.- 102 p.; Freiburg (unpublished diploma thesis).

Lageman, R. & Pool, W. (2001): Thirteen years electro-reclamation in the Netherlands.- In: Czurda, K., Haus, R., Kappeler, C. & Zorn, R. (eds.), EREM 2001, 3rd Symposium and Status Report on Electrokinetic Remediation. Schr. Angew. Geol. Karlsruhe, 63: 1/1-1/17; Karlsruhe.

Lageman, R. (1993): Electroreclamation - Applications in the Netherlands.- Environ. Sci. Technol., 27 (13): 2648-2650.

Lageman, R., Pool, W. & Seffinga, G.A. (1989): Electro-Reclamation: Theory and Practice.- Chemistry & Industry, 18: 585-590.

Lageman, R.; Pool, W. & Seffinga, G.A. (1991): Elektrosanierung: Sachverhalt und zukünftige Entwicklungen.- In: Jessberger, H.L. (ed.): Erkundung und Sanierung von Altlasten; Rotterdam (Balkema).

Li, R.S. & Li, L.Y. (2000): Enhancement of electrokinetic extraction from lead-spiked soils.- J. of Env. Eng., 126 (9): 849-857.

Li, Z.. Yu, J.-W. & Neretnieks, I. (1997): Removal of Pb(II), Cd (II) aand Cr (III) from sand by electromigration.- J. Hazard. Mat., 55: 295-304.

Lindgren, E.R., Kozak, M.W. & Mattson, E.D. (1991): Electrokinetic Remediation of Contaminated Soils: An Update.- In: Post, R.G. & Wacks, M.E.: Waste Management '92 - Proc. of the Symp.: 1309-1314; Tucson (Univ. of Ariz. Press).

Lindgren, E.R., Kozak, M.W. & Mattson, E.D. (1994): Electrokinetic Remediation of Unsaturated Soils.- In: Tedder, D.W. & Pohland, F.G.(eds.): ACS Symposium Series 554: Emerging Technologies in Hazardous Waste Management IV.: 33-50; Washington/DC (American Chemical Society).

Lo, I., Lai, K. & Kjeldsen, P. (2004): Field monitoring of Fe^0 PRB for removal of chlorinated hydrocarbons.- In: Proceedings, Fourth international conference on remediation of chlorinated and recalcitrant compounds, Monterey, Calif. Columbus, Ohio (Battelle).

MacKenzie, P.D., Horney, D.P. & Sivavec, T.M. (1999): Mineral precipitation and porosity losses in granular iron columns.- J. Haz. Mat., 68: 1-17.

Maini, G., Sharman, A.K., Sunderland, G. Knowles, C.J., Jackman, S.A. (2000): An integrated method of incorperating sulfur-oxidizing bacteria to enhance removal of copper from contaminated soil.- Env. Sci. Technol., 34 (6): 35-60.

Matthess, G. (1990): Die Beschaffenheit des Grundwassers.- 2nd ed.: 498 p.; Berlin, Stuttgart (Gebrüder Borntraeger).

McMahon, P.B., Dennehy, K.F. & Sandstrom, M.W. (1999): Hydraulic and geochemical performance of a permeable reactive barrier containing zero-valent iron, Denver Federal Center.- Ground Water, 37 (3): 396-404.

Meggyes, T. (2005): Construction methods of permeable reactive barriers. - In: Roehl, K.E., Meggyes, T., Simon, F.-G. & Stewart, D.I. (eds.): Long-term Performance of Permeable Reactive Barriers. Trace Metals and Other Contaminants in the Environment, 7: 27-52; Amsterdam (Elsevier).

Menon, R.M., Hsu, C., & Yeung, A.T. (1996): Experimental and modelling studies on electro-kinetic extraction of lead from Georgia kaolinite.- In: Kamon, M. (ed.): Env. Geotechnics., Vol.2: 1039-1044; Rotterdam (Balkema).

Mermut, A.R. (ed., 1994): Layer Charge Characteristics of 2:1 Silicate Clay Minerals.- CMS Workshop Lectures, 6: 134 p.; Clay Minerals Society, Boulder, CO.

Mitchell, J.K. & Yeung, A.T. (1991): Electrokinetic Flow Barriers in Compacted Clay.- Transp. Res. Record, 1288: 1-9.

Moore, A.M. & Young, T.M. (2005): Chloride interactions with iron surfaces: Implications for perchlorate and nitrate remediation using permeable reactive barriers.- J. Env. Eng., 131 (6): 924-933.

Morrison, S.J. (2003): Performance evaluation of a perm3eable reactive barrier using reaction products as tracers.- Environ. Sci. Technol., 37: 2302-2309.

Napier, J., (1846), Phil. Mag., Vol. 29, No 10.

Narasimhan, B. & Ranjan, R.S. (2000): Electrokinetic barrier to prevent subsurface contaminant migration: theoretical model development and validation.- J. Cont. Hydr., 42: 1-17.

Nathanail, J., Bardos, R.P. & Nathanail, P. (2001): Contaminated Land Management: Ready Reference.- 480 p.; London (EPP Publications).

Niederbacher, P. & Nahold, M. (2005): Installation and operation of an adsorptive reactor and Barrier (AR&B) system in Brunn am Gebirge, Austria.- In: Roehl, K.E., Meggyes, T., Simon, F.-G. & Stewart, D.I. (eds.): Long-term Performance of Permeable Reactive Barriers.- Trace Metals and Other Contaminants in the Environment, 7: 283-309.; Amsterdam (Elsevier).

O'Hannesin, S.F. & Gillham, R.W. (1998): Long-term Performance of an In Situ "Iron Wall" for Remediation of VOCs.- Ground Water, 36 (1): 164-170.

O'Hannesin, S.F. & Gillham, R.W. (2005): A current overview of permeable reactive barrier technology.- Available on the internet at www.portofentry.com.

Page, M.M. & Page, Ch.L. (2002): Electroremediation of Contaminated Soils.- J. of Inv. Eng., 128 (3): 208-219.

Pamukcu, S. & Wittle, J.K. (1992): Electrokinetic Removal of Selected Heavy Metals from Soil.- Environmental Progress, 11 (3): 241-250.

Pamukcu, S. (1994): Electrokinetic Removal of Coal Tar Constituents From Contaminated Soils.- Final Report, Electric Power Research Institute, EPRI TR-103320, Project 2879-21, March 1994.

Pamukcu, S. (1997): Electro-Chemical Technologies for in-situ restoration of contaminated subsurface soils.- EJGE Paper: 37 p.; www.ejge.com/1997/Ppr9704/Ppr9704.htm.

Pamukcu, S. (2005): Electrically Enhanced Transformation of Contaminants in Clay Rich Subsurface.- Presentation at the EREM Conference May 2005, Ferrara, Italy.

Phillips, D.H., Gu, B., Watson, D.B., Roh, Y., Liang, L. & Lee, S.Y. (2000): Performance Evaluation of a Zerovalent Iron Reactive Barrier: Mineralogical Characteristics.- Environ Sci. Technol., 34: 4169-4176.

Phillips, D.H., Watson, D.B., Roh, Y. & Gu, B. (2003): Mineralogical characteristics and transformations during Long-term operation of a zero-valent iron reactive barrier.- J. of Envir. Quality, 32 (6): 2033-2045.

Pourbaix, M. (1966): Atlas of electrochemical equilibria in. aqueous solutions.- 644p.; Oxford (Pergamon Press).

Probstein, R.F. & Hicks, R.E. (1993): Removal of Contaminants from Soil by Electric Fields.- Science, 260: 498-503.

Probstein, R.F. (1994): Physicochemical Hydrodynamics - An Introduction.- 2nd ed.; New York (Wiley & Sons).

Quincke, G. (1861) Pogg. Ann. Physik, Vol. 113: 513 p.

Reddy, K.R. & Chinthamreddy, S. (2003): Sequentially enhanced electrokinetic remediation of heavy metals in low buffering clayey soils.- J. of Geotech. and Geoenv. Eng., 129 (3): 263-277.

Reddy, K.R. & Chinthamreddy, S. (2004): Enhanced Electrokinetic Remediation of Heavy Metals in Glacial Till Soils Using Different Electrolyte Solutions.- J. of Env. Eng., 130 (4): 442-455.

Reddy, K.R., Danda, S. & Saichek, R.E. (2004): Complicating Factors of Using Ethylenediamine Tetraacetic Acid to Enhance Electrokinetic Remediation of Multiple Heavy Metals in Clayey Soils.- J. of Env. Eng., 130 (11):1357-1366.

Reddy, K.R., Parupudi, U.S., Devulapalli, S.N. & Xu, C.Y. (1997): Effects of soil composition on the removal of chromium by electrokinetics.- J. Hazard. Mat., 55, 135-158.

Reed, B.E., Mitchell, J.K., Thompson, J.C. & Hatfield, J.H. (1995): Chemical Conditioning of Electrode Reservoirs during electrokinetic Soil flushing of Pb-contaminated Silt Loam.- J. Environ. Eng., 121 (11): 805-815.

Reuss, F. (1809): Mém. Soc. Naturalistes Moscou, 2: 327 p.

Reuss, F.F. (1809), Sur un nouvel effet de l'électricité galvanique.- Mémoires de la Société Impériale des Naturalistes de Moscou, Vol. 2, 327-337.

Roehl, K.E. & Czurda, K. (2002): PEREBAR - A European Project on the Long-Term Performance of Permeable Reactive Barriers.- In: Prokop, G. (ed.): Proc. 1st IMAGE-TRAIN Cluster Meeting Karlsruhe November 7-9, 2001, 23-31; Vienna (Federal Environmental Agency of Austria).

Roehl, K.E., Huttenloch, P. & Czurda, K. (2001): Permeable sorption barriers for in-situ remediation of polluted groundwater - reactive materials and reaction mechanisms.- In: GREEN 3, The Exploitation of Natural Resources and the Consequences, 466-473; London (Telford).

Roehl, K.E., Meggyes, T., Simon, F.-G. & Stewart, D.I. (2005): Long-term Performance of Permeable Reactive Barriers.- Trace Metals and Other Contaminants in the Environment, 7: 244 p.; Amsterdam (Elsevier).

Roehl, K.E. & Gregolec, G. (2005): Implementation of Remediation Technologies - Theory and Practice.- Land Contamination & Reclamation, 13 (2): 123-136; London (EPP Publications).

Roine, A. & Anttila, K. (2006): Eh-pH-Diagrams (Pourbaix-diagrams).- Available on www.outotec.com.

Röhrs, J., Ludwig, G. & Rahner, D. (2002): Electrochemically induced reactions in soils - a new approach to the in-situ remediation of contaminated soils? Part 2: remediation experiments with a natural soil containing highly chlorinated hydrocarbons.- Electrochimical Acta, 47 (9):1405-1414.

Roh, Y., Lee, S.Y. & Elless, M.P. (2000): Characterization of corrosion products in the permeable reactive barriers.- Environ. Geol. 40 (1-2): 184-194.

Rust, C.F., Schulze-Makuch, D. & Bowman, R., (2005): Removal of the Human Pathogen Giarida intestinales from Ground Water.- Presented at the 2005 NGWA Groundwater Summit, San Antonio, TX, April 17-20.

Saichek, R.E. & Reddy, K.R. (2005): Electrokinetically enhanced remediation of hydrophobic organic compounds in soils: a review.- Environ. Sci. Technol., 35: 115-192.

Sass, B., Gavaskar, A., Yoon, W., Reeter, C. & Drescher, E. (2002): Geochemical factors affecting performance and longevity of permeable reactive barriers.- In: Proceedings, Third international conference on remedaiton of chlorinated and reacalcitrant compounds, Monterey, Calif. (Battelle Press).

Schwartz, D.T., Bueler, M.F., Christiansen, D.X. & Davis, E.J. (1997): In-situ monitoring of electrochemical transport processes in Hanford grout vault soil.- J. Haz. Mat., 55: 23-37.

Segall, B.A. & Bruell, C.J. (1992): Electroosmotic Contaminant-Removal Processes.- J. Environ. Eng., 118 (1): 84-100.

Segall, B.A., O'Bannon, C.E. & Matthias, J.A. (1980): Electro-Osmosis Chemistry and Water Quality.- J. Geotech. Eng. Div., 106 (GT10): 1148-1152.

Shapiro, A.P. & Probstein, R.F. (1993): Removal of Contaminants from Saturated Clay by Electroosmosis.- Environ. Sci. Technol., 27 (2): 283-291.

Simon, F.-G. & Meggyes, T. (2000): Removal of organic and inorganic pollutants from groundwater using permeable reactive barriers - Part 1. Treatment processes for pollutants.- Land Contamination & Reclamation, 8 (2): 103-116.

Smoluchowski, M. (1921): Elektrische Endosmose und Strömungsströme.- In: Handbuch der Elektrizität und des Magnetismus, 2: 366-428; Leipzig.

Steger, H. (2005): Elektrokinetische In-situ-Sanierung LCKW-kontaminierter gering durchlässiger Lockergesteine.- Diss. Univ. Karlsruhe.

Steger, H., Zorn, R., Haus, R. & Czurda, K. (2001): Removal of tetrachlorethylene from finegrained soils by electrokinetic processes.- In: Czurda, K., Haus, R., Kappeler, C. & Zorn, R. (eds.): EREM 2001, 3rd Symposium and status report on electrokinetic remediation, Schr. Angew. Geol. Karlsruhe, 63: 21-1-21-14; Karlsruhe.

Stern (1924): Zur Theorie der elektrischen Doppelschicht.- Z. Elektrochem., 30: 508-516.

Stumm, W. & Morgan, J.J. (1996): Aquatic Chemistry: Chemical equilibria and rates in natural waters.- 1022 S.; New York (John Wiley & Sons).

Thevanayagam, S. & Rishindran, T. (1998): Injection of nutrients and TEAs in clayey soils using electrokinetics.- J. of Geotech. and Geoenv. Eng. 124 (4):330-338.

Thornton, R.F. & Shapiro, A.P. (1995): Modeling and Economic Analysis of In Situ Remediation of Cr(VI)-Contaminated Soil by Electromigration.- In: Tedder, D.W. & Pohland, F.G. (eds.): ACS Symposium Series 607: Emerging Technologies in Hazardous Waste Management V: 33-47; Washington/DC (American Chemical Society).

Ursini, O., Lilla, E. & Montanari, R. (2005): Zeolites as selective ion trapper during the electrokinetic process for copper polluted soils.- EREM 2005, 5th Symposium on Eletrokinetic Remediation – Fundamental and Industrial Aspects: Ferrara, Italy.

U.S. EPA (1995): In situ remediation technology: electrokinetics.- EPA/542-K-94-007.

U.S. EPA (1997): Electrokinetic Laboratory and Field Processes Applicable to Radioactive and Hazardous Mixed Waste in Soil and Groundwater.- EPA/402-R-97-006.

U.S. EPA (1998): Sandia National Laboratories in-situ electrokinetic extraction technology – Innovative Technology Evaluation Report.- EPA/540-R-97-509.

U.S. EPA (1996): A Citizen´s Guide to Treatment Walls. - U.S. EPA Remedial Technology Fact Plane, EPA/542/F-96-016: 5 p.

U.S. EPA (1998): Permeable Reactive Barrier Technologies for Contaminant Remediation. - U.S. EPA Remedial Technology Fact Plane, EPA 600/R-98/125: 102 p.

U.S. EPA (1999): Field Applications of In Situ Remediation Technologies: Permeable Reactive Barriers. - U.S. EPA Remedial Technology Fact Plane, EPA 542-R-99-002: 122 p.

U.S. EPA (2004): Evaluation of permeable reactive barrier performance.- Preparation for the FRTR by the Tri-Agency Permeable Reactive Barrier Initiative. EPA 542-R-04-004: 45p.

U.S. EPA (2002): Field Applications of In Situ Remediation Technologies: Permeable Reactive Barriers. - U.S. Environmental Protection Agency, 30 p.

Van Cauwenberghe, L. (1997). Electrokinetics – Technology Overview.- Ground-Water Remediation Technologies Analysis Center, seen at http.//www.gwrtac.org.

Vance, D.B. (2002): Ground Water and Redox Potential.- Available on http://2the4.net/index.html.

Vancýsek, P. (1993): Ionic Conductivity and Diffusion at Infinite Dilution.- CRC Handbook of Chemistry and Physics: 5-90; Boca Raton, FL (CRC Press).

Virkutyte, J., Sillanpää, M., Latostenmaa, P. (2002): Electrokinetic soil remediation – critical overview.- The Sci. of the total Env., 289: 97-121.

Vidic, R. D. (2001): Permeable reactive barriers: case study review.- GWRTAC E-Series Technology Evaluation Report TE-01-01, Ground-Water Remediation Technologies Analysis Centre, Pittsburgh, PA.

Vogan, J.L., Focht, R.M., Clark, D.K. & Graham, S.L. (1999): Performance evaluation of a permeable reactive barrier for remediation of dissolved chlorinated solvents in groundwater.- J. Haz. Mat., 68: 97-108.

Wagner, J.-F. (1992): Verlagerung und Festlegung von Schwermetallen in tonigen Deponieabdichtungen. Ein Vergleich von Labor- und Geländestudien. - Schr. Angew. Geol. Karlsruhe, 22: 246 p.; Karlsruhe.

Waxman, M.H. & Smits, L.J.M. (1967): Electrical Conductivities in Oil Bearing Shaly Sands.- Soc. of Petroleum Engineers, Proc. of 42nd Annual Fall Mtg., Houston, Tx., SPE-1863-A, V-145-V-160.

Weng, C-H. & Huang, C.P. (2004): Preliminary Study on Treatment of Soil Enriched in Chromite Ore Processing Residue by Electrokinetics.- Practice Periodical of Haz., Toxic, and Radioactive W. Manag., 8 (2): 67-72.

West, L.J. & Stewart, D.I. (1995): Effect of zeta potential on soil electrokinesis.- Geotechnical Special Publication, 46 (2): 1535-1549.

West, L.J., Stewart, D.I., Binley, A.M. & Shaw, B. (1997): Resistivity imaging of electrokinetic transport in soil.- In: Yong, R.N. & Thomas, H.R. (eds.): Geoenvironemental Engineering: 565-574; London (Telford).

Wilkin, R.T. & Puls, R.W. (2003): Capstone report on the application, monitoring, and performance of permeable reactive barriers for groundwater remediation: Volume 1 - Performance evaluation at tow sites.- EPA/600/R-03/045a U.S. Environmental Protection Agency.

Wilkin, R. Swewll, G. & Puls, B. (2001): Rate of microbial biomass accumulation at two permeable reactive barrier sites.- Eos Trans AGU 82(47).

Wilson, D.J., Rodriguez-Maroto, J.M. & Gomez-Lahoz, C. (1995a): Electrokinetic remediation. I: Modeling of simple systems.- Separation Sci. and Techn., 30 (15): 2937-2961.

Wilson, D.J., Rodriguez-Maroto, J.M. & Gomez-Lahoz, C. (1995b): Electrokinetic remediation. II: Amphoteric metals and enhancement with a weak acid.- Separation Sci. and Techn., 30 (16): 3111-3128.

Wong, J.S.H., Hicks, R.E. & Probstein, R. (1997): EDTA-enhanced electroremediation of metal-contaminated soils.- J. Hazard. Mat., 55: 61-79.

Yabusaki, S., Cantrell, K., Sass, B. & Steefel, C. (2001): Multicomponent Reactive Transport in an In Situ Zero-Valent Iron Cell.- Environ. Sci. Technol., 35: 1493-1503.

Yang, G.C.C & Long, Y.-W. (1999): Removal and degradation of phenol in a saturated flow by in-situ electrokinetic remediation and Fenton-like process.- J. Haz. Mat., B69: 259-271.

Yeung, A. T., Scott, T. B., Gopinath, S., Menon, R. M. & Hsu, C. (1997): Design, Fabrication, and Assembly of an Apparatus for Electrokinetic Remediation Studies.- Geotechnical Testing Journal, 20 (2): 199-210.

Yeung, A.T. & Dalta, S. (1995): Fundamental Formulation of Electro-Kinetic Extraction of Contaminants from Soil.- Can. Geotech. J., 32 (4): 569-583.

Yeung, A.T. & Hsu, C. (2005): Electrokinetic remediaton of cadmium-contaminated clay.- J. of Env. Eng., 131 (2): 298-304.

Yeung, A.T. & Mitchell, J.K. (1993): Coupled fluid, electrical and chemical flows in soil.- Géotechnique, 43 (1): 121-134.

Yeung, A.T. (1990): Coupled flow equations for water, electricity and ionic contaminants through clayey soils under hydraulic, electrical and chemical gradients.- J. Non-Equil. Thermodyn., 15 (3): 285-299.

Yeung, A.T., Hsu, C. & Menon, R.M. (1996): EDTA-Enhanced Electrokinetic Extraction of Lead.- Journal of Geotechnical Engineering, 122 (8): 666-673.

Zhou, D., Zorn, R. & Czurda, K. (2003): Electrochemical remediation of copper contaminated kaolinite by conditioning anolyte and catholyte pH simultaneously.- J. of Env. Sciences, A15 (3): 396-400.

Zorn, R., Steger, H., Haus, R. & Czurda, K. (2001): Elektrokinetik - Einführung, Ergebnisse aus Labor- und Feldversuchen.- In: Burkhardt, G., Egloffstein, T. & Czurda, K. (Hrsg.): Altlasten 2001 – Neue Verfahren zur Sicherung und Sanierung, Beiträge zum Seminar 20.-21.06.01 in Karlsruhe, Band 4: 71-82; Karlsruhe (ICP Eigenverlag Bauen und Umwelt).

Zorn, R., Haus, R., Steger. H., Czurda, K. & Borst, M. (2003): Electroremediation: In situ Treatment of Chromate Contaminated Soil.- INCORE: International Conference on Abatement of Groundwater Contamination in Urban Areas, Perspectives resulting from recent R& D-Results, Proceedings 25.06.2003 - 26.06.2003 Stuttgart.

Zorn, R. (2005): Elektrokinetische Bodensanierung: Numerische Modellierung des Strofftransportes unter Einfluss eines elektrischen Gradienten.- XXII+154p.; Karlsruhe.

World Wide Web:

http://www.rtdf.org

http://www.prb-net.org

http://www.rtdf.org

http://www.clu-in.org

http://www.rubin-online.org

http://itrcweb.org

http://www.powellassociates.com

http://www.outotec.com

http://www.hsc.csu.edu.au

http://www.outokumpu.com/hsc